Mechanical and physical guidance of osteogenic differentiation and matrix production

Thesis submitted to the University of Sheffield for the degree of Doctor of Philosophy

Robin Delaine-Smith

Department of Materials Science and Engineering

January 2013

ACKNOWLEDGMENTS

I would like to thank my family and friends for their support and for putting up with me over the course of these four years. I have worked many long nights and weekends, and without their understanding I would not have been able to get to this point. Two of the most important people in my life, my parents, have been brilliant

ever since I started University as an undergraduate many years ago and I want them to know that I appreciate everything they have ever done for me and it is thanks to them that I have been able to reach where I am today.

My final thank you goes out once again to Gwen, you have been so supportive of me right from the start and I am really grateful to you for giving me this opportunity and for believing in me.

Acronyms

%	percentage
α	alpha
β	beta
μg	microgram
μl	microlitre
μM	micromolar
2D	two dimensional
3D	three dimensional
AA	ascorbic acid-2-phosphate
ALP	alkaline phosphatase
ANOVA	analysis of variance
ADMSC	adipose-derived mesenchymal stem cell
ASC	adult stem cell
AR	Alizarin red S
ATP	adenosine triphosphate
BCS	bovine calf serum
βGP	β-glycerophosphate
BMP	bone morphogenic protein
BMSC	bone marrow stem/stromal cell
BSA	bovine serum albumin
Ca^{2+}	calcium
CD	cluster of differentiation
CH	chloral hydrate
cm	centimetre
cm^2	square centimetre
cm^3	cubed centimetre
CO_2	carbon dioxide
COL1	type 1 collagen
COX2	cyclooxygenase 2
DAPI	4',6-diamidino-2-phenylindole
DCM	dichloromethane
DED	de-epithelialized dermis

Dex	dexamethasone
dH$_2$O	deionised water
DMEM	Dulbecco's Modified Eagle's Medium
DMSO	dimethyl sulphoxide
DNA	deoxyribonucleic acid
ECM	extracellular matrix
EDTA	ethylenediaminetetraacetic acid
ERK	extracellular signal-regulated kinase
ESC	embryonic stem cell
F	fungizone
FAK	focal adhesion kinase
FBS	fetal bovine serum
FCS	fetal calf serum
FITC	fluorescein isothiocyanate
FM	fibroblast media
FSS	fluid shear stress
g	gram
h	hour
HA	hyaluronic acid
HCl	hydrochloric acid
HDF	human dermal fibroblast
HDMS	human dermal mesenchymal stem cells
hESMP	human embryonic stem cell-derived mesenchymal progenitor
Hz	hertz
ICT	intraciliary transport
IFT	intraflagellar transport
IGF	insulin-like growth factor
kDa	kilodaltons
kPa	kilopascals
L	litre
M	molar
MAPK	mitogen-activated protein kinase
MC3T3	Mus musculus calvaria
MEM	minimum essential medium

mg	milligram
MG63	human osteosarcoma cells
min	minute
mL	millilitre
MLO-A5	murine long bone osteocyte A5
mm	millimetre
mM	millimolar
MP	multiphoton
MPa	megapascal
mRNA	messenger ribonucleic acid
MSC	mesenchymal stem cells
MTS	3-(4,5-dimethylthiazol-2-yl)-5-(3-carboxymethoxyphenyl)-2-(4-sulfophenyl)-2H-tetrazolium
MTT	3-(4,5-dimethylthiazol-2-yl)-2,5-diphenyltetrazolium bromide
n	number
NA	numerical aperture
NaOH	sodium hydroxide
nm	nanometre
nM	nanomolar
nmol	nanomole
NM	non-dex containing media
NO	nitrogen oxide
O_2	oxygen
OCN	osteocalcin
OD	optical density
OFF	oscillatory fluid flow
OM	osteogenic media
ON	osteonectin
OPN	osteopontin
P/S	penicillin/streptomycin
Pa	pascal
PBS	phosphate-buffered saline
PGE_2	prostaglandin E2
pH	potential of hydrogen

PCL	polycaprolcatone
PLGA	poly(lactic-co-glycolic acid)
PU	polyurethane
RNase	ribonuclease
RT-PCR	reverse transcriptase polymerase chain reaction
RUNX2	runt-related transcription factor 2
SD	standard deviation
SEM	scanning electron microscopy
SHG	second harmonic generation
siRNA	small interfering ribonucleic acid
SKP	skin-derived precursors
SR	Sirius red
t	time
TE	tissue engineering
Tecoflex	polyurethane elastomer
TGF-β1	transforming growth factor beta-1
THF	tetrahydrofuran
TRITC	tetramethyl rhodamine isothiocyanate
VD3	vitamin D3

Summary

Tissue engineering and regenerative medicine strategies until now have mostly relied on static culture using chemical stimulation to induce cell differentiation. However, these strategies neglect the dynamic environment in which cells reside in the body where they are surrounded by a chemically and physically well-defined three-dimensional (3D) topography. Not only does this environment control cellular differentiation, but its structure also determines the mechanical function of that tissue. Alongside physical cues, external mechanical forces play an essential role in the homeostasis of many tissues, particularly bone. In order to develop tissue engineered constructs that are suitable for implantation, it may be important to incorporate these essential cues into pre-culture methods and in order to do this, a better understanding of the cellular responses is required.

The main aim of this research was to understand how physical and mechanical cues affect cell behaviour, differentiation and matrix production, with particular emphasis on osteogenesis and collagen organisation. In order to achieve this, electrospun scaffolds were fabricated with controllable fibre orientation for studies involving fibroblast matrix organisation, and the affect on the differentiation of osteoprogenitor cells. Short bouts of tensile loading were conducted using a previously established bioreactor model for conditioning collagen-producing cells. A simple rocking platform method for subjecting cells to fluid-flow was also investigated for its potential to enhance osteogenesis and collagen organisation. This system was further used to study the role of the primary cilium for the mechanotransduction of bone cells. The overall goal was to understand how to manipulate cell differentiation and matrix production in order to develop a more suitable construct with correct tissue structure in a rapid manner.

Monitoring of the major structural matrix protein collagen was achieved using the minimally-invasive technique of second harmonic generation, which was optimised. Electrospun scaffolds with a random architecture caused cells to deposit matrix in a similar random manner, however highly aligned scaffolds caused deposited collagen to orientate in the fibre direction giving superior tensile properties. Further to this, random fibres appeared to be more favourable for the differentiation of osteoprogenitor cells than highly aligned substrates.

Short bouts of tensile stimulation of collagen producing cells on 3D substrates caused an increase in collagen deposition. Another stimulation method, a simple rocking platform, created oscillatory fluid shear stress (FSS) suitable for stimulation of osteogenic cells and enhanced collagen organisation. Further to this, human dermal fibroblasts could be induced to form a mineralised matrix when cultured in osteogenic media, which was further enhanced with FSS.

It was also demonstrated that this simple rocking system could be used to test a wide variety of loading parameters. Finally, rocking was used to examine the role of the primary cilium in the load-induced mineral deposition response of bone cells. When mature bone cells were subjected to FSS, primary cilia shortened in length and removal of primary cilia resulted in loss of the load-induced matrix response suggesting that primary cilia are mechanosensors in bone cells.

CONTENTS

LIST OF FIGURES

LIST OF TABLES

CHAPTER ONE: Background to present work

1.1 Introduction to current clinical problems

Organ failure or major tissue loss can result in serious health problems that can dramatically affect the quality and length of a person's life. Surgical treatments are often needed when damaged tissue fails to spontaneously heal in order to restore some function to the affected area. The current normal practice is to implant graft tissue from a donor site; however, there are complications associated with tissue grafting, dependant on the method. The preferred method is to use donor tissue taken from a different site in the patient (autologous), but the availability of autologous donor tissue is limited, especially in patients who suffer from chronic disease. Donor tissue extraction also requires further surgical procedures and donor site morbidity can occur. Other less preferred methods are to take donor tissue from a different individual (allogeneic) or a different species (xenogeneic), but these carry the risk of pathogenic transfer resulting in infections and there is the possibility of immunological rejection (Murugan and Ramakrishna 2007). An alternative is an artificial replacement, for example, joints often require implants made from metals or polymers to replace the damaged area, but these do not have the ability to undergo wound healing and remodelling. They can also cause mechanical mismatch and cause wearing of the native tissue. These drawbacks are present due to the implanted materials being a nonliving tissue with a finite lifespan (the average for a total joint replacement is 10–20 years) resulting in the need for future surgery to revise the implant, especially in younger people who are still growing, or in middle-aged people who are now living in a time with increasing life expectancy. Cases of mal-union or non-union prevent the bone healing naturally and the standard treatment for these is to use metallic components including pins, screws and rods involving invasive surgery. They often require multiple surgeries and healing time can be prolonged. Metal implants have good mechanical strength and durability, which make them seem suitable for bone replacement; however they can cause numerous problems for the patient including stress shielding, stiffness and chronic pain.

1.2 Tissue engineering

1.2.1 Introduction

Tissue engineering (TE) has become a major discipline in the field of regenerative medicine and presents potential solutions to the problems associated with current therapies in the treatment of tissue defects caused by trauma, diseases, and age-related conditions. The basic principles of TE (Fig. 1.1) involve taking a suitable cell source, expanding them in culture to obtain the required number of cells, and then seeding them on a suitable scaffolding material, ideally with similar chemical, physical, and mechanical properties to the target tissue. The scaffold and culture environment then promotes the organization, growth, and development of the cells into a fully functioning tissue (Murugan and Ramakrishna 2007). This would be implanted into the effected tissue and the scaffold material would harmlessly degrade leaving the cells and their own matrix to integrate with new tissue.
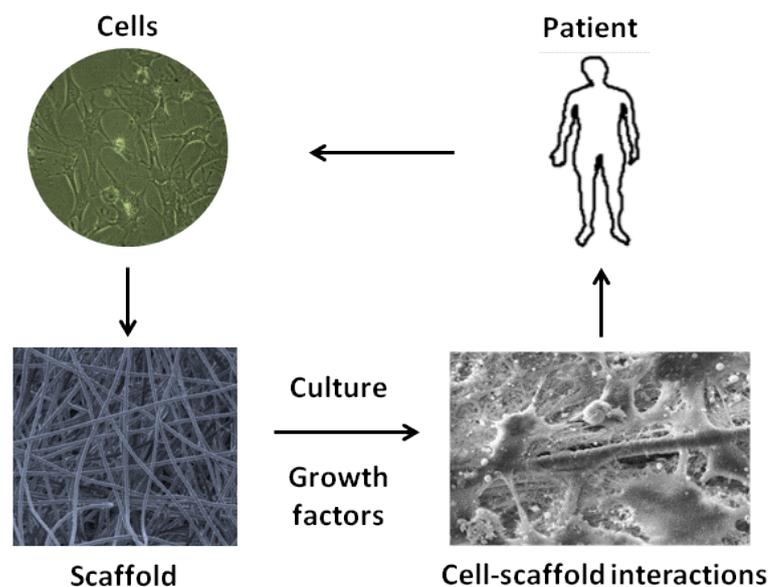
Figure 1.1: The basic principle of tissue engineering strategies. Cells are taken from a patient or donor and cultured on a scaffold material before implantation into the affected area of the patient.

Ideally, tissue engineers would have access to mature cells of the target tissue that are capable of making new matrix in a rapid manner. However, this is often not the case due to limit supply of differentiated cells, especially if the patient suffers from disease or has suffered major tissue loss. One promising alternative for the development of new tissues is the use of stem cells, cells that are able to form many

different types of tissue and have self-renewal ability. While there have been advancements in our understanding of the behaviour and capabilities of stem cells, we are still unable to precisely control their differentiation, which is a major limiting factor in the development of successful TE therapies. It is well known that biochemical cues, such as cytokines, growth factors, and signalling events (Augello and De Bari 2010) can control the function of stem cells as well as environmental factors (e.g., surface chemistry and topography) (Dalby *et al.* 2007b; Reilly and Engler 2010) but it is also becoming clear that mechanical forces can greatly influence stem cell behaviour. External mechanical forces are likely to play a major role in developing the optimum culture conditions for TE constructs.

There are several advantages that successfully implemented tissue engineering strategies would have over current treatments. An implanted engineered construct would mean that fewer surgical steps would be needed; essentially the affected area would be cleaned and prepared followed by subsequent implantation of the construct. This means that risks associated with multiple surgeries are reduced and the wound will be allowed to heal properly at the normal rate. The implanted tissue engineered construct will mature and remodel while integrating seamlessly with the native tissue preventing problems associated with material/tissue mismatching. The overall aim then is that costs of treatments will be reduced with fewer steps required than current treatments and with no future surgical interventions necessary.

1.2.2 Requirements of tissue engineering

In order for tissue engineering strategies to be successful, the tissue engineer must elucidate which materials and culture conditions are the most appropriate for the development of a suitable tissue engineered construct *in vitro* that is ready for implantation *in vivo* that reduces subsequent healing time. Firstly, this includes selection of a healthy cell source that is easily available and capable of lineage-specific differentiation into a mature cell native to the required tissue. Secondly, the appropriate culture conditions must be identified that allows the chosen cell to proliferate, migrate and differentiate into the required tissue. This includes identifying the best media formulations along with any chemical stimuli required for inducing or enhancing differentiation and when is the right time to apply these. The mechanical properties of the tissue engineered construct ideally should match that of

the tissue being replaced to avoid mechanical failure or mismatch. This could include using a starting material that already has the required properties of the target tissue but essentially comes down to being able to produce the appropriate matrix components and matching how it is organised within the target tissue. Another important point to consider is that many tissues in the body, especially the musculoskeletal tissues, are load bearing and experience mechanical forces and this could be in the form of compression, tension, or fluid flow-induced shear stresses. Therefore, it seems necessary that tissues should be pre-conditioned using the appropriate mechanical forces in order to prepare the tissue engineered construct for the forces it will experience *in vivo*. Mechanical matching is also important for triggering the correct biochemical pathways to induce cellular differentiation and matrix formation. Mechanical forces could also help increase matrix production and subsequently reduce healing time, and they may contribute to matrix organisation resulting in a stronger and more suitable construct.

1.3 Tissue structure and composition

1.3.1 Introduction to extracellular matrix

Tissues are complex structures and are typically well organised into a three dimensional (3D) architecture that is thought to play a major role in the biological functions of the tissues. Amongst this 3D network, all tissues contain a non-living portion called the extracellular matrix (ECM) which is essentially a ground substance containing a complex nano-micro fibrous environment complete with ridges and pores that serves to provide structural support to the cells. There are three major structural proteins; collagen, fibronectin, and laminin, as well as many other components including elastin, fibrillin, tenascin, glycosaminoglycans, and proteoglycans. The distribution and organisation of these components throughout the body is very specific (Hay 1991) and may well contribute to developmental processes (Eyal-Giladi 1995). In skin for example, there is very little ECM between the tightly packed epithelial tissue of the outermost layer, the epidermis. The dermis is an example of a dense irregular connective tissue because the fibres are closely interwoven but not highly organised. Specialised connective tissues such as tendon

or bone are referred to as dense regular connective tissues because the majority of tissue is made up of fibrous ECM tightly packed in parallel arrays. As well as this, the ECM facilitates tissue growth by acting as a substrate for cellular-adhesion and migration, and it is thought to regulate cellular proliferation and function by providing growth factors (Bissell and Barcellos-Hoff 1987).

1.3.2 Collagen

Collagen is the most abundant protein in the human body and one of the major constituents of the ECM and a major structural component of the specialised connective tissues such as bone, cartilage, tendon/ligament and skin. So far there have been at least 28 distinct types of collagen identified in the human body based on their molecular sequences and generally categorized into fibril or non-fibril form (Heino 2007). All members of the collagen family share a common structural feature in the form of at least one triple helical domain (Eckes *et al.* 2010). Collagens are found throughout the body in different tissues in varying amounts and each one has its own distinct role. Major types of collagen include the fibril-forming collagens (types I, II and III), that provide structural strength, the basement membrane-associated collagens (types IV, VII), and transmembrane collagens (XIII and XVII) that form cell-ECM contact sites. The most abundant collagen is type I, which forms large fibrous networks, followed by type III, which forms much finer fibres. By dry weight, type I collagen (Col I) makes up about 30% of bone matrix (Hollinger *et al.* 2005), 70-80% of ligaments, 75-85% of tendons, and 56-70% of skin (Martin *et al.* 1998). In human skin, Col I and collagen type III (Col III) account for 80% and 15% of dermal collagen respectively, whereas in bone only small amounts of Col III, V and XII exist (Hollinger *et al.* 2005).

A collagen molecule (called a tropocollagen) has a triple helix structure formed by three α polypeptide chains coiling together giving an overall rope-like appearance. Collagen type I is a heteropolymer made up of two poly peptide chains [α1(I)]2 and one chain of [α2(I)]1 and collagen type III fibrils are formed by three poly peptide chains called [α1(III)]3. The primary structure of α polypeptide chain has the primary structure $(Gly-X-Y)_n$ where X and Y are often proline or hydroxyproline. Post-translational modifications are made to the collagen molecule in order to form stable collagen cross-links. Tropocollagen molecules are then arranged into groups called

fibrils and the diameter of these fibrils can range anywhere between 50 and 500nm and collagen fibrils can then be packed together to form much larger collagen fibres in the micrometer range (10-50 µm) (Screen *et al.* 2004) (Fig. 1.2). Depending on the tissue type, they can be organised into large bundles of well organised, parallel fibres as seen in tendon or concentric layers of fibres as seen in compact bone. Col I is present in loose connective tissue, which often lines epithelial tissue, as relatively sparse fine fibres and it is also present in dense connective tissue like skin as much thicker, more abundant fibres. One of the key roles of collagen is to resist pulling and its inherent strength is due to its structure and organisation starting at the molecular level and right up to the micro-scale fibre bundles, which can be likened to that of a piece of rope. This makes all tissues containing collagen strong in tension and while collagen is only very slightly elastic, it is quite flexible allowing movement as seen in skin. The structural integrity of collagen fibres are maintained by the presence of non-collagenous matrices which surround the fibres and help bind them together. Human dermis undergoes fundamental structural changes in the collagen network as it ages, caused by internal and external factors. The main cause of these changes is a decline in collagen content due to reduced neosynthesis and continued degradation of collagen fibres.
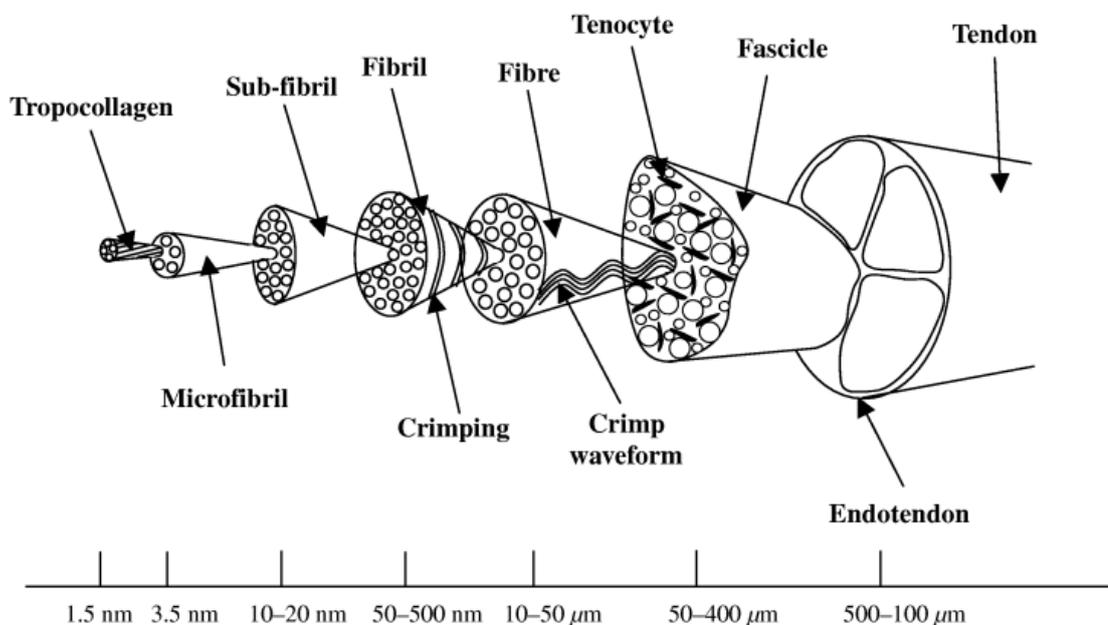
Figure 1.2: Schematic showing the hierarchical organisation of collagen in tendon. Reprinted from Screen *et al.* 2004 with kind permission from John Wiley and Sons.

1.3.3 Collagen orientation

An important factor with regards to the mechanical properties of tissue is the orientation of the collagen fibres. In bone for example, the mechanical properties exhibited are due to the predominately orientated structure of the Col I fibrils. It has been shown that collagen fibres that are orientated more longitudinally (relative to the long axis of the bone) have stronger tensile properties than bone made up of more transversely orientated collagen, which is stronger in compression (Reilly *et al.* 1997; Riggs *et al.* 1993). Similar findings have also been seen in the long curved bones of animals where the regions that are usually subjected to tension have a predominately longitudinal orientation (higher tensile properties) and regions subjected to higher levels of compression have a more transverse orientation (better compressive properties) (Skedros and Hunt 2004). Collagen in skin is organised into randomly orientated, woven sheets to facilitate the stretching that it receives in multiple directions (Fig. 1.3a). Collagen fibres in tendon are organized into long crimped, uniaxial bundles in the direction parallel to the tension that they receive (Screen *et al.* 2004) (Fig. 1.3b). As a result of this, tendon and ligaments have shown tensile properties up to 500 times higher parallel to the fibre direction when compared to the perpendicular direction (Lynch *et al.* 2003). Other matrix proteins also play an important role in the mechanics of tissues, for example elastin in skin allows connective tissues to resume their shape after stretching or contraction.
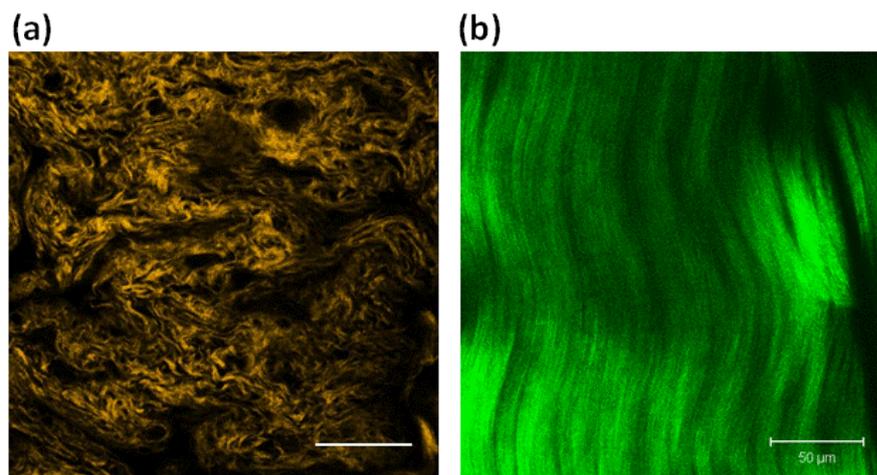
Figure 1.3: Collagen organisation can be visualised in two differentially organised tissues; human DED (de-epithilialized dermis) (a); and rat tail tendon (b) using second harmonic generation (SHG) imaging. Scale bars are 50 μm. Images captured by Author.

1.4 Examining collagen production and organisation

1.4.1 Introduction

Monitoring the production and organisation of the fibrous collagen network is of particular importance in all load-bearing tissues as it is the principal determinant of tissue structure, and associated mechanical properties that dictate the biomechanical function of the tissue. Current techniques for examining matrix production and organisation in 3D tissue-engineered constructs both *in vitro* and *in vivo* are often associated with highly invasive procedures that result in sacrifice of the sample. There are a few well-established standard methods for either visualising (e.g. antibody immunohistochemical, histology) or quantifying (hydroxyproline crosslink assay, qPCR) collagen but these techniques are invasive and often time consuming, requiring preparation steps such as fixation and staining. Most techniques do not provide sufficient information on structural organisation, and those that do can alter matrix organisation through preparation steps. There are a number of physical methods that have been used to image collagen organization in tissues including polarized light microscopy, small and wide-angle x-ray scattering, and polarization sensitive optical coherence tomography (PSOCT) (Ugryumova *et al.* 2005; Ugryumova *et al.* 2006). PSOCT allows for depth imaging on tissue attached to subchondral bone, however, the depth and lateral resolution of the technique are too low to be able to sufficiently determine any minor changes in structure that may occur through disease for example. The ideal technique would be one that could penetrate deep into tissues, is non-invasive, and allows for sufficient depth and lateral resolution.

1.4.2 Multiphoton microscopy

Multiphoton microscopy may serve to satisfy this criteria and it has been used to image biological systems ranging from cultured cells (Zoumi *et al.* 2002), to whole tissues (Campagnola *et al.* 2002; Zipfel *et al.* 2003; Zoumi *et al.* 2002) and also living organisms (Sun *et al.* 2004). It utilises excitation wavelengths in the infrared region owing to its nonlinearity, which allows for increased tissue penetration compared with normal fluorescent imaging techniques, while also maintaining high spatial resolution. Signal can be generated via interactions with naturally occurring

endogenous structures within a sample without the need for external staining or sample fixing (Schenke-Layland *et al.* 2006). This allows the sample to be imaged in its non-altered form in a minimally invasive way. Two-photon techniques allow for precise optical sectioning without the use of a pinhole due to the exciting photons concentrating all the power at the focal point (Campagnola *et al.* 2002) resulting in improved axial and lateral resolution. This also minimises photobleaching and phototoxicity outside of the focal plane. With the use of near infrared (IR) lasers, sample penetration is greater and this also allows for higher contrast imaging (Campagnola and Loew 2003) which is particularly useful for 3D tissue engineered constructs.

The two nonlinear processes that can be used with multiphoton microscopy are two-photon fluorescence (TPF) and second harmonic generation (SHG). There are a number of endogenous fluorophores that have been identified in the extracellular matrix, such as flavoproteins, keratin, and elastin (figure 1.4), and these can be imaged using TPF (Schenke-Layland *et al.* 2006). TPF is a resonant process, which occurs when a fluorescent molecule absorbs the energy provided by two photons simultaneously, shifting an electron into an excited energy state (Oheim *et al.* 2006). Relaxation to the ground state follows this causing fluorescence to occur, and the energy of the emitted photon is less than that absorbed from the original two photons (Oheim *et al.* 2006). SHG in particular could be highly advantageous for tissue engineers as it is capable of imaging non-centrosymmetric molecules such as the major ECM component collagen (Freund *et al.* 1986).
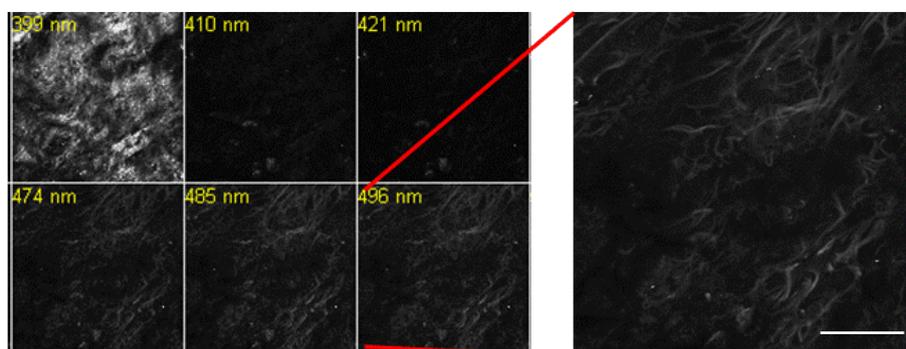
Figure 1.4: Multiphoton excitation (800 nm) of human DED shows the presence of matrix with endogenous flurophores in emission windows 474-496 nm. Scale bar is 50 μm. Image captured by author.

1.4.3 Second harmonic generation

SHG can be generated using a short pulse multiphoton (MP) laser, such as a femtosecond laser, whereby the non-centrosymmetric molecule is excited by two near-infrared incident photons of equal wavelength and low energy which scatter non-linearly, resulting in the formation of a visible photon at half the wavelength and twice the energy of the original photons. This new photon can be detected at half the wavelength of that used to excite the sample. During the excitation process, no absorption occurs and so there is no loss of coherence (Prasad 2003). Collagen is a strong emitter of SHG (Zipfel *et al.* 2003) and the intensity of the resulting SHG image is influenced by a multitude of factors including the quantity of collagen present, the type of collagen, and the fibril organisation and alignment (Bayan *et al.* 2009; Matcher 2009).

It has been suggested that proteins such as collagen are efficient generators of SHG because dipole interactions are enhanced by the chiral nature of the helices, an effect which is further enhanced by the number of helices (Campagnola *et al.* 2002). Collagen molecules have a highly crystalline triple helical structure with no centre of symmetry and so it is not surprising that it is a strong emitter of SHG. SHG therefore allows for the non-invasive imaging of the development of a collagenous matrix without sacrificing a sample *in vitro* or taking a biopsy *in vivo* and so remodelling, turnover and scaffold degradation can be observed. SHG is polarization sensitive and so the intensity is dependent on the angle between the fibres and the polarization of the excitation source. The maximum signal intensity is obtained when the fibre axis is parallel to the plane of polarization, and the minimum intensity is generated when the fibre axis is perpendicular to the polarization.

SHG signal is propagated either in the same direction as the incident laser beam (forward) or scattered backwards. Most of the signal generated will be in the forward direction due to the coherent nature of the process, but the ratio of the two signals will vary depending on the sample properties (Oheim *et al.* 2006). The two signals can also provide varying (yet complimentary) information about the sample contents. It has been suggested that backward scattering can distinguish between younger and older collagen fibrils due to changes in fibril size (Williams *et al.* 2005) and therefore

would be very useful for monitoring developing collagen as within a tissue engineered construct.

1.4.4 SHG wavelength dependence

It has been suggested that SHG intensity is also dependent on the excitation wavelength used (Theodossiou *et al.* 2006). Previous studies have been conflicting as to which wavelength, if any, produces a more intense SHG signal from collagen (Zipfel *et al.* 2003; Zoumi *et al.* 2002) with many studies suggesting that 800-860 nm excitations gives the most intense SHG. Zoumi et al., (2002) imaged a polymerized gel containing COL I from rat tail and observed a bell shape curve for excitation intensities (730-880 nm) centred around 800 nm. Theodoussiou et al., (2006) imaged cryosections of rat tendon using excitation wavelengths of 830-920 nm in both forward and backward propagation modes at varying angles. SHG intensity varied depending on propagation direction, with peaks at 845, 880, 895, and 915 nm for backwards and 880 for forwards.

Wavelength dependence is of interest with regards to imaging delicate samples. A tissue engineered construct in its early stages of development will contain an immature and developing collagenous matrix that is less-well organized than mature tissue. Therefore, it will more susceptible to photo-damage and is less likely to give an intense signal so the excitation wavelength that provides the most intense signal is desirable. Another important feature is that the use of different wavelengths may serve as a method of differentiation between different materials and structures (e.g. between scaffold and ECM). It has also been shown that the use of longer wavelengths increases tissue penetration as well as minimizing cellular damage (Campagnola and Loew 2003; Zipfel *et al.* 2003). Sample depth has been shown to affect the signal intensity of two-photon imaging techniques (Balu *et al.* 2009). Tissue phantoms containing fluorescent and non-fluorescent beads were imaged using 800 nm and 1300 nm excitation. TPF signal intensity dropped off more quickly at 800 nm and signal was indistinguishable from noise at a depth of 175 µm for 800 nm compared with 300 µm for 1300 nm. It was suggested that this was due to increased scattering occurring at shorter excitation wavelengths (Balu *et al.* 2009).

1.5 Fibroblasts

Fibroblasts are a heterogeneous population of cells of mesenchymal origin, found in abundance in many tissues around the body, particularly the connective tissues. They are generally defined by their spindle shape (fusiform) morphology (Fig. 1.5). Fibroblasts are the primary cell responsible for synthesis and deposition of ECM components during development, growth and maintenance, as well as during wound healing, especially in bone, cartilage, tendon and ligaments, adipose, and skin. They also recruit other cell types during tissue repair by releasing growth factors and cytokines and they produce proteases for later stage remodelling (Eckes *et al.* 2010). During wound healing, fibroblasts can transform into myofibroblasts, a cell that causes the wound to contract and deposits excessive matrix (Gabbiani 2003). While having similar morphologies, fibroblasts from different anatomical sites around the body have their own characteristic phenotype and gene-expression profile, as well as differences in ECM proteins that are synthesized (Chang *et al.* 2002). Dermal fibroblasts proliferate and mobilise in response to chemotactic, mitogenic and modulatory cytokines (Chang *et al.* 2002).

Human dermal fibroblasts

Figure 1.5: Phase contrast images of human dermal fibroblasts cultured on tissue culture plastic showing morphology at 24-72 h after attachment. Scale bar is 50 μm. Images captured by Author.

Restoration of damaged tissue requires synthesis, deposition and remodelling of ECM proteins during both early and late phases of wound healing. During wound healing, fibroblasts synthesize most of the ECM and produce proteases for later-stage remodelling. They also release numerous growth factors and cytokines that act on other cell types to regulate tissue repair and scarring (Eckes *et al.* 2010). Fibroblasts become migratory, proliferative and biosynthetically active cells after the initial

inflammatory response to a wound, after which they lay down matrix and remodelling into a highly organized architecture takes place. Secreted matrix is assembled into a fibrillar network whereby cell integrins attach to cell-binding portions of the ECM e.g. the Arginine-Glycine-Aspartic acid (RGD) on fibronectin. Matrix proteins are unwound by the process of pulling apart multiple bound integrins, which reveals self-associated domains (Mao and Schwarzbauer 2005). These domains then become part of the matrix that is organised into fibrillar bundles.

Fibroblasts in culture will behave in a way that is affected by age of donor, passage number, subtype of fibroblast and the anatomical site. Younger fibroblasts tend to migrate faster and double in population quicker than older donor fibroblasts and elderly donor fibroblasts have also been shown to be less responsive to various supplements including ascorbic acid (Phillips *et al.* 1994).

1.6 Bone structure and physiology

1.6.1 Introduction

Bone is the major structural-support tissue of the human body and has many essential functions. It is load bearing and allows movement by supporting muscular contraction as well as providing protecting for many internal organs. It also serves as a mineral reservoir and provides a rich array of growth factors and cytokines, as well as housing red marrow from which new red and white blood cells are formed. The basic building block of bone ECM is mineralized collagen I fibrils, with collagen comprising about 90% of the total protein in bone (Weiner and Wagner 1998). Collagen fibres form the foundation for which the mineral portion of bone is deposited in highly ordered arrays at collagen nucleation points and this composite structure is responsible for the lightweight strength of bone. In a typical adult human there are 206 bones made up of many different shapes and sizes, however the structure is comprised of two major architectural types; cancellous (also called spongy or trabecular bone) and cortical (also called compact). Cancellous bone is more porous (50-90 % porosity), which allows bone to be lightweight. It comprises around 20 % of the total bone volume and is located at the centre of some bones and surrounds the bone marrow. Cortical bone is a highly ordered structure of aligned

mineralized collagen fibres organized into concentric sheets and is mainly responsible for the high tensile and strength of bone (Martin *et al.* 1998). It is found mainly as the outer part of bones or in some cases it comprises whole sections (the mid-shaft of long bones) where it acts as a shield against external forces. Bone can resist extremely high loads and will undergo many millions of cycles before succumbing to fatigue.

At the microscopic level, bone is found in two forms, woven and lamellar. Woven bone is immature bone that is composed of unorganized coarse fibres with no preferred orientation. Lamella bone is characterized by highly organized collagen fibres and formation of this type of bone begins around one month after birth. Lamellar bone protects important organs like the brain (the skull) and is particularly prominent in major structural bones like the long bones in leg, which resist impact. Due to the disorganisation of fibres found in woven bone, it has isotropic properties, while lamellar bone is highly anisotropic due to a preferred fibre orientation. The mechanical behaviour of lamellar bone is dependent on the direction of applied force and the greatest resistance will be found in the direction parallel to the fibre direction. Lamellar bone is arranged longitudinally around vascular channels called the central canal, combining to form an osteon, which is the major structural unit of cortical bone (Fig. 1.6). Cortical bone is made up of many of these osteons packed tightly together with a network of interstitial canals (canaliculi) for nutrient transfer running between lamellae arranged circumferentially.
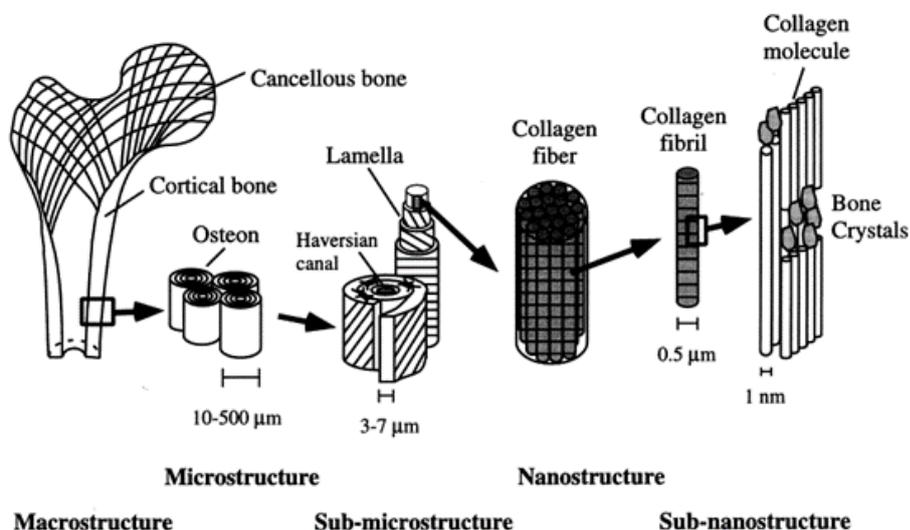
Figure 1.6: The hierarchical structure of bone from the nano-scale to the micro-scale. Reprinted from Rho *et al.* (1998) with kind permission of Elsevier.

1.6.2 Cells in bone

There are four major bone cell types each of which has a defined role and function; osteoblasts (matrix-producing cells), osteocytes (matrix-maintaining cells), osteclasts (matrix-resorbing cells), and osteoprogenitor cells. For healthy bone tissue maintenance, all of these cells are required. Osteoblasts mature into osteocytes and are derived from pluripotent mesenchymal stem cells or osteoprogenitor cells (Fig. 1.7), whereas osteoclasts are derived from hematopoietic precursors found in the bone marrow.

Osteoblasts are the major organic matrix producing cell in bone and are responsible for laying down the type I collagenous matrix as well as the other non-collagenous bone proteins and plasma proteins. Osteoblasts can deposit 0.5-1.5 µm of non-calcified organic bone matrix (osteoid) per day (Sommerfeldt and Rubin 2001). Specialised, inactive osteoblasts called bone lining cells are present at quiescent bone surfaces. They are part of the intracellular communication network and it is though that they direct the formation of new bone (Sodek and McKee 2000).

| Osteoprogenitors | Osteoblasts | Osteocytes |
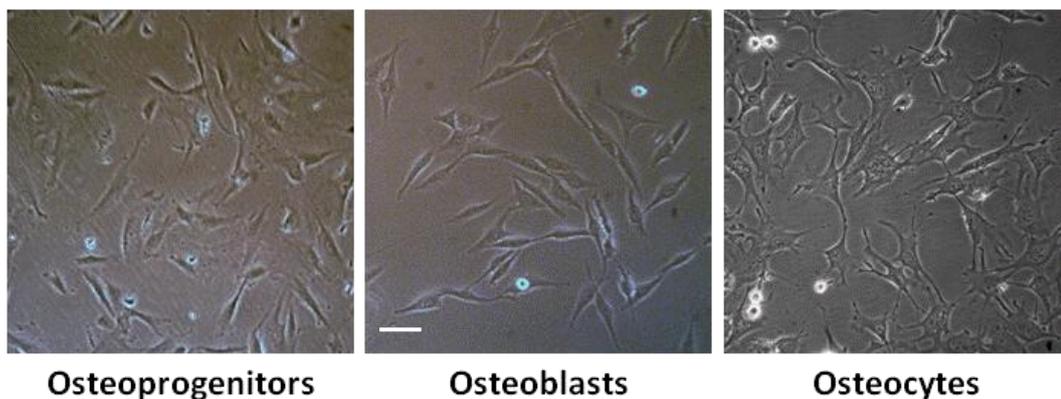
Figure 1.7: Phase contrast images representing the three major bone cells responsible for bone matrix formation and maintenance. Osteoprogenitor (hESMP); osteoblast (MG63); pre-osteocyte (MLO-A5). Scale bar is 25 µm. Images captured by author.

Osteocytes are mature osteoblasts encased in bone matrix and are the most abundant cells in mature bone. They are smaller than osteoblasts and possess a stellate shape expressing a high number of cytoplasmic processes. They have a reduced number of synthesising and secretory organelles but have a higher nucleus/cytoplasmic ratio (Sodek and McKee 2000), and are able to affect protein secretion with the primary function of bone maintenance. Osteocytes are able to communicate with other cells

within bone using their extensive cell processes that penetrate through the bone canaliculi and make contact via gap junctions with the processes of other osteoyctes or even those of osteoblasts (Baylink and Wergedal 1971). It is thought that osteocytes are responsible for sensing mechanical load in bone resulting in communication with osteoblasts and osteoclasts to remodel bone (Tatsumi *et al.* 2007).

Osteoclasts are large, multinucleated cells derived from hematopoietic stem cells in the bone marrow and are responsible for bone resorption as part of the bone remodelling process. They have a high abundance of mitochondria indicating a high level of activity. They break down mineralised bone through the secretion of lysosomal enzymes and once activated, an osteoclast is capable of resorbing as much bone matrix as the amount of bone formed by up to 10 generations of osteoblasts (Hollinger *et al.* 2005)

Osteoprogenitors are undifferentiated, multipotent cells capable of forming new bone by transformation into a matrix-secreting osteoblast. A common osteoprogenitor is a mesenchymal stem cell (MSC) residing in bone marrow stroma and this is recruited to a wound site by specific cues where it differentiates.

1.6.3 Bone mechanobiology

Mechanical forces play an essential role in the physiology and homeostasis of many tissues in the body especially bone. The skeleton is primarily responsible for bearing load and providing structural support. Bones positioned around the body are structured in a way to resist the loading they are subjected to, which also determine the shape of the bone. In order for normal bone structure to be maintained, the correct amount of loading is required and without it, bone becomes weakened and may fracture upon normal load. In the absence of loading, as with spaceflight or prolonged bed rest, bone formation, mineral content and matrix production is reduced resulting in weaker, more brittle bones (Janmey and McCulloch 2007). During walking bones such as the femur and tibia experience cyclic loading in the form of compression and tension, which forces fluid through the lacunocanalicular network creating shear forces across osteocytes embedded within the bone matrix. This repeated loading also acts as a pumping system to move oxygenated and

nutritious fluid around the bone whilst removing waste products (Bassey and Ramsdale 1994).

When osteocytes experience fluid shear *in vivo* they produce secondary messenger signals which may then stimulate the differentiation of osteoblasts from progenitor cells in order to form new bone. This may also inhibit osteoclast function and so there is less bone resorption (Whitfield 2007). As mentioned previously, bone cells *in vivo* often experience forces in the microstrain region (<0.2 %), however *in vitro*, bone cells are often stimulated using strains much greater than this (5-15 % strain). Bone cells subjected to mechanical forces *in vitro* also produce secondary messengers but the level of strain required to upregulate some of these markers are only seen using supraphysiological strains (>0.3 %) (Owan *et al.* 1997).

In bone, it is thought that osteocytes are the main mechano-sensing cells, which are able to detect skeletal activity from the movement of interstitial fluid caused from repeated compression and stretching of bone during various loading activities (Aubin and Bonnelye 2000). Studies *in vitro* have shown that mechanical strain causes an upregulation of nitric oxide (NO) in osteocytes, which enhances osteoblast proliferation and subsequent prostaglandin E_2 (PGE_2) release (Johnson *et al.* 1996). It has also been observed *in vitro* that osteoblasts are also sensitive to mechanical forces (McCoy and O'Brien 2010). As well as fully differentiated bone cells, osteoprogenitor cells have also displayed sensitivity to mechanical stimulation *in vitro* (Delaine-Smith and Reilly 2011). Different mechanical stimuli appear to favour different lineages and mostly resulted in enhancement of differentiation (See Appendix 2 for review details).

Along with bone, other tissues in the body are subjected to different forces at differing magnitudes depending on their role and position. Tissue deformation can be described by how much strain is experienced, which is a measure of the change in length of the tissue compared to its original length, and this can be caused by compression, tension and shear forces. During exercise, tendon can strain in tension as much as 5 % whereas bone peaks much lower at around 0.2-0.3 % under compression and tension due to being a much stiffer tissue. If bone is strained much higher than this (0.7 %) it can start to fail (Whitfield 2007).

1.7 Scaffolds for tissue engineering

Most tissue engineering strategies involve the use of a scaffold material in order to support cellular matrix deposition and guide the formation of new tissue. This would act as an artificial ECM and provide cells with an architecture that allows them to adhere, proliferate, migrate and differentiate. The goal is to seed the appropriate cells on the scaffold and implant this into the affected area of the body either with or without pre-culture *in vitro*. The scaffold would then degrade harmlessly at the same rate as the cells deposit new matrix in the place of the scaffold. As most scaffold materials do not have sufficient mechanical properties for the target tissues, pre-culture methods are likely to be required. Another strategy involves implantation of a cell-free scaffold material in a hope that the native cells will migrate into the scaffold and form new tissue. Scaffolds can also function as delivery vehicles for cells for example to deliver MSCs to a skin wound to promote healing and angiogenesis (Walker *et al.* 2012). Scaffold properties influence cell survival, growth and migration, as well as gene expression and matrix production especially *in vitro*.

It is thought that the ideal scaffold should mimic the native ECM as closely as possible so that the correct physiological and biological functions are performed, and also to match mechanical properties. The characteristics required for the ideal scaffold will vary according to the type of tissue that requires healing. However, all scaffolds should have some basic essential characteristics that are required for the ideal development of tissue (table 1.1). Achievement of these criteria is largely dependent on the choice of base materials and the scaffold fabrication technique.

Materials used for scaffolds can either be naturally-derived, such as collagen, chitosan and gelatine, or of synthetic origin including polylactic acid (PLA), polyglcolic acid (PGA), and polycaprolactone (PCL). Naturally-derived materials are favourable for their chemical and biological properties but they often suffer from poor mechanical stability. Synthetic polymers on the other hand generally have improved mechanical properties but most materials in their raw form lack the required biological functionality. However, synthetic polymers can be processed with modifiable surfaces and tailored to offer a wide range of functional properties. Another advantage is that they do not run the risk of causing immunogenic responses, which can occur with collagen-based materials. However, while naturally-

derived materials are biodegradable, not all synthetic materials are, while others can take years to degrade. Any synthetic polymer that is to be used for biomedical applications must firstly be approved by the relevant authorities, normally the US Food and Drug Administration. Synthetic and naturally-derived materials can also be combined to produce a new scaffold material that utilizes the advantages of each base material.

Biocompatable	Biologically compatible with target tissue
Biodegradable	Ideally degrades at the same rate as tissue formation
Non-toxic	Should not cause cells to die
Non-immunogenic	Should not cause cells to signal immune responses
3D structure or surface topography	To replicate ECM topography and support 3D tissue growth
Porous with interconnected pores	Space for cells to adhere, migrate and secrete matrix; to allow revascularization; efficient mass transport
High surface area to volume ratio	To allow high cell density attachment and proliferation
Mechanical strength	To withstand *in vivo* forces and replicate mechanical environment so cells function correctly.

Table 1.1: Basic essential criteria for the ideal scaffold material for use in TE strategies.

A number of different techniques have been used to fabricate a wide variety of scaffold types including molecular self-assembly (Whitesides and Boncheva 2002), freeze drying (Schoof *et al.* 2001), drawing (Ondarcuhu and Joachim 1998), electrohydrodynamic jet printing, two-photon polymerisation and lithography (Koroleva *et al.* 2012), each of which has its own advantages and disadvantages. The types of scaffolds that can be produced include (but are not limited to) hydrogels, metal meshes, porous foams, printed 3D structures, fibrous mats, and bioactive glasses, each possessing their own unique properties and features. However most of these methods are not capable of producing nano- and micro- fibrous scaffolds with

controlled pore size or fibre geometry as well as highly aligned substrates. Another technique that promises to achieve these points is electrospinning, and it has become a popular choice for scaffold fabrication.

The size of the scaffold fibres and pores are considered to be of great importance when it comes to replicating the proper phenotypic cell expression. It is generally acknowledged that if the scaffold is made up of fibres with a diameter that is equivalent to or larger than the size of the cell then the proper phenotypic cell expression may not be achieved within the ECM (Boland *et al.* 2006)**.** Cells are typically between 10 and 100µm (Stevens 2005) in diameter and so pore sizes must also be of a sufficient size in order for the cells to be able to migrate into the scaffold. As mentioned earlier, the native ECM is found in different forms in the human body, examples include the randomly woven fibres of skin or the highly organised fibres of tendon, which means that it is ideal for scaffolds to be constructed of the correct arrangement to allow for proper tissue function and phenotypic expression. Scaffold architecture is also important for replicating mechanical properties of the tissue.

While many different types of scaffolds have been designed for tissue engineering purposes, 3D culture still has many problems to overcome. These limitations include limited cell in-growth into scaffolds, leading to a shell of cells around the surface of the scaffold instead of desired uniform 3-D cell distribution. It is thought that this occurs because of limited nutrient and waste exchange inside the scaffold before implantation (Hollinger *et al.* 2005; Salgado *et al.* 2004). The correct molecular and macroscopic architecture of the engineered tissue is likely to be important for proper tissue function. The outcome of implanted engineered tissue will ultimately be governed by the clinical variables of each patient such as gender, habit, age, health, systemic conditions and anatomy. In addition, the different regions of the body will have different functional loads and vascularity. Therefore, control of these environments to generate tissue formation, cell function, differentiation, and angiogenesis is a huge challenge for clinical application of tissue engineering.

1.8 Electrospinning

1.8.1 Introduction

Electrospinning is the term widely used for the process of producing fibres from a solution or melt using electrostatic forces. It traces its roots to the more established technique of electrospraying in which electrostatic forces are employed with the aim of controlling droplet formation (Fenn *et al.* 1989). The main difference between the two techniques comes when the melt or solution contains a polymer at a concentration that is sufficiently high enough to cause molecular chain entanglement (Xie *et al.* 2008) resulting in a fibre being drawn. Electrospinning is a straightforward and versatile technique that offers itself to a wide range of polymers and composite materials capable of producing continuous fibres with typical diameters in the range of a few micrometers down to tens of nanometers (Rutledge and Fridrikh 2007). The main advantages of electrospinning include the production of fibrous mats with high surface area to volume ratios, controllable fibre diameter, and the production of highly aligned substrates.

1.8.2 System setup

The basic configuration of an electrospinning rig (figure 1.8) consists of a spinneret (typically a hypodermic syringe needle), a high voltage power pack (normally in the range of 1-30kV) and a grounded collector. The chosen polymer is dissolved using an appropriate solvent, which must be viscous enough for fibres to form. The polymer solution is pumped at a constant rate out of the needle tip using a mechanically controlled syringe pump with the needle connected to the high voltage power pack in order for the solution to become charged. A grounded metallic collector is positioned a determined distance away from the needle tip (called the working distance, Wd) and this can be placed either horizontal to, above or below the tip depending on setup. The collector is often in the form of either a grounded metal flat sheet or a rotating barrel.

The most basic setup for an electrospinning rig is to have the needle positioned vertically above a static, square collector with the advantage being simplicity. However, this makes the resultant fibre mat prone to bead formation due to dripping from the needle tip, and uneven scaffold distribution tends to occur. In order to form

a more evenly distributed fibrous mat, a rotating collector can be used. This not only allows for the formation of a scaffold with random fibre alignment but also one with highly orientated fibres using high speed rotation (>1000rpm).
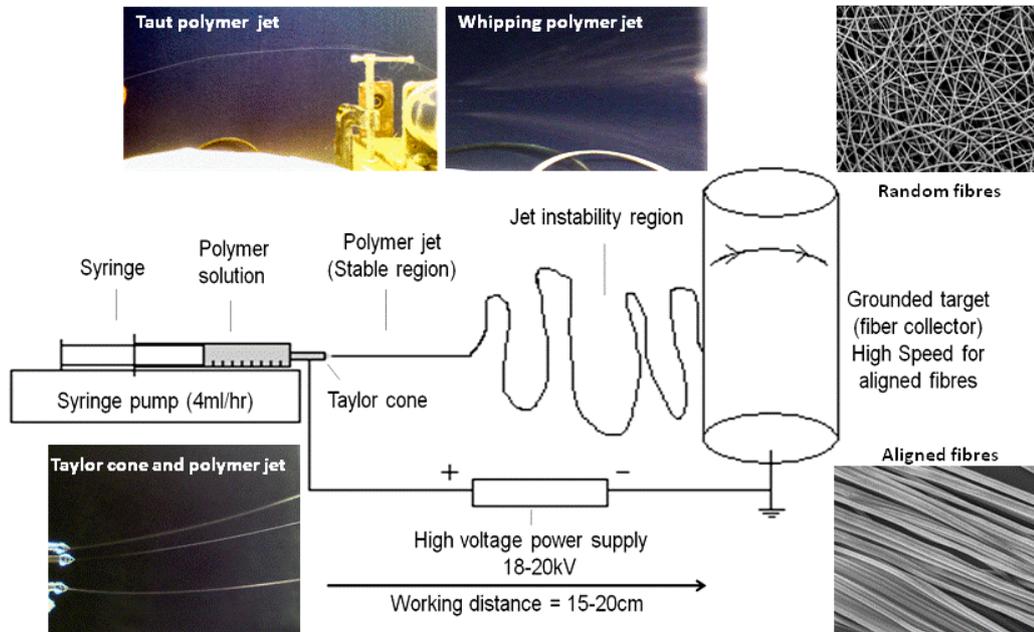
Figure 1.8: Schematic of a typical electrospinning apparatus. Values quoted for flow rate, voltage, and working distance are typical of the conditions used in this thesis. Polymer jet images show the formation of a Taylor cone and subsequent jetting of the polymer solution along with appearance during formation of random fibres (whipping jet) or aligned fibres (taut jet).

1.8.3 Spinning mechanism and theory

Although the process of electrospinning is relatively easy to implement, the mechanism behind the formation of the fibres is complex. Upon applying an electric potential to the contained solution, the induced charge shifts towards the free surface of the solution where electrostatic repulsion occurs. This repulsion effect works against the elasticity and the surface tension of the solution causing a deformed droplet to appear called the Taylor cone (Taylor 1964). When a critical charge density is reached, the electrostatic forces overcome the viscolelastic force and the surface tension resulting in a charged fluid jet emitting from the tip of the cone. This fluid jet seeks out a path to ground and whilst doing so, undergoes two distinct phases of flight. The first period is a 'stable' phase where the jet moves in a straight line but it then encounters a second 'unstable' phase where the jet accelerates and

41

elongates whilst moving in a random whipping motion towards the collector. This instability was originally thought to be due to the phenomenon of 'splaying' (Doshi and Reneker 1995) where mutual repulsion causes the polymer strands of the jet to separate out, but there is evidence to suggest that a 'whipping' mode (Reneker *et al.* 2000) is the primary cause of instability where the jet undergoes a growth of lateral displacement. While in transit, the jet thins out and the solvent evaporates allowing for the formation of thin fibres, which land as a non-woven mat on the collector. The formation of aligned fibres is achieved by inhibiting this whipping motion, either by increasing the stability of the jet or by reeling in the jet so fast that it becomes taut and so no unstable phase occurs.

1.8.4 Electrospinning and tissue engineering

A big breakthrough came in the 1990's when Reneker's group showed that many organic polymers could be used to form fibres via electrospinning (Reneker and Chun 1996). It was then that TE researchers began to realise the potential of electrospining as a technique to fabricate fibrous scaffolds that could mimic the native ECM. Since then, over 100 different types of polymer have been successfully electrospun into fibres (Burger *et al.* 2006) and the resulting scaffolds have been applied to numerous TE and regenerative medicine applications. Electrospun scaffolds have been used as supporting structures for the regeneration of skin (Blackwood *et al.* 2008), bone (Ma *et al.* 2011), tendon/ligaments (Lee *et al.* 2005a), muscles, and for nerve guidance (Daud *et al.* 2012; Murray-Dunning *et al.* 2011). Like the ECM, electrospun scaffolds can potentially act as a reservoir for growth factors (Phipps *et al.* 2012) and for the localised delivery of drugs (Canton *et al.* 2010). Delivery of cells to a wound bed to aid or restore tissue function has also been investigated, for example, epithelial cell delivery to the cornea (Deshpande *et al.* 2010).

There are a wide range of polymers available for use in the production of electrospun scaffolds including both naturally-derived and synthetic types and it is important to consider the required properties for the tissue to be regenerated when choosing a suitable polymer. Choice of processing conditions is important in determining the nature of the fibrous mats that are produced. Fibre diameter is affected by choice of solvent, molecular weight and concentration of polymer, polymer flow rate, applied

voltage, collector distance as well as environmental conditions including temperature, humidity and air flow. Fibre diameter also controls scaffold pore size with smaller fibres yielding smaller pores.

1.8.5 Natural polymers

Chitin/Chitosan: Chitin is a naturally abundant polymer extracted from the exoskeleton in shellfish and chitosan is derived from chitin. Chitosan shows good biocompatibility, it is biodegradable, and it is also non-toxic, which has lead to its use as a wound dressing (Min *et al.* 2004). Chitosan shows a high level of plasticity and good adhesive properties, which makes it a suitable binder for a variety of biomedical applications and it has also proved useful in promoting tissue growth specifically for bone regeneration (Murugan and Ramakrishna 2004).

Collagen: One of the most widely used naturally derived polymers is collagen, and it is not surprising as it is the most abundant protein in the ECM. It comes in two main forms, either extracted from natural tissue or in a purified form (known as reconstituted collagen), which is produced by biochemical processing. It has properties that are favourable in tissue engineering such as biocompatibility, it is biodegradable and it is non-toxic. However, collagen in the form taken straight from natural tissue can cause immunogenic responses and so its use is limited. Using reconstituted collagen significantly decreases this immunogenic risk however, it is relatively expensive. While collagen may seem like the ideal scaffold material, recent studies have shown that when it is electrospun in the normal way, it actually loses its properties and effectively becomes gelatine-like (Zeugolis *et al.* 2008). It has also been seen to degrade far too quickly for suitable cell culture times meaning that some form of treatment is needed after spinning (Zhong *et al.* 2006a).

Gelatin: Gelatin is obtained via extraction from collagen effectively making it a denatured form of collagen. It has physicochemical and biological properties quite similar to those of collagen, (Huang *et al.* 2004) however it does exhibit some properties not seen in collagen. It has favourable properties such as biocompatibility, it is bioresorbable, and unlike some forms of collagen, it does not trigger immunogenic responses. It is widely used in tissue engineering as a scaffold material (Mo *et al.* 2000) and a surface coating for promoting cell adhesion (Delaine-Smith *et al.* 2012) particularly for bone tissue engineering.

1.8.6 Synthetic polymers

Poly(lactic acid) (PLA): PLA is a hydrophobic polymer that is biocompatible, biodegradable, and non-toxic, and it is frequently used in the design of tissue-engineered scaffolds particularly in the field of neural regeneration (Murray-Dunning *et al.* 2011; Yang *et al.* 2004a) and bone formation (Ngiam *et al.* 2011). It has two enantiomeric forms, L-lactide (PLLA) and D-lactide (PDLA), but PLLA is used predominantly in tissue engineering due to its higher biocompatibility and its slower rate of degradation. The principle mode of degradation is via hydrolysis into lactic acid (a metabolic by-product), which is effectively dealt with by the body. PLLA also exhibits high strength and modulus (Inai *et al.* 2005) further making it an attractable polymer.

Poly(glycolic acid) (PGA): PGA is a hydrophilic polymer that is biocompatible, biodegradable, and non-toxic, and has also found use as tissue-engineered scaffolds. It degrades via hydrolysis into glycolic acid (a metabolic by-product) that is effectively dealt with by the body and this happens at a rate faster than that of PLA due to PGA being relatively more amorphous whereas PLA is more crystalline (Blackwood *et al.* 2008). PGA is quite a stiff polymer and it shows high tensile strength and modulus.

Poly(lactic-co-glycolic acid) (PLGA): PLGA is a copolymer made up of the previously discussed homopolymers of PLA and PGA. It is very attractive in that it is possible to manipulate the rate of degradation and mechanical strength by altering the composition of the copolymeric units. PLGA degrades by hydrolysis of its ester linkages and has a more amorphous structure than its individual homopolymers meaning that a copolymer of 50:50 PLGA would degrade faster than each homopolymer. To increase the longevity of PLGA, the amount of PLA can be increased and common ratios used are 75:25 and 85:25 PLA:PGA. It has found wide use in tissue engineering applications and shows much promise in the repair of connective tissues, in particular skin (Blackwood *et al.* 2008), cornea (Deshpande *et al.* 2010), and the urethra (Selim *et al.* 2011).

Poly(-ε-caprolactone) (PCL): PCL is a biodegradable polyester derived from crude oil. It is about ten times less stiff than PLGA but remains elastic over a wider range and has a larger plastic region (Li *et al.* 2007). PCL is a synthetic, aliphatic polyester

formed by ring opening polymerisation of e-caprolactone. It is biocompatible and has good mechanical properties. In contact with water PCL undergoes degradation via hydrolysis with the degradation products being incorporated into the tricarboxylic acid cycle. It degrades at a rate slower than that of PLLA and PLGA mixtures. Electrospun scaffolds of PCL have been used widely in tissue engineering strategies and have shown a good ability to mimic the native ECM (Ma *et al.* 2005). They can easily be drawn into aligned fibres and for this reason have generated favourable use in neuronal repair (Daud *et al.* 2012). PCL has been shown to support osteogenic differentiation of mature bone cells and has been used widely for supporting the osteogneic differentiation of MSCs.

Polyurethane (PU): PUs are a group of synthetic polymer biomaterials that have been used to make implantable medical devices for a long time due to their biocompatibility, excellent mechanical properties and durability. PUs are made up of alternating chains of hard and soft segments with urethane links. By selecting the right intermediates for synthesising PUs, one can engineer a wide range of mechanical and biological properties (Guelcher *et al.* 2007). The soft segment is in the form of a polyol; typically either a polyester or a polyether, while the hard segment is a diisocyanate group. The components that make up a PU can be represented by three basic segments described by the following formula:

$$P - (D(CD)_n - P)_n$$

Where *P = the polyol, D = diisocyanate, C = chain extender, either hydroxyl or amine group (D and C combine to make the hard segment).*

They come in many forms from rigid and flexible foams, to cast and thermoplastic elastomers. Many PUs in the past were non-biodegradable but in recent years, many biodegradable forms have been produced (Guelcher 2008), which has increased interest in their use as scaffolds (Khan *et al.* 2008). Electrospun PUs are very elastic in nature when compared to most other polymers, making them ideal for soft tissues (Guan *et al.* 2005) and tissues that undergo high strains (Pedicini and Farris 2003).

Co-polymers: Combinations of natural and synthetic polymers have also been electrospun (co-spinning) in order to achieve further desirable properties and targeted at specific tissue engineering applications. Some examples include

PCL/collagen for supporting adult stem cell differentiation (Fu and Wang 2012), polyurethane-nanohydroxyapatite for bone TE (Khan *et al.* 2008), and polyurethane/gelatine meshes for vascular grafts (Detta *et al.* 2010).

1.9 Substrate effect on cells

Cell differentiation has traditionally relied on chemical stimulation with various growth factors but it is becoming apparent that substrate properties including composition, stiffness, and patterning, can influence this. Cell-generated forces caused by myosin bundles slipping down actin filaments are transmitted to the ECM surrounding the cells. Cells can feel their environment and as they pull on the ECM they sense the resistance to deformation by this substrate, which triggers signals via mechanically-sensitive proteins allowing communication between the extracellular and intracellular environments. MSCs are known to migrate from bone marrow into a multitude of different tissues that contain different ECM compositions (Pittenger *et al.* 1999), which raises the possibility of their susceptibility to variations in matrix composition.

It has been shown that by altering surface topography, MSC behaviour can be affected (Dalby *et al.* 2007a; Dalby *et al.* 2007b). Substrates of Poly(methylmethacrylate) (PMMA) substrates containing semi-disordered (~120 nm) pits spaced 200 nm apart where shown to upregulate osteogenic genes compared with the ordered pits or flat substrates (Dalby *et al.* 2007b). In another study, MSCs were cultured on titanium nanotubes of 100 and 30 nm diameter, with the large tubes promoting osteogenic gene expression and the smaller tubes promoting proliferation (Oh *et al.* 2009). These tubes were both shown to have the same roughness and so the outcome was most likely dependent on the formation of focal adhesions which regulates a cells ability to adhere and generate force. It has been seen that controlling MSC attachment and cell shape can affect differentiation preference by using the cell's ability to spread on a surface or create traction on it (McBeath *et al.* 2004a). Well-spread MSCs express common osteoblastic markers associated with calcifying bone proteins and this is dependent on the cell being able to apply traction to the material. MSCs that are limited in their ability to spread and generate substrate

tension tend to develop lipid deposits typically found in adipocytes (McBeath *et al.* 2004a). Native ECM has a fibrillar architecture containing a specific distribution of RGD-containing binding sites and so this must be considered for the future design of scaffold materials. The use of planar surfaces could affect the way a cell attaches and senses its environment and so differentiation may not occur in the same way as the human body.

Coatings on rigid planar surfaces do not replicate the physiological mechanical environment of most cell types, which can result in loss of function (Engler *et al.* 2008). The mechanical strength (or elasticity) in cell niches located in different tissues can vary over many orders of magnitude from relatively rigid calcifying bone (>30 kPa) (Engler *et al.* 2006) to much softer brain tissue (0.1 kPa) (Krieg *et al.* 2008). During development, there are natural variations in matrix elasticity and spatial and temporal changes may guide cells through maturity into tissues (Zamir *et al.* 2003). This matrix elasticity dependence on directing cell differentiation was realised in a pioneering study by Engler *et al.* (2006). Undifferentiated MSCs were grown on polymer gels of differing stiffness, chosen to mimic specific tissue types, in the absence of specific growth factors. Precursor proteins specific to that individual tissue lineage were expressed by MSCs on the gel of appropriate elasticity (Engler et al. 2006).

Cells have an inherent sensitivity to their surroundings and they will tend to migrate in the direction of long straight fibres, a phenomenon called contact guidance theory (Barocas and Tranquillo 1997). There is much evidence to suggest that *in vitro* manipulation of collagen fibril orientation can be achieved using either highly orientated substrate scaffolds (Wang *et al.* 2003; Zhong *et al.* 2006b). Several studies using fibroblasts cultured on orientated substrates have induced cell orientation followed by collagen orientation (Lee *et al.* 2005a; Wang *et al.* 2003). Lee and co-workers (Lee *et al.* 2005a) seeded human ligament fibroblasts onto electrospun aligned fibres of polyurethane and then applied tensile strain from which they found that the collagen produced was orientated in the direction of this strain. Bone cells cultured on scaffolds have also been seen to re-orientate themselves when they have been subjected to mechanical strain (Ignatius *et al.* 2005). Integrins are arranged differentially on fibrillar substrates when compared with planar surfaces (Cukierman *et al.* 2001) and so culture on fibrils may alter the distribution of focal contacts. This

could influence how the cells feel the stiffness of the culture matrix and also influence how they differentiate.

1.10 Cell sourcing for tissue engineering

1.10.1 Introduction

One of the most important aspects of all regenerative medicine strategies is the sourcing of an appropriate cell type that is capable of regenerating new tissue without causing complications. The ideal cell type would be one that is easy to obtain with a minimally invasive biopsy, easily expandable *in vitro*, nonimmunogenic, and possesses the ability to differentiate into a variety of cell types with specialized functions (Stock and Vacanti 2001).

Mesenchymal stem cells (MSCs) are a promising cell source that match these requirements and have received much attention due to their multi-potent differentiation potential, self-renewing ability, and apparent immunosuppressive properties (Jaiswal *et al.* 1997; Pittenger *et al.* 1999). They can be obtained from the stroma of adult bone marrow and progenitor cells with similar phenotypic characteristics and differentiation capabilities have been obtained from a variety of other adult tissues including adipose (De Ugarte *et al.* 2003; Zuk *et al.* 2001), tendon (Rui *et al.* 2011), and skeletal muscle (Asakura *et al.* 2001; Bosch *et al.* 2000), as well as fetal tissues such as umbilical cord blood (Erices *et al.* 2000; Goodwin *et al.* 2001) and amniotic fluid (Soncini *et al.* 2007). The use of MSCs for regenerative medicine would mean that tissue-specific cells would not be required from the already damaged or diseased tissue. MSCs have been induced in vitro to differentiate into cell types of the musculoskeletal system, including bone, cartilage, tendon/ligament, and fat (Fig. 1.9). More controversially, researchers have claimed that MSCs differentiate into other tissue types such as smooth muscle, endothelial, and nervous tissue (for a recent review, see (Nombela-Arrieta *et al.* 2011). There are no strong ethical and political issues associated with MSCs compared to embryonic stem (ES) cells making them an attractive cell source for TE and regenerative medicine therapies.
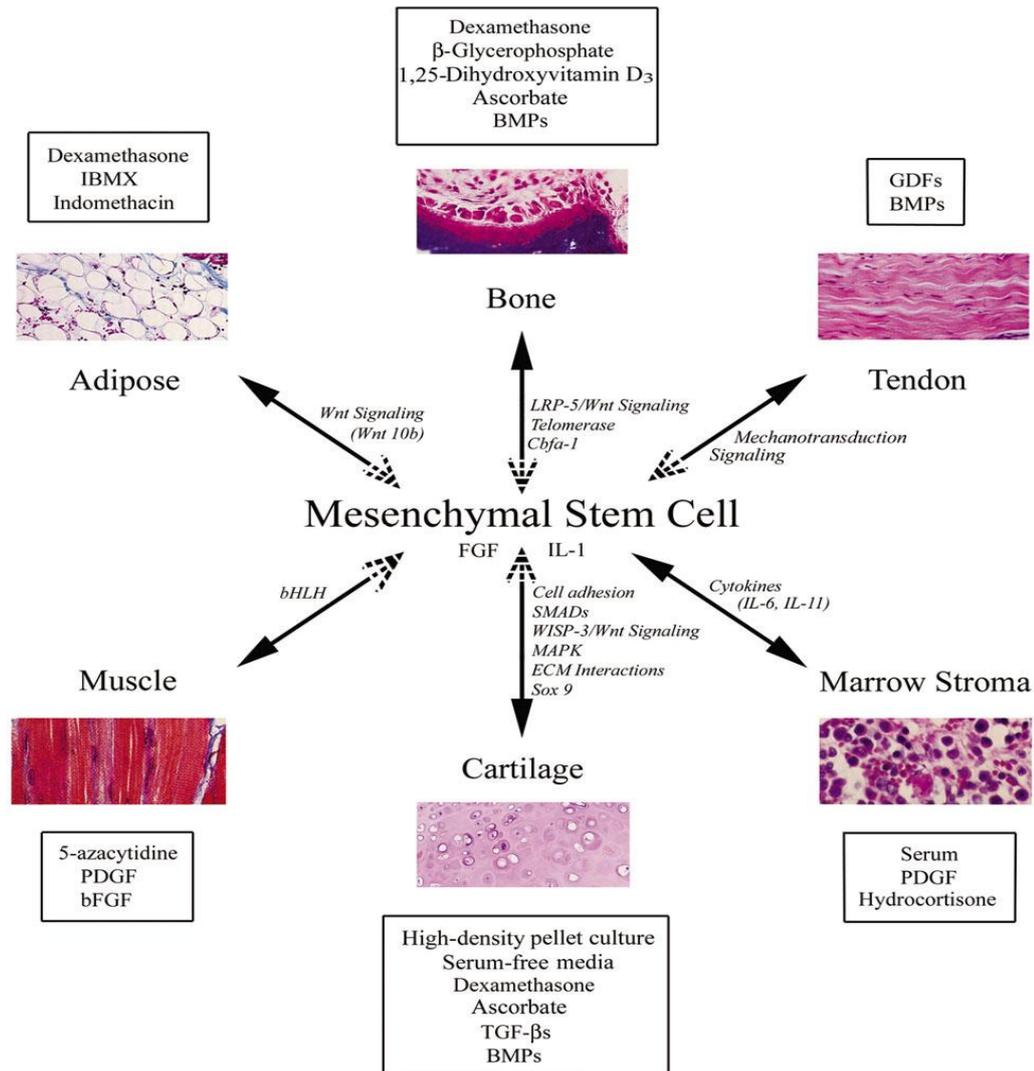
Figure 1.9: Diagram summarising the lineage potential of adult human MSCs. The figure depicts the *in vitro* culture conditions (boxed) used to promote the differentiation into the lineage depicted and some of the signalling pathways and transcription factors involved in the process (italics). Dotted arrow heads denote possibility of 'reverse' differentiation. Reprinted from Arthritis Research and Therapy (Tuan *et al.* 2003), BioMed Central, with kind permission of Professor Tuan.

1.10.2 Embryonic and adult stem cells

Two of the major types of stem cell suggested to have applications in regenerative medicine are embryonic stem cells (ESC), which are present in the early stages of development from the inner cell mass of the blastocyst-stage embryo, and adult stem cells (ASCs), which reside in adult tissue. ESC are considered pluripotent as they are able to differentiate into all cell types in the body and have an unlimited self-renewal capacity, whereas ASC are termed multipotent as they have a limited self-renewal

capacity and can only form a few different tissue types. ESC rapidly proliferate during growth and could be considered an ideal, inexhaustible cell source for tissue replacement, however, the ability for ESC to rapidly form tissue has also lead to teratoma formation (Ben-David and Benvensity 2011). There is also ethical opposition to the clinical use of ESC. On the other hand, stem cells in the adult body do not pose the same ethical concerns and being specialized cells should not produce teratomas, although there may be some cancer risk associated with their therapeutic use (Chanda *et al.* 2010).

1.10.3 Mesenchymal stem cells

MSCs are multipotent ASCs located within the stroma of the bone marrow and other tissues and are therefore also referred to as multipotent stromal cells. It has been recommended that MSCs grown in vitro by plastic adherence selection should be termed "multipotent MSCs," as it is not clear if they possess all the characteristic of true stem cells (Nombela-Arrieta *et al.* 2011). MSCs are nonhematopoietic progenitors capable of extensive self-renewal with potential immunosuppressive properties. hMSCs have been isolated from numerous tissue types and have been shown to differentiate into multiple cell types of the mesoderm, particularly the skeletal tissues, but also may differentiate into cell types of ectodermal and endodermal origin. MSCs were first isolated from bone marrow by Friedenstein *et al.* (1966), who demonstrated their osteogenic potential, but since then populations of cells with similar characteristics have been obtained from other tissues. MSCs are a heterogeneous population and up until now no unique cell-surface markers for MSC identification have been found, although there are some general guidelines for defining an MSC. MSCs should adhere to tissue culture plastic and express the specific surface antigen markers CD73, CD90, and CD105; be negative for CD11b, CD19 or CD34, CD45, CD79a, and HLA-DR; and be able to differentiate into osteoblasts, chondroblasts, and adipocytes *in vitro* (Dominici *et al.* 2006).

MSCs are most commonly sourced from bone marrow by iliac crest biopsy, and there have been extensive investigations into the potential use of bone marrow MSCs (BMSCs). The potential therapeutic benefits of MSCs extend further than their direct contribution to tissue healing by differentiation into the specific cell type of the damaged tissue, they also participate indirectly in wound healing by secretion of

bioactive proteins including growth factors, chemokines, and antiapoptic agents (Rehman *et al.* 2004). Production of these proteins plays an important role in local cellular dynamics, promotion of angiogenesis, and recruitment of cells including other ASCs, which can then aid in the healing process (Meirelles *et al.* 2009). MSCs also act as an immunosuppressant by inter-acting with B and T lymphocytes, Natural Killer cells, and monocytes (Sioud *et al.* 2011), which means they may be suitable as a source of allogenic cells (Koc *et al.* 2002).

While MSCs seem to have a great potential to aid regenerative medicine and tissue engineering strategies, there are still some limitations that need to be addressed. MSCs are commonly sourced from bone marrow, however harvesting of bone marrow is an invasive and painful procedure, and the number of MSCs obtained is relatively small (1 in 100,000 cells) (Caplan 2007). It has also been demonstrated that the number of MSCs obtained from the bone marrow of elderly patients is decreased along with their differentiation potential (Caplan 2007). This may limit the repair of large defects using autologous MSCs, especially in elderly patients, and so finding ways to increase the number of useable cells is a key goal. Alternatively, methods using allogenic MSCs may have to be considered.

The scarcity of BMSCs has lead tissue engineers to search other tissue types for a more accessible and abundant source of cells with MSC capabilities. One promising source is adipose tissue, which can be obtained from any donor regardless of body fat content, using an easily tolerated harvesting procedure. These cells, termed by some as adipose-derived mesenchymal stem cells (ADMSCs) or adipose-derived stem cells (ADSCs), are thought to be present in larger numbers than BMSCs, and also have multi-differentiation potential including osteogenesis, chondrogenesis, and adipogenesis (Seong *et al.* 2010) as well as other phenotypes including Schwann-like cells (Kaewkhaw *et al.* 2011).

1.10.4 Dermal fibroblasts as osteogenic progenitors

Another recently identified tissue that might harbour a suitable cell source for bone repair is the dermis of skin. Dermal fibroblasts (DFs) were initially thought to be terminally differentiated but it has been reported that they may be more plastic than first thought and are able to switch their lineage preference (Rutherford *et al.* 2002; Sommar *et al.* 2009) while numerous studies report that multipotent progenitor cells

reside in the dermal tissue of rodents and humans (Bartsch *et al.* 2005; Chen *et al.* 2007; Toma *et al.* 2001; Xue and Li 2011; Young *et al.* 2001). Multipotent precursor cells expressing nestin and possessing both neural and mesodermal differentiation capabilities were isolated from mammalian dermis by Toma *et al.* (2001) and termed skin-derived precursors (SKPs). Dermal cell populations have also been isolated that contain cells with the ability to differentiate into osteogenic, chondrogenic, and adipogenic phenotypes when cultured under defined conditions, showing positive expression of vimentin but not nestin (Bartcsh *et al.* 2005; Chen *et al.* 2007). Chen *et al.,* (2007) established single cell clones from dermal foreskin fibroblasts and found that around 30% upregulated ALP and Osteocalcin (OCN) mRNA along with strong staining of deposited calcium when cultured in osteogenic media. Others have observed osteogenic differentiation from a population of skin cells (Buranasinsup *et al.* 2006; Lorenz *et al.* 2008). Lorenz *et al.,* (2008) observed an upregulation in OCN and Osteonectin (ON) mRNA in cells derived from human juvenile foreskin when cultured in osteogenic media while Buranasinsup *et al.,* (2006) observed positive ALP and mineral staining in cells derived from middle-aged human skin biopsies. These results show that fibroblast populations derived from the dermis are heterogeneous in nature and contain progenitor cells with varying degrees of differentiation potential including osteogenesis. The relationship between these different types of multipotent cells remains unclear and further investigation is required. Due to the large quantities of available skin, the ease with which it can be obtained, and the high proliferative capacity of dermal fibroblasts (Lorenz *et al.* 2008; Lysy *et al.* 2007), dermal multipotent cells offer a promising cell source for bone tissue engineering strategies.

1.10.5 Stem cell niche

MSCs in vivo reside in what is known as the stem cell niche containing many biochemical factors that regulate their behaviour. Mechanical forces in the form of compression, tension, and fluid-induced shear are all present in the bone marrow (Gurkan and Akkus 2008) but very little is known of their nature of these forces and how they affect stem cell mobilization and function. As well as external mechanical stimuli, there are intracellular tensile forces at focal adhesions as a result of cell–extracellular matrix (ECM) interactions and recent studies suggest that both intrinsic and extrinsic forces play a key role in MSC differentiation (Guilak *et al.* 2009).

1.10.6 Osteogenic differentiation of MSCs *in vitro*

MSC differentiation can be stimulated in vitro under controlled conditions and then confirmation of the progression along a specific lineage can be observed using phenotypic makers associated with that tissue type. This generally involves growing the cells in an optimized medium including supplements or growth factors and then observing the expression of differentiation pathway signals and ECM components that form the infrastructure of that tissue, via assays of gene upregulation and matrix secretion. The differentiation of MSCs into an osteoblast-like cell and subsequent osteogenesis is one of the most extensively studied differentiation pathways.

An early marker of osteogenic differentiation is a switch in the morphology of MSCs from a fibroblastic, fusiform to a more cuboidal, osteoblast-like shape and experience of an initial proliferative phase. This is accompanied by mRNA expression of Runt-related transcription factor-2 (RUNX-2), osteonectin matrix protein (ON), the growth factors bone morphogenic protein 2 (BMP-2) and transforming growth factor-beta1 (TGF-β1), the enzyme alkaline phosphatase (ALP), and the abundant matrix protein collagen type I (Col I). Later stage differentiation markers include expression of other matrix proteins such as osteopontin (OPN) and osteocalcin (OCN), as well as secretion of the major ECM components, first Col I, and at a later stage bone mineral. The mineral found in bone is carbonated hydroxyapatite a form of calcium phosphate, but most studies identify the presence of a calcium salt by alizarin red staining or a phosphate salt by von Kossa staining without further characterization of the mineral chemistry.

The most commonly used osteogenic medium for MSCs typically contains ascorbic acid (AA) or its phosphate salt, beta-glycerophosphate (βGP), and dexamethasone (Dex), applied for at least 7 days up to several weeks. AA is required for the production of stable collagen, the major matrix protein of bone, and plays a critical role as a cofactor in the hydroxylation of proline residues in the collagen molecule (Kielty *et al.* 1993). βGP provides inorganic phosphate for synthesis of bone-like mineral by the cells (Chang *et al.* 2000). Dex is a non-protein, synthetic glucocorticoid and is a component of multiple differentiation media formulae including osteogenic, chondrogenic, and adipogenic media. In its absence, or the absence of other osteogenic inducers in 2D static culture, there is incomplete

osteogenesis (Porter *et al.* 2003). However, Dex has also been shown to have an inhibitory effect on collagen production and high levels (0.1-1 µM) have been shown to induce adipogenesis (Beresford *et al.* 1992). Other additives have been used to enhance osteogenic induction in combination with the previously described supplements or alone, including the growth factors, TGF-β1 and BMPs, as well as vitamin D3 (VD3) (Seong *et al.* 2010; Vater *et al.* 2011). BMPs belong to the TGF-super family and appear to stimulate osteogenic differentiation *in vitro* and *in vivo*; however, their effect *in vitro* may be species-specific (Diefenderfer *et al.* 2003). For example, in order to stimulate *in vitro* osteogenesis of hMSCs, BMP-2 requires a specific defined medium in which serum is removed or the extracellular regulated-kinase pathway 1 and 2 (ERK1/2) is inhibited and either insulin or insulin-like growth factor (IGF) is added (Osyczka and Leboy 2005).

1.11 Mechanical forces

1.11.1 Introduction

Cells and tissues in the human body are subjected to a wide variety of external forces, which influence their growth, development, and maintenance (Vogel 2006). For example, it is well demonstrated that if bone does not receive adequate loading, as occurs during space flight or prolonged periods of bed rest, then bone mass and density decrease (Janmey and McCulloch 2007), whereas exercise in the form of high-impact loading increases bone density (Bassey and Ramsdale 1994). In other tissues such as muscles, tendon, skin and vessels, cells continuously recognize alterations in mechanical forces and adapt their biological function (Kjaer 2004). Many researchers have explored these mechanical influences *in vitro* and subsequently, many different cell types have been demonstrated to be highly mechanosensitive (Orr *et al.* 2006). Recent TE strategies for MSC differentiation have involved attempts to simulate the physiologically relevant mechanical environment by reproducing the forces experienced *in vivo* in an *in vitro* setting.

1.11.2 Mechanical regulation of cells

Culturing cells on tissue culture plastic or on a scaffolding material under static conditions (no external mechanical forces) in the presence of differentiation media is the simplest and most commonly used method of developing tissue engineered constructs. However, culture under static conditions excludes the important role mechanical forces contribute to the growth, development, and maintenance of tissues under physiological conditions. Previous studies have shown that dynamic culture in 3D can stimulate production of early stage bone markers and cause cells to infiltrate the scaffold material better than static counterparts (Cartmell *et al.* 2003; Jaasma and O'Brien 2008). A wide variety of external mechanical forces act on cells and tissues *in vivo* including compression, tension, torsion, fluid shear stress, and hydrostatic pressure. These forces have all been shown to influence the behaviour and differentiation of cells *in vitro* and so incorporation of external force into culture methods could help produce a more suitable construct. As all cell types that MSCs differentiate into are strongly mechanosensitive, it is not surprising that undifferentiated MSCs are also mechanosensitive. In response to mechanical stimulation, numerous signalling pathways are initiated and FSS causes a release of Ca^{2+}, NO, ATP and prostaglandin E_2 (PGE_2) within seconds to minutes.

While the mechanical environment *in vivo* of load bearing tissues such as bone, cartilage, and endothelium have been well characterized, little is known about the mechanical environment of the MSC niche in vivo (Gurkan and Akkus 2008). The differentiation of MSCs occurs during fetal development, in children and adolescents during growth and in adults during tissue maintenance, such as bone remodelling. MSCs are also involved in the wound healing response, for instance, in a healing fracture and all of these are environments where extracellular forces are in abundance and are thought to influence the action of the MSCs (Henderson *et al.* 2007; Lacroix *et al.* 2002; Morgan *et al.* 2008).

Despite the lack of understanding of the mechanical environment of differentiating MSCs *in vivo*, it has become clear that MSCs respond strongly to mechanical loading *in vitro*. Some of these forces may be considered "supraphysiological"; however, from the TE perspective, the important parameter to elucidate is the loading regime that will ensure precise differentiation and best accelerate matrix

production and/or improve matrix quality either in vitro, prior to implantation, or in vivo, after implantation. A wide variety of mechanical stimuli have been used in an attempt to either induce or enhance MSC differentiation *in vitro* including stretch (Huang *et al.* 2009), compression (Sittichokechaiwut *et al.* 2010), fluid shear (Delaine-Smith *et al.* 2012), ultrasound (Angle *et al.* 2011), vibrations (Edwards and Reilly 2011), and magnetic particle stretching (Glossop and Cartmell 2010).

1.11.3 Mechanical stimulation of MSCs

Mechanical stimulation of MSCs in vitro has shown that hydrostatic pressure induces chondrogenic differentiation in hMSCs (Luo and Seedhom 2007), tensile strain applied to MSCs enhances osteogenesis and inhibits adipogenesis (Sen *et al.* 2008; Simmons *et al.* 2003), and fluid shear forces upregulate genes associated with osteogenesis (Arnsdorf *et al.* 2009; Yourek *et al.* 2010). For a full review on the effect of different mechanical stimuli on MSC differentiation see Delaine-Smith and Reilly (2011) (See APPENDIX 2). However, due to the wide range of types of mechanical stimulus, the large array of possible conditions, and the different chemical stimulants available, the optimum conditions for MSC differentiation along a specific lineage remain elusive. A better understanding of the mechanical control of MSC differentiation is important when designing bioreactor conditions for growing constructs. In particular, reproducible dynamic culture conditions, capable of scale-up, will need to be devised in order for such constructs to be engineered in a laboratory for economically viable clinical use (Archer and Williams 2005).

1.12 Methods of mechanical stimulation

1.12.1 Introduction

The optimum durations, magnitudes, and frequencies of mechanical loading for lineage-specific differentiation of MSCs is not known due to the difficulty of undertaking multiple loading regimens within one set of experiments. The response of MSCs to loading are likely to be age-specific, may be specific to site of origin, and appear to depend on how differentiated the cells are at the time of loading, as well as whether loading is performed in conjunction with biochemical supplements.

There are many ways in which researchers have stimulated cells with mechanical forces in vitro and while there is a wide range of experimental apparatus, they can generally be categorized into the primary type of stimulation they provide. For each stimulation mode, the stimulus can be applied in 2D (monolayer) or 3D and differences between cells cultured in 2D and 3D have been observed in terms of cellular morphology and migration strategies, matrix adhesion, gene and protein expression, and responses to fluid flow (Pedersen and Swartz 2005). A wide variety of mechanical stimuli have been used in order to either induce or enhance cellular differentiation *in vitro* and these are reviewed in Delaine-Smith and Reilly (2011) and in more detail in Brown (Brown 2000) and El Haj and Cartmell (El Haj and Cartmell 2010). Two mechanical stimulation methods of significance with regards to the loading bone cells receive *in vivo* will be discussed here; tensile loading, and fluid flow-induced shear stress (FSS).

1.12.2 Tensile loading

When a sample is stretched, it will experience tensile strain and this will result in an increase in length of the sample. Stretching is experienced in the body by many tissue types including bone, tendons and ligaments, skin and vascular tissue. There are a number of ways in which cells have been stretched *in vitro* but ultimately most methods are based on two primary designs; uniaxial (and multiaxial) grip tension and substrate bending. Longitudinal stretch requires a deformable substrate and can be in the form of static stretch, where the sample is held at a specific strain for a fixed period of time, or dynamic stretching where strain is applied in cycles. Gripped tensile loading is performed mainly on cell-seeded constructs and involves gripping the sample at the ends with the cells seeded in the middle of the sample away from the gripped area. Substrate bending involves cells seeded on a flexible substrate placed over a number of pivot points with an external load or displacement being applied to the ends. This is normally performed in 2D on a monolayer of cells as the apparatus is often a specially built flat culture dish. In each of these methods, there will be some compression forces exerted due to substrate deformation in the direction perpendicular to the applied tension (Poisson effect). Also, cyclic tension can subject the cells to major or minor fluid shear stresses as they are moved backward and forward through the media simulating the flow of fluid over the cells (Thompson *et al.* 2010).

When cells are seeded in a 3D gel or porous scaffold, tensile loading can also stimulate the flow of nutrients into and out of the scaffold (Cartmell *et al.* 2003). In 3D culture, the forces that the cells experience will also depend on the scaffold architecture. A gel-based scaffold, for example, will deform almost entirely uniformly and so the force resulting from the applied strain should be relatively homogeneous on each cell throughout the scaffold. This is in contrast to a randomly orientated fibrous scaffold or a foam scaffold, where cells will be attached to fibres or struts that are not in the same plane as the applied strain and so the forces experienced throughout the scaffold will be heterogeneous. The applied strain is usually then referred to as a global strain.

1.12.3 Fluid flow-induced shear stress

Fluid flow-induced shear stress (FSS) is created when a fluid passes over the surface of an object. This type of force is thought to be one of the major influencing mechanical stimuli experienced *in vivo* especially in bone where it is thought that shear forces acting on osteocytes, caused by interstitial fluid movement in the lacunar-canalicular system, result in a biochemical response to initiate remodeling (Klein-Nulend *et al.* 2005). For 2D systems, various experimental apparatus have been used to study the effects of shear stress on monolayers of cells. Commonly used systems include the cone and plate system (Frangos *et al.* 1988), the parallel plate flow chamber system (Jacobs *et al.* 1998), rotating disk or radial flow devices (Deligianni *et al.* 2001), an oscillating orbital shaker system (Hubbe 1981), and a rocking "see saw" system (Delaine-Smith *et al.* 2012; Hoey *et al.* 2011). The first system involves a plate containing cells in which rotation is forced around a cone axis that stands perpendicular to the plate. The fluid shear stresses experienced are spatially homogenous due to the differences in radial position and ultimately the relative velocities of the cells. The parallel plate flow system consists of a relatively long rectangular chamber with an opening at both ends and a pressure gradient created between the two, which causes a uniform laminar flow to develop between the two. These systems are able to apply well-defined parameters allowing for easy modelling of the shear forces experienced. There are many commercially available parallel plate systems, many of which were designed for endothelial cell work, and cell attachment studies, as well as many in house designs (Anderson and Tate 2007). The oscillating orbital shaker and the rocking platform systems are less-well defined

in terms of the shear stresses they produce but both of these systems are simple to use and can accommodate many samples simultaneously.

More recently, bioreactors for 3D culture have been designed to allow for the cells on scaffolding materials to be subjected to flow-induced shear forces (El Haj and Cartmell 2010). Some common designs include rotating wall vessels, spinner flasks, and perfusion systems. Perfusion flow bioreactors induce mechanical forces on cells seeded on scaffolds by passing the culture medium through the porous scaffold which passes over the cells exposing them to fluid shear stresses. As well as applying a fluid shear force, nutrient transfer to cells is improved as the media is constantly being forced through the scaffold and therefore cells in the centre are able to receive a greater supply of nutrients.

Differences between cells cultured in 2D and 3D have been observed in response to fluid flow (Pederson and Swartz 2005). This is most likely due to the fact that cells in 2D are subjected to shear forces at their surface whereas in 3D, cells are subjected to interstitial forces that flow all around them (Morris *et al.* 2010). However, in many 3D scaffolds cells are attached in a single layer to scaffold pores and so may experience fluid shear on their apical surface in a similar way to cells attached in a 2D parallel plate flow chamber. This means that we can potentially still learn a lot from use of 2D fluid flow systems and translate it into 3D systems.

1.13 Mechanotransduction

1.13.1 Introduction

Cells are able to sense and respond to mechanical forces and convert them into biochemical signals using mechanosensitive receptors in a process called mechanotransduction (Liedert *et al.* 2008; Nomura and Takano-Yamamoto 2000). This phenomenon is believed to occur due to some common mechanisms regardless of cell type and while known mediators of mechanotransduction have been identified the exact roles that they play are still being investigated. These mechanisms may alter with the stage of maturity of a cell and so as a stem cell differentiates down a specific lineage, the cell surface and the intracellular signalling mechanisms will

most likely change. Suggested mechanotransduction mechanisms include junctions between the cell and ECM (integrins and focal adhesions), cell to cell adhesions (cadherins and gap junctions), the cell cytoskeleton (microfilaments, microtubulules, and intermediate filaments) and membranes (ion channels and caveolae). Other suggested mechanisms include the pericellular glycocalyx and the primary cilia.

One key theory is that a response results from cytoskeletal deformations caused by integrin pulling (Iqbal and Zaidi 2005). Integrins are transmembrane proteins that couple the cellular cytoskeleton to the ECM; they cluster at focal adhesion points on the cell surface forming an integrin–ligand bond with the ECM. This integrin-ligand bond resists external forces, which enables the force to be transferred across the plasma membrane and into the cell causing deformation of the cytoskeleton. When forces are applied to these adhesion sites, various signal pathways are activated including focal adhesion kinase (FAK) and extra-cellular signal-regulated protein kinase (ERK). A second mechanism involves regulation of membrane proteins which may be stretch-activated ion channels, or G-protein coupled receptors, where the plasma membrane is deformed by an external force causing an influx/efflux of ions into/out of the cell (Liedert *et al.* 2008). Another potential sensor is the glycocalyx, a pericellular GAG-proteoglycan layer, which surrounds the cell membrane. When fluid moves past the cell, such as during blood flow past endothelial cells or interstitial fluid flow in the osteocyte's lacunar-canalicular system, the glycocalyx creates a drag force resulting in deformation of the cellular membrane and transduction of the applied force (Morris *et al.* 2010; Reilly *et al.* 2003; Weinbaum *et al.* 2007). More recently, the primary cilium has been implicated as a mechanosensor in a wide variety of cell types including bone. Primary cilia are immotile microtubule-based organelles, one per cell, that protrude from the cell surface and have been seen to exist in most mammalian tissue types (Pitaval *et al.* 2010). They are populated with receptors that participate in numerous signalling events and are believed to act as sensors to fluid flow. While it has been known for some time that primary cilia play an important role in many biological pathways (Badano *et al.* 2006) it is just being realised that this hair-like structure may be a key regulator of biological responses in bone cells to mechanical forces and this will be discussed in detail in the next section.

1.13.2 Primary cilia

Cell biologists have known about the existence of the primary cilium for over 100 years (Zimmerman 1971), however it was only in the last ten years that it was hypothesised to act as a mechanosensor in bone (Whitfield 2003, 2007). The primary cilium is a non-motile microtubule-based hair-like organelle that protrudes from the apical surface of most mammalian cells. The primary cilium extends from the mother centriole continuous with the cell membrane and unlike the motile cilia, which are present in multiple numbers, it has only nine microtubule pairs around the periphery and is absent of a central microtubule doublet (Hoey *et al.* 2012a). Cells have a maximum of one primary cilium, which forms several hours after mitosis when cultured *in vitro* and this can take several days to grow to full size (Wheatley *et al.* 1996). Not all cells generate a primary cilium and spatial confinement is a major regulator of ciliogenesis (Pitaval *et al.* 2010). A typical cilium ranges from 1-10 μm in length but this varies with cell type and culture conditions (Gardner *et al.* 2010; Hoey *et al.* 2012a) .

Primary cilia have been shown to be present in most mammalian cells and it is believed that they play a vital role in the normal function of human cells and tissues (Berbari *et al.* 2009). If normal primary cilia function is lost due to aberrations in genes controlling their structural development, absence of key functional components, or damage, then it this can have major clinical implications. For example, primary cilia have been implicated in many human diseases and developmental abnormalities, including hepatic and pancreatic defects, polycystic kidney disease, blindness and obesity, as well as pattern abnormalities in the skeleton (Praetorius and Spring 2005; Wheatley *et al.* 1996). In renal tubular epithelia cells, the primary cilium has been shown to serve as a chemosensor (Praetorius and Spring 2005) and has also been implicated as a mechanosensor to fluid flow (Praetorius and Spring 2003). When human kidney cells were subjected to FSS, there was an increase in intracellular Ca^{2+} caused by bending of primary cilia, however, once primary cilia were removed this Ca^{2+} influx disappeared (Praetorius and Spring 2003).

Since the bending of a kidney cell's primary cilium enables the cell to sense fluid flow, the bending of an osteocyte's primary cilium by moving extracellular

fluid is likely to do the same thing (Whitfield 2003). Malone *et al.* (2007a) have shown that the primary cilium of osteoblastic cells can deflect during fluid flow (Fig.1.10) and proposed that primary cilia might be sensory organelles that translate extracellular chemical and mechanical cues into cellular responses in bone. Hoey *et al.* (2011) showed that signalling molecules released into culture media by ostoblasts in response to fluid flow where primary-cilia dependent. This suggests that primary cilia play a role in osteogenic responses to flow in both osteoblasts and osteocytes.
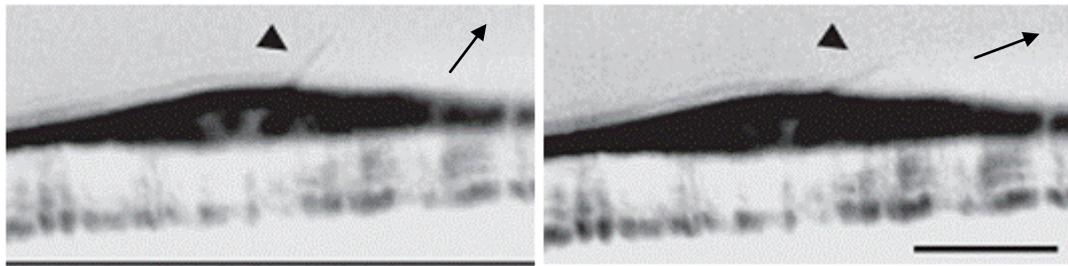
Figure 1.10: Primary cilium (indicated by triangle) in a MC3T3 cell stands relatively upright when cultured under static conditions (a). When fluid is passed across the cell surface, shear stresses (0.036 Pa) act on the primary cilia causing it to tilt in the direction of flow (left to right in this case). Scale bar is 5μm. Adapted and reprinted with kind permission from Prof. C. Jacobs (Malone *et al.* 2007).

There are a number of theories on how primary cilia may transduce a mechanical signal into a biological response. It has been proposed that the primary cilium acts as a cantilever system, which bends or deflects upon application of fluid shear stress or cell-matrix deformation, resulting in a mechanosensory signal transducing to the cell. This includes activation of stretch-activated ion channels localised at the base of the primary cilium at the point where bending occurs (Nauli *et al.* 2003). Another theory it that transmembrane proteins are present on the primary cilium, making them more exposed to fluid shearing than they would be otherwise (Janmey and McCulloch 2007). The proposal of the primary cilium as a lever- arm has raised the assumption that the longer the cilium the more sensitive it will be to small shear forces and vice versa. Previous studies have shown that differing levels of mechanical force can cause the primary cilia to remodel and alter its length in cartilage (McGlashan *et al.* 2010) and in tendon (Gardner *et al.* 2011).

Only a few studies have investigated mechanotransduction mechanisms in MSCs but investigations that have taken place observe many mechanisms common to that of

mature mesenchymal cells (Liedert *et al.* 2008) such as the cytoskeletal changes. Mechanically mediated upregulation of ERK1/2 is common to osteogenic MSCs (Glossop and Cartmell 2009; Kim *et al.* 2007; Simmons *et al.* 2003) and mature (You *et al.* 2001) bone cells. Recently, it was shown that the primary cilia of hMSCs are required for the modulation of osteogenic and adipogenic differentiation pathways in static conditions (Tummala *et al.* 2010). Further to this, the primary cilium was shown to mediate oscillatory fluid flow-increases in osteogenic genes in hMSCs (Hoey *et al.* 2012b). This exciting finding indicates that targeting the primary cilium using oscillatory fluid flow may be beneficial for bone tissue engineering strategies.

1.14 Aims and objectives of research project

The main aim of the work in this thesis was to understand how mechanical and physical cues affect cellular differentiation, specifically osteogenesis, and collagen matrix deposition. This contributes to the long term goals of trying to understand how engineered tissues can be manipulated so that we can improve their structural and mechanical properties, as well as efficiently guiding the differentiation of progenitor cells. From a clinical point of view, reducing the time it takes to create a fully-developed tissue-engineered construct (reducing healing time) with correct tissue structure and function is of great importance.

In order to achieve this aim, the project was broken down into a list of objectives:

1. **Fabricate electrospun scaffolds with controllable fibre orientation**
    * Fabricate fibrous scaffolds possessing a randomly orientated or highly aligned architecture.
    * Characterisation of electrospun scaffolds: physical and mechanical properties.
    * Fabricate elastic fibres suitable for use as a substrate for the dynamic conditioning of cells.

2. **Identify a suitable method for imaging collagen organisation**
    * Investigate the potential of second harmonic generation for imaging collagen structure and organisation.
    * Optimise SHG conditions for imaging tissue-engineered collagen on fibrous scaffolds.

3. **Investigate the osteogenic potential of two human cell types**
    * Human dermal fibroblasts (HDFs) as a potential source of osteoprogenitors.
    * Human embryonic derived mesenchymal progenitor (hESMP) as a suitable MSC model cell line.

4. **Study how fibre orientation affects cell behaviour and matrix deposition**
   - Observe influence of random and aligned fibres on dermal fibroblasts.
     - i. Morphology, viability, and migration.
     - ii. Collagen production and organisation, mechanical properties.
   - Observe influence of random and aligned fibres on hESMP cells.
     - i. Morphology, viability, migration.
     - ii. ALP activity, mineral deposition.
     - iii. Collagen production and organisation, mechanical properties.

5. **Study the effects of tensile forces on collagen matrix production**
   - Dynamic tension of collagen-producing cells on 3D scaffolds, in an already established loading model.
     - i. PU open-porous foam scaffolds
     - ii. PU electrospun fibres

6. **Fluid-flow stimulation of osteogenic cells**
   - Investigate the potential of a simple platform rocker to create fluid flow-induced shear stress suitable for stimulating osteogenic cells.
   - Study the effect of oscillatory FSS on osteogenic progenitor cells.

7. **Study the role of primary cilia in bone mechanobiology**
   - Identify the primary cilium in mature bone cells.
   - Identify the optimum conditions for removing the primary cilia.
   - Study the effect that primary cilia removal has on the loading response of bone cells to FSS.

The main hypothesis of this project was that cell differentiation and matrix deposition would be influenced by both the orientation of fibres in electrospun scaffolds and the application of mechanical forces.

CHAPTER TWO: Materials and Methods

2.1 Materials

1. MLO-A5 mature osteoblast/early osteocyte murine cells (kindly donated by Professor Lynda Bonewald, University of Missouri, Kansas City, USA, under MTA agreement with the University of Texas Health Science Center at San Antonio).

2. MC3T3-E1 early stage osteoblast murine cells (kindly donated by Dr A. Scutt, University of Sheffield)

3. Primary human dermal fibroblasts isolated from skin obtained from consenting patients undergoing abdominoplasty or breast reduction operations (According to local ethically approved guidlines, NHS Trust, Sheffield , UK) and stored in Kroto Research Institute's tissue bank, University of Sheffield (licensing number 12179).

4. MG63 human osteocarcoma cell line (kindly donated by Dr A. Scutt, University of Sheffield)

5. Human embryonic stem cell-derived mesenchymal progenitor hES-MP 002.5 (hESMP) cells (Cellartis, Gothenburg, Sweden).

6. Polyether polyurethane industrial grade foam (Caligen Foam Ltd, Lancashire, UK (kindly donated by Professor Anthony J. Ryan, Department of Chemistry, University of Sheffield, UK)) for use as an interconnected open pore scaffold.

7. Poly(ε-caprolcatone) (80kDa Mn) (Sigma, Dorset, UK) for fabrication of electrospun mats.

8. Tecoflex® SG-80A polyurethane (Lubrizol Advanced Materials, MA, USA) for fabrication of electrospun mats.

9. Poly(D,L-lactide-co-glycolide) (lactide:glycolide (75:25)) Mw 66-107k (Sigma, UK) for fabrication of electrospun mats.

10. Dichloromethane, Tetrahydrofuran and Dimethylformamide (Sigma, UK) for electospinning solvents.

11. Human dermal fibroblast and MG63 basal culture media: Dulbecco's Modified Eagle's Medium (DMEM) (Biosera, East Sussex, UK) supplemented with 10% Fetal calf serum (FCS), 2mM L-glutamine (L-g) and

100mg/ml penicillin and streptomycin (P/S) (both 1%) (All obtained from Sigma, UK).

12. MLO-A5 and MC3T3-E1 basal culture media: Minimum Essential Medium Alpha Eagle (α-MEM) (Lonza, Castleford, UK) supplemented with 10% FCS, 1% L-g and P/S.

13. hESMP basal culture media: α-MEM supplemented with 10% FCS, 1% L-g and P/S, and 4nM fibroblast growth factor-basic recombinant human (bFGF) (Sigma, UK).

14. Fibroblastic media (FM): basal DMEM supplemented with 50 µg/ml ascorbic acid-2-phosphate (AA) (Sigma, UK).

15. Non-dex containing osteogenic media (NM): basal α-MEM supplemented with 50 µg/ml (AA) and 5 mM β-glycerophosphate (β GP) (Sigma, UK).

16. Osteogenesis media (OM): any basal media supplemented with 50 µg/ml AA, 5 mM βGP and 100nM Dexamethasone (Dex) (Sigma, UK).

17. Loading media (LM): DMEM supplemented with 2% FCS and 1% P/S.

18. Porcine gelatine (Sigma, UK).

19. MTT (3-(4,5-Dimethylthiazol-2-yl)-2,5-diphenyltetrazolium bromide) cell viability assay (Sigma-Aldrich, Dorset, UK).

20. MTS (CellTiter 96$^{®}$ AQ$_{ueous}$ Non-Radioactive Cell Proliferation Assay) (Promega, Southampton, UK).

21. DAPI [4'-6-Diamidino-2-phenylindole] (Sigma Aldrich, Dorset, UK) 1 mg/ml.

22. Phalloidin-TRITC (Phalloidin-Tetramethylrhodamine B isothiocyanate) (Sigma, UK) at 0.5 mg/ml.

23. Picro-Sirius red stain: direct red dye and saturated Picric acid (Sigma, UK) at 1 mg/ml for staining collagen.

24. Alizarin red stain (Sigma, UK) at 1 mg/ml diH$_2$O for staining deposited calcium.

25. Quant-iT™ PicoGreen$^{®}$ dsDNA reagent assay kit (Invitrogen, UK) for total cellular DNA quantification.

26. ALP Yellow (pNPP) Liquid Substrate system for ELISA (Sigma, UK) for measuring alkaline phosphatase (ALP) activity in cells.

27. PGE$_2$ Assay kit (Parameter, R&D Systems, Abingdon, UK) for quantitative determination of Prostaglandin E$_2$ in cell culture supernates.

28. Glutaraldehyde (25 %, Grade 1 for SEM) (Sigma, UK).

29. Hexamethyldisilazane (HMDS) (Sigma, UK) for SEM.

30. Monoclonal anti-Collagen I antibody produced in mouse (Sigma, UK) for use as primary antibody in tissue-engineered collagen staining.

31. Monoclonal anti-acetylated α-tubulin antibody produced in mouse (clone 6-11B-1) (Sigma, UK) for primary cilia and microtubule staining.

32. Biotinylated anti-mouse IgG (H+L) secondary antibody (made in goat), and fluorescein streptavidin and Texas Red streptavidin tertiary antibodies (Vector, Peterborough, UK), used for all antibody protocols.

33. Goat serum (Sigma, UK) for use as blocking agent in primary cilia staining.

34. Chloral hydrate (Sigma, UK) for primary cilia removal.

35. Electrospinning apparatus: 1. Department of Chemistry, University of Sheffield (with kind permission from Prof. Anthony J. Ryan, and Dr Patrick A. Fairclough); 2. University of Pisa, Prof. Emo Chiellini group; 3. University of Strathclyde, Dr Richard Black group.

36. BOSE ElectroForce 3200 (ELF3200) for mechanical testing and mechanical conditioning of samples equipped with a 22N load cell (ElectroForce Systems Group, BOSE, Minnesota, USA).

37. Biodynamic chamber for use with BOSE ELF3200 (Electroforce Systems Group, BOSE, Minnesota, USA) for sterile culture while mechanically stimulating cells.

38. Platform rocker (STR6) (Stuart equipment, Staffordshire, UK) for application of fluid-induced shear stress.

39. FLx800 microplate fluorescence reader (BioTek, UK).

40. Image Express™ epifluorescent fluorescent microscope (Axon Instrument, UK).

41. Zeiss Axioskop 2 FS MOT laser-scanning confocal microscope (upright and inverted) equipped with LSM 510 Meta detector (Carl Zeiss MicroImaging GmbH, Germany).

42. Chameleon Ti:sapphire tuneable (700 − 1060 nm) multiphoton laser (Coherent, CA, USA).

43. Scanning electron microscopy (SEM) (Department of Biomedical Science, University of Sheffield).

44. Marine grade steel rings (2cm diameter, 1 cm inner hole diameter) for cell seeding.

45. Medical grade stainless steel dental wire (diameter 0.8-1mm) for holding down scaffolds.

46. Image analysis software: Image Processing and Analysis in Java (ImageJ) (developed by National Institutes of Health).

47. Image analysis software: LSM Image Browser (downloaded from Carl Zeiss microscopy).

48. Data analysis software: GraphPad Prism 5, GraphPad InStat 3, Microsoft Excel and Origin Pro 8.0.

2.2 Methods

2.2.1 Cell preparation

2.2.1.1 General cell culture conditions

All cells were cultured in T-75 flasks using the appropriate basal medium for expansion and kept in a humidified incubator at 37 ^{o}C with 5 % CO_2. Media changes were performed every 2-3 days along with observations of cell morphology and cell density and when cells reached confluence they were passaged. Briefly, cell media was removed and cells were washed with PBS twice before adding 2ml of trypsin-EDTA and incubating for 5 min to detach cells. The trypsin-EDTA reaction was then halted with media and detached cells in suspension were centrifuged at 1000rpm for 5 min to for a cell pellet. The supernatant was poured off and cells were resuspended in a known volume of media and a cell count was performed using a haemocytometer and cells were then split 1:10 to new flasks. Cells to be used in future experiments were suspended in a 10 % DMSO in FCS solution and placed in a isopropanol jacket and stored at -80°C for one day before moving to -196°C the following day for long term storage. Harvested cells were placed into fresh, warm media and seeded into culture flasks before changing the media the following day.

2.2.1.1 Human dermal fibroblasts

Primary human dermal fibroblasts (HDFs) were harvested from skin biopsies by firstly stripping away the outer epidermal layer and then dissecting the dermis and

placing in collagenase overnight to remove the dense collagen matrix. The remaining material and cell populations were then washed free of collagenase with PBS and placed into culture flasks. Extracted cells were provided at passage 1. HDFs were split 1:10 at each passage and only cells between passage 2 and 8 were used in experiments to allow for the outgrowth of any other non-fibroblastic cells present and to avoid the use of 'old' fibroblasts.

2.2.1.2 Osteoblastic cell lines

Three different osteblastic cell lines were used in the presented work; MG63 human osteocarcoma cells, MC3T3 murine early stage osteoblasts, and MLO-A5 murine late stage osteoblast/early stage osteocytes. MG63 cells were used from passages 50-60 and split at 1:10. MC3T3-E1 cells were used between passages 20-30 and also split at 1:10. MLO-A5 cells were used between passages 25-30 and were split at 1:20.

2.2.1.3 Human embryonic stem cell derived mesenchymal progenitors (hESMP)

These cells were split 1:10 and cultured on 0.1 % gelatine coated surfaces and expanded in 4nM fibroblast growth factor-basic recombinant human (bFGF) as stated by the manufacturer (Cellartis). Cells were used for experiments between passages 3-10 in most cases. Cells could be expanded up to passage 20 but were observed to begin to lose their fibroblastic morphology after passage 12 and ALP activity and mineral depositing ability also reduced.

2.2.2 Cell culture in two dimensions

For all 2D experiments, the required number of cells was added to the required volume of media and seeded into the well plate and evenly distributed using a gentle back and forth, side to side rocking motion, but no swirling. Cell number was determined on the basis of the length of the culture period; often if cells became too dense then they would peel off. Gelatine (0.1 %) coated wells were used for all cell types for all rocking experiments.

2.2.3 Cell culture in three dimensions

2.2.3.1 Scaffold preparation

All scaffolds were prepared the day before the start of the experiment. Electrospun scaffolds were cut using either a circular cork borer or a scalpel blade. For PU foam scaffolds, a template was firstly drawn with a permanent marker pen and then cut using scissors. Once scaffolds were cut to the appropriate size for experiments, they were sterilised in a culture plate containing 0.1 % peracetic acid and rocked steadily for three hours. Peracetic acid is a potent anti-microbiological agent and therefore a very effective sterilising agent. Sterilisation studies were carried out to compare the effectiveness of 0.1 % peracetic acid and 70% ethanol whereby scaffold pieces were sterilised in either solution and then placed in sterile media with or without antibiotics and left in a dry incubator at 37°C. Ethanol treated scaffolds cultured without antibiotics became infected after 5 days whereas 0.1% peracetic acid scaffolds remained sterile for 6 months.

After sterilisation, scaffolds were washed three times with PBS for 5 minutes each to remove any remaining peracetic acid. For electrospun PCL, scaffolds were then thoroughly wet-through with PBS using a pipette in order to increase the hydrophilicity of the scaffold (Fig. 2.1a). Scaffolds being prepared for HDF, MG63 or MC3T3 seeding were then submerged in culture media containing serum and scaffolds being prepared for seeding with hESMPs or MLO-A5s were soaked in 0.1 % gelatine solution. All scaffolds were then left to rock gently over night under sterile conditions at room temperature. Excess media or gelatine solution was removed before cell seeding.

2.2.3.2 Cell seeding

Two different cell-seeding methods were utilised for 3D scaffolds; ring confinement and low volume seeding (Fig. 2.1b). Ring confinement seeding was used for all experiments involving electrospun PCL; a steel ring (10 mm internal diameter) was placed on top of the scaffold centre and filled with 500 µl of media. The medium was then allowed to seep through the scaffold until the medium level reached equilibrium with the region outside the ring. Then the cell suspension (volume no greater than 50 µl) was dropped inside the ring. The volume of cell suspension was

chosen so not to disturb the equilibrium between media outside and inside the ring. If a large volume of media is placed inside the ring then media will flow outside the ring and draw the cells towards the edge of the inner circle. The ring was removed 24 h after seeding and the scaffold was covered with fresh media.
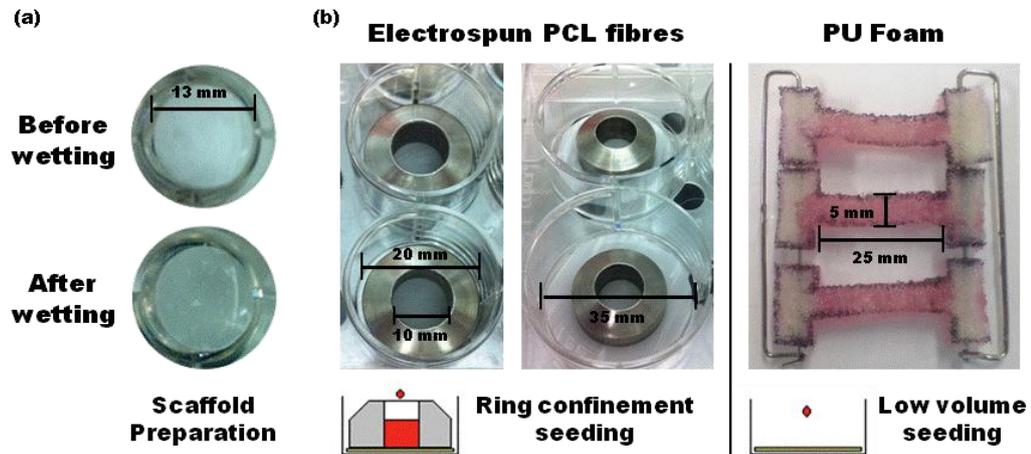
Figure 2.1: Electrospun PCL scaffolds were cut using a hole-punch, sterilized, and then wet-through with PBS using a pipette gun (appearance before and after wetting (a)). Ring confinement cell-seeding was used for electrospun PCL scaffolds whereby a ring was placed on top of the scaffold centre containing a 500 μl medium after which the cell suspension was added (b). For PU foam and electrospun Tecoflex, low volume seeding was used whereby 60 μl of cell suspension was dispersed evenly across the scaffold centre and left for 90 min to allow cell attachment, after which fresh medium was added. Red circles show cell pellet. 12-well and 6-well plates are shown with PCL fibres. PU foam scaffolds are mounted on dental wire brackets and black lines show pen markings.

Low volume seeding was used for PU foams and electrospun tecoflex scaffolds involved in dynamic loading studies; 60 μl of cell suspension (containing the required number of cells) was dispensed onto the central portion of the scaffold and cells were allowed to attach for 90 minutes before scaffolds were submerged in fresh media. It was found that 60 μl was the optimum volume of media that could be held in the scaffolds using the chosen dimensions and so the cells were retained within the scaffold and had the chance to attach.

For both seeding methods, scaffolds were transferred to new well-plates 24 h after seeding and fresh media was added along with any required supplements.

2.2.4 Fluorescent staining of cell nucleus and cytoskeleton

Cell nucleus staining was performed using DAPI (4′,6-Diamidino-2-phenylindole dihydrochloride), which forms fluorescent complexes with natural double-stranded DNA, and will stain live and dead cells. DAPI can be imaged under the blue wavelength.

Cell cytoskeletal staining was performed using phalloidin-TRITC (phalloidin-Tetramethylrhodamine B isothiocyanate). Phalloidin is a fungal toxin that binds to polymeric and oligomeric forms of actin. TRITC conjugate allows for imaging under the orange-red wavelengths.

Samples were washed free of media with PBS (x3) and then fixed in 10% formalin solution for 15 minutes at room temperature, followed by washes with PBS 3 times allowing the cells to keep their structures and preventing degradation. To increase cell membrane permeability, a 0.5% Triton-X solution was applied to samples for 5 minutes and then washed away. A solution of 1 µg/ml of DAPI and 1 µg/ml phalloidin-TRITC in PBS was added to each well to cover the samples. Samples were then covered with aluminium foil and left at room temperature for 20 min. The solution was removed and replaced by PBS and cells were imaged on an epifluorescent or confocal microscope.

2.2.5 Assessing cell viability and cell number

2.2.5.1 MTT assay

MTT (A3-(4,5-dimethylthiazol-2-yl)-2,5-diphenyltetrazolium bromide) assay is a frequently used methods for measuring cell growth and viability. The yellow MTT solution is reduced by active mitochondria in live cells to form an insoluble dark blue or purple formazan salt (Fig. 2.2). This salt is easily visualised to confirm the presence of live cells and it can be subsequently quantified by measuring the absorption of dissolved salt supernatant using a plate reader at 540 nm. The absorbance is directly related to the amount of formazan salt formed and is assumed to represent the number of live cells.
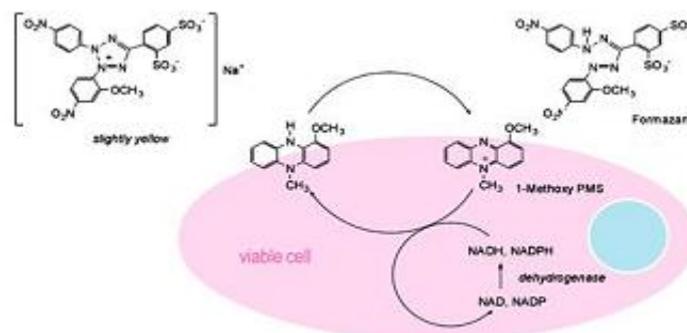
Figure 2.2: A schematic representation showing the reduction of MTT to formazan. This reduction takes place only when mitochondrial dehydroxygenase enzyme in live cells is active. The MTT terazolium compound is reduced by cells into a colored insoluble formazan (blue or purple) and therefore conversion is often used as a measure of viable (living) cells.

MTT assay was performed firstly by removing media from cells and washing with PBS before incubating with MTT solution (1mg/ml in PBS) for 40 minutes at 37°C. The solution was then removed and the insoluble formazan salt was dissolved in 0.125% acidified isopropanol. Finally, the absorbance of the resulting solution was determined using a 96-well plate reader at 570nm referenced at 630nm.

2.2.5.2 MTS assay
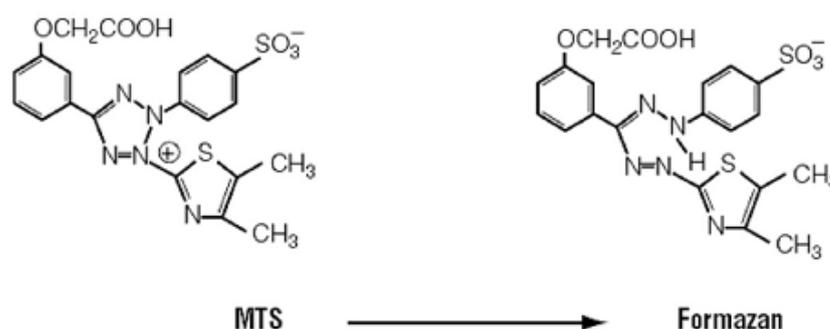
Figure 2.3: The MTS terazolium compound is bioreduced by cells into a coloured formazan product that is soluble in tissue culture medium.

MTS (3-(4,5-dimethylthiazol-2-yl)-5-(3-carboxymethoxyphenyl)-2-(4-sulfophenyl)-2H-tetrazolium) assay is another colorimetric method to determine the number of viable cells in culture. Similarly to the MTT assay, the yellow MTS tetrazolium compound is reduced by live cells into a pink formazan product that is soluble in culture medium (Fig. 2.3). This conversion is also presumably

74

accomplished by NADPH or NADH produced by dehydrogenase enzymes in metabolically active cells.

MTS assay was performed firstly by removing media from cells and washing with PBS before incubating with diluted (1:10 in PBS) yellow MTS solution for 2-3 hours at 37°C. The resulting solution was yellow (no viable cells) or orange-red (viable cells) and the absorbance was determined using a 96-well plate reader at 490 nm.

2.2.5.3 Total DNA

Total DNA was measured using a fluorescent Quant-iT™ PicoGreen® dsDNA reagent assay kit (Invitrogen, UK), which is used as a measure of total cell number through the binding of a fluorescent dye to double stranded DNA in the cells. Cells cultured in 2D were washed with PBS 3 times and a known volume of carbonate buffer solution (0.2M NaHCO3, 0.2M Na_2CO_3, 0.1% Triton X-100) was applied for 2 min. Cells were then scraped and all buffer solution and cell debris was pipetted into a bijou. Cells cultured on scaffolds were washed well with PBS 3 times (5 min each) and a known volume of buffer solution was pipetted into a bijou and the scaffold with cells was placed directly into this. Scaffold samples were then vortexed for 10 s followed by 5 min centrifugation at 10, 000 rpm to disrupt the cells on the scaffold. All samples were left at 4°C overnight. In order to extract cellular DNA, samples were freeze-thawed 3 times before 100 µl of cell lysate was added to 200 µl of Tris-buffered EDTA solution (provided in kit, diluted 1:20) containing the Quant-iT™ PicoGreen® (diluted 1:400). Fluorescence intensity was recorded using a FLx800 microplate fluorescence reader (BioTek, UK) using 485 nm excitation and 520 nm emission. Total DNA was converted to ng DNA/sample using the following formula taken from a standard curve:

$$DNA\ (ng) = Vol_{sample} * ((0.1366 * TDNA_{485Ex/520Em}) + 2.0087)$$

2.2.6 Analysis of cell-deposited collagen

2.2.6.1 Picro-sirius red staining for collagen production

Picro-sirius red staining is a routine method for the qualitative identification of collagen in tissue sections or that deposited by cells. If collagen is present it will form a strong red staining complex that can then be destained for semi-quantitative analysis. Sirius red is a strong anionic dye whereby the sulphonic groups of the dye attach to the amino acid groups belonging to lysine and hydroxyproline as well as the guanidine groups of arginine on the collagen molecule. The bound dye then aligns itself parallel to the long axis of the collagen molecules. The dye is not specific and so stains all types of collagen but it can be used as a fluorescent marker of collagen and suffers very little from photo-bleaching.

Before application of the stain, media was removed from samples and then three PBS washes were carried out to ensure full media removal. Samples were then fixed for 20 min in 3.7% formaldehyde, which was then removed and three PBS washes were performed again. Direct red dye was added to saturated picric acid (1mg/ml) and then applied to fully cover each sample. Samples were then left to shake mildly for 2 h (2D) or 18 h (3D) at room temperature. Excess dye was then washed clear with dH_2O until no more red colouring was eluted after which the sample was left to air dry in a clean environment. The bound dye was observed either under a light microscope or using a digital camera at normal magnification. For quantitative analysis, samples were destained with a known volume of 0.2 M NaOH:Methanol (1:1), under mild shaking for 15 min (2D) or 30 min (3D) resulting in a clear-red solution. Absorption was then measured at 490nm using a 96-well plate reader.

2.2.6.2 Collagen type I antibody staining

Collagen type I antibody staining was performed on cells as a comparison to SHG imaging using the following optimised protocol:

1. Culture media was removed and cells washed with PBS 3 times.
2. Cells were fixed in 2.5 % glutaraldehyde for 15 min followed by 3 PBS washes.

3. Blocking solution (5 % bovine serum albumin (BSA)) was added for 1 h at room temperature.

4. Primary antibody (monoclonal anti-collagen I) was applied at 1:500 and left overnight at 4°C.

5. Secondary antibody (botinylated anti-mouse) was added at 1:1000 for 1 h at room temperature.

6. Tertiary antibody (conjugated Streptavidin-Texas Red) was added at 1:100 for 30 min at room temperature.

7. Counterstaining was performed with DAPI (1:1000) for 15 min at room temperature.

N.B. All antibody solutions contained 1 % BSA. 3 x 5min PBS washes were performed after each staining step. It was found that 3.7 % formaldehyde inhibited the binding of the antibody to collagen and so was not suitable for fixing.

Samples stained with Col I antibody were imaged on the confocal microscope.

2.2.6.3 Second harmonic generation imaging

Collagenous tissue or deposited collagen fibers from cultured cells were visualised from second harmonic generation (SHG) images obtained using a Zeiss Axioskop 2 FS MOT upright laser-scanning confocal microscope equipped with a tuneable (700-1060 nm) Chameleon Ti:sapphire multiphoton laser. SHG emission was collected in the backwards scattering direction filtered through a primary dichroic (HFT KP650) before entering a descanned LSM 510 Meta detector capable of collecting emissions in narrow 10 nm bandpass filters. SHG emissions should be present in the collection window at half the wavelength of the excitation source. For wavelength dependence studies of tissue samples and electrospun scaffolds, excitation was performed using a range of wavelengths (760-1000 nm) and collected as either a lambda stack or collected in the 10 nm bandpass filter at half the wavelength of the excitation laser. Lambda stacks were composed of a series of narrow 10 nm bandpass filters from 360-700 nm and collected using the LSM 510 Meta detector. In order to match the laser power at each excitation wavelength, a power meter was used to match laser intensity to laser power. For all imaging of tissues and tissue-engineered collagen produced by cells in 2D culture and on electrospun scaffolds, a 40x 1.3 NA (numerical aperture) oil immersion objective. Imaging of cell-deposited collagen for

all experiments was performed using an excitation wavelength of 940 nm and emissions were collected in the 10 nm bandpass filter centred around 474 nm. The pinhole was set to maximum at all times and for each set of experiments, conditions were optimised and kept constant in terms of excitation power, detector gain, and scan speeds. Conditions were kept constant for each experimental time point.

Fresh rat tail tendon and DED were stored in complete DMEM at 4 ^{o}C and 37 ^{o}C respectively and imaged while still wet.

2.2.7 Assessment of osteogenesis

2.2.7.1 Alkaline phosphatase activity

Alkaline phosphatase (ALP) activity in osteo-induced cells was assessed using a colorimetric assay involving the conversion of p-nitrophenol phosphate substrate to p-nitrophenyl and recording the rate of colour change from colourless to yellow. Cell lysate for ALP assessment was taken from the same cell solution used to extract TDNA using the same extraction techniques (See 2.2.5.3). Cell lysate was incubated for 30 min before adding 20 µl to 180 µl of p-nitrophenol phosphate substrate (Sigma, UK) followed by incubation for 5 min. The subsequent conversion to p-nitrophenyl was measured by recording the rate of colour change from colourless to yellow at 405 nm. ALP activity was calculated as nmol of p-nitrophenol converted per minute where 22.5 nmol (K) equals 1 absorbance value (A_{405}). ALP activity was calculated using the following formula:

$$\text{ALP activity (nmol pNPP converted per min)} = \Delta A_{405} * K * V_{total}/V_{sample}$$

Where V_{total} is the volume of cell lysate added to the sample and V_{sample} is the amount of sample added to the ALP solution. ALP activity was then normalised to total DNA.

2.2.7.2 Prostaglandin E$_2$ (PGE$_2$) assay

PGE$_2$ plays an important role in the functional adaptation of bone cells to mechanical loading. PGE$_2$ release into the media by MLO-A5 cells after mechanical stimulation was determined using a Parameter PGE$_2$ assay kit following the manufactures

protocol. Briefly, the assay is based on the forward sequential competitive binding technique in which PGE_2 present in the sample competes for horseradish peroxidise (HRP)-labelled PGE_2 for a limited number of binding sites on a mouse monoclonal antibody. PGE_2 in the sample is allowed to bind to the antibody in the first incubation. During the second incubation, HRP-labelled PGE_2 binds to the remaining antibody sites. Following a wash to remove unbound materials, a substrate solution is added to the wells to determine bound enzyme activity. The colour development is stopped, and the absorbance is read at 405nm (A_{405}). Colour intensity is inversely proportional to the concentration of PGE_2 in the sample. PGE_2 concentration was calculated from the formula of a plotted standard curve:

$$PGE_2 \text{ concentration} = EXP\ ((A_{405} - 0.2146)/\text{-}0.025)$$

This assay was used in chapter 8. Cells subjected to mechanical stimulation were incubated in fresh medium for 2 hours before collection of the medium.

2.2.7.3 Alizarin red S staining

Alizarin red S is a dye that binds to Ca^{2+} ions to form a strong red complex and is commonly used as an indicator of calcium deposition in mineralising cells and tissues. Samples were washed and fixed as with Sirius red staining (see 2.2.6.1) followed by three washes with dH2O to remove any non-cell produced calcium ions. Alizarin red S dye was added to dH_2O (10mg/ml) and the pH adjusted to 4.1 using ammonium hydroxide before applying to fully cover each sample and placing under mild shaking for 15 min at room temperature. Excess dye was then washed clear using dH_2O and samples were then allowed to air dry in a clean environment before qualitative analysis under light microscope or normal magnification with a digital camera. For quantitative analysis, samples were destained with a known volume of 5 % perchloric acid, under mild shaking for 15 min, resulting in a clear-dark yellow solution. Absorption was measured at 405nm using a 96-well plate reader. Calcium and collagen staining were not carried out on the same samples as they were both found to grossly interfere with each other, in either order, resulting in losses of deposited calcium or collagen.

2.2.8 Mechanical conditioning of cells

2.2.8.1 Tensile loading of cells on scaffolds

Dynamic tensile loading of cell-seeded substrates was performed using a sterile (autoclaved) BioDynamic chamber mounted on a BOSE ELF 3200 (Fig. 2.4). Up to three samples were mounted on dental wire frames to allow for simultaneous multiple sample stimulation. For Tecoflex samples, brackets were placed in between the frames to keep the samples taut. All static samples were mounted in frames in the same way as loaded samples. Samples were loaded into the biodynamic chamber in the laminar flow hood and the ends of the dental wire frames were inserted into the grips (Tecoflex brackets then removed). The chamber was filled with 200 ml of loading media, sealed, and then mounted onto the ELF 3200.
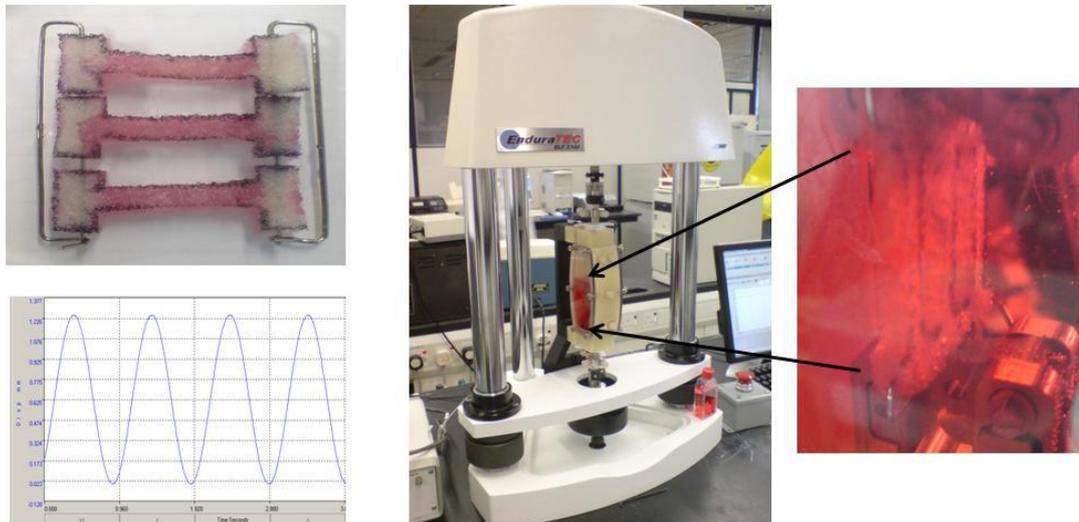
Figure 2.4: Cell seeded PU foam scaffolds mounted on dental wire brackets used in tensile conditioning experiments. BOSE ELF 3200 with biodynamic chamber for subjecting cells to tensile forces is shown with a close up view of how the scaffolds are mounted inside the chamber. A sine wave created the dynamic loading profile.

Dynamic tension was performed using a sine waveform at 1 Hz for 2 hours for all samples, while the strain and loading days were varied. During loading, paired-static samples were placed outside of the incubator in the same loading media. The loading force and displacement data was monitored using WinTest 4.1 software provided by BOSE.

2.2.8.2 Application of fluid flow-induced shear stress to cells

Cells were exposed to fluid flow-induced shear stress (FSS) using a platform rocker (Fig. 2.5). When a culture plate is placed on the platform, the see-saw rocking motion causes fluid in each well to move back and forth under the influence of gravity causing shearing across the cells. The rocking platform had a fixed maximum tilt angle of 6 degrees and a variable speed dial allowing for alterations to cycle time. For all FSS experiments, cells were cultured in 6-well culture plates (previously coated for 30 min in 0.1 % gelatine) containing 2 ml of media. Cells of each media type were either cultured under static conditions (no forces) or subjected to fluid flow-induced shear stress (FSS) (also referred to as 'rocked' group). All bouts of rocking were performed outside of the incubator and statically cultured samples were also placed outside of the incubator for the same amount of time.
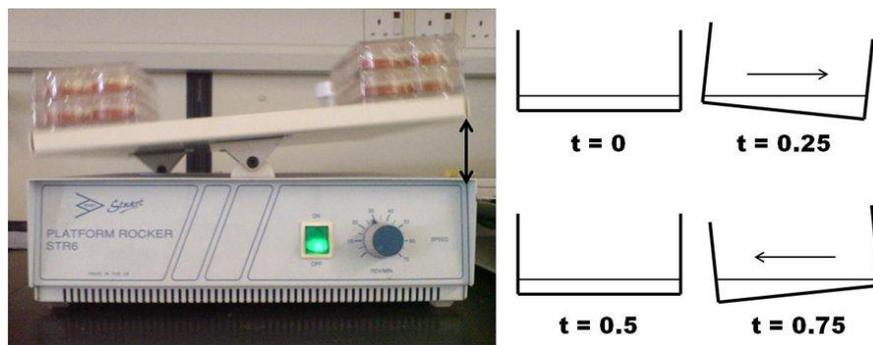
Figure 2.5: Platform rocker used to subject cells to fluid flow-induced shear stress. Schematic shows gravitational movement of media in a well during one cycle (where t = time during one cycle).

2.2.9 Fabrication and characterisation of electrospun scaffolds

2.2.9.1 Electrospun scaffold fabrication

Polymers to be used for the fabrication of fibrous scaffolds via electrospinning were firstly dissolved in a suitable solvent at a specific polymer concentration and left on a magnetic stirrer at room temperature for 24-48 hours to ensure full dissolution. Solutions were generally prepared 1-2 days before they were electrospun but in some cases, fully dissolved polymeric solutions were stored at room temperature for up to one week before use but were not electrospun after one week. Fibrous scaffolds were fabricated using the electrospinning setup shown in figure 1.8 of chapter 1. A sheet of aluminium foil was wrapped around the rotating collector and fibres were

collected on this until the desired scaffold thickness was achieved. Scaffolds were then placed under vacuum at room temperature for 24 h to remove any excess solvent and then stored in sealed plastic bags at 4 $^{\circ}$C and used for experiments within 6 months of fabrication.

2.2.9.2 Physical characterisation

The fibre distribution and mean diameter of electrospun fibres was determined using ImageJ software from SEM micrographs. The image was assigned the correct scale and then a line was drawn across fibres from edge to edge and the distance recorded. For random and aligned PCL fibres spun at 4 ml/hr, images from three different scaffolds were analysed (n > 150 fibres). For all other scaffolds, at least two images were used for fibre analysis. The distribution of fibre orientation for random and aligned PCL was plotted from analysis of SEM micrographs also using ImageJ. For aligned scaffolds, a predominant fibre direction was determined (set as 0 $^{\circ}$) and fibre agreement or deviation from this was plotted.

For water contact angle measurement, scaffolds were cut into 1 cm diameter circular discs using a cork borer and the water contact angle was measured using a Goniometer (ramé-hart). A small drop of dH$_2$O was dispensed onto the scaffold using a micro-needle and the contact angle was measured.

Scaffold porosity was determined firstly by calculating scaffold density by cutting scaffolds into 1.3 cm diameter circles, measuring the thickness with a micrometer, and weighing on a 5 decimal place balance. Scaffold porosity was then calculated using the following formula:

$$\varepsilon = (1 - \rho/\rho_0) * 100$$

Where ρ = density of scaffold and ρ_0 = density of the bulk material.

2.2.9.3 Mechanical characterisation

Mechanical testing of materials and scaffolds containing cells was performed using a BOSE ELF 3200 along with WinTest 4.1 software. Scaffolds without cells were cut into a dog-bone shaped narrow strip of roughly 25 mm in length and 5 mm in width around the central region. Scaffolds with cells were cut into rectangular strips of 25 mm length and 10 mm width. The samples were strained at a rate of 0.1 mm/s and

the maximum strain distance was 12mm for scaffolds without cells and 6 mm for scaffolds with cells. The resulting force produced by the scaffold was measured using a 22 N load cell and the force and displacement data collected was used to generate stress/strain curves. From these curves, the Young's modulus of elasticity (*E)* was generated as well as the tensile strength at 50 % strain for scaffolds with cells (see example in Fig. 2.6).
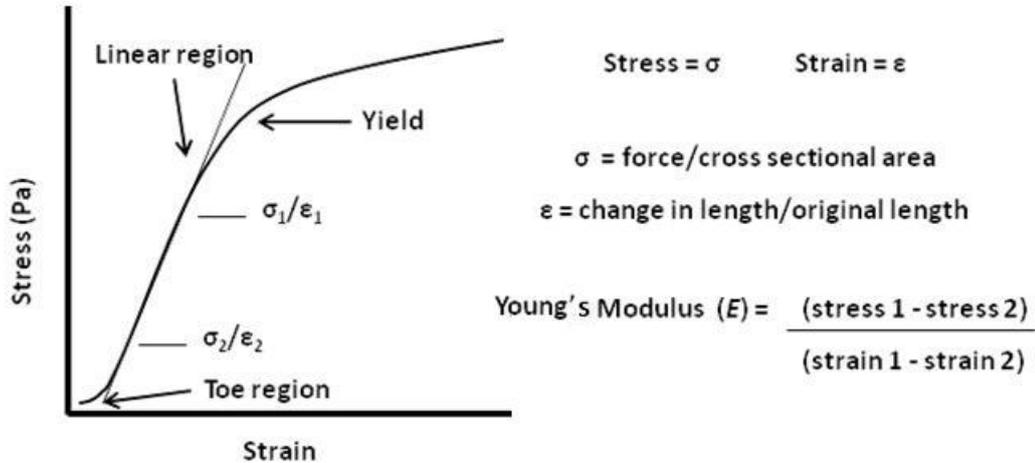
Figure 2.6: An example stress/strain curve obtained by tensile testing of a sample. The Young's modulus of elasticity can be calculated from the gradient of the sharpest slope known as the elastic (linear) region.

2.2.10 Scanning electron microscopy

2.2.10.1 Electrospun scaffolds

Scaffolds were cut into a 1 cm diameter circle using a hole punch and mounted on a carbon dot stuck to a metal stub. Samples were then sputter coated with a thin layer of gold under vacuum for 3 minutes in order to create a conductive surface for the electrons. Samples were imaged using an acceleration voltage of 10 kV and spot size of 3. SEM was performed in the Department of Biomedical Sciences at the University of Sheffield.

2.2.10.2 Electrospun scaffolds with cells

To visualise cells and matrix on scaffolds, the following procedure was used:

1. Culture media was removed and 3 PBS washes (5 minutes each) were performed.
2. Samples were fixed with 2.5 % glutaraldehyde for 1 h at room temperature.
3. This was then removed and 3 PBS washes (15 min each) were performed followed by a 5 min rinse in dH$_2$O.
4. A serious of dehydration steps were performed with 100 % ethanol (EtOH): 35 %, 60 %, 80 %, 90 %, 100 % for 15 min each.
5. Hexamethyldisilazane (HDMS) treatment:
   a. 1:1 EtOH:HDMS for 1 h
   b. 100 % HDMS for 5 min x 2
6. HDMS was removed and left to dry in a dessicator for at least 1 h.
7. Samples were stored in a clean and dry environment until imaging.

2.2.11 Primary cilia studies

2.2.11.1 Primary cilia antibody staining

Primary cilia have axonemes containing tubulin, therefore they can be detected by immunostaining with anti-tubulin antibodies. The primary cilia was visualised in MLO-A5 cells, HDFs and hESMPs using the following antibody staining protocol:

1. Media was removed from the cells followed by 3 PBS washes.
2. Cells were fixed with 3.7 % formaldehyde for 15 min followed by 3 PBS washes.
3. 0.5% Triton X-100 was applied for 10 min followed by 3 PBS washes.
4. Blocking solution (5 % goat serum) was applied for 1 h at room temperature.
5. Primary antibody (anti-acetylated α-tubulin) (1 µg/ml) was applied for 24 h at 4°C.
6. Secondary antibody (biotinylated anti-mouse) (2 µg/ml) was applied for 1 h at room temperature.

7. Tertiary antibody (conjugated Streptavidin) (10 µg/ml) was applied for 30 min at room temperature.

8. Cells were counterstained with DAPI (1 µg/ml) for 15 min.

N.B. All antibody solutions contained 1 % goat serum for blocking and 0.1 % Tween and 3 PBS washes (5 min each) were performed between each staining step.

Primary cilium counting for FSS experiments was performed using fluorescent images from three separate samples of each condition.

2.2.11.2 Chloral hydrate treatment

In order to disrupt the structure of the primary cilia, 4mM chloral hydrate (CH) solution was applied to MLO-A5 cells for 24, 48 or 72 h. After CH removal and one PBS wash, cells were either stained with anti-acetylated α-tubulin, or for rocking experiments, cells were cultured in fresh medium for 24 h before being subjected to rocking.

2.2.12 Statistical Analysis

All experiments were performed a minimum of two times with triplicate samples for each condition where possible. For imaging of samples, some experiments were limited to one sample per condition per experimental run due to time constraints. To test for significant differences between two sample means, an unpaired Student's t-test was performed preceded by an F-test to test for significant differences between standard deviations between sample populations. For comparisons between more than two means, one-way ANOVA was preformed followed by Tukey's post-hoc test. All graphs are plotted as mean ± SD unless stated otherwise and significant differences are marked for $P < 0.05$. Single images are always chosen to be representative of the experimental outcome.

CHAPTER THREE: Electrospun scaffold characterisation and experimental optimisation

This chapter concerns the production and characterisation of electrospun scaffolds and the main preliminary work that was performed in order to optimise experimental methods for use in future work performed in results chapters 4-8. Each section contains brief introduction/aims, followed by results; some sections contain a short discussion; and all sections finish with a summary including how the results will be interpreted or translated into the future work.

3.1 Characterisation of electrospun scaffolds

3.1 Introduction

Electrospinning allows for the formation of nano- to micro-fibrous polymer scaffolds with controllable fibre orientation, which makes it an attractive technique for use in tissue engineering applications. Scaffolds can be produced that contain fibres of random orientations with isotropic properties as well as scaffolds containing fibres that are highly aligned and exhibiting anisotropic orientations. Alterations in the fibre orientation would allow one to model different architectures that are experienced in the body, for example, random fibres might represent a wound model or dermal tissue, whereas highly aligned fibres might represent tendon or organised mature bone. It would then be possible to study how scaffold architecture affects the differentiation of cells and whether matrix organisation can be controlled.

Although nano-fibres are predominant in most tissues, they often bundle together to form larger micro-sized fibres and cells are nestled in between these large bundles. As electrospun fibres become smaller, so does the pore size of the resulting mats due to increased fibre packing density. This means that it is more difficult for cells to migrate into the scaffold, nutrient transport/waste removal into and out of the scaffold is less efficient, and there is less room for cells to deposit new matrix.

While there are a large number of polymers available for use with electrospinning, a number of important considerations were made in order to choose a polymer suitable to complete all the necessary scaffold work outlined in the aims and objectives of chapter 1. Initially PLGA (75:25) was investigated for its use as an electrospun scaffold and was used for comparing the efficiency of different cell seeding methods.

However, fibrous mats of PLGA were observed to contract greatly when seeded with cells meaning that scaffolds needed to be constrained and PLGA itself was not cost-effective. Therefore the use of PCL fibres was investigated owing to its known biocompatibility and biodegradability; that fact that it is durable and easy to handle (even when wet), and its good mechanical properties. PCL fibres have been shown to support the culture of many cell types, and they also support the osteogenic differentiation of mature and progenitor cells. PCL was also more cost effective than PLGA. Therefore it appeared to be a suitable material to investigate the effect of scaffold architecture on matrix production and orientation.

The main aim of this work was to produce and characterise random and aligned electrospun micro-fibres of PCL for use as scaffolds to study cell behaviour and matrix production in later work. Another aim was to produce electrospun fibres of a polyurethane elastomer for use as a stretchable substrate to support the mechanical conditioning of cells. Finally, some of the electrospinning parameters were varied in order to see what affect these had on the resulting fibres.

3.1 Results

A tabulated list of all the conditions used for electrospinning polymer fibres are shown in table 3.1.1 along with the corresponding figure.

Polymer (w/w)	Solvent system	Flow rate (ml/h)	Voltage (kV)	Working distance (cm)	Collector speed (rpm)	Figure
PCL (15 %)	DCM	4	11	20	200	3.1.1
PCL (15 %)	DCM	4	11	20	2000	3.1.2
PCL (15 %)	DCM	3	11	20	200	3.1.4a
PCL (15 %)	DCM	3	11	20	2000	3.1.4b
PCL (15 %)	DCM	0.25, 0.5, 2, 4	11	20	2000	3.1.5a
PCL (15 %)	DCM	3	20	10, 20, 30, 40	2000	3.1.5b
PCL (15 %)	DCM	4	25	20	200	3.1.6
Tecoflex (10 %)	THF:DMF (0.7:0.3)	4	15	20	200	3.1.8a
Tecoflex (7.5 %)	DCM	4	13	20	200	3.1.8b
Tecoflex (7.5 %)	DCM	4	13	20	2000	3.1.8c
Tecoflex (7.5 %)	DCM	4	25	20	200	3.1.9

Table 3.1.1: Complete list of solution and experimental parameters for electrospinning of polymers. PCL is poly(caprolactone); DCM is dichloromethane; THF is tetrahydrofuran; DMF is dimethylformamide. Collector used was a rotating mandrel.

Electrospun PCL fibres: Random orientation
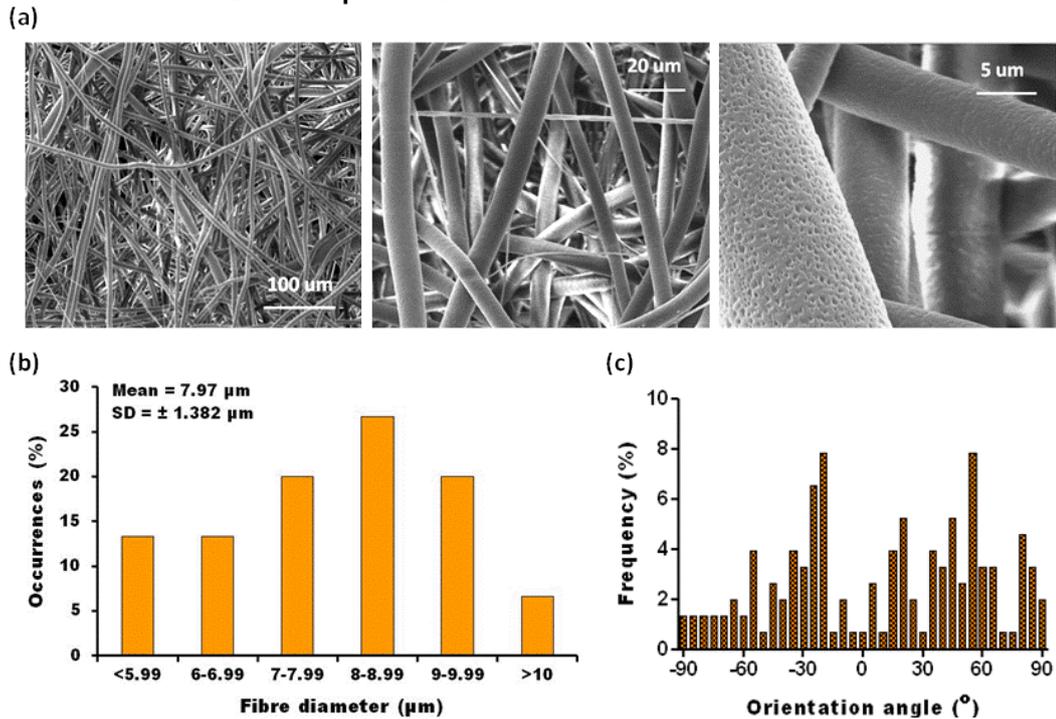
Figure 3.1.1: Electrospun PCL fibres with a random orientation formed from a solution of PCL (80 kDa) 15 w% in DCM. Conditions were 4 ml/h flow rate, 11 kV, 20 cm working distance. SEM micrographs (a) show different magnifications. Fibre diameter distribution (b) and frequency of fibre orientation (c) were calculated from 150 fibres (n = 3).

Electrospun microfibers of PCL were produced using a 15 w% solution in dichloromethane (DCM) and scaffolds containing randomly orientated fibres (Fig. 3.1.1) were fabricated as well as scaffolds containing highly aligned fibres (Fig. 3.1.2) by increasing the speed of the rotating collector 10-fold. Mean fibre diameter of each scaffold orientation did not vary significantly however fibre orientation, porosity and pore size were different. High magnification of each scaffold revealed surface features on individual fibres that looked like small micron/nano closed pores.

PCL fibrous scaffolds were then stretched in order to generate stress/strain curves (Fig. 3.1.3). Aligned scaffolds of PCL had a 10-fold higher Young's Modulus of elasticity (*E*) when stretched parallel to the fibre direction compared with randomly orientated fibres. The end of the elastic region was less well defined in the random fibres and the strain profile also continued to increase up to 100 % strain compared with aligned fibres which showed a gradual decrease in stress after the elastic region.

Electrospun PCL fibres: Aligned
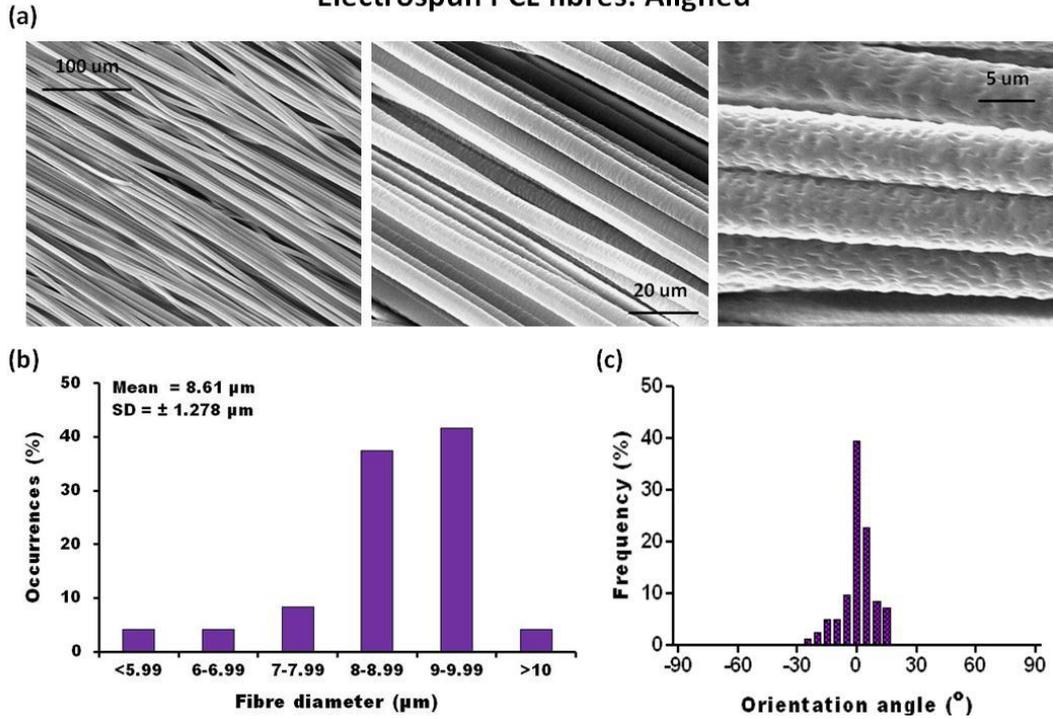
Figure 3.1.2: Electrospun PCL fibres with a high degree of alignment were formed from a solution of PCL (80 kDa) 15 w% in DCM. Conditions were 4 ml/h flow rate, 11 kV, 20 cm working distance, and 2000 rpm (collector). SEM micrographs (a) show different magnifications. Fibre diameter distribution (b) and frequency of fibre orientation (c) were calculated from 150 fibres (n = 3).
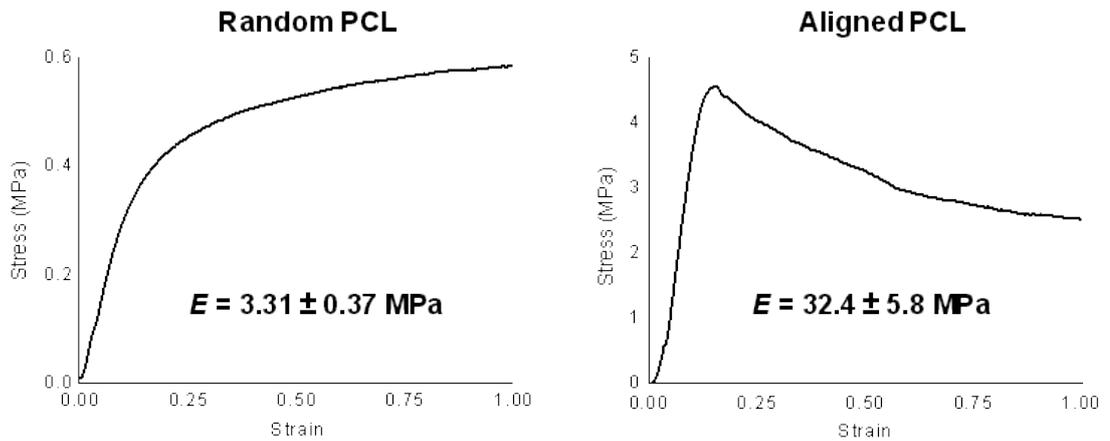
Figure 3.1.3: Stress/strain curves for random and aligned electrospun PCL fibres. Scaffolds were cut into 25 mm by 5 mm strips and stretched at 0.1 mm/s to 100 % strain. Notice the difference in the scale for stress which is ten-fold higher for aligned fibres. Curve is representative for n = 6.

A comparison of physical and mechanical properties for random and aligned PCL fibres (from figures 3.1.1-3.1.2) is shown in table 3.1.2. Random scaffolds were more porous and had a higher water contact angle than aligned scaffolds.

Scaffold	Mean Fibre diameter	Porosity (%)	Water contact angle (°)	Young's Modulus (Mpa)	TS at 100 % strain (MPa)
Random	7.97 ± 1.38	85.5 ± 1.8	135 ± 3	3.31 ± 0.37	0.59 ± 0.07
Aligned	8.61 ± 1.28	77.3 ± 1.1	64 ± 4 (Parallel) 118 ± 17 (Across)	32.4 ± 5.8 (Parallel) 0.037 ± 0.01 (Across)	4.58 ± 0.63 (Parallel) 0.017 ± 0.004 (Across)

Table 3.1.2: Physical and mechanical properties of random and aligned electrospun PCL scaffolds fabricated at 4 ml/hr. Parallel refers to values obtained in the direction of fibre orientation and across refers to values obtained perpendicular to the fibre direction. Values are quoted as mean ± SD (n = 6).

Random and aligned PCL fibres were also formed using the same conditions previously but with a flow rate of 3 ml/hr (Fig. 3.1.4). Mean fibre diameter was reduced by nearly 25 % and was very similar for both random and aligned scaffolds indicating that a reduction in flow rate reduces fibre size.
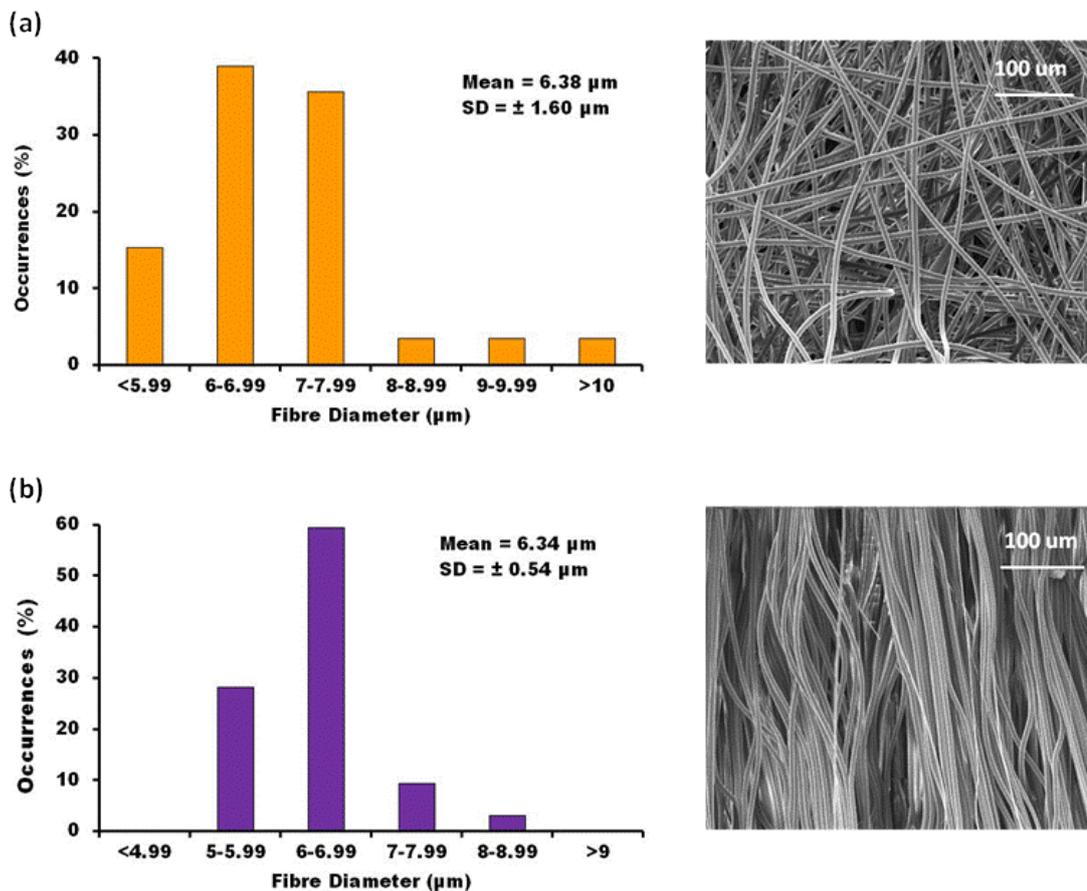
Figure 3.1.4: Distribution of diameters for random and aligned electrospun PCL fibres at a flow rate of 3 ml/h, 11 kV, 20 cm Wd along with SEM micrographs. Data is for n >50 fibres.

The effect of flow rate and working distance (Wd) on aligned fibre diameter was examined for four conditions. Increasing the flow rate resulted in a significant increase in mean fibre diameter (Fig. 3.1.5a) which was directly proportional for all but one increase (0.5-2 ml/hr). Altering the Wd from 10-40 cm did not have a significant effect on mean fibre diameter (Fig. 3.1.5), although at the greatest distance (40 cm) the diameter was the lowest. When fibres were formed using a relatively high voltage (25 kV), mean fibre diameter reduced and the fibre diameter distribution was more spread resulting in a larger standard deviation (Fig. 3.1.6).
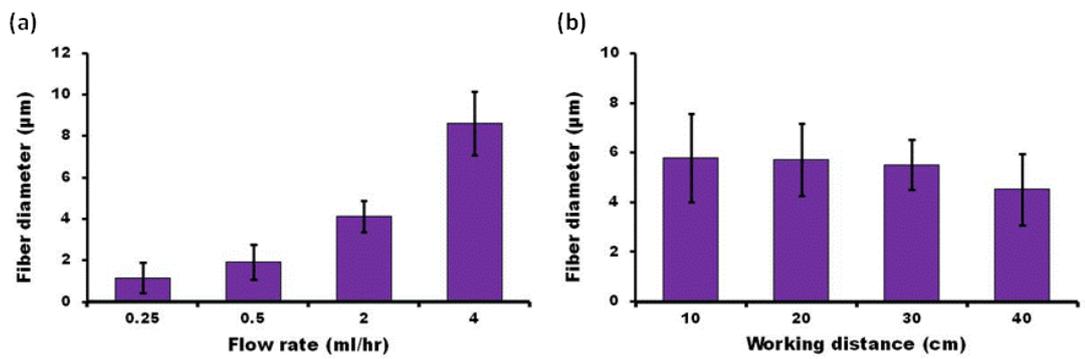
Figure 3.1.5: Mean fibre diameter of aligned electrospun PCL fibres resulting from varying the flow rate (a) and the working distance (b). Conditions were; (a) 0.25, 0.5, 2 or 4 ml/h flow rate, 11 kV, 20 cm Wd, 2000 rpm (collector); (b) 3 ml/hr, 20 kV, 10, 20, 30, or 40 cm Wd, 2000 rpm. Data is mean ± SD for n >50 fibres (n = 2).
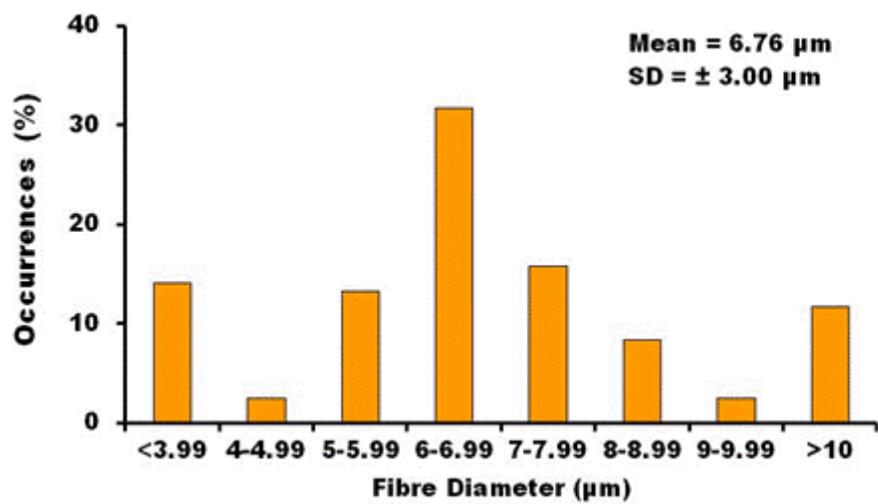
Figure 3.1.6: Mean fibre diameter of electrospun PCL fibres resulting from using a voltage of 25 kV. A higher voltage causes greater instability in the polymer jet resulting in a greater distribution in fibre diameters. Other conditions: 4 ml/h, 20 cm Wd, 200 rpm. Data is for n >50 fibres (n = 2).

SEM micrographs were obtained from the underside of the fibres (the side that first lays down in the collector) which had a much flatter and smoother appearence (Fig. 3.7) than fibres imaged from the top side. The closed pores that were obsevred on the top of the fibres were alos not present.
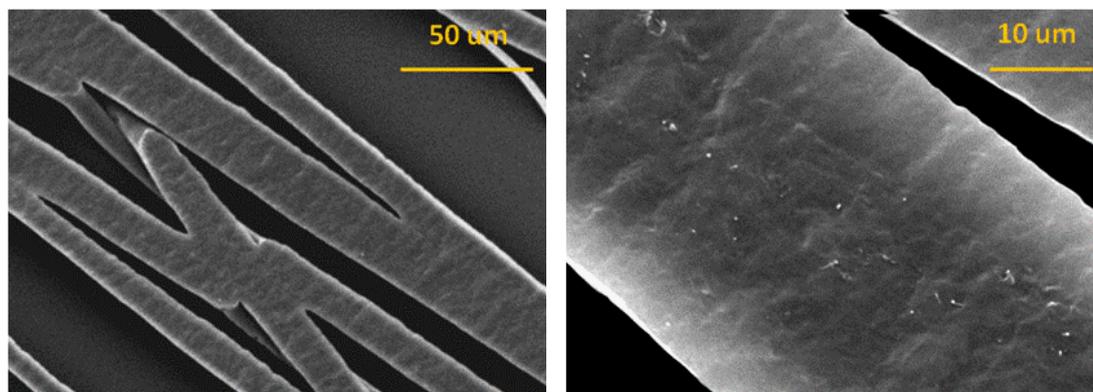
Figure 3.1.7: SEM micrographs of electrospun PCL 15 w% DCM fibres imaged from the underside (bottom) of the mat. Image shows fibres on the bottom side are flat and relatively smooth compared with fibres on the top.

Electrospun Tecoflex was initially produced from a 15 % w solution with THF:DMF but SEM micrographs revealed dark patches on the scaffolds (most likely the scaffold still contained solvent) and very little porosity (Fig. 3.1.8a). Cell viability at day 7 was also very low (Fig. 3.1.8d Tecoflex (a)) and so a new scaffold was produced to address these issues. Tecoflex fibres were produced from a solution of 7.5 w% in DCM and SEM micrographs showed a clearer picture and the scaffold also had larger pores than before (Fig. 3.1.8b). Cell viability at day 7 was also improved compared with the previous Tecoflex fibres. Aligned fibres of Tecoflex were also produced and in their relaxed state they were shown to curl round along themselves (Fig. 3.1.8c).

Tensile testing showed that aligned fibres stretched parallel to the fibre direction had a 10-fold higher E than random fibres. The stress/strain profiles also showed that scaffolds of both fibre orientations had an elastic region greater than 100 % strain and so these scaffolds could be useful as substrates for dynamic condition of cells.
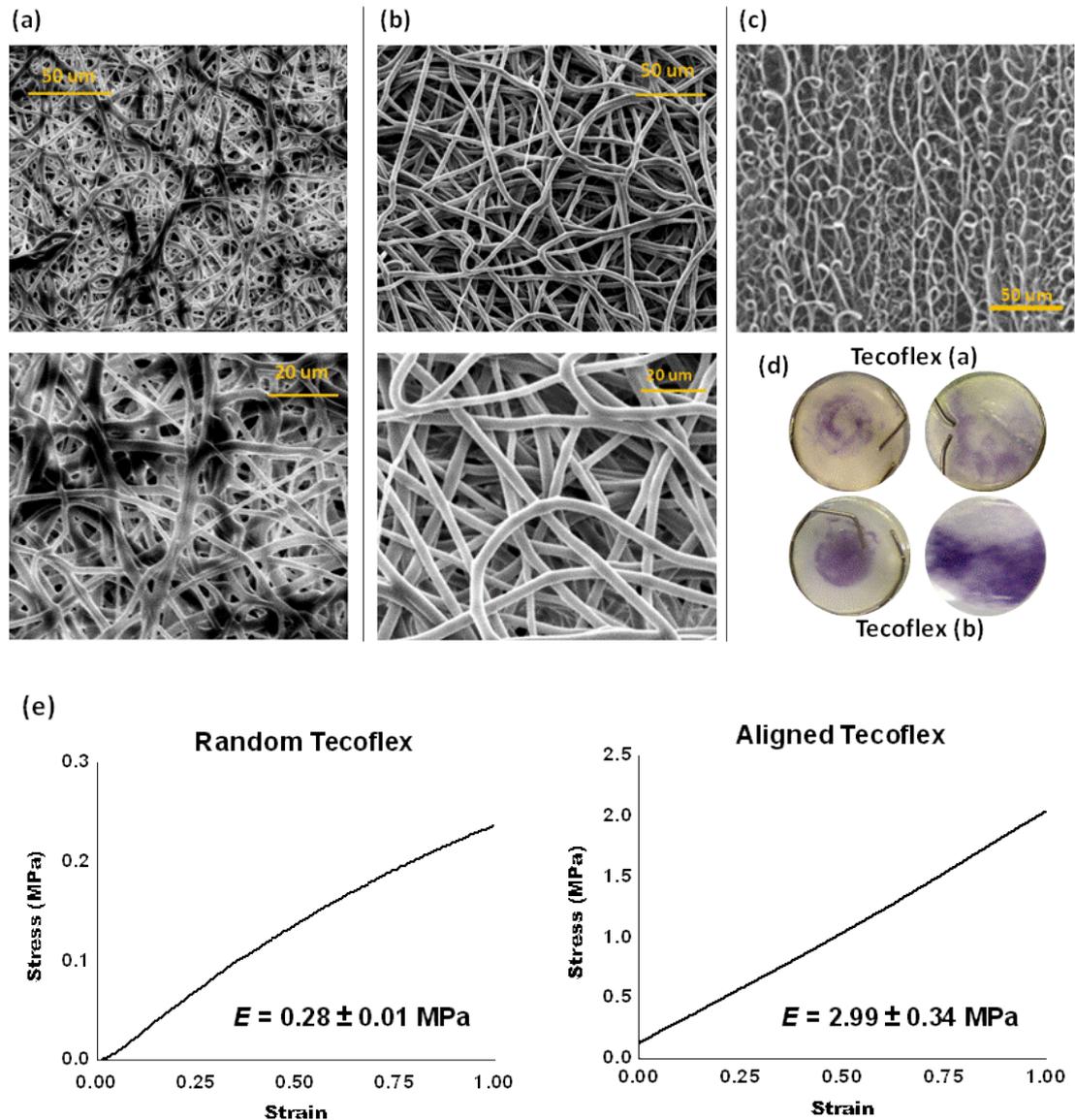
Figure 3.1.8: SEM micrographs of electrospun Tecoflex 10 w/w % THF:DMF (0.7:0.3) (a) or 7.5 w/w % DCM random (b) or aligned (c) fibres. MTT assay at day 7 (d) of human dermal fibroblasts seeded on Tecoflex-THF:DMF (a) (top) or Tecoflex-DCM (b) (bottom) using ring confinement (left) or low volume (right) seeding methods. The tensile profile of random and aligned Tecoflex (DCM) is shown (e). Notice the difference in the stress scale which is ten-fold higher for aligned fibres. Data representative for n = 5.

When electrospun Tecoflex was produced using a 2-fold higher voltage, fibres formed had two predominant diameters, large micron fibres (5-8 microns) and smaller 1-2 micron fibres (Fig. 3.1.9).
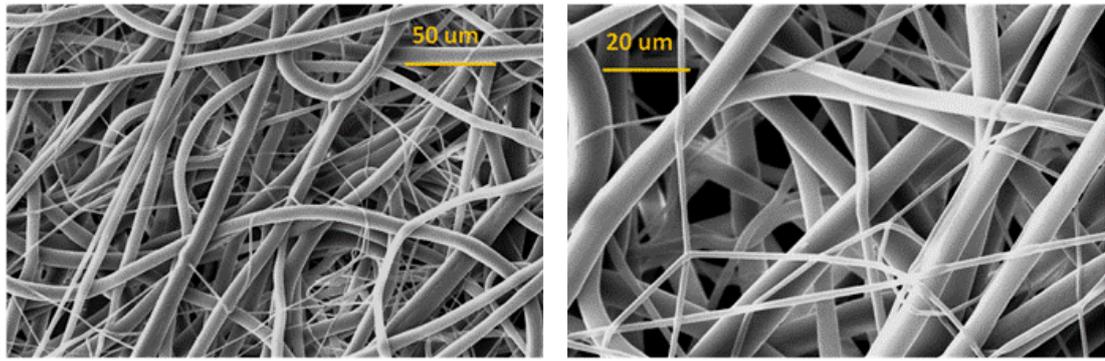
Figure 3.1.9: SEM micrographs of electrospun Tecoflex (7.5 w% DCM) fibres. Images show micro- and nano-fibres intertwined with each other. This was a direct result of increasing voltage (25 kV).

3.1 Discussion

Electrospun PCL scaffolds with randomly organised or highly aligned micro-fibres were successfully fabricated with similar mean fibre diameter. This was achieved using the same conditions (4 ml/hr, 11 kV, 20 cm) for both scaffolds. The working distance (Wd) is an important parameter in the formation of randomly orientated fibres as increasing this allows for a larger instability region and so the polymer jet can be drawn into smaller fibres. For aligned fibres, the Wd was shown to have little influence on fibre diameter (Fig. 3.5b) as there is no whipping of the jet, rather the fibre is drawn by the high speed rotational collector. Increasing the collector speed allows for additional drawing and increases chain alignment. The aligned fibres were not perfectly orientated due to the rapid deposition of fibres on the grounded, high speed rotating collector, there is not enough time for the charge on each fibre to be dissipated and so newly deposited fibres will repel each other. This causes some fibres to deviate at a slight angle from the main parallel axis and so the fibrous mat is not perfectly orientated. On the plus side, this does mean that some fibres will cross over each giving the scaffold more structural integrity and making the scaffold easier to handle.

The fibre diameter distribution was more spread for random fibres most likely due to the unstable region (which cannot be controlled) but the standard deviation of mean fibre diameter for both scaffolds was quite similar. It was seen that using a relatively high voltage results in a greater fibre diameter distribution and a large standard deviation and so using a low voltage is favourable. Although a scaffold composed of two different small and large fibre sizes may be useful for cells with the smaller

fibres supporting faster cell migration while the larger fibres offer larger pores are room to deposit matrix (Fig. 3.8). Pores in aligned scaffolds are smaller and essentially a different shape compared with random mats due the orientation of the fibres, and the higher packing density of the aligned mats. This also means that the aligned scaffolds are less porous than the random scaffolds. Fibres of both scaffolds showed surface features in the form of nano-micro closed pores giving the fibres an inherent roughness.

Electrospun fibres have a fibrillar structure with alternating crystalline and amorphous regions within each fibril. The fibrillar structure of electrospun fibres is mainly due to the electrospinning 'drawing effect' resulting in elongation of the polymer jet and subsequent molecular orientation in the direction of the fibre axis. Fibres produced by electrospinning are typically stronger than fibres produced by other techniques such as melt-spinning due to this drawing process. This results in electrospun fibres having higher Young's modulus and ultimate tensile strength (UTS) than fibres produced via melt-spinning.

When random fibrous mats are formed by electrospinning, they exhibit isotropic mechanical properties similar to the composition of the polymer (Li *et al.* 2007). However, the formation of aligned fibrous mats resulted in a scaffold with anisotropic properties, and this was 100-fold stronger parallel to the direction of fibre alignment. As a fibre is stretched and deformed, it goes through a period of linear elastic deformation and then when the slope of the stress strain begins to level off, this is the plastic deformation region, which continues until the sample fails. Stress/strain curves of random and aligned PCL were different in appearance, with random fibres experiencing a continued increase in stress during plastic deformation, whereas aligned fibres showed a decrease in stress. The end of the elastic region for each scaffold also had a different appearance. The length of the elastic region is determined by how well aligned or taut the interfibrillar non-crystalline molecules are. Tauter fibres lose elasticity and undergo plastic deformation quicker resulting in intrafibrillar shearing (Peterlin 1983). The fibres in random scaffolds have to unravel before they are all stretched parallel to the direction of strain.

Choice of solvent for polymer dissolution is an important parameter for a number of reasons. Solvent polarity can affect the diameter of electropsun fibres directly or

indirectly. You *et al.* (2006) fabricated electrospun fibres of PLGA after dissolution in chloroform or HFP, two solvents with differeing polarity with chloroform possessing a much lower dielectric constant. The resulting fibres formed from the HFP solution were nearly 3 times the size of those formed from the chloroform solution (You *et al.* 2006). Some solvents such as those with low volatility or fluorinated solvents are often retained in the resulting scaffold and can affect the biological performance of the scaffold, with particular regards to cell toxicity. This may explain the poor cell viability on THF:DMF Tecoflex fibres. DCM is a volatile solvent hence why it was chosen for spinning all of the scaffolds.

Tecoflex was shown to have a large elastic region and so would most likely be suitable for use as a substrate for subjecting cells to dynamic strain. However, this high degree of elasticity is detrimental to the structural integrity of the aligned fibres which curl up on themselves and cause the scaffold as a whole to fold inwards.

3.1 Summary

- Random and aligned fibrous scaffolds of PCL were formed using electrospinning, with similar fibre diameters.
- Aligned electrospun fibrous substrates had anisotropic mechanical properties showing a 10-fold increase in stiffness when stretched parallel to fibre direction.
- Flow rate and voltage affect the resulting mean fibre diameter and distribution of fibre diameters respectively.
- Mechanical properties can be enhanced by heat annealing, but this also results in decreased pore size.
- Tecoflex has a large elastic strain profile and appears suitable as a substrate for future cyclic mechanical conditioning of cells.
- Electrospun PCL fibres formed at 4 ml/h with fibre diameters of 8 µm will be used for future work regarding substrate effect on cell behaviour, differentiation, and matrix production/organisation.

3.2 Ascorbic acid and Sirius red staining

Ascorbic acid (AA) is well known to play an essential role in the synthesis of stable collagen by mediating the hydroxylation of proline and lysine to enable the formation of the collagen triple helix (Kielty *et al.* 1993). AA has been seen to support collagen synthesis in fibroblasts and bone cells, independent of fibroblast age, and also appears to be necessary for strain-induced increases of the mechanical properties of fibroblast-seeded scaffolds (Garvin *et al.* 2003; Maehata *et al.* 2007). So it appears that AA is an essential requirement for stable collagen production as well as loading-induced responses of mature fibroblastic cells.

A common method for identifying and quantifying collagen is Sirius red (SR) staining. SR (normally prepared in saturated picric acid) is a strong anionic dye that stains collagen when its sulphonic acid groups react with the basic amino groups belonging to lysine and hydroxylisine (Taskiran *et al.* 1999). The molecules of the dye are elongated and attach parallel to the long axis of the collagen fibre, which causes a visual enhancement when using polarisable microscopy. It has been demonstrated that SR is not specific for just one type of collagen but many types (Types I, II, III, IV, V) (Walsh *et al.* 1992). It has also been shown that noncollagenous proteins do not significantly interfere with the assay or uptake the dye (Walsh *et al.* 1992). Collagen can also be quantified using the more expensive hydroxyproline (HPr) assay, with HPr accounting for about 10 % of the collagen molecule, but it has been shown that the SR assay is just as reliable (Taskiran *et al.* 1999). SR staining has some advantages over the HPr assay including visualisation of collagen location, and it can also be used as a fluorescent marker which does not suffer significant photobleaching. This makes the SR assay an inexpensive and reliable assay for quantifying total collagen in tissue engineering applications.

The aims of this work was to (a) observe the extent by which AA affected HDF behaviour with regards to cell viability and collagen production over 21 days of culture and (b) to determine suitable time points for future collagen quantification using Sirius red staining. The addition of AA in HDF culture on electrospun scaffolds was also performed in order to observe if PCL fibres supported AA-related increases in cell viability and collagen production at day 14.

3.2.1 Results
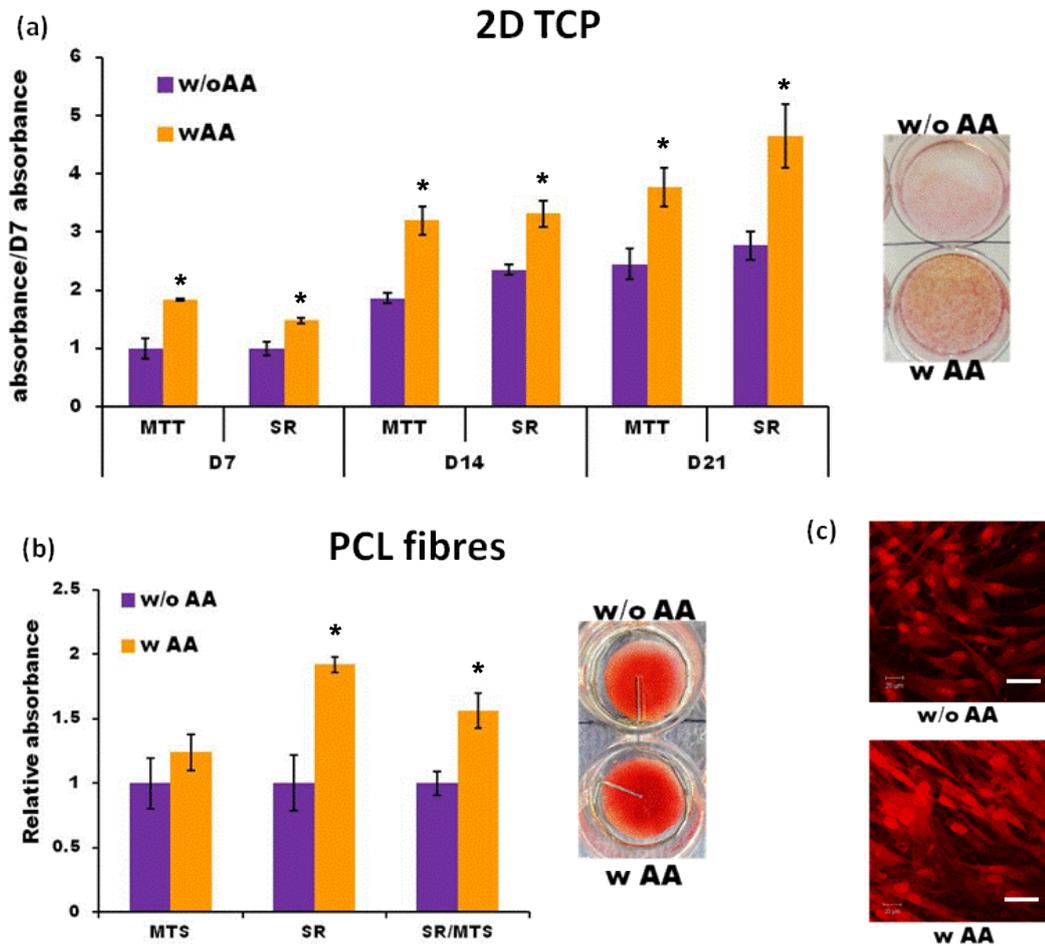
Figure 3.2.1: Affect of AA on cell viability and collagen production for HDFs on 2D TCP (a) or on electrospun PCL fibres (b). For 2D, data is normalised to absorbance at day 7 of cells w/o AA. All images show SR staining at day 14; fluorescent images (c) show cell-deposited collagen in 2D. Scale bar is 50 μm. Data is mean ± SD (n = 6). *P <0.05.

Cell viability doubled from day 7-14 but only increased slightly from day 14-21 (Fig. 3.2.1). Collagen deposition increased during the culture period in a similar fashion but for AA$^+$ cells the increase in collagen deposition from day 14-21 was much greater than for AA$^-$ cells. In 2D, cell viability and collagen production was significantly higher at all time points for AA$^+$ cells than AA$^-$ cells. The largest difference in collagen production was observed at day 21 were AA$^+$ cells had nearly 2-fold more collagen than AA$^-$ cells. On electrospun PCL at day 14, cell viability was highest for AA$^+$ cells but this difference was not statistically significant from AA$^-$ cells. However, collagen production was 2-fold higher with AA suggesting that more collagen per cell was produced than AA$^-$ cells. Fluorescent images of Sirius red

staining in 2D showed that AA⁻ cells possessed few fibres whereas AA⁺ cells had a more intense signal and an increased number of fibres.

3.2.2 Summary

- AA enhanced cell viability and collagen deposition of HDFs in 2D and on PCL fibres.

- AA enhanced cell viability to a greater extent in 2D compared with PCL fibres, but more collagen per cell was produced on PCL scaffolds.

- This suggests that the affect of AA on collagen production appears to be most effective when cells have reached confluence.

- Increases in collagen deposition can be monitored at days7, 14 and 21.

- Future experiments concerned with collagen production will use media containing AA.

3.3 Second harmonic generation imaging

The ability to monitor long-term matrix development is important as the successful production of a tissue-engineered construct requires a well-defined body of differentiated cells and ECM. It is important that the construct be monitored in a way that allows for its uninterrupted continued development so that the differentiation process is not affected or the construct damaged. Second harmonic generation (SHG) (introduced in Chapter 1) can be used to image collagen deposition and organisation in a minimally invasive fashion and so it holds much promise as a useful imaging technique in tissue engineering.

Some studies have shown that SHG signal is dependent on excitation wavelength (Theodossiou *et al.* 2006; Zoumi *et al.* 2002) and determining the wavelength that yields the most intense signal is desirable when collagen is immature and disorganised. SHG intensity is dependent on a number of factors relating to collagen including the amount present, how mature it is, the fibre diameter, the organisation, and the alignment relative to the incident laser. The maximum signal intensity will occur when the axis of the collagen fibril is parallel to the polarization of the laser (Freund *et al.* 1986).

There were a number of aims to this optimisation work:

1. Perform wavelength dependent studies on collagenous tissues to observe which produces the most intense signal.
2. Perform wavelength dependent studies on PCL electrospun scaffolds of varying orientations.
3. Compare the difference between SHG imaging, Sirius red fluorescencence, and Col I antibody staining.
4. The potential of this technique for imaging tissue engineered collagen in real time or after fixation.

3.3.1 Results: Wavelength dependence of collagenous tissue
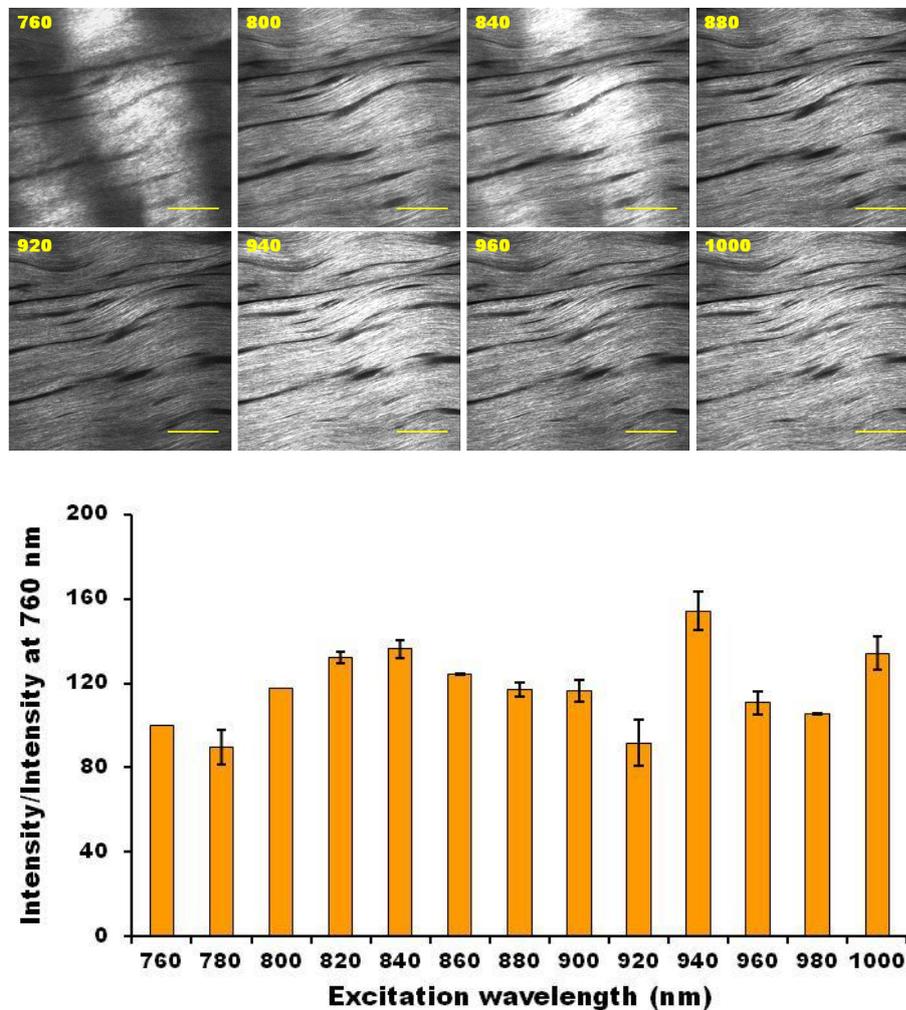
Figure 3.3.1: MP excitation of rat tendon at 760-1000 nm (20 nm intervals) and subsequent collection of SHG in half-excitation wavelength emission bin. Images show SHG traces from a selection of excitation wavelengths where the yellow number represents the excitation wavelength in nm. Pixel intensity normalised 760 nm pixel intensity was plotted as mean ± SD (n = 2). Scale bars are 50 μm.
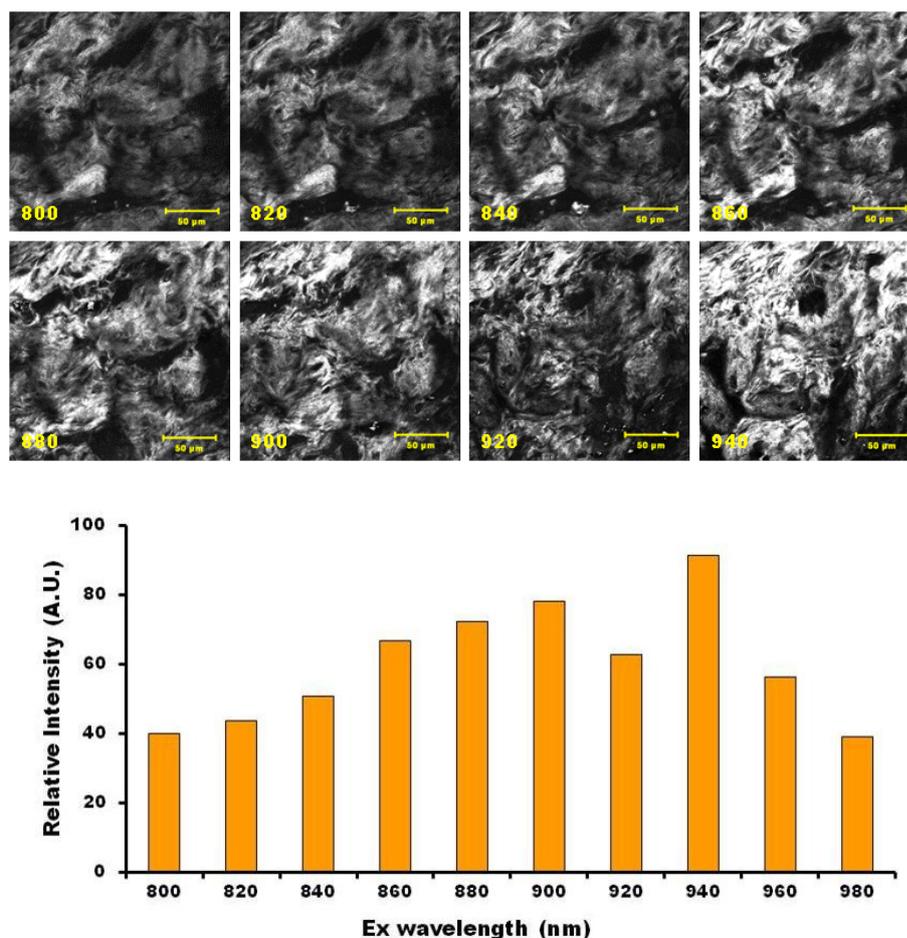
Figure 3.3.2: MP excitation of DED (de-epithelialized dermis) at 800-980 nm in 20 nm intervals and subsequent collection of SHG in half-excitation wavelength emission bin. Images show SHG traces from a selection of excitation wavelengths where the yellow number represents the excitation wavelength in nm. Data is total pixel intensity for n = 1. Scale bars are 50 μm.

Rat tendon was excited at 760-1000 nm (20 nm increments) and SHG was collected in the back scattered geometry at the appropriate half excitation wavelength emission bin. Differences were seen in the overall pixel intensity of the images, as well as the pixel intensity at localised areas. SHG intensity oscillated over the excitation wavelength range tested (760-1000 nm) peaking at 840, 940 and 100 nm and dipping at 780, 920 and 980 nm (Fig. 3.3.1). The highest intensity was observed at 940 nm and SHG was relatively even across the image however other wavelengths such as 760 and 840 nm showed light and dark SHG bands. Image quality also appeared to vary at different wavelengths, for example, SHG using excitation at 760 nm produced a relatively hazy image compared with that using excitation at 940 nm.

For human DED (de-epithilialized dermis), SHG intensity also oscillated but the peaks and troughs were located at different wavelengths compared to those of the rat tendon with the exception of the largest peak which similarly was observed at 940 nm (Fig. 3.3.2). The light and dark SHG banding observed using some excitation wavelengths with the rat tendon was not obvious when imaging DED.

Rat tendon was a stronger emitter of SHG than DED and so could be easily visualised at a lower power (10 mW) compared with DED (25 mW). This is due to the superior structural organisation of tendon including thicker fibre bundles and a high degree of orientation.

3.3.2 Results: Wavelength dependence of electrospun scaffolds
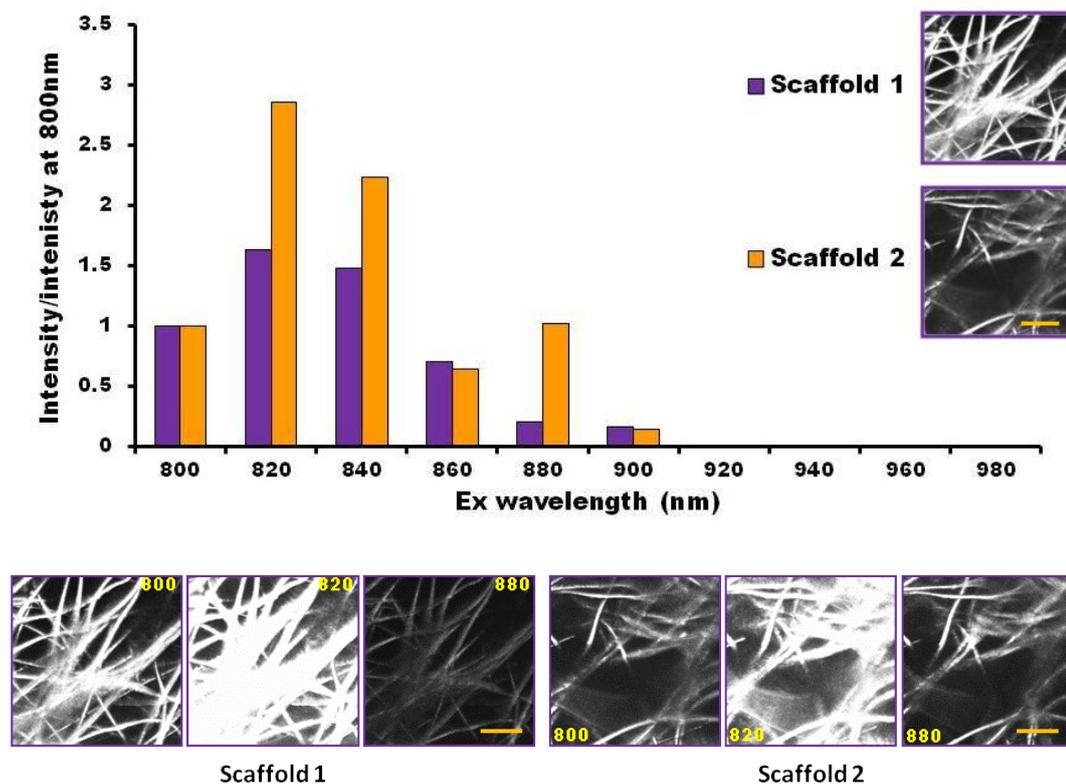
Figure 3.3.3: MP excitation of two different randomly orientated fibrous PCL electrospun scaffolds at 800-980 nm in 20 nm intervals and subsequent collection of SHG in half-excitation wavelength emission bin. Data is total pixel intensity normalised to total pixel intensity at 800 nm for each scaffold. Images show scaffold SHG intensity at 800, 820 and 880 nm excitation. Scale bar is 50 μm.

Electropsun PCL fibres were imaged using MP excitation across a range of wavelengths and SHG was obtained in the same fashion as with the tissues. In contrast to the collagen imaged in the tissues, SHG intensity decreased as the

excitation wavelength increased, before no detectable SHG was observed at 940nm Ex. For two different random fibrous scaffolds, there was a difference in magnitude of the normalised intensity (normalised to 800nm) at each excitation wavelength (Fig. 3.3.3) and scaffold 2 had a much more intense signal at 880nm Ex than scaffold 1. Aligned scaffolds orientated either parallel or perpendicular to the imaging stage had different signal intensities at 880nm and 920nm, with perpendicular fibres producing more SHG (Fig. 3.3.4).
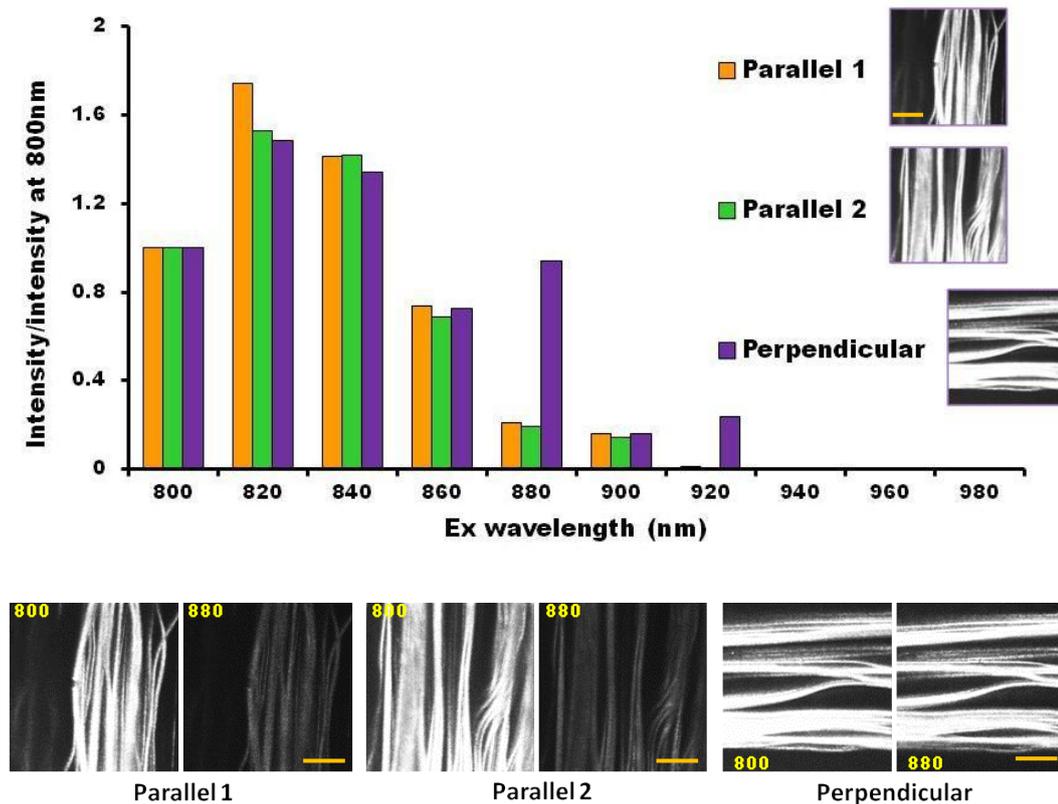
Figure 3.3.4: MP excitation of three aligned fibrous PCL electrospun scaffolds at 800-980 nm in 20 nm intervals and subsequent collection of SHG in half-excitation wavelength emission bin. Two scaffolds were orientated on the microscope stage from back to front (parallel) and one was orientated across the stage from right to left (perpendicular). Data is total pixel intensity normalised to total pixel intensity at 800 nm for each scaffold. Images show scaffold SHG intensity at 800 and 880 nm excitation. Scale bar is 50 μm.

3.3.3 Results: Tissue engineered collagen

HDFs were seeded on PCL fibres and imaged for SHG at day 21 (Fig. 3.3.5). Using an excitation wavelength of 800 nm, cells, scaffold fibres, and matrix were all visible resulting in an inhibition of the collagen signal. At an excitation wavelength of

940nm, SHG from collagen was clearly visible while any signal from the scaffold or cells was not observed.
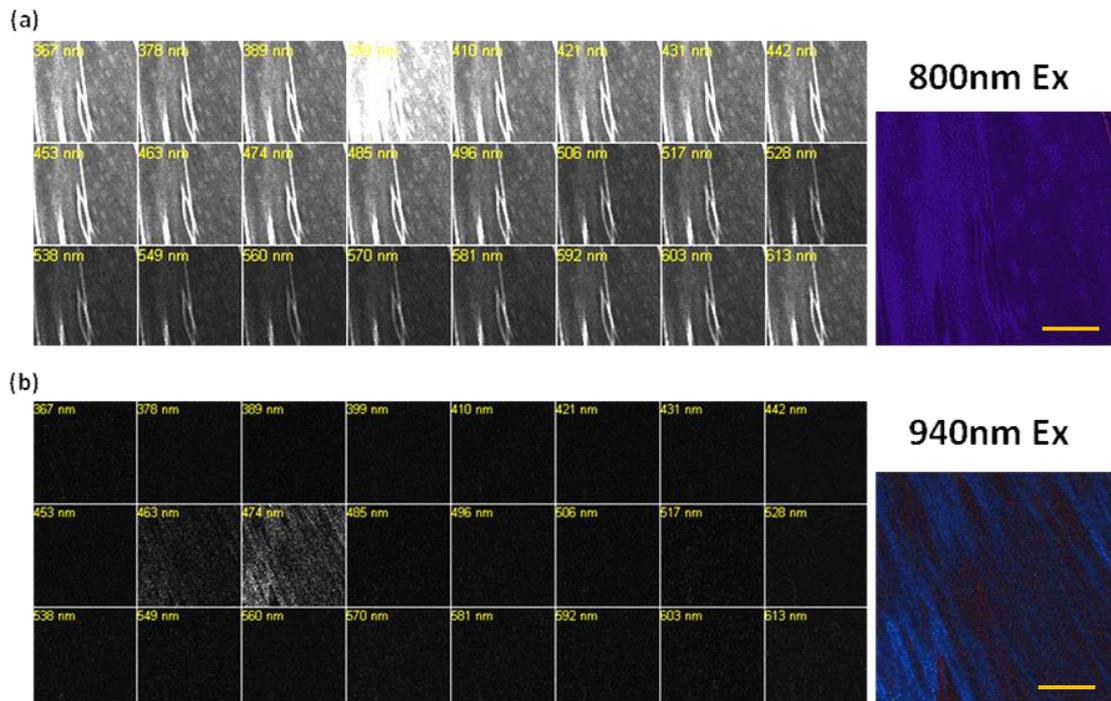
Figure 3.3.5: Two-photon excitation of HDFs seeded on PCL fibres was performed at day 21 using 800 nm and 940 nm and signal was collected using a lambda stack made up of narrow 10 μm collection bins from 367-613 nm. Excitation at 800 nm (a) showed matrix, cells, and scaffold was present in all collection bins and was most intense in the half excitation bin (SHG bin 399 nm). Excitation at 940 nm showed SHG from collagen clearly present in the SHG bin (474 nm). Scale bar is 50 μm.

Next, cell-seeded scaffolds were imaged using 940nm Ex at two depths after 10 % formalin fixation or without fixation (Fig. 3.3.6). SHG from unfixed samples was clear and collagen fibres could be seen at both depths. SHG of fixed samples was much less intense at both depths, especially 5 μm, and the fibrous appearance if the collagen was replaced with a more grainy texture.

Fixed samples were then imaged after staining with DAPI and phalloidin TRITC to see if combined imaging could be carried out with SHG. Figure 3.3.7 shows that imaging SHG and DAPI/phalloidin on the same samples was possible.
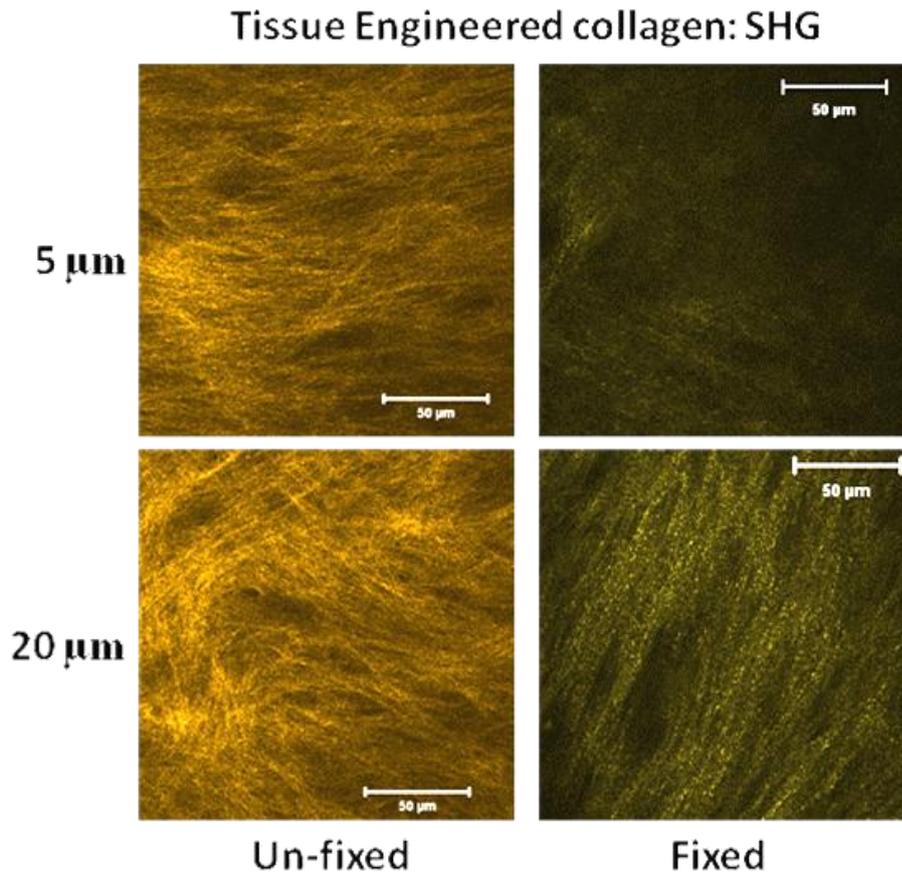
Figure 3.3.6: SHG collected from collagen deposited by human dermal fibroblasts cultured on PCL fibres at 21 days. Samples were imaged either in natural form (un-fixed) or fixed with 3.7 % formaldehyde, at 5 or 20 μm into the scaffold. Un-fixed samples had a more intense and fibrous appearance, while fixed samples were faint at 5 μm and there was no obvious fibrous structure.

Finally, three methods of imaging collagen produced by HDFs on random and aligned PCL scaffolds were compared, Sirius Red (SR) fluorescence, Col I antibody staining, and SHG (Fig. 3.3.8). All methods were able to give information on the orientation of the samples but the SR and Col I methods did not give much information on the nature of the collagen fibres and this was particularly true for aligned samples. They also seemed to stain pro-collagen inside the cell meaning that the cell staining inhibited collagen visualisation outside of the cell. SHG on the other hand gave a much clearer image which was in the form of a fibrous matrix. Differences in matrix orientation could be clearly seen between samples.
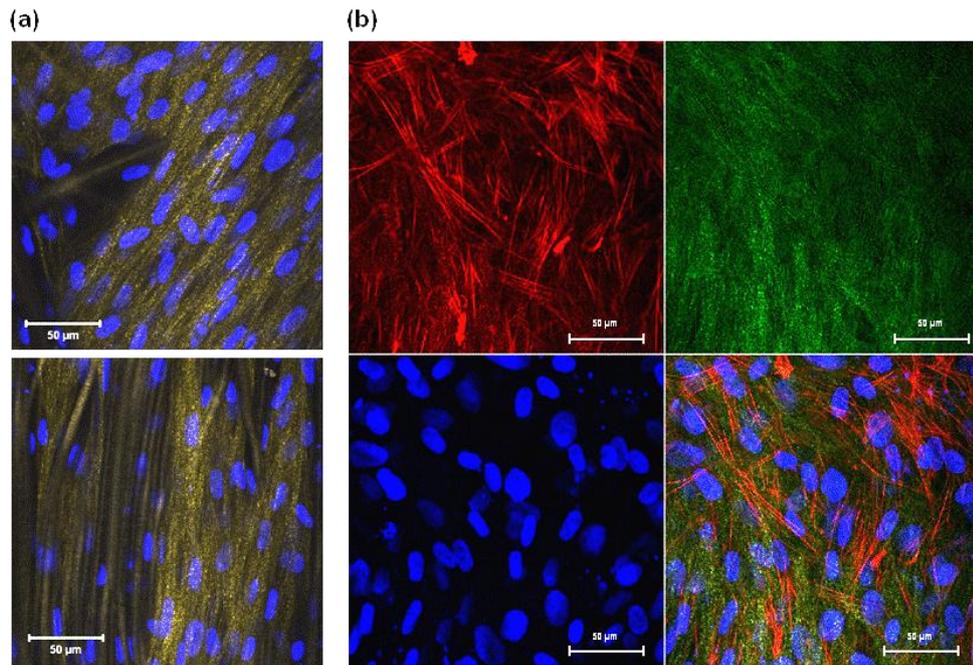
Figure 3.3.7: SHG collected from collagen deposited by human dermal fibroblasts cultured on PCL fibres after fixation at 21 days. Samples were stained with DAPI (blue-nucleus) and PCL fibres can be seen in grey with SHG in yellow (a). Samples were also stained with phalloidin-TRITC (red-cytoskeleton) and combined with SHG (green) (b). Scale bars are 50 μm.

Sirius Red　　**Col I antibody**　　**SHG**
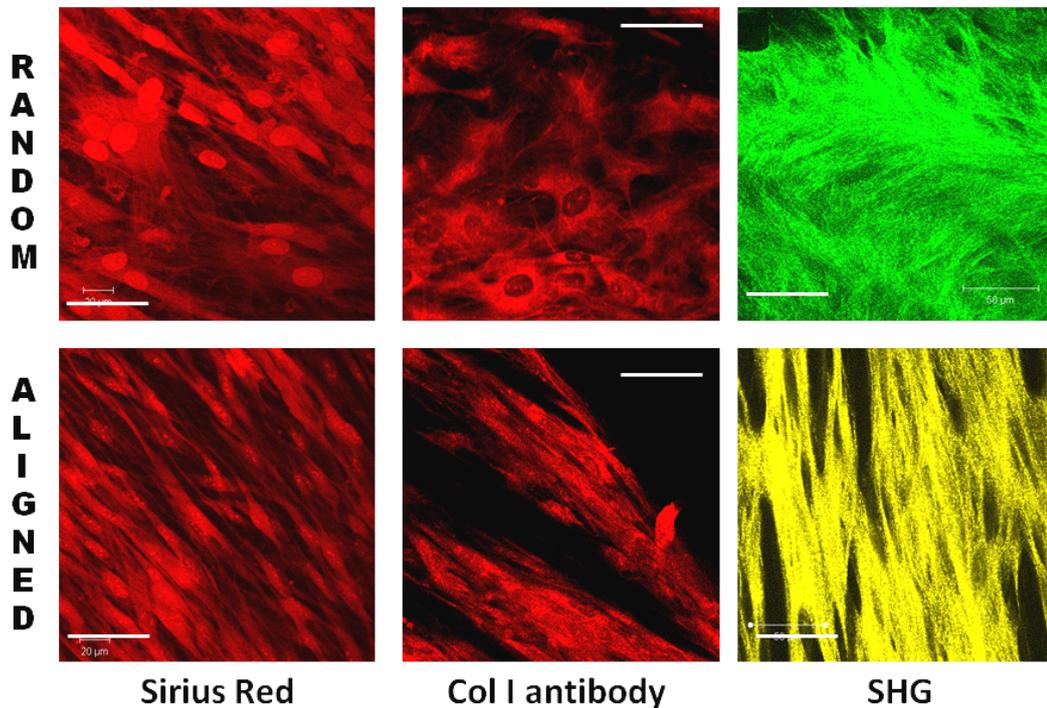
Figure 3.3.8: Collagen deposition on random and aligned PCL fibres by human dermal fibroblasts was visualised using three confocal-based imaging techniques; Sirius Red fluorescence (red), Col I antibody staining (red), and SHG (green and yellow). Scale bars are 50 μm.

3.3.4 Summary

- SHG is a minimally invasive technique that can be used to image tissue-engineered collagen without any sample preparation.

- SHG gives information on collagen deposition and organisation, and signal intensity is dependent on both these factors.

- Higher excitation wavelengths are favourable for collagen SHG and removal of interfering background fluorescence.

- 940 nm excitation yields the most intense SHG for collagen.

- SHG cannot be detected from PCL fibres at 940 nm excitation.

- SHG can also be used to image collagen on fixed samples, but signal is weakened and fibrous structure is lost.

- SHG will be used for monitoring collagen matrix deposition in future work.

3.4 Osteogenic differentiation of hESMPs

The human embryonic stem cell-derived mesenchymal progenitor 002.5 (hESMP) cell line is a mesenchymal progenitor cell line that was derived from hESC lines (Karlsson *et al.* 2009). They do not express typical pluripotent markers (Oct-4 or Nanog) found in undifferentiated ESCs. They have a morphology similar to MSCs and have been characterised as desmin$^+$, vimentin$^+$, and nestin$^-$, as well as expressing MSC markers CD105, CD166, CD10, and CD 13. They also are able to differentiate *in vitro* towards the three common mesenchymal tissue lineages of bone, cartilage, and adipose. There are a number of advantages of using an MSC cell line over primary MSCs including:

1. Being readily available, without the requirement for suitable donors.
2. Being easy to culture and have an excellent proliferative capacity.
3. Avoidance of donor variation associated with primary MSCs.

These cells can be passaged up to 20 times while retaining proliferative capacity and were observed to undergo osteogenic differentiation *in vitro* at P16 (data not shown).

At present there is no data on the effect of varying the concentration of the osteogenic inducer dexamethansone (dex) on hESMP osteogenesis. Therefore, the

aim of this work was to observe what affect dex concentration (0, 10 or 100nM) had on cell number and osteogenic ability of hESMPs, assayed by total DNA, ALP activity, collagen production and calcium deposition in 2D.

3.4.1 Results
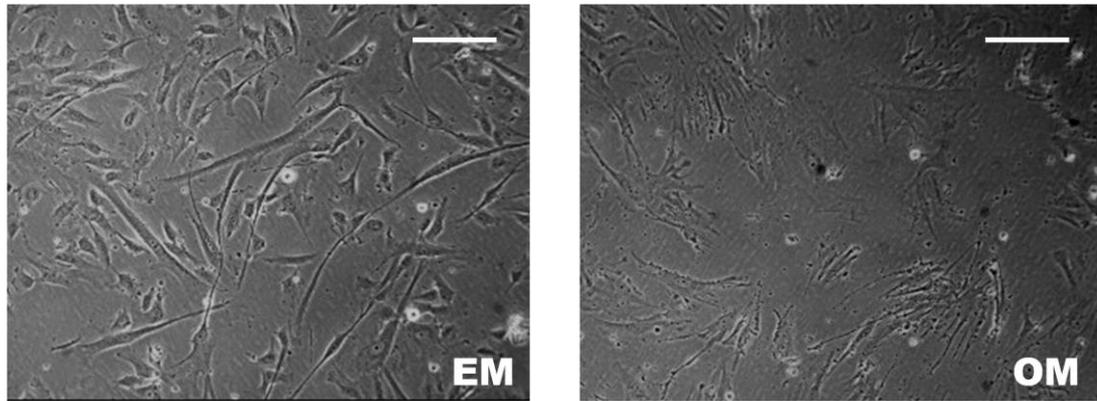
Figure 3.4.1: Phase contrast images showing hESMP morphology after 7 days of culture in either expansion media (EM) or osteogenic media (OM). Scale bar = 50µm
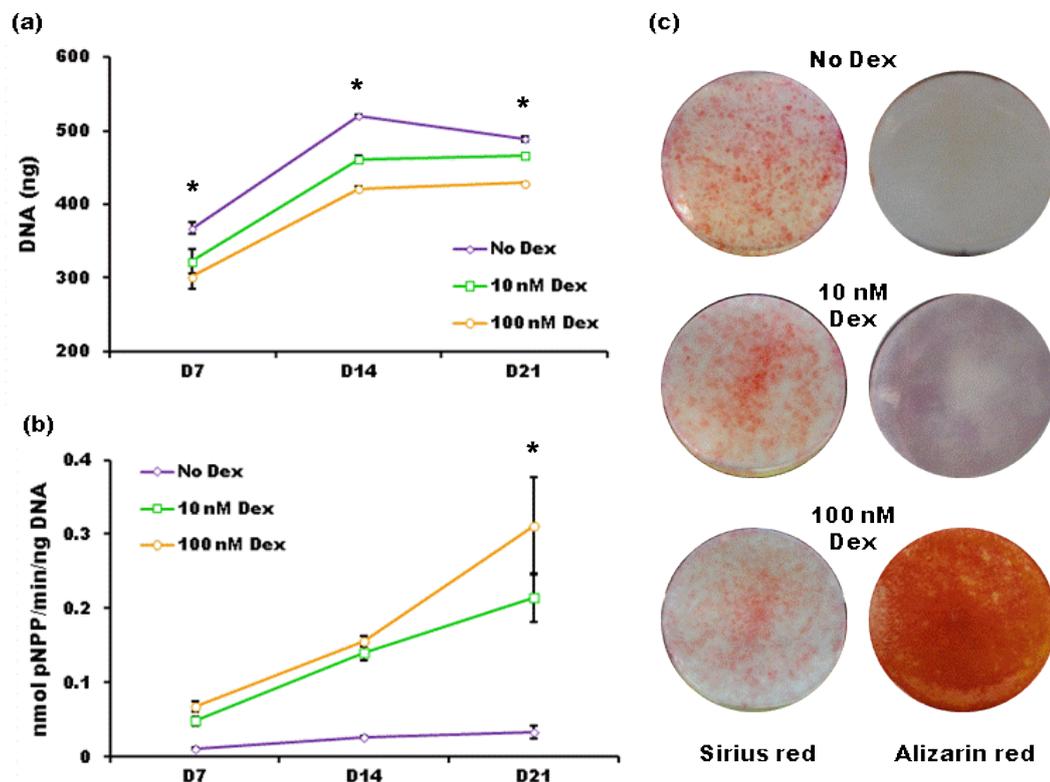
Figure 3.4.2: Effect of dex concentration (0, 10 and 100 nM) on hESMPs cultured on TCP assayed by total DNA (a) and ALP activity (b) (D7, 14 and 21), and collagen (D14) and mineral deposition (D21) (c). All data is mean ± SD (n = 6). *$P <0.05$%

Osteogenic media induced a morphological switch in hESMP cells (Fig. 3.4.1) from a fibroblast to a flatter, more square-like shape typical of an osteoblast. Total DNA increased from day 7-14 for all media groups (Fig. 3.4.2a) but only minor increases were seen from day14-21 (10-100 nM) apart from cells with 0 nM dex that decreased slightly. A lower dex concentration corresponded to higher total DNA, showing that dex affects cell number. ALP activity (Fig. 3.4.2b) of 10 nM and 100 nM groups showed no difference at days 7-14 however, at day 21 the 100 nM dex group was 1.5-fold higher. Cells with 0 nM dex had a much lower ALP activity at all time points. Sirius red staining of collagen at day 14 showed that increasing dex concentration resulted in less staining (Fig. 3.4.2c). Mineral deposition at day 21 was observed only in the 100nM dex group (Fig. 3.4.2c).

3.4.2 Summary

- Dexamethasone induced an osteogenic morphology in hESMP cells, and increased ALP activity.
- Increasing dex concentration resulted in a lower cell number and lower collagen production.
- At day 21, hESMPs cultured in 100 nM of dex had the highest ALP activity and were the only cells to deposit mineral.
- 100 nM of dex will be used for future work with hESMP cells.

3.5 HDF Osteogenesis

Fibroblasts derived from the dermis of humans have been show to express mesenchymal surface antigen immunophenotypes and posses osteogenic, chondrogenic, and adipogenic multipotent differentiation potential (Chen *et al.* 2007; Xue and Li 2011; Young *et al.* 2001). Due to the large quantities of available skin, and the ease with which it can be obtained, progenitor cells derived from the dermis offer a promising cell source for bone tissue engineering strategies.

A number of studies have observed that that mesenchymal differentiation potential of DFs is reduced or absent at later passages (Chen *et al.* 2007; Lysy *et al.* 2007). Lysy *et al.* (2007) showed that dermal fibroblasts of <P3 and >P3 had similar mesenchymal phenotypic markers CD45, CD34, CD73 and CD90. However, HDFS

up to passage 3 deposited mineralised matrix and expressed OCN, BSP, and Col I mRNA *in vitro*, whereas cells after P3 did not.

Many names have been given to the populations of multipotent cells obtained from dermis including skin-derived progenitors/precursors (SKPs) (Toma *et al.* 2001), dermal mesenchymal stem cells (DMSCs) (Bartsch *et al.* 2005), multipotent fibroblasts (MFBs) (Chen *et al.* 2007), and dermal multipotent cells (DMCs) (Xue and Li 2011). For this work I am only investigating the osteogenic potential of HDFs and so essentially I have deemed them as osteogenic progenitors from dermis, however as dermal fibroblasts are the major cell type found in the dermis I will still refer to them as HDFs. Variations in the osteogenic ability of hBMSCs between donors have been observed (Siddappa *et al.* 2007) and it seems likely that this would occur in HDFs from different donors also. Therefore, in order to avoid the complication of donor variation at this stage, only HDFs from the same patient were used for all experiments.

The aim of this optimisation work was to; (i) determine if primary HDFs could be induced to an osteogenic lineage assayed by ALP activity (early marker) and calcium deposition (late marker) and; (ii) observe what effect cell passage number had on these markers. The ultimate goal was to assess if HDFs were suitable for future fluid flow experiments concerning the enhancement of mineralised matrix.

3.6.1 Results

HDFs at P3 were cultured in fibroblastic media (FM) or osteogenic media (OM) for 7 days with noticeable differences in cell morphology (Fig. 3.5.1a). FM cultured cells showed a typical fibroblastic morphology while OM cultured cells had spread out more and mostly adopted a cuboidal morphology typical of an osteoblastic cell. ALP activity increased under all conditions from day 14 to 21 and was significantly higher in OM cultured cells at all passages then FM cultured cells (Figure 3.5.1b). Interestingly, ALP activity was lowest in OM cultured cells at P3 at day 14 and highest at P4 at day 21, while all other passages had similar values at each time point. There was no observed calcium deposition in FM cultured cells at day 21; however, cells cultured in OM showed strong calcium staining at P2-3 (Fig. 3.5.1c). Calcium deposition in OM cells decreased dramatically from passages 4-6.
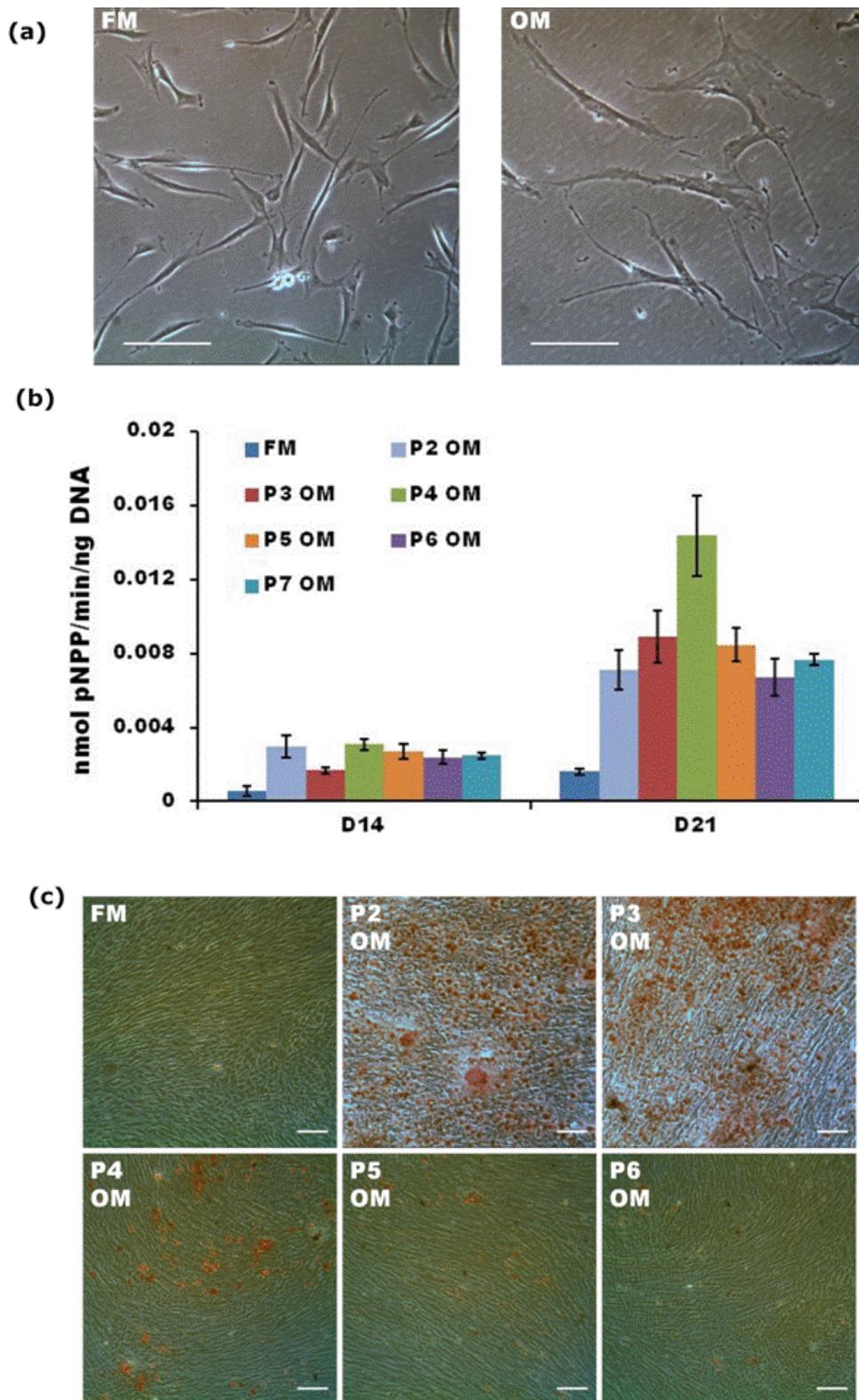
Figure 3.5.1: Human dermal fibroblasts (HDFs) were cultured in fibroblastic media (FM) or osteogenic media (OM) and assayed for cell morphology at day 7 (a), and ALP activity (b) and calcium deposition at day 21 (c) at different passage numbers P2-7). ALP is mean ± SD (n = 3-6) and (a) and (c) show representative images for n = 3. Scale bars = 100 μm.

3.5.2 Discussion

ALP activity is considered an early indicator of osteogenic differentiation, however, ALP activity did not appear to directly correlate to the amount of mineral deposition, which was highest at P2-3, and significantly reduced at P4. A study by Agata *et al.* (Agata *et al.* 2010) investigating hBMSCs showed that while ostoegenic gene expression (ALP, OC, BSP, Col I) did not alter *in vitro* between passages 1 and 3, mineral deposition was much lower at P3 than P1. This suggests that *in vitro* mineralisation potential is reduced with increasing passage number. Sidappa *et al.* (2007) also noticed that hBMSCs were only able to mineralise *in vitro* at or before P3, losing this ability at P4. However, ALP is still a useful marker for assessing osteogenesis. Siddappa *et al.* (2007) also showed that donors with a higher percentage of ALP positive hBMSCs produced more deposited mineral compared to donors containing a lower percentage of ALP positive cells. It has also been shown that bone-forming cells have a higher ALP activity than non-bone forming cells (Agata *et al.* 2010).

This study shows that typical osteogenic media is able to upregulate osteogenic markers in HDFs however, the extent of their potential as a source of bone cells is still unknown. Studies comparing the osteogenic potential of DFs and other mesenchymal stem cells have been rare. He *et al.* (2011) compared the osteogenic potential of dermal fibroblasts with ADMSCs and BMSCs and found similar cell surface marker protein expressions (CD90, CD73, CD105) between all three types. But while DFs had the highest proliferation potential they also had the lowest osteogenic differentiation potential, although they did stain positive for ALP and calcium deposition. They went on to derive a subpopulation of highly purified osteogenic progenitor cells from the dermis using bone morphogenic protein receptor type IB (BMPRIB) immunogenic sorting. In another study, ADMSCs and HDFs were also examined for their phenotypic and differentiation characteristics by Blasi *et al.* (2011); both of which were found to equally express CD90, CD44, CD105 and possess similar osteogenic capabilities.

In contrast to these previous results, a number of studies have shown that while DF populations express surface antigens similar to MSCs, they are not able to differentiate into an osteogenic phenotype (Wagner *et al.* 2005). Differences between

studies may include variation in the frequency of osteogenic progenitors in the initial isolation as well as tissue source and donor age. It is also possible that bone-forming cells are lost during culture and passaging, or that progenitor cells senesce and lose their osteogenic abilities. DFs are a heterogeneous population containing progenitor cells with varying magnitudes of differentiation potential, along with lineage committed fibroblasts (Chen *et al.* 2007).

Other important features of MSCs are their immunosuppressive, anti-inflammatory and angiogenic potential, which are important regenerative properties. Blasi *et al.* (2011) showed that ADMSCs posses stronger angiogenic and anti-inflammatory activity than HDF cell lines. This may partly explain why dermal fibroblasts are less efficient in promoting wound healing then MSCs. However, primary dermal fibroblasts have been found to have a population of cells within them that are pre-angiogenic (Krajewska *et al.* 2011).

3.5.3 Summary

- HDFs may contain a population of osteogenic progenitors, which were able to upregulate ALP and deposit mineral in osteogenic media.
- The ability of HDFs to deposit mineral *in vitro* reduced after P3 and disappeared almost completely at P6 (D21).
- These cells have the potential to be a source of osteogenic progenitor cells.
- Future work will concentrate on HDFs ≤P3.

3.6 Mechanical stimulation using a simple rocking platform

One of the major forces that contribute to the mechanical environment of bone cells are oscillatory fluid-flow induced forces caused by fluid movement through interstitial bone space caused by repetitive loading and unloading of the bone. Bone cells have been shown to be highly responsive to fluid flow *in vitro*, showing an upregulation of may osteogenic markers including osteocalcin (OC), osteopontin (OP), BMP2 and 7, bone sialoprotein (BSP), PGE_2, ALP, Col I (McCoy and O'Brien 2010). A number of studies have shown that constant mechanical stimulation of cells can lead to tolerance of the cell to the load. To overcome this cellular desensitization,

some researchers have inserted rest periods or periods of low flow, which seems to be beneficial for many osteogenic genes.

While it is has been established that mechanical forces can influence bone cell differentiation, it is still not clear what the best conditions are to achieve this. This is mainly due to the number of parameters that are relevant – the magnitude, frequency and duration of the stimulus, the number of rest periods, the point of initiation, and the culture conditions e.g. chemical supplements. Therefore, a simple system that is capable of mechanically stimulating a large number of samples and testing a wide variety of parameters would be ideal.

A rocking 'see-saw' system holding culture wells containing media is able to create fluid shear stresses (FSS) by gravitational media movement that may be suitable for stimulating cells. This simple system is an easily accessible device that can accommodate large numbers of samples and has many advantages over other more commonly used apparatus including; smaller amounts of medium per sample, cheap and easy operation, no special chambers required and high throughput. It can potentially be used outside of an incubator for intense, short bouts of loading, or inside for long term, low intensity stimulation without interruption.

MLO-A5 bone cells were chosen for use in the work as previous studies in our group have shown that MLO-A5 cells are sensitive to short bouts of loading (Morris *et al.* 2010; Sittichockechaiwut *et al.* 2009). MLO-A5s are thought to represent a fully differentiated late-stage osteoblast or an early-stage osteocyte and have been shown to rapidly mineralise in culture even in the absence of βGP (Kato *et al.* 2001) Therefore they are ideal for studying the short-term and long-term mineralised matrix deposition response of bone cells to load.

The aim of this work was to firstly observe the potential of the rocking platform to influence the differentiation of MLO-A5 cells by monitoring total DNA, ALP activity and collagen and calcium deposition over 21 days. The second aim was to test a number of different loading parameters on the mineral forming ability of MLO-A5s seeded at two seeding densities over a shorter culture period of 12 days.

3.6.1 Results: long-term loading
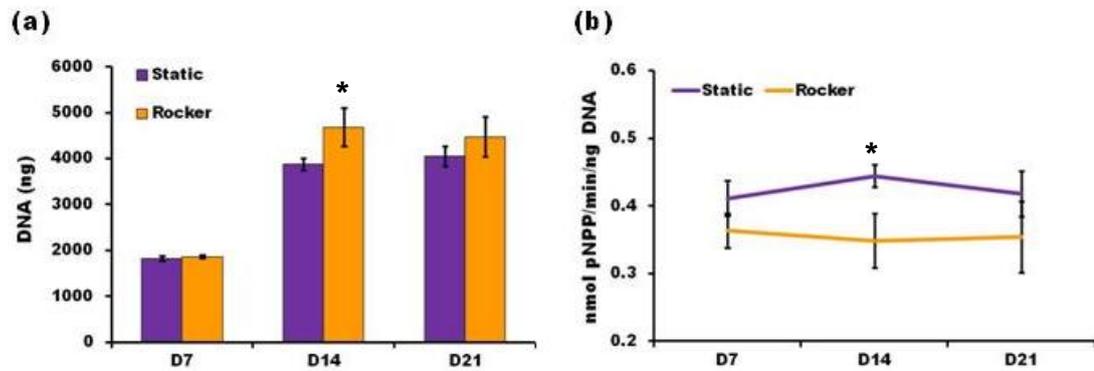
Figure 3.6.1: Total DNA (a) and normalised ALP activity (b) of MLO-A5 cells assayed at days 7, 14 and 21 after static culture or rocking. Data is mean ± SD (n = 6). *$P < 0.05$.
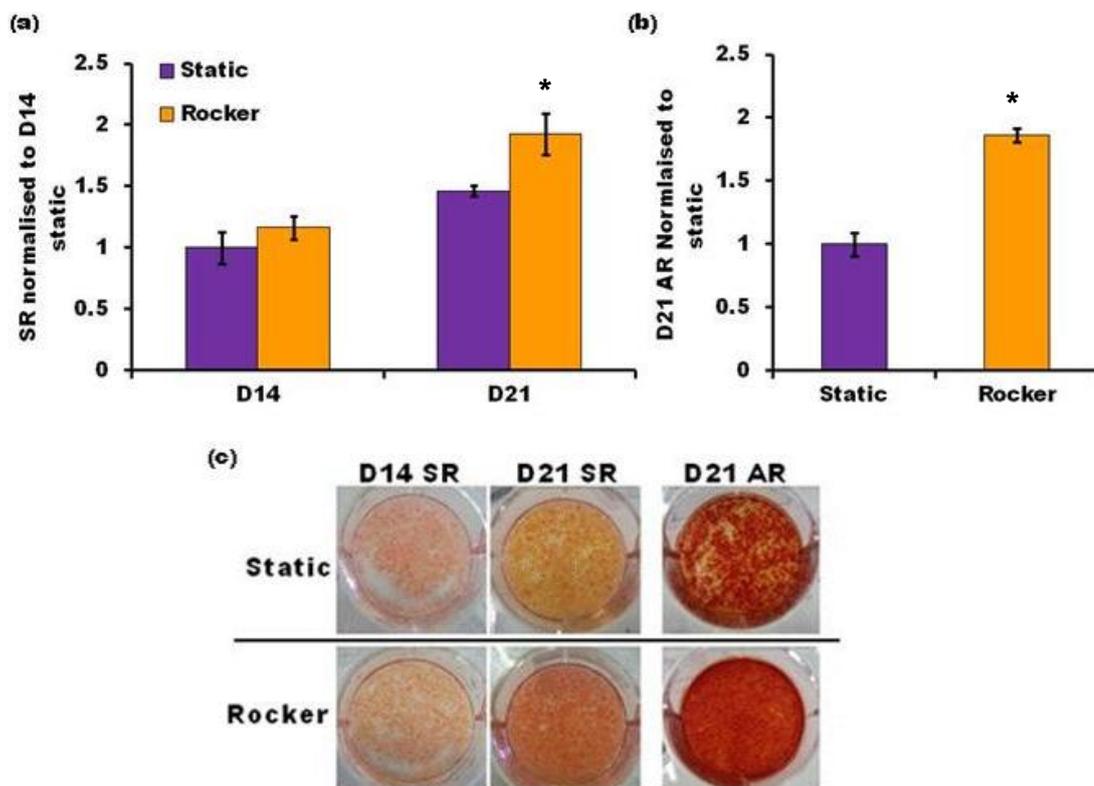
Figure 3.6.2: Collagen staining by Sirius red at days 14 and 21 (a), and calcium staining by Alizarin red at day 21 (b) of MLO-A5 cells after static culture or rocking (45 cycles/min, 1 h/day for 5 days/week). SR and AR staining can be visualised (c). Data is mean ± SD (n = 6-9). *$P < 0.05$.

MLO-A5 cells were subjected to bouts of rocking starting from day 3 (45 cycles/min, 1 h/day, 5 days/week) or cultured under static conditions. Total DNA

115

was significantly higher in rocked cells at day 14 than those cultured in static (Fig. 3.6.1a). Cells subjected to oscillatory FSSs had lower ALP activity at all time points compared with static controls (Fig. 3.6.1b) and this was significant at day 14 ($p<0.05$). Collagen production was slightly higher in rocked samples at day 14 but by day 21, cells subjected to FSSs had produced 33 % more collagen and had a 2-fold increase in deposited calcium compared with static controls, both of which were significant ($p<0.05$) (Fig. 3.6.2b). Alizarin red staining of MLOA5 cells at day 21 showed that static controls had patchy calcium deposits while rocked cells showed a more uniform deposition across the whole of the well (Fig. 3.6.2c).

3.6.2 Results: Short-term loading and variable loading parameters

Six different loading regimes were used to stimulate MLO-A5 cells (Table 3.6.1) by changing a number of loading parameters including; the number of cycles; the time of daily stimulation; the insertion of rest days; and initiating loading in the first or second half of the culture period.

Figure 3.6.3 shows calcium deposition (AR staining) by MLO-A5s at day 12 after static culture or one of the six rocking regimes. For all rocker regimes at both cell densities, there was a significant increase in calcium deposition compared with their respective static controls ($p<0.05$). For 10, 000 cells, regimes 2 and 6 had the highest amount of deposited calcium (Fig. 3.6.3a). For 25, 000 cells, regime 4 had the highest amount of deposited calcium (Fig. 3.6.3b). As well as a denser stain, all rocker regimes had a more uniform stain across the well compared with static samples especially regimes 2 and 6 for 10, 000 cells and regimes 1, 2, 4, and 5 for 25, 000 cells.

Regime	Cycles/min	Time (h)	Rest Days	Load days
1	45	1	N	D3-10
2	45	2	N	D3-10
3	45	1	Y	D3-5, 8-10
4	30	1	Y	D3-5, 8-10
5	45	1	Y	D2-6
6	45	1	Y	D6-10

Table 3.6.1: Loading regimes for testing the effects of oscillatory FSS on calcium deposition response by MLO-A5 cells using a rocking platform.
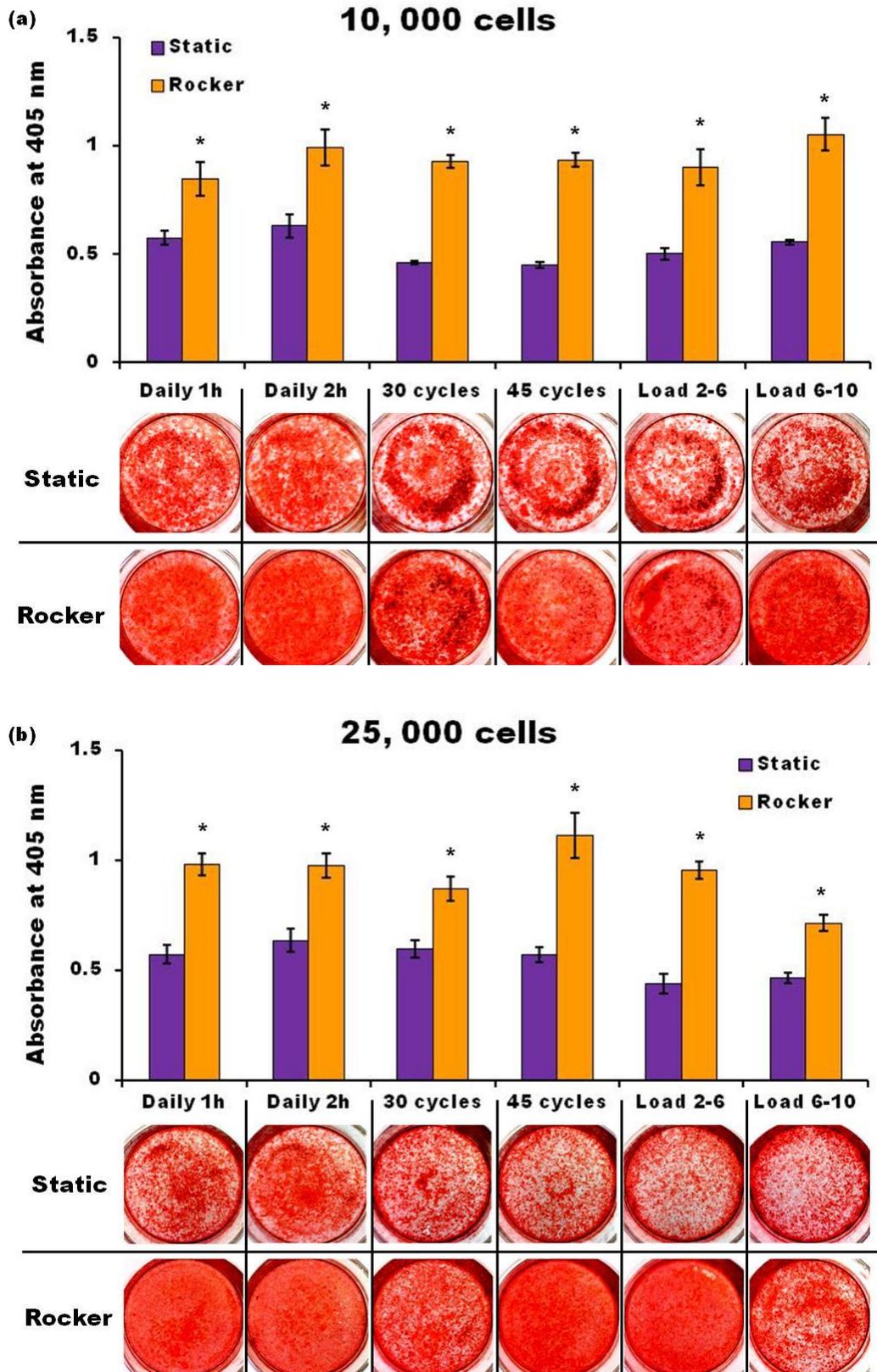
Figure 3.6.3: The effect of FSS produced during different loading regimes using a simple rocking platform on calcium deposition by MLO-A5s seeded in 2D at 10, 000 (a) or 25, 000 (b) cells/well. Deposited calcium was assayed at day 12 using AR staining and can be visualised for each condition below the respective bar data. Data is mean ± SD (n = 6). *P <0.05 verses respective static control.

Calcium deposition was also normalised to static controls for each regime to take into account the differences between static regimes (Fig. 3.6.4). Noticeable differences were observed not only between rocker regimes for a given cell density but also between cell densities for the same rocker regime. For 10, 000 cells, normalised calcium was higher for samples with rest periods compared with daily loading. For 25, 000 cells, normalised calcium was also higher with rest periods compared with daily loading and increasing the cycle number also caused an increase in deposited calcium. Loading the cells in the first half of culture was more beneficial than loading cells in the second half of culture. Significant differences for calcium deposited between cell densities were observed for daily 1 hour loading, 30 cycles/min, and initiation of loading in the first or second half of culture.
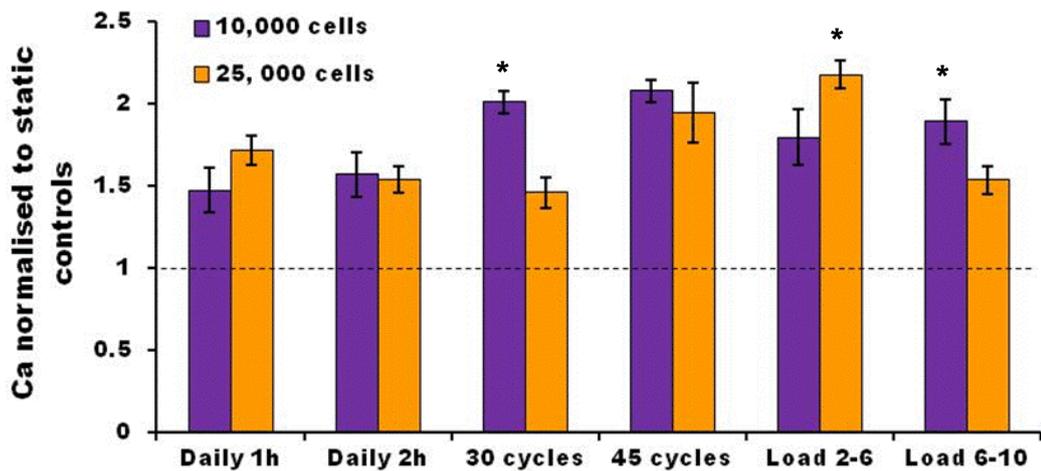
Figure 3.6.4: Calcium deposited by MLO-A5 cells in response to different rocking regimes was normalised to respective static controls for both 10, 000 and 25, 000 cell-seeding densities. assayed at day 12 using Alizarin red S staining. Data is mean ± SD (n = 6). *P <0.05* is reported for significant differences between cell densities rocked using the same conditions.

3.6.3 Discussion

Zhou *et al.* (Zhou *et al.* 2010) estimated that the shear stresses experienced at the bottom of a standard 6-well using a rocking platform are in the range of $5\text{-}10 \times 10^{-2}$ Pa. In 2D fluid flow systems, the range of fluid shear stresses that appear to best stimulate bone cell differentiation is 0.5-1 Pa whereas in 3D fluid flow culture, most researchers have used shear stresses in the range of $1\text{-}5 \times 10^{-2}$ Pa, which are two orders of magnitude lower than most 2D experiments (McCoy and O'Brien 2010). A range of shear stresses as low as 1×10^{-4} and as high as 1.2 Pa are able to increase

expression of ALP, PGE$_2$, OPN, OC, RunX2 and Col I, as well as increased mineralised matrix production (Cartmell *et al.* 2003; Jaasma and O'Brien 2008; Sikavitsas *et al.* 2005). Therefore, this system seems suitable for stimulation of osteogenic cells.

Most researchers allow for 24-72 hours attachment time before subjecting cells to flow. However, the results show that cells may benefit from early loading when cells are confluent as with 25, 000 cells. Differences in the responses of different cell densities may be attributed to cell-cell contacts. 25,000 cells reach confluence within 24 hours whereas 10, 000 cells take around 96 hours.

3.6.4 Summary

- Gravitational fluid flow created by a simple rocking platform system is suitable for stimulating osteogenic cells.
- Long term and short term loading resulted in an enhancement of ostoegenic differentiation in MLO-A5 cells.
- Varying the loading parameters resulted in different load-induced responses of MLO-A5 cells.
- This system is a simple, high-throughput technique that could be used for numerous applications involving the use of fluid flow stimulation including;
    - Stimulation of osteoprogenitor cells
    - Studying fluid flow effects on matrix organisation
    - Studying mechanotransduction mechanisms
    - Testing a wide range of loading and culture parameters
- Future work will use this system for some of the applications mentioned above.

CHAPTER FOUR: The effect of scaffold fibre orientation on the behaviour and collagen organisation of fibroblasts

4.1 Introduction

The micro-architecture of many human tissues is dictated by controlled cellular alignment, which determines the biological and mechanical function of the tissue. In order to replicate this, it is important that tissue engineered constructs mimic the 3D architecture *in vivo*.

There are a number of techniques that have been developed with the aim of controlling cellular behaviour on both the micro- and nano-scale (Khademhosseini *et al.* 2006) by controlling the cell environment. There are many examples of where defined micro- and nano-architectures have been generated by chemical or topographic patterning on 2D surfaces to control cellular alignment and behaviour (Dalby *et al.* 2007b; Hasirci and Kenar 2006), however these do not reflect the 3D nature of most *in vivo* tissues and translating these technologies into 3D scaffolds remains a major challenge.

3D tissue engineered constructs typically consist of cells seeded into synthetic or natural scaffolds that may be in the form of a hydrogel or a porous structure with the aim of forming a 3D network of cells and matrix (Khademhosseini *et al.* 2009). However, many scaffold types are unable to precisely control cell behaviour and this means there is no well-defined cellular organization, which ultimately results in poor ECM organization compared with native tissue. Scaffold porosity (the space available for cell growth and matrix deposition) and pore size plays a significant role in allowing cell infiltration and nutrient diffusion. Scaffold fabrication techniques like salt leaching and lyophilisation often generate pore sizes that are on the order of hundreds of microns (Lee *et al.* 2005b; Menard *et al.* 2000), and this results in cells stretching out along the pore wall as if it was a 2D flat or slightly curved surface. It has been suggested for bone that the optimal pore size for cell growth and bone formation is >300 μm to allow for sufficient nutrient diffusion (Karageorgiou and Kaplan 2005). However, voids of this size are difficult for cells to bridge. In the body, most cells have multiple attachments to different points within a 3D

architecture, which enables them to migrate and proliferate as well as facilitating controlled secretion of matrix.

Collagen is strong in tension and how it is organised ultimately determines the mechanical properties of the native tissue. Therefore, monitoring collagen production by cells in culture is of great importance and this ideally requires a technique that is minimally-invasive. Collagen is a strong emitter of SHG and the intensity of the signal produced depends on how much collagen has been deposited and how well organised it is (bundle size and orientation). As it requires no sample preparation, the collagen is imaged in its secreted form.

It has been shown previously that fibroblast orientation controls the alignment of cell-secreted collagen (Wang *et al.* 2003). Therefore, in order to control cell orientation and subsequent matrix organisation, the use of a construct with a controllable architecture that matches the relevant anatomical architecture is ideal. When human ligament fibroblasts (HLFs) were seeded on aligned nanofibres, they adopted an elongated spindle shape orientated in the fibre direction (Lee *et al.* 2005a). Significantly more collagen was also synthesised on aligned nanofibers compared with randomly orientated ones, which was also organised in the fibre direction. This suggests that cellular morphology is a major contributing factor to how ECM is produced and organised, and that matrix orientation could be controlled if the orientation of the cell was controlled.

Therefore, it is hypothesized that by using the electrospun mats with controllable fibre orientation, one could control the cell morphology and subsequent matrix orientation. The fabricated electrospun scaffolds have high porosity and a high surface area to volume ratio, which allows for the attachment of a large number of cells. The fibrous structure also enables cells to attach to multiple fibres in a 3D fashion and migrate across the scaffold.

The main aims of this chapter was to observe how random and aligned PCL electrospun micro-fibres controlled cell behaviour over 21 days and what affect this had on subsequent matrix production and organisation. SHG was used to monitor the production and organisation of collagen at different scaffold depths and scaffold mechanical properties were tested over time to see how the cell-secreted matrix

affected these properties. Fibroblasts were selected for use in this study due to their high collagen producing potential and major role in matrix remodelling of wounds.

4.2 Methods

4.2.1 Culture on electrospun PCL scaffolds

HDFs were seeded on random (7.97 µm) and aligned (8.61 µm) fibrous electrospun PCL scaffolds (see chapter 3) at a density of 100, 000 cells using the ring confinement method. For studies involving quantification of total DNA and collagen, and visualisation of collagen and cell morphology, scaffolds were cut into circles (d = 1.3 cm) with a thickness of 300 µm and dental wire was used to pin down scaffolds to avoid the scaffold folding. For migration studies, scaffolds were cut into circles (d = 3 cm) and cells were seeded in the centre. For mechanical testing, scaffolds were cut into strips 2.5 cm in length and 1 cm in width with a thickness of between 100-150 µm.

4.2.2 Cellular assays

- Cell viability and migration were determined using MTT assay at days 3, 7 and 12.
- Cell morphology: DAPI and Phalloidin TRITC at day 7 and 21.
- Total DNA measurement at days 7, 14, and 21.
- Quantitative collagen staining using 0.1 % Picrosirius red solution at days 7, 14 and 21.
- Qualitative collagen production and organisation using SHG collected at days 14, and 21 at varying depths.
- Mechanical testing of HDF-seeded constructs was performed at days 2, 7, 14, and 21.

4.2.3 Statistics

All experimental assays were performed two or three times in triplicate (n = 6 or 9). Collagen visualisation using SHG (n = 3) was performed on one sample of each condition during each experimental repeat. Cells cultured on random and aligned scaffolds were compared for statistical differences using an unpaired Student's t-test.

Where comparisons of more than two sample means were made, one-way ANOVA followed by Tukey's post-hoc test was performed.

4.3 Results

4.3.1 Cell viability and Migration

Cell viability, assayed by MTT activity, increased with culture time on both scaffold orientations suggesting that cells proliferated over the course of the culture period (Fig. 4.1a). At day 3, cell viability was significantly highest on aligned scaffolds (*p<0.05)* but by day 7 both scaffolds showed similar viability. At day 12, cell viability was almost 2-fold greater on randomly orientated scaffolds which was also a 2-fold increase from day 7, whereas cells on aligned fibres had only increased about 30 % from day 7. Cell migration was observed from images obtained of the soluble purple product formed by the MTT stain (Fig. 4.1b).
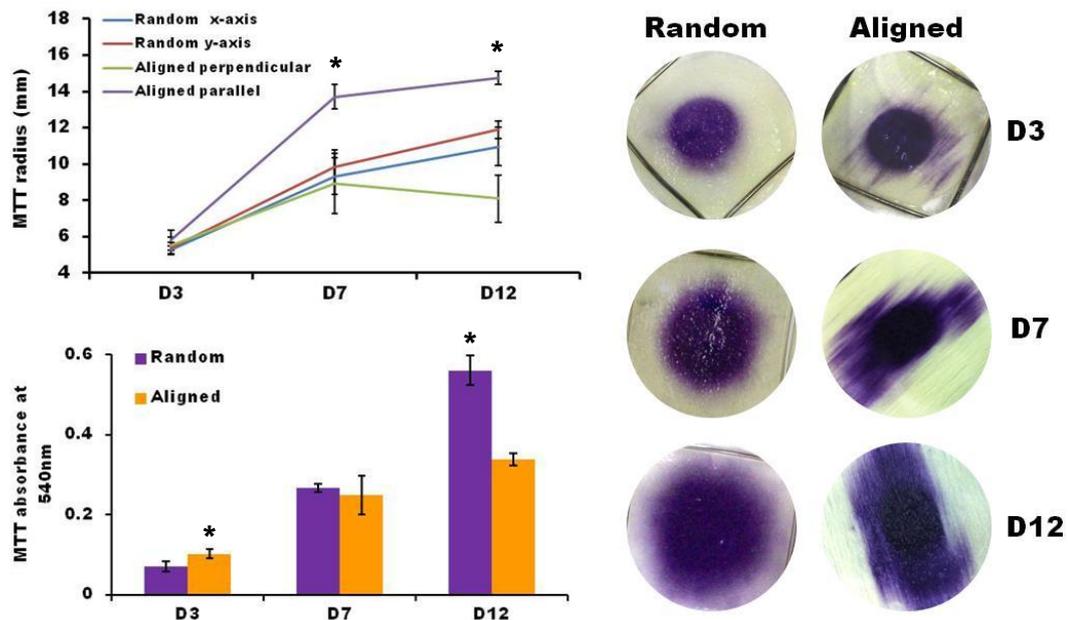
Figure 4.1: HDFs were seeded into the centre of random and aligned fibres and an MTT assay was performed at days 3, 7 and 12 to observe cell migration and viability. Cells on random scaffolds migrated equally in all directions whereas cells on aligned scaffolds preferred to migrate in the direction of the fibre. Data is mean ± SD (n = 6). *P <0.05.*

At day 3, both scaffolds showed a similar circular stain from where the cells were seeded in the metal ring but the stain was darker on the aligned mat and some cells had already appeared to have migrated along the fibre direction slightly. At day 7,

cells on aligned scaffolds had migrated along the fibre direction and had reached the edges of the scaffold, whereas cells on random scaffolds had begun to migrate evenly in all directions increasing the diameter of the stained area almost 2-fold. By day 12, cells on aligned scaffolds had covered the scaffold from end to end in the direction of the fibre orientation, whereas cells on the random mats continued to spread evenly away from the centre of the scaffold.

4.3.2 DNA and Sirius red staining
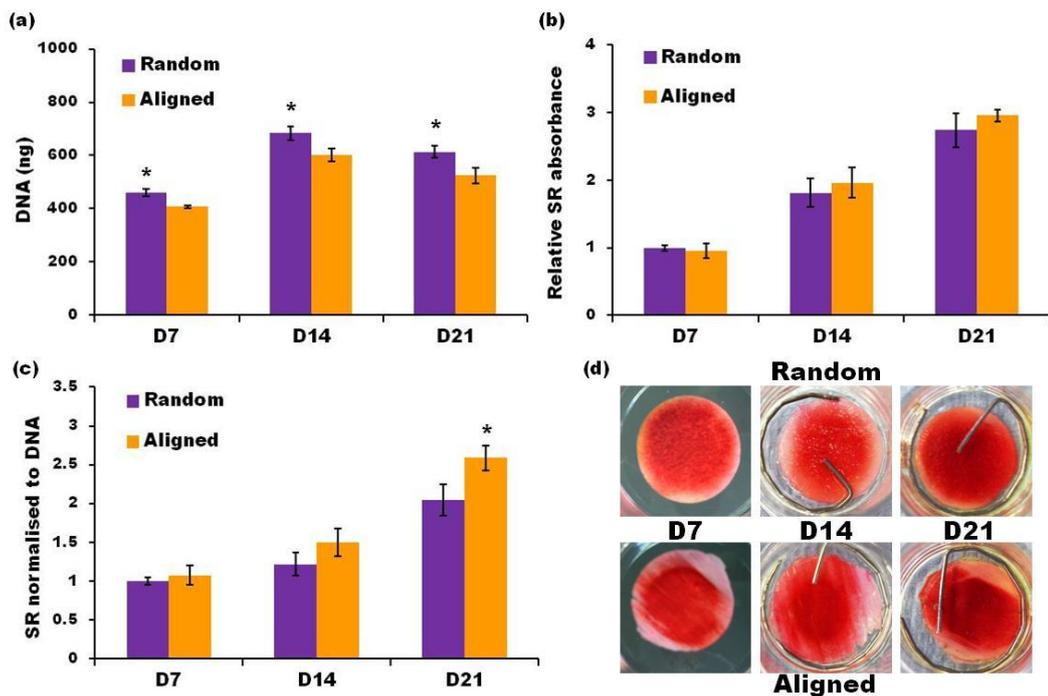
Figure 4.2: HDFs seeded on random and aligned electrospun PCL fibres. Total DNA (a) was highest at all time points for cells on random fibres. Sirius red staining increased on both scaffolds from day 7-21 and total collagen (b) was similar at all time points on both scaffolds. Collagen normalised to DNA showed cells on aligned scaffolds produced more collagen per cell (c). SR staining can be visualised at days 7-21 (d). Data is mean ± SD (n = 6-9). *P <0.05.

Total DNA increased in both scaffold orientations from day 7 to 14 and then reduced slightly at day 21 (Fig. 4.2a). At all time points, DNA levels were significantly higher (*p<0.05)* in random scaffolds by 10-15 % most likely due to greater cell infiltration into the scaffold. Total collagen was assayed at days 7, 14 and 21 and the amount of collagen deposited increased in both scaffolds in a linear fashion over the course of the culture period (Fig. 4.2b). Total collagen deposition was similar at all time points between cells on both scaffold orientations. However, when total

collagen was normalised to DNA content, cells on aligned scaffolds had higher levels at day 14 and significantly higher levels at day 21 (*p<0.05*) (Fig. 4.2c) suggesting that cell alignment induces more collagen production per cell than cells on randomly orientated fibres. Sirius red staining can be seen to cover the scaffold evenly by day 21 on random fibres but only covered the scaffold from end to end in the fibre direction from where the cells were seeded on aligned scaffolds (Fig. 4.2d).

4.3.3 Cell Morphology
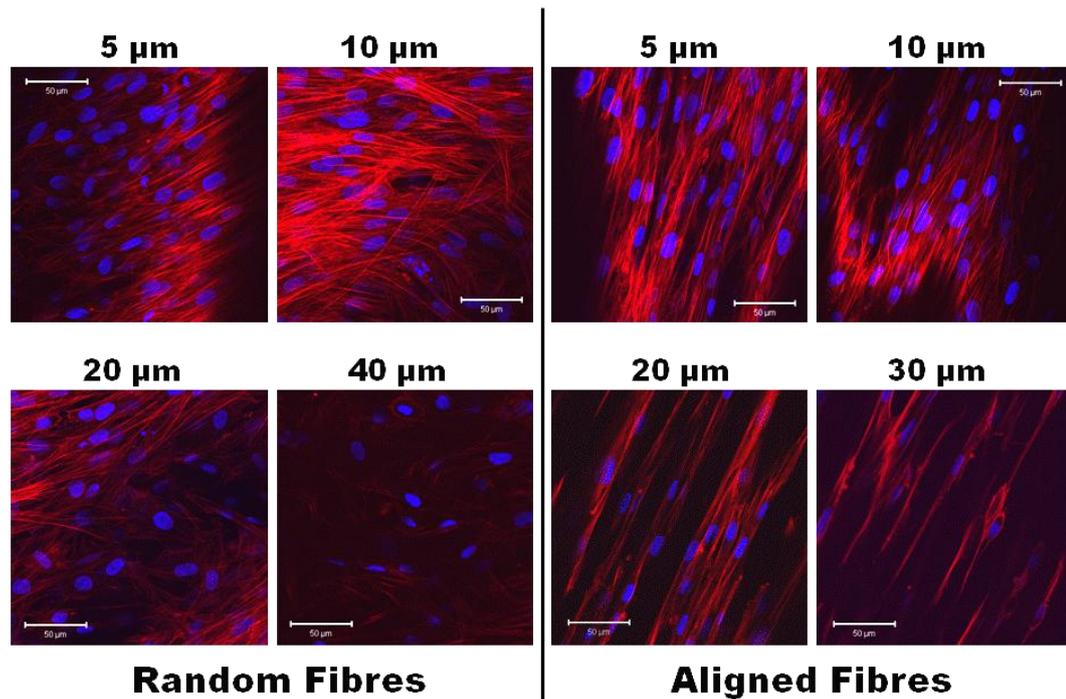
Figure 4.3: Cell nucleus (DAPI in blue) and cytoskeleton (phalloidin TRITC in red) of HDFs seeded on random and aligned scaffolds at day 7 imaged at different depths. Cells on random fibres had spindle shaped morphologies at the lower depths (5-10 μm) but were branched out across multiple fibres at deeper depths (20-40 μm). Cells on aligned fibres had spindle shaped morphology at all depths and were aligned in the direction of the fibres.

At day 7, cells seeded on random fibres showed different morphologies depending on the depth at which they were found in the scaffold (Fig 4.3). On the top surface of the scaffold (5 μm), cells were spindle shaped, tightly packed, and appeared orientated though the direction of cell orientation changed across the scaffold (not shown). At 10 μm deep, cells were spindle shaped and also star shaped as some cells were attached to multiple fibres causing them to branch out. At 20-40 μm deep, most of the cells were attached to multiple fibres and spread out in a star shape with the

number of cells decreasing with increasing depth. On aligned fibrous mats, cells were also spindle shaped on the surface (5 µm) but were more elongated than cells on random mats and also orientated in the direction of fibre alignment. This was also observable at 10-30 µm deep but at 20-30 µm, HDFs were also observed to have attached to individual fibres and elongated further still. Cell number also reduced with increasing depth. Cells on aligned fibres were not observed 40 µm deep.

Cells imaged at day 21 (Fig. 4.4) on the random scaffolds showed a similar trend in cell morphology at all depths compared with day 7 but more cells were now observable with depth. On the aligned fibres, while most cells were still orientated in the fibre direction at depths of 5-20 µm, there were also a number of cells that no longer aligned with the fibres suggesting that cellular orientation was being lost. At 40 µm cells were still orientated in the fibre direction.
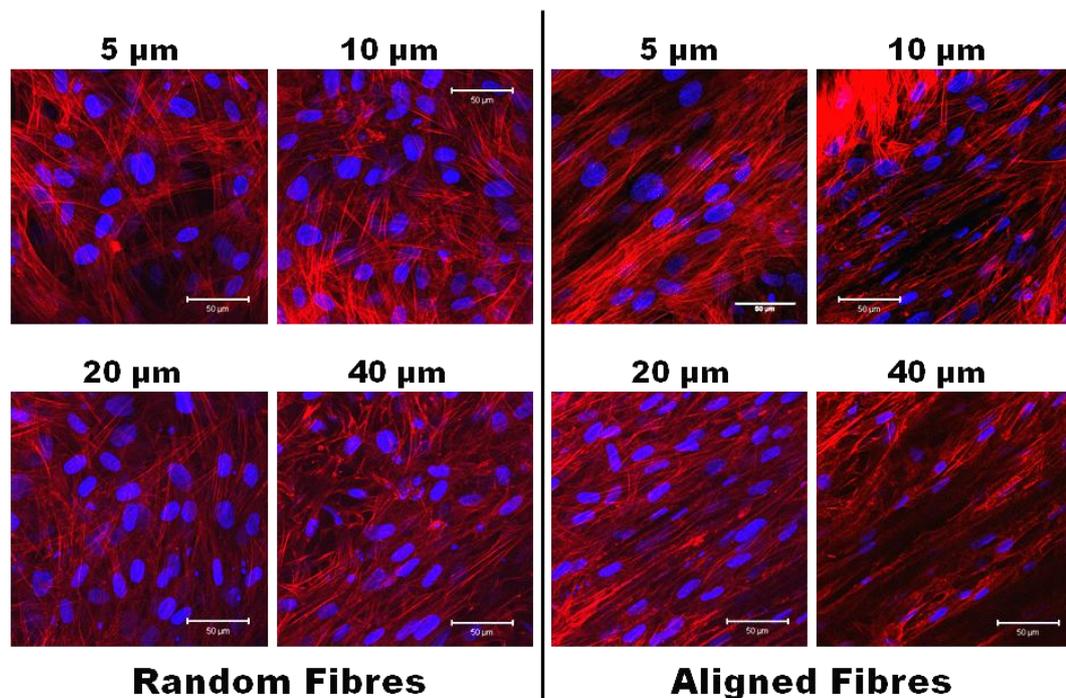
Figure 4.4: Cell nucleus (DAPI in blue) and cytoskeleton (phalloidin TRITC in red) of HDFs seeded on random and aligned scaffolds at day 21 imaged at different depths. Cells on random fibres had a branched star shaped morphology at all depths. Cells on aligned fibres were mostly still spindle shaped and aligned in the fibre direction but some cells were no longer orientated.

4.3.4 Second Harmonic Generation of collagen

SHG was obtained from cell-secreted collagen at different depths on both scaffold orientations at days 14 (Fig. 4.5) and 21 (Fig. 4.6). At day 14, SHG from random scaffolds showed a fibrous matrix with no preferential orientation at all depths. The most intense images were at the 10-20 μm depths, although there was less area coverage at 20 μm. At 20 μm deep, the collagen fibres were spread in all directions. The signal at 40 μm was very weak indicating only a small amount of collagen had been deposited at this depth. On the aligned fibres, SHG showed matrix orientation in the direction of the fibre alignment at all depths and SHG was most intense at 10 and 20 μm depths. At 40 μm deep, there was a faint SHG signal and the collagen was still orientated. Comparing SHG between random and aligned fibres, signal was more intense at all depths on aligned scaffolds, and this was most evident at 10-20 μm, but random fibres appeared to show more area coverage. This indicates that cells on aligned scaffolds could have produced more collagen at these depths or that the collagen was better organised than on random fibres.
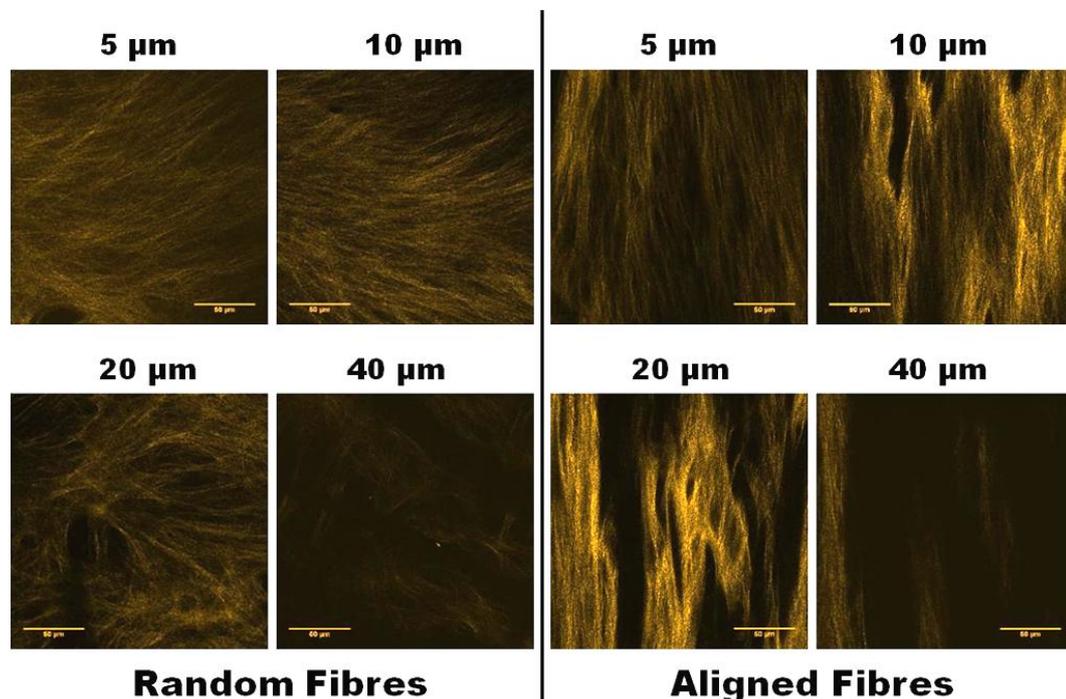
Figure 4.5: SHG images of collagen matrix produced from HDFs seeded on random and aligned scaffolds at day 14 taken from different depths. An increase in SHG intensity suggests an increase in collagen production and/or a more organised collagen fibrous network. Collagen on random scaffolds appears randomly orientated in no preferential direction whereas collagen on aligned scaffolds is organised in the direction of scaffold fibre alignment. Scale bars are 50 μm.
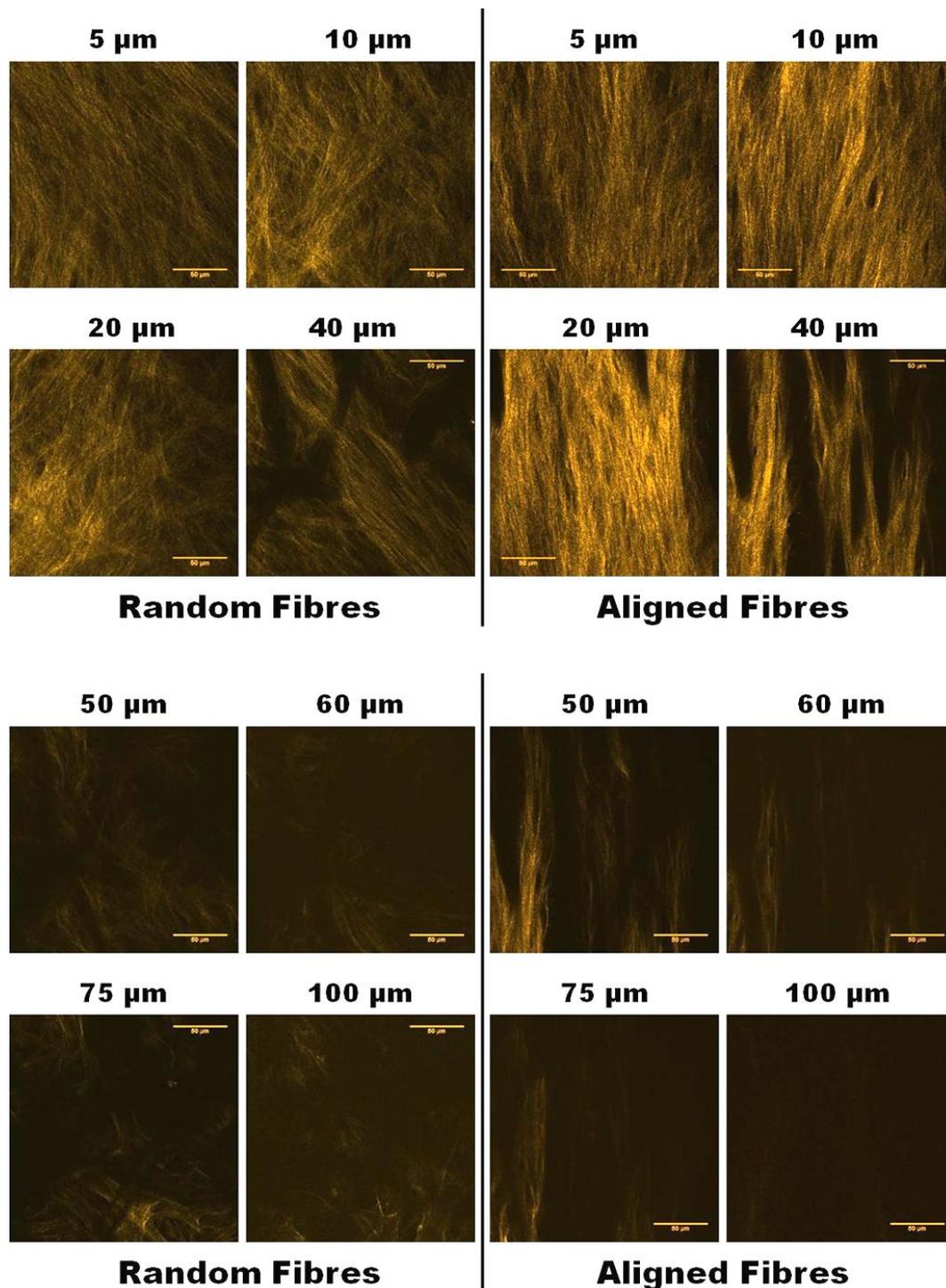
Figure 4.6: SHG images of collagen matrix on random and aligned scaffolds at day 21 at different depths. SHG intensity and area coverage is greater at all depths than the equivalent depths at day 14 suggesting increased collagen deposition and organisation. Collagen on random fibres was randomly orientated while collagen on aligned scaffolds appeared aligned in the fibre direction. Settings for images taken at 75-100 μm on both scaffolds were optimised in order to see collagen SHG. Scale bars are 50 μm.

At day 21, signal intensity and area coverage was increased for both scaffolds at all depths indicating continued collagen deposition and/or organisation over the culture period. As with day 14, at all depths the collagen matrix appeared randomly orientated on random fibres but orientated in the scaffold fibre direction on aligned scaffolds. The greatest intensities for both scaffolds were at the depths of 10-20 μm, and at this time point there was a large increase in SHG intensity at 40 μm deep for both scaffolds. SHG intensity was also greater on the aligned scaffolds at all depths compared with random scaffolds. SHG images were also obtained up to 100 μm into the scaffolds but due to the weak signal using the previous settings, imaging parameters were maximised in order to get as bright an image as possible. Images showed the same trends as before but at 100 μm there appeared to be more collagen present in the random scaffold than the aligned scaffold.

4.3.5 Tensile properties of cell seeded scaffolds

In order to test what effect the deposited matrix had on scaffold mechanical properties, cell seeded scaffolds were tested for the Young's modulus of elasticity (E) and the tensile strength at 50% strain (TS) across the culture period (Fig. 4.7).

As expected, E was highest at all time points on the scaffolds stretched parallel to the fibre direction, then on the random scaffolds, then on the scaffolds stretched perpendicular to the fibre direction. All three scaffold orientations seeded with cells had significantly higher E and TS at all time points compared with scaffolds with no cells, indicating that the cells and deposited matrix made the scaffold stronger. Both E and TS increased with time on all cell seeded scaffolds with the exception of days 2-7 which had similar properties for all scaffolds. For perpendicular scaffolds, there was a dramatic increase in E from days 14 to 21 and a similar trend in the TS from days 7-14. E of randomly orientated scaffolds increased from 3 MPa (no cells) to 7 MPa (day 21 with cells), whereas E of aligned scaffolds showed a much larger increase from 30 MPa (no cells) to over 60 MPa (day 21 with cells).
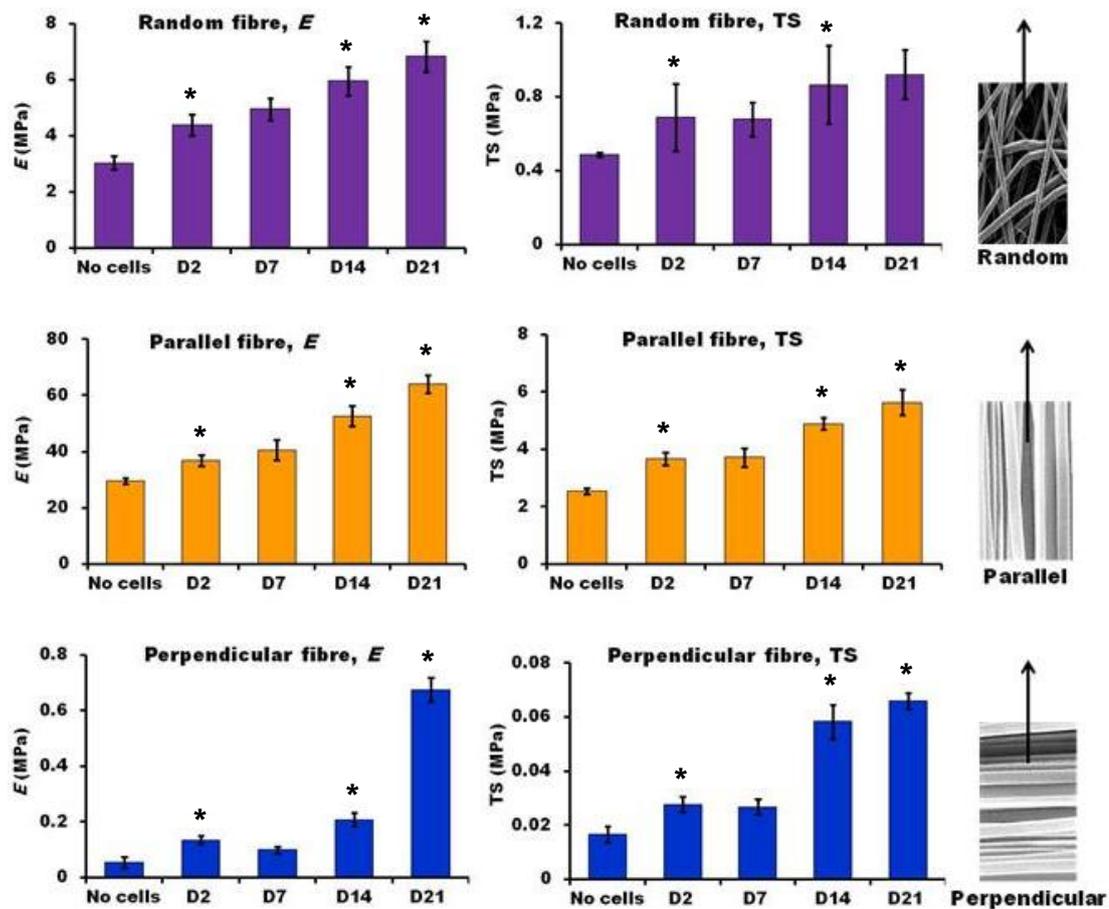
Figure 4.7: Tensile testing was performed on blank and HDF-seeded PCL scaffolds of different fibre orientation to observe scaffold properties at day 0 (no cells) and days 2, 7, 14, and 21 (with cells). Notice the difference in the size of the scales for each scaffold orientation (parallel > random > perpendicular). Images on right hand side indicate respective scaffold orientation along with arrow showing direction of tensile force applied. Data is mean ± SD (n = 6 for random and parallel or n = 3 for perpendicular). *$P <0.05$ verses previous day tested.

4.4 Discussion

In order to develop tissue engineered constructs that are suitable for implantation, it is important that physiological function is replicated as well as tissue mechanical properties. To achieve this, scaffold materials should mimic the native ECM and be able to control cell behaviour and differentiation to match the biological function of the *in vivo* tissue. This study has shown that electrospun PCL scaffolds with controllable fibre orientation can influence cell behaviour which in turn influences collagen production and organisation. This study utilises the minimally-invasive technique of SHG to image collagen production and organisation by cells in fibrous scaffolds over time. SHG was able to show how collagen infiltrates the scaffold with

time and how its deposition and organisation varies at different depths within the construct. The resulting matrix organisation was shown to affect the mechanical properties of the constructs.

Fibrous scaffolds have been shown to promote cellular proliferation and differentiation because cells attach and organize around fibres with diameters smaller than their size (Laurencin *et al.* 2006). Scaffolds composed of randomly orientated or highly aligned fibres replicate two major types of tissue-fibre organisation found within the body. Scaffolds made of randomly orientated fibres generally contained cells that were attached to multiple fibres in a star shape, especially deeper into the scaffold where there were fewer cells. Cells on aligned fibres tended to attach to one individual fibre and were and were spindle shaped and elongated in the fibre direction. On the surface of randomly orientated scaffolds, cells were densely packed and appeared to show cellular alignment; however, alignment did not occur in any favoured direction and changed throughout the scaffold (not shown). Alternating patches of common alignment also occurs on 2D substrates when cells become highly confluent. On aligned scaffolds, cell orientation was determined by the direction of the fibres and so their orientation can be controlled in a precise manner. The deviation of alignment of some cells on the aligned scaffolds close to the surface at day 21 may be due to the cells no longer 'feeling' the fibres and perhaps branching across the other cells. It may be that these scaffolds need some form of mechanical strain, either statically fixed or dynamic, in order to maintain alignment after this time point (Deng *et al.* 2009; Lee *et al.* 2005a).

Induced cellular orientation along well organized fibres has been reported in a number of cell types and it is believed that various integrins are involved in this fiber-induced cell adhesion. Vinculin is an actin-binding protein ubiquitously expressed and used as a marker for both cell-cell and cell-ECM (focal adhesion) adherents-type junctions. HDFs on flat PMMA substrates showed vinculin staining clustered around the cell periphery, however on nanofibres the integrin receptors were scattered across the entirety of the cell located everywhere the cell interacted with a fibre (Liu *et al.* 2009). On microfibres, the integrin receptors were located along the edge of the fibre where the cell was adherent (Liu *et al.* 2009). These results indicate that integrin receptors could easily follow nano-micro surface features. It has also been seen that hASCs seeded on random fibrous mats possessed

short and random focal adhesion plaques whereas cells on aligned fibres had long focal adhesion plaques orientated in the fibre direction (Fu and Wang 2012) as confirmed by vinculin staining.

Alterations in cell shape and cell-matrix adhesions are functionally and physically coupled to the genes by the tissue matrix, and therefore alterations in cell morphology affect cell behaviour and gene expression (Brammer *et al.* 2009). HDF alignment on the highly orientated scaffolds appeared to result in a greater cell elongation than those seeded on random fibrous mats. It has been shown that elongation of the cell cytoskeleton also facilitates distortion and elongation of the cell nucleus, which affects cell differentiation and promotes DNA synthesis (Brammer *et al.* 2009). Although total collagen was equal on both scaffolds at all time points, when this was normalised to DNA, aligned scaffolds had more collagen per cell at day 21. Similar findings have been reported elsewhere, and it has been suggested that this may be due to denser collagen packing on aligned scaffolds due to the collagen fibres aligning with each other (Lee *et al.* 2005a). In a study by Koepsell *et al.* (Koepsell *et al.* 2011), matrix production was seen to increase on scaffolds with increasing alignment especially with regards to collagen**.** However, that study compared scaffolds of differing fibre diameter as well as porosity and so it is not conclusive that alignment alone caused the observed differences in cell behaviour and matrix production.

Cell number (measured by DNA) was higher at all time points on random fibres compared with aligned fibres. This is most likely due to the higher porosity of the random scaffold allowing cells to better infiltrate the deeper regions. However, the increase was only 10-15 % and this may be due to the fact that the cells on the aligned scaffolds pack in more tightly together than on the random fibres due to their common orientation. Also the higher porosity on the surface of the random mats is likely to cause the cells to take more time to form a dense layer compared with on the aligned scaffolds. In this study, cells were seeded into a small area in the centre of a large scaffold to investigate how cells migrate on different fibre arrangements showing that cells prefer to migrate along straight fibres rather than span two fibres or go across from fibre to fibre go, a phenomenon called cell contact guidance theory (Barocas and Tranquillo 1997). While cell proliferation was not directly measured in this work, a cell viability (MTT) assay was performed that can give us an indication

of cell proliferation when its value increases over time. Cell viability started highest on aligned scaffolds (D3) and finished highest on random scaffolds (D12). On random fibres, cells migrate in all directions at a steady rate, whereby cell migration on aligned scaffolds is faster in the fibre direction but very limited across the fibres. Initially, cells migrate fast along the aligned fibres but once they reach the end of the scaffold and run out of space, there is little increase in MTT. Also cells appear to migrate deeper into random fibrous scaffolds than the aligned fibres and so both of these factors are likely to account for the differences in MTT at day 12.

Fibre diameter and pore size are two important physical factors that can control cell behaviour in electrospun fibrous mats and are considered important in replicating proper phenotypic expression (Boland *et al.* 2006). The pore size of as-spun scaffolds made via electrospinning, is controlled mainly by the fibre diameter, with large pore sizes resulting from larger fibre diameters. As fibres become smaller, pore size and porosity of the scaffolds decrease due to increased fibre packing density. Cells are typically between 10 and 100 µm in diameter (Stevens 2005) and so pores must be of sufficient size to facilitate cell migration into the scaffold. A number of studies have shown that as fibre size is reduced cell proliferation tends to increase and matrix gene expression has been shown to be initially higher. On PLGA random fibres, Col I and elastin expression was initially lower in HDFs (day 7) on microfibres compared with nanofibrous but was higher at day 28 (Kumbar *et al.* 2008). One reason for these observations may be that scaffolds with increased fibre diameter have a greater inter-fibre distance meaning the lower fibre surface density makes it more difficult for cells to adhere to neighbouring fibres. The lower porosity of the nanofibrous mats allows faster initial matrix growth before cells bridge the larger gaps of the microfibers. Then due to the higher scaffold porosity there is more space to deposit matrix. In contrast to this, a number of studies have found that cell proliferation and cell density was not sensitive to fibre diameter or orientation (Bashur *et al.* 2006; Lee *et al.* 2005a), while others found that smaller fibres resulted in lower cell densities (Badami *et al.* 2006; Kwon *et al.* 2005). These observations may be a result of the cell type used. It has also been seen that cells align on scaffolds with orientated fibres regardless of fibre diameter (Bashur *et al.* 2006). A study by Lowery *et al.* (2010) showed that the pore size had a greater impact on cell proliferation than fibre diameter. Therefore, it seems that pore size may be the key

factor in determining how well cells migrate across and infiltrate inside a scaffold. In combination with overall porosity, pore size will also ultimately determine how much tissue in-growth there will be. Larger pores also allow for better nutritional supply into the scaffold and so the cells are more likely to survive further into a scaffold with larger pores.

It has been shown that fibre size can influence cell spreading (Badami *et al.* 2006; Bashur *et al.* 2006). Fibroblasts spread out more on microfibres (3.6 µm) compared with nanofibres (0.14-0.78 µm) (Bashur *et al.* 2006). Explanations for diminished cell spreading on submicron fibres are related to the role of the focal adhesion complexes in mediating cell adhesion to biomaterials. Vinculin staining has shown that focal adhesions can be larger than 1 mm (Badami *et al.* 2006; den Braber *et al.* 1998) and so it is possible that submicron fibres undermine cell spreading by limiting focal adhesions size. In addition, the density of cell attachment proteins adsorbed to submicron fibers may be less than that on larger fibres, which would diminish the number of integrin receptors engaged in cell adhesion. There may also be a limit on the size of fibres that can be used. It is believed that cell expression of phenotypic markers is not achievable with the use of scaffolds containing fibre diameters that are equivalent to, or larger than the cell diameter (Murugan and Ramakrishna 2007). Overall, it would seem that electrospun scaffolds need to be fabricated to suite the specific need of the cell type being used and tissue to be constructed with regards to fibre diameter, pore size, and fibre orientation.

The fibres used in this study had a mean diameter of around 8-8.5 µm, and while this is at least an order of magnitude higher than the size of ECM fibres found in most native tissues (50-500 nm) (Screen *et al.* 2004), the cells appeared to grow well across the culture period and deposited a well organised collagen matrix. In tissue such as tendon, collagen fibrils are organised into larger fibres in the micrometer range that are tightly packed in orientated bundles. Therefore, the aligned microfibers used in this study seem quite relevant to the *in vivo* organisation of these tissues. While the fibre diameter was the same for both scaffolds in this study, the pore sizes of random and aligned scaffolds were different. Scaffolds with highly orientated fibres tend to have smaller pores compared with randomly orientated mats due to a higher packing density. They are also narrower and more elongated due to the way the fibres align. This is an uncontrolled variable in the comparison of these

scaffolds, but the high packing density of the aligned fibres is required in order to offer structural integrity to the scaffold. Also, tissues with this high degree of fibre orientation in the body are also always tightly packed together most likely for the same reason.

Fibrous sheets produced by electrospinning are essentially layered in one plane and so continuously depositing fibres on top of each other results in a dense fibre packing towards the middle of the scaffold. This causes pore sizes to decrease towards the centre of the scaffold and makes it harder for cells to infiltrate. There are many tissues in the body that have ECM organised in one plane, such as dermis, and the fibrous network is essentially like a series of layers stacked on top of each other. A strategy of layering up sheets of cell-seeded electrospun scaffolds to allow the construction of a thick 3D construct has been tested (Hong and Madihally 2010). Using this technique, complex architectures can also be formed by layering a combination of different fibre orientations to mimic more complex tissues with depth dependent architectural organisations, for example cartilage (Matcher 2009). It is also possible to increase scaffold porosity by co-spinning with a very fast degrading or water-soluble polymer e.g. PEG (Milleret *et al.* 2011) or using mechanical techniques such as ultrasonication (Lee *et al.* 2011) to force apart fibres thus allowing greater cell penetration and nutrient diffusion. A combination of these techniques may allow for the production of large 3D constructs with controllable porosity and fibre orientation.

Matrix orientation, and more specifically, collagen orientation, dictates the mechanical properties of connective tissues and so it is important that it is organised in a way to mimic the native tissue. In the study, the novel technique of SHG was used to image the temporal production and organisation of collagen at different depths within the scaffolds. Depth imaging of matrix production is important because what we see on the scaffold surface is most likely not what we will see inside the scaffold. Also it will take time for matrix to be produced further in the scaffold (due to cell migration and limited nutrient supply) so it is important that this can be monitored. SHG intensity is dependent on a number of factors including, amount of collagen, fibre diameter, packing density, and orientation (Matcher 2009). It is quite clear that SHG intensity was higher for all depths on aligned scaffolds than on random scaffolds. The collagen matrix appears highly orientated on aligned

scaffolds whereas fibrils appear to orientate in all directions on random scaffolds. The collagen alignment is retained throughout the orientated scaffold whereas it changes throughout the random scaffold.

Mechanical testing showed the influence that the matrix orientation had on the construct mechanical properties. While all scaffolds became stronger with time, parallel tested fibres had the largest increases in E and UT_{50} as a result of the orientated collagen. The E of parallel stretched fibres was 250 times (day 14) and 100 times (day 21) greater compared with perpendicular stretched fibres. Scaffolds tested perpendicular to the fibres had very low properties until day 21, which is the same time point at which some cells on the surface started to change their direction of orientation. Randomly orientated scaffolds were about 10 times less stiff than parallel fibres at all time points supporting the organisation in all directions as seen in the SHG images.

These types of orientated fibrous scaffolds could have great value for use in the engineering of tissues where there is one dominant fibre direction such as in ligaments, tendons, muscles and bone for example. As well as this, fibrous scaffolds with random orientations may be useful for replicating the native ECM of tissues that are not as well orientated but still contain a well organised, dense fibrous network such as skin or the bladder.

4.5 Conclusions and future work

Cell behaviour can be controlled by altering the fibre arrangement of electrospun scaffolds, which seems to have a direct effect on collagen production and organisation. The different fibre architectures that can be produced via electrospinning show promise in the production of scaffolds that mimic the native ECM of many different tissues. Cell orientation resulted in increased collagen production per cell and the organisation of a highly orientated collagen matrix throughout the depth of the construct. This in turn contributed to greater mechanical strength of constructs over time when stretched parallel to the collagen fibril direction compared with perpendicular stretching. At present, scaffold infiltration by cells and subsequent matrix deposition needs improving in order to produce large 3D constructs that are clinically viable. This may be accomplished by combining a

number of techniques involving layering up, increasing pore size, and combining dynamic bioreactors to improve nutrient supply to the scaffold centre. For orientated tissues, it seems likely that some form of mechanical stimulation (static or dynamic) may be required in order to retain cell and matrix alignment and to produce a stronger construct. SHG imaging is an important minimally-invasive tool for monitoring collagen production and organisation. When combined with non-descanned detectors, collagen could be imaged many hundreds of micro-meters into the construct, allowing for greater depth profiling.

4.6 Summary

- Fibre orientation can control cell behaviour including cell alignment, morphology and migration.
- Cells tend to migrate along a straight, uninterrupted fibre rather than across fibres.
- Orientated cells produce more collagen per cell and this is well organised in the direction of scaffold alignment.
- SHG is a minimally-invasive technique that allows monitoring of collagen production and organisation in tissue engineered constructs.
- Collagen orientation dictates the tensile properties of the tissue engineered construct making it stronger parallel to the fibre direction.

CHAPTER FIVE: The effect of scaffold fibre orientation on the behaviour and differentiation of osteogenic progenitor cells

5.1 Introduction

In the body, human MSCs (hMSCs) are known to migrate to sites of inflammation and become incorporated into many different tissue types were they assist tissue repair and regeneration either through the secretion of chemokines or by differentiation into the mature native cell (Rehman *et al.* 2004). MSC differentiation at the wound site is likely to be initiated and directed by cues from the local microenvironment. These complex environments consist of soluble factors, cell-cell interactions and cell-extracellular matrix interactions (Wong *et al.* 2004).

Many tissues in the musculoskeletal system, especially those that are load bearing, exhibit a preferential direction of fibrous matrix alignment organised to resist the load to which they are habitually subjected. These tissues are anisotropic and have different mechanical properties depending on the direction of the mechanical forces with the strongest tensile properties found in the strain direction parallel to the fibre orientation direction. Mature bone tissue has a well organised, hierarchical structure, comprised mainly of collagen fibres and hydroxyapitite mineral, the building blocks of mineralised tissue (Weiner and Wagner 1998). These collagen fibres are preferentially orientated within a layer of bone which are then organised into concentric layers or a helical arrangement. Both components have a definitive role in maintaining the structural integrity of bone. The collagen fibres resist tensile forces and are packed to prevent bending, while the apatite crystals embedded within the fibres resist compressive forces (Summitt and Reisinger 2003). Therefore, being able to recreate this structural anisotropy found in musculoskeletal tissues is an important goal in order to restore proper tissue function and to avoid mechanical mismatch.

MSCs do not reside alongside osteocytes in mature compact bone and so there must be a way of triggering MSC migration to the wound site and their subsequent differentiation. In a healing wound, where progenitor cells are likely to be present, the ECM will resemble a more porous and disorganised structure compared. The bone marrow stroma, where bone progenitor cells reside, is also organised in a very

different way to the osteon environment. With these differences in mind, it seems likely that ECM organisation plays a role in the behaviour and differentiation of progenitor cells. Cell-ECM interactions have been shown to regulate cell behaviour including proliferation and differentiation (Zamir and Geiger 2001). Regulation of osteogenesis in hMSCs has been achieved using cell-ECM contacts (Mizuno and Kuboki 2001; Salasznyk *et al.* 2004), which triggered osteoblastic-specific expression of alkaline phosphatase (ALP), eventually leading to the formation of a mineralized collagenous matrix.

The successful differentiation of MSCs along the musculoskeletal lineages has been achieved on electrospun fibres (Li *et al.* 2005; Yoshimoto *et al.* 2003)**.** There have been numerous studies that have demonstrated the suitability of PCL scaffolds for supporting MSC proliferation differentiation into an ostoeblastic phenotype (Yoshimoto *et al.* 2003) *in vitro*. Aligned synthetic electrospun fibrous scaffolds could be potentially very useful for mimicking the orientated collagen fibres that are found in bone matrix. On the other hand, random electrospun fibres could be more representative of a disorganised, developing wound model.

It has been established that surface topography on the micro- and nano-scale can influence cell behaviour. With regards to orthopaedic applications, osteogenesis in osteoprogenitor and mesenchymal stem cells has been induced using topographical cues (Dalby *et al.* 2007b; Kumar *et al.* 2011). Previous *in vitro* studies have also shown that osteogenic differentiation of MSCs can be influenced by scaffold fibre diameter and orientation. Rat MSCs were seeded on non-woven fibres with different diameters (2-42 μm) showing ALP activity and osteocalcin gene expression to be greatest on fibres with diameters of 9-12 μm (Takahashi and Tabata 2004). hMSCs seeded on aligned collagen thread scaffolds had a significantly lower osteocalcin expression at day 14 compared with hMSCs seeded on random threads (Kishore *et al.* 2012). The influence of the orientation of electrospun microfibers on the osteogenesis of MSCs has rarely been investigated and to our knowledge there are no longer term studies on how fibre orientation affects matrix deposition and organisation.

The main aim of this chapter was to study the influence that electrospun PCL fibre orientation had on the behaviour, osteogenic differentiation, and matrix production

of progenitor hESMP cells. In addition to this, matrix organisation and construct mechanical properties were also investigated. A small number of comparisons between TCP and PCL fibres were also made. We were also interested in comparing the response of the mature bone cell line MLOA5, cultured on the same fibres, to see if different stages of cell maturity resulted in a preference for different fibre orientations.

5.2 Methods

5.2.1 Cell culture

The human embryonic cell-derived mesenchymal progenitor cell line (hESMP) was used between passages 3-7 for all assays. The mature bone cell line MLOA5 (P25-30) was used as a model of a mature osteoblast for comparison with the hESMPs.

5.2.2 Culture on electrospun fibrous scaffolds

Cells were seeded on random (7.97 µm) and aligned (8.61 µm) fibrous electrospun PCL scaffolds (see chapter 3) at a density of 150, 000 cells using the ring confinement method. For studies involving quantification of total DNA, ALP activity, collagen and calcium, and visualisation of cell morphology, collagen and SEM imaging, scaffolds were cut into circles (d = 1.3 cm) with a thickness of 300 µm and dental wire was used to pin down scaffolds to avoid the scaffold folding. At day 1, basal media was changed to either NM or OM for hESMPs and NM for MLOA5 cells. For migration studies, scaffolds were cut into circles of 3 cm diameter and cells were seeded in the centre. For mechanical testing, scaffolds were cut into strips 2.5 cm in length and 1 cm in width with a thickness of between 100-150 µm.

5.2.3 Cellular assays

- Cell viability and migration were determined using MTT assay at days 5, 10 and 15.
- Cell morphology: DAPI and phalloidin TRITC at day 7 visualised by Image Express™ fluorescent microscope.
- Total DNA measurement at days 7, 14, and 21 for hESMPs; and at day 12 for MLOA5s.
- ALP activity at days 7, 14, and 21 for hESMPs; and at day 12 for MLOA5s.

- Quantitative collagen staining using 0.1 % Picrosirius red solution at days 14 and 21 for hESMPs; and day 12 for MLOA5s.

- Quantitative deposited calcium staining using 0.5 % Alizarin red S at days 21 and 28 for hESMPs; and day 12 for MLOA5s.

- Qualitative collagen production and organisation using SHG collected at days 14, and 21 for hESMPs. Images were obtained at sample depths of approximately 10 and 20 µm.

- SEM images were obtained for hESMP-seeded constructs at days 21 and 28; and at day 12 for MLOA5s.

- Mechanical testing of hESMP-seeded constructs, cultured in OM was performed at days 2, 7, 14, and 21.

5.2.4 Statistics

All experimental assays were performed two or three times in triplicate (n = 6 or 9). Collagen visualisation using SHG (n = 2) and SEM imaging (n = 3) were performed on one sample of each condition during each experimental repeat. Cells cultured using the same media were compared for statistical differences between random and aligned scaffolds using an unpaired Student's t-test. Where comparisons of more than two sample means were made, one-way ANOVA followed by Tukey's post-hoc test was performed.

5.3 Results

5.3.1 Effect of fibre orientation on MLOA5 cells

MLO-A5 cells adopted different cell morphologies depending on the fibre orientation (Fig. 5.1). On random fibres, cells were more spread out and had a star-like shape while attached to multiple fibres. On aligned scaffolds, cells were spread along individual fibres in the direction alignment adopting a spindle shape.

At day 12 of culture, total DNA was highest in random scaffolds compared with aligned but this was not significant (Fig. 5.2a). ALP activity normalised to DNA was 20 % higher in cells cultured on random scaffolds compared with aligned scaffolds ($p<0.05$) (Fig. 5.2b). Total collagen content assayed by Sirius red staining was significantly higher on random scaffolds compared with aligned ($p<0.05$) but when

this was normalised to total DNA there was no difference (Fig. 5.2c-d). Total deposited calcium was significantly higher in aligned fibrous scaffolds than on random scaffolds ($P<0.05$) and this was also the case when normalised to DNA (Fig. 5.2e).
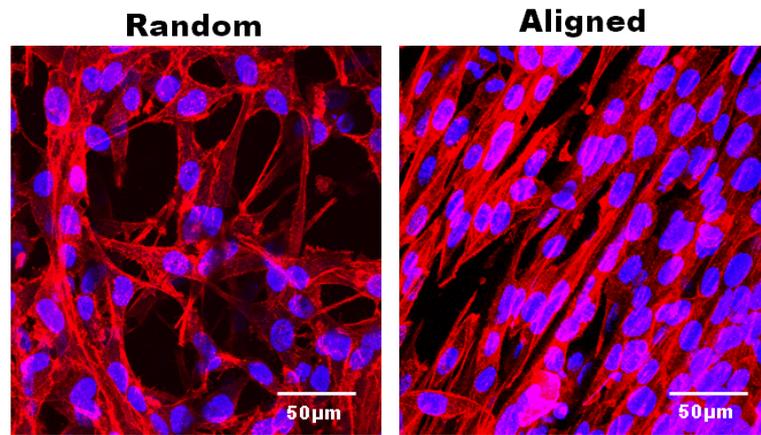
Figure 5.1: Morphology of MLO-A5 cells on random and aligned electrospun PCL fibres at day 5 of culture. Cell nucleus (DAPI -blue) and actin cytoskeleton (Phalloidin TRITC-red) shows distinctly different cell morphologies on random and aligned fibres. Representative images are shown (n = 3).
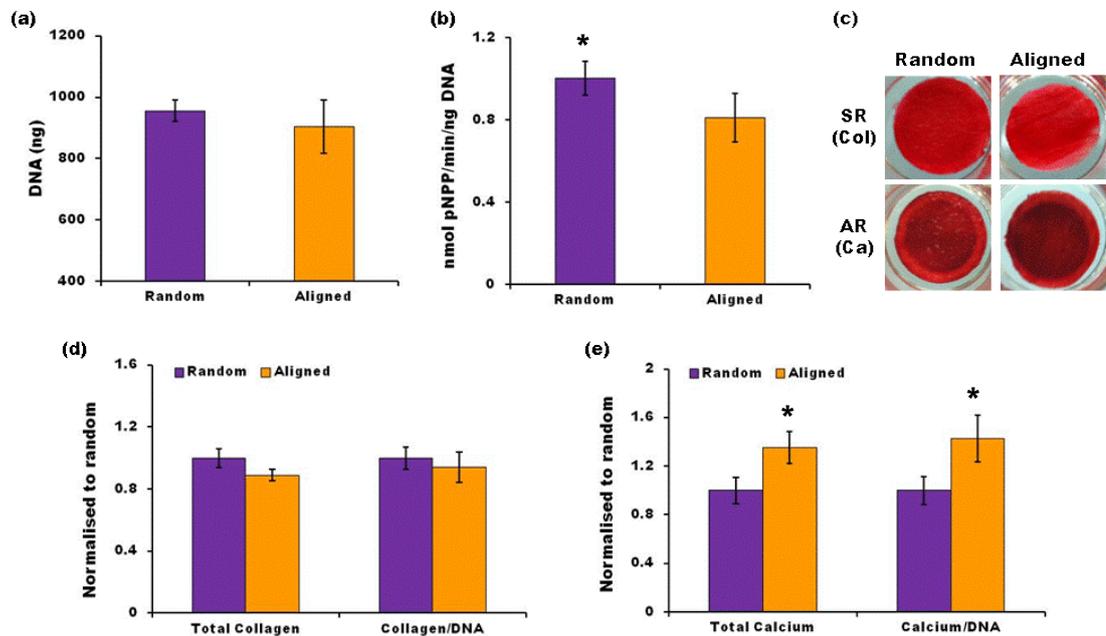
Figure 5.2: MLOA5 cells cultured for 12 days on random or aligned electrospun PCL fibres were assayed for total DNA (a), ALP activity (normalised to DNA) (b), and stained for collagen production (c and d) and calcium deposition (c and e). All data is mean ± SD (n = 9). *P < 0.05.

SEM images collected at day 12 showed that on both types of scaffold, there was a confluent layer of cells covering the scaffold surface and closer inspection showed cells had penetrated into the scaffold (Fig. 5.3). There appeared to be no preferential direction of cell alignment on random fibrous scaffolds, however, on aligned scaffolds cells appeared to be orientated in the direction of the fibres. On both scaffolds, thin matrix fibres can be seen and these appear to be more orientated in a preferred direction on the aligned scaffold compared with the random. Also on the aligned scaffold there is more visible mineral compared with the random scaffold, which also appears to be deposited along the direction of fibre orientation.
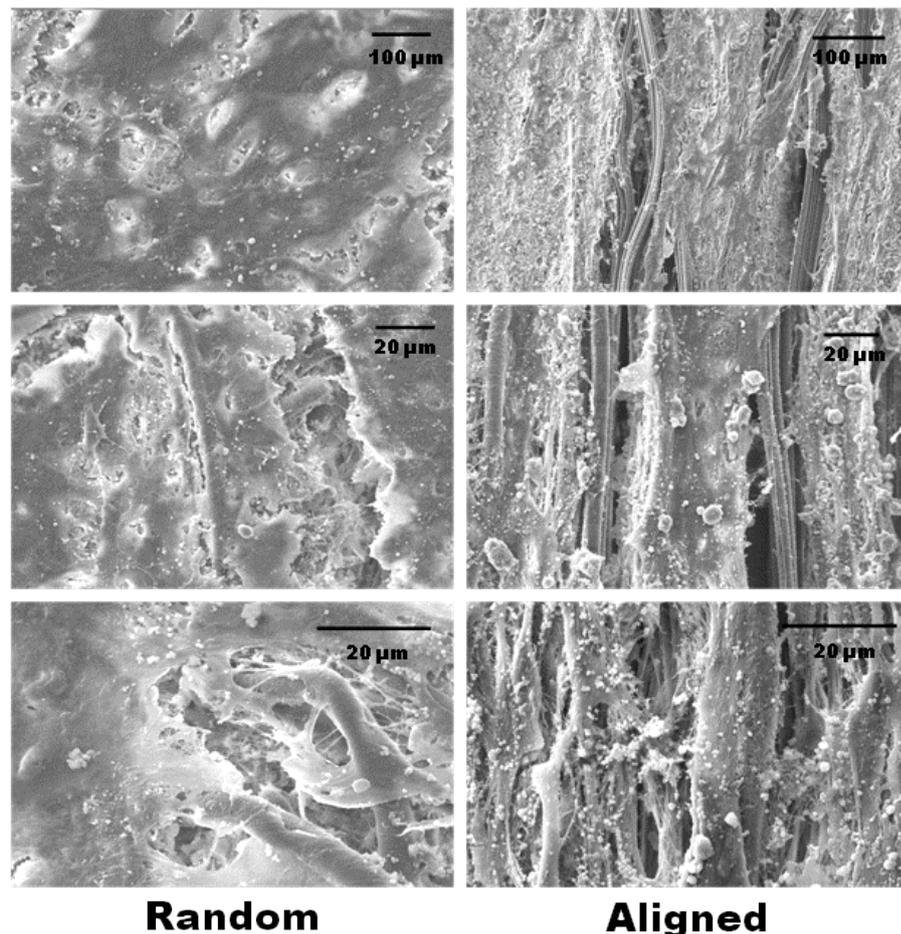
Figure 5.3: SEM micrographs of MLOA5 cells cultured for 12 days in NM on random or aligned electrospun PCL fibres. Images show cell-seeded constructs at different magnifications. Representative images are shown (n = 3).

5.3.2 The effect of fibre orientation on hESMP cells

5.3.2.1 Cell migration, viability, and morphology

Cells on random scaffolds began migrating after day 5 and moved outwards across the scaffold evenly in all directions (Fig. 5.4a-b). Cells on aligned scaffolds had already begun to move slightly in the fibre direction at day 5, and by days 10 and 15 cells had migrated significantly further parallel to the fibre direction than perpendicular to the fibre direction. Cells had migrated further parallel to the fibre direction of aligned fibres than in any other direction on both scaffolds at all time points. Cell viability (Fig. 5.4c) was significantly higher on random fibres at days 5-10 compared with aligned but by day 15 aligned fibres had a slightly higher viability.
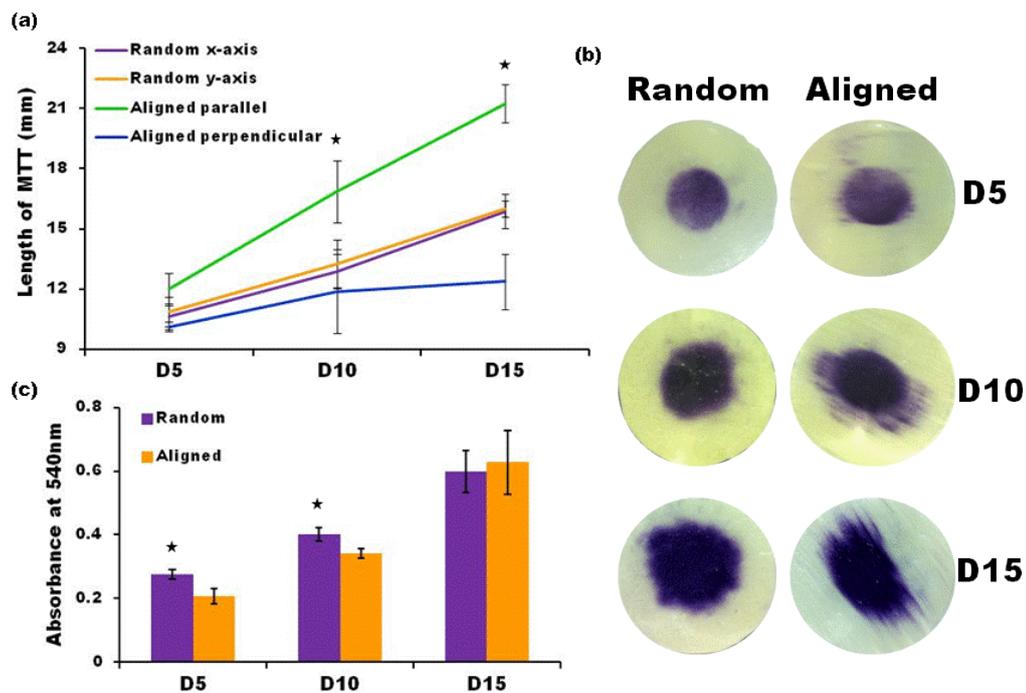
Figure 5.4: Cell migration and viability of hESMP cells on random and aligned PCL was assessed using MTT assayed at days 5, 10 and 15. Migration (a-b) was measured as the length of the MTT stain from end to end across the x- and y-axis on both scaffolds (parallel or perpendicular to fibre direction on aligned scaffold). Cell viability was the resulting MTT stain measured at 540nm (c). All data is mean ± SD (n = 6). *P <0.05.

Cell morphology at day 7 showed that cells cultured in NM were generally less-well spread than cells cultured in OM on all surfaces (Fig. 5.5). Cells on TCP and random fibres were arranged in all directions while cells on aligned fibres were orientated in the direction of fibre alignment.
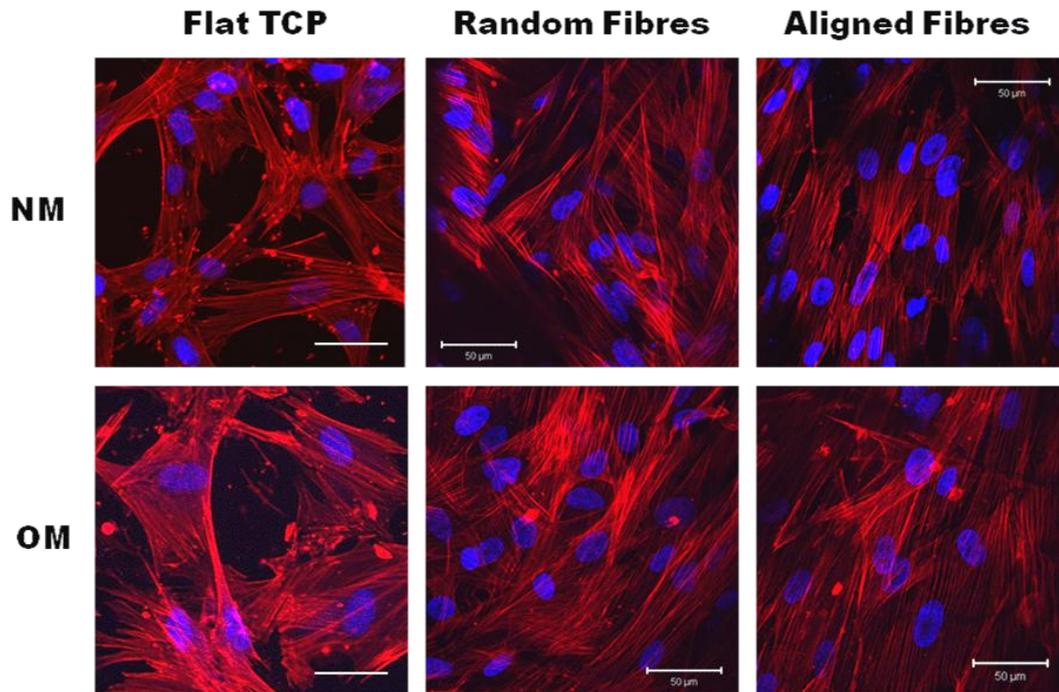
Figure 5.5: Morphology of hESMP cells cultured on tissue culture plastic (TCP) and random and aligned PCL fibres observed with DAPI (nucleus-blue) and phalloidin TRITC (actin cytoskeleton-red) staining at day 7. Images are representative for n = 6. Scale bars are 50 μm.

5.3.2.2 Total DNA and ALP activity

Total DNA increased from day 7-14 and showed similar levels at each time point for all samples (Fig. 5.6a). This suggests that cells in all conditions proliferated from day 7-14. However, at day 21 total DNA was unchanged for samples cultured in OM, however there was a slight increase for cells cultured on random fibres in NM and an even larger increase for cells cultured on aligned fibres in NM. ALP activity was greater in samples cultured in OM compared with NM at all time points, and ALP activity continued to increase in all samples from day 7-21 (Fig. 5.6b). For all samples, the increase in ALP activity from day 14-21 was greater than from day 7-14 suggesting a greater commitment to differentiation at this later time point. For cells cultured in NM, ALP activity on random fibres was significantly higher at days 14 and more so at day 21 compared with aligned fibrous scaffolds ($p<0.05$). For cells cultured in OM, ALP activity was significantly higher at day 21 in random fibrous scaffolds compared with aligned fibrous scaffolds ($p<0.05$).
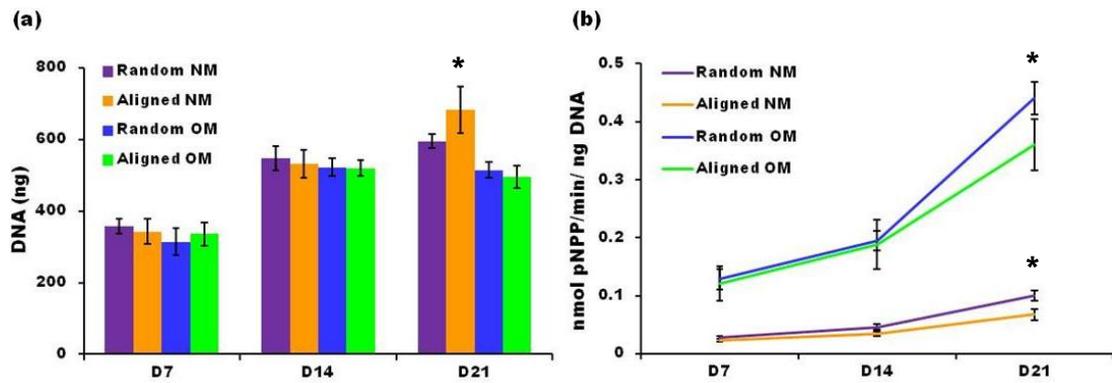
Figure 5.6: Total DNA content (a) and ALP activity (normalised to DNA) (b) at day 7, 14, and 21 of hESMP seeded random and aligned fibrous constructs cultured in NM or OM. Data is mean ± SD (n = 9). *P <0.05* indicates significant difference between scaffold type cultured with the same media.

A comparison of normalised ALP activity was carried out between cells cultured on random and aligned PCL fibres and 2D TCP. When cultured in OM, cells seeded on either scaffold had higher ALP activity at days 7 and 21 (Fig. 5.7a) compared with TCP. At day 21, ALP activity on random fibres was significantly higher than on TCP (*p<0.05*). When cultured in NM, cells seeded on either scaffold had higher ALP activity at all time points than TCP (Fig. 5.7b) and this was significant at days 7 and 21 (*p<0.05*). From day 14-21, ALP activity only slightly increased on TCP samples whereas there was a sharp increase on aligned and random fibrous samples. These results suggest that fibrous PCL scaffolds favour osteogenic differentiation over TCP.
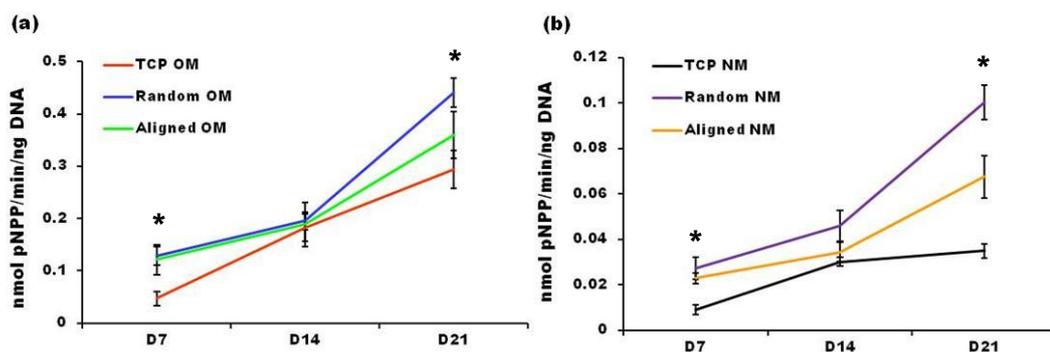
Figure 5.7: Normalised ALP activity of hESMP seeded random and aligned fibrous scaffolds compared with TCP cultured in OM (a) or NM (b) at days 7, 14 and 21. Notice the difference in scale (y-axis) between media conditions. Data is mean ± SD (n = 9). *P <0.05* indicates cells cultured on random fibres have significantly different normalised ALP activity for both media conditions compared with TCP.

146

5.3.2.3 Collagen production and SHG

Collagen production increased more than 2-fold for all conditions from day 14-21. Total collagen production (Fig. 5.8a) was significantly higher on random scaffolds than aligned scaffolds at both time points ($p<0.05$) and the same was true when collagen was normalised (Fig. 5.8b). Cells cultured in NM had higher total collagen than cells cultured in OM for each respective scaffold type however when this was normalised, there was more collagen per cell for hESMPs cultured in OM than NM on aligned scaffolds. At day 21, OM cultured cells produced a darker SR stain (Fig. 5.8c) but it was not as dense as the stain on NM cultured fibres.
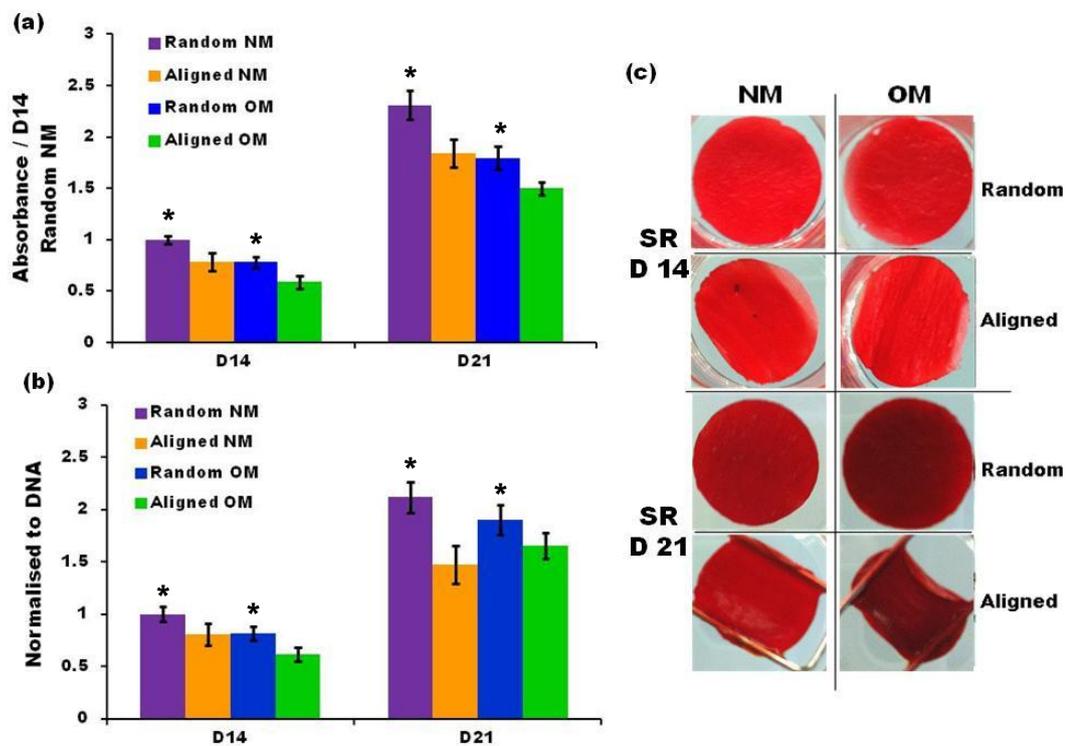
Figure 5.8: Random and aligned PCL seeded with hESMPs were assayed by SR staining for total collagen deposition (a) and collagen normalised to total DNA (b) at days 14 and 21. SR stain can be visualised for all conditions (c). Data is mean ± SD (n = 9). *P <0.05.

To further explore collagen deposition and how it was organised, SHG was performed at days 14 and 21 at two different depths (10 and 20 µm). At day 14, collagen on random fibres was disorganised compared with collagen on aligned scaffolds, which was orientated in a preferential direction (Fig. 5.9a). Interestingly, at a depth of 10 µm, collagen fibres deposited on aligned scaffolds were not orientated in the fibre direction but off set at a slight angle. SHG intensity appeared

greater on random scaffolds than on aligned scaffolds at a depth of 20 µm, indicating more deposited collagen and agreeing with the SR results. SHG intensity increased drastically from day 14 to 21 indicating greater collagen deposition and also agreeing with the SR results.
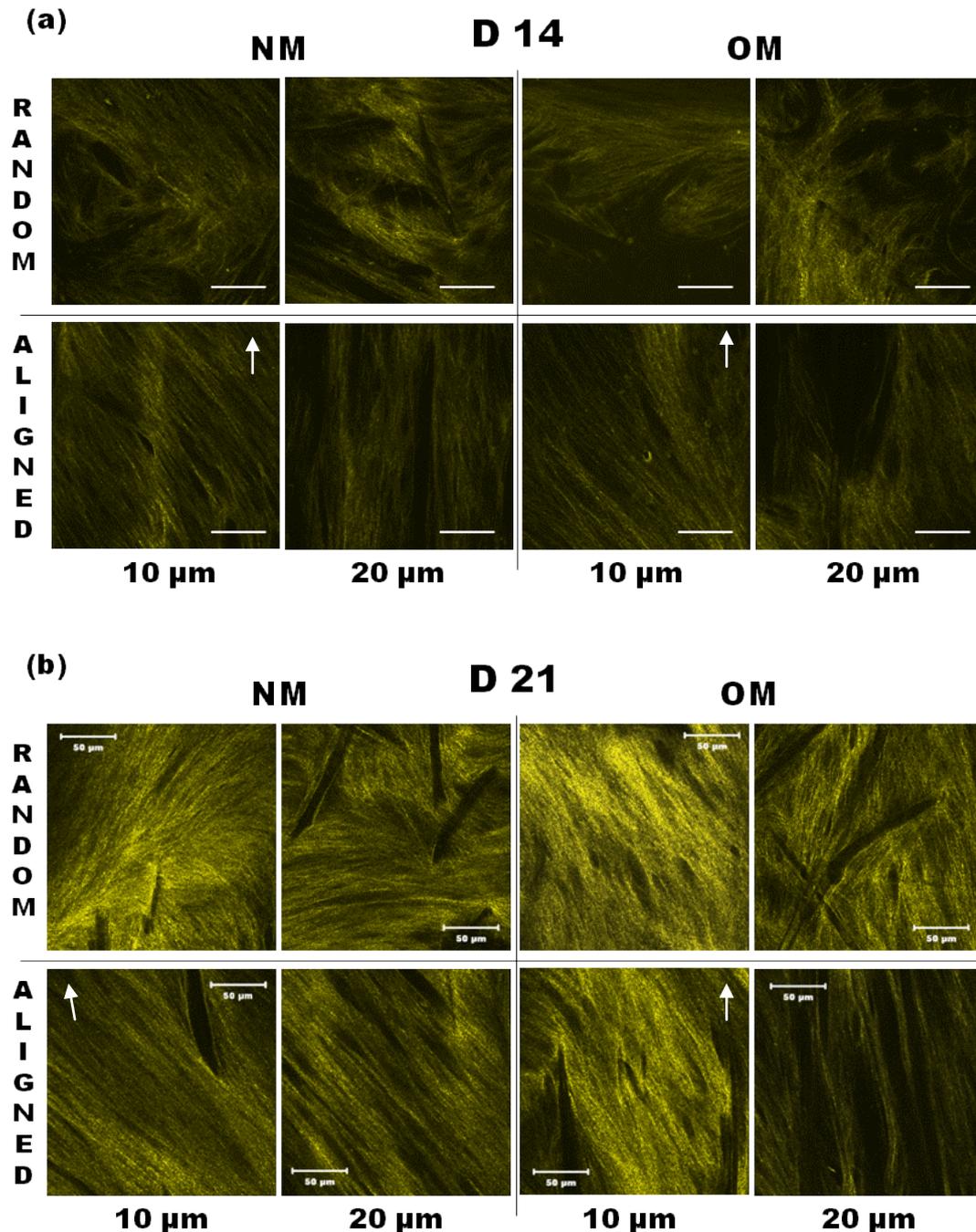
Figure 5.9: Second harmonic generation was captured for hESMP cells cultured on random and aligned scaffolds at days 14 and 21 at two separate depths from the scaffold surface (10 and 20 µm). Arrows indicate direction of aligned scaffold fibre orientation. Images are representative from n = 2. Scale bars are 50 µm.

At day 21, collagen deposited on random fibres showed no preferential organisational direction in contrast to collagen on aligned fibres (Fig. 5.9b). A similar trend was observed on aligned fibres as with day 14 in that collagen was orientated at an angle off set from the direction of scaffold fibre orientation. SHG intensity appeared higher for random scaffolds compared with aligned scaffolds, however there did not appear to be much difference between cells cultured in NM or OM, suggesting that OM scaffolds may be better organised into thicker bundles.

5.3.2.4 Calcium production
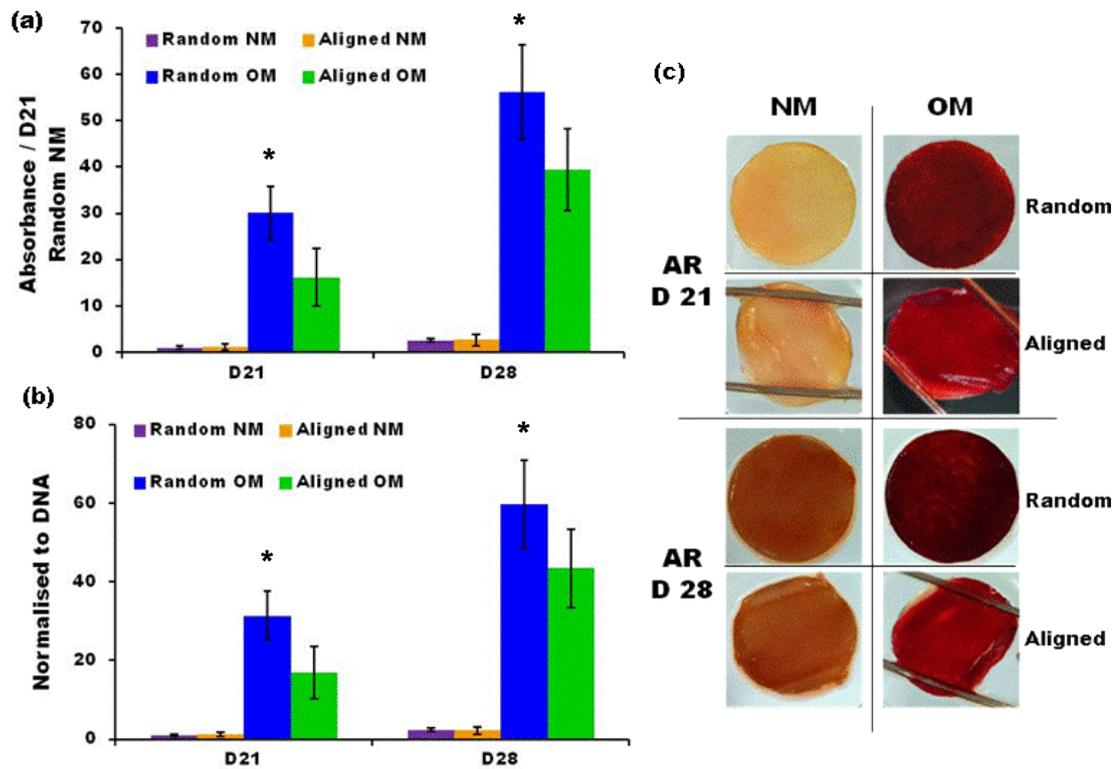
Figure 5.10: Random and aligned PCL fibres seeded with hESMPs were assayed for deposited calcium by AR staining at days 21 and 28 (a) and normalised to total DNA (b). AR staining of deposited calcium on scaffolds was visualised at days 21 and 28 (c). Diagrams show dental wire on aligned images used to hold scaffold down. Data is mean ± SD (n = 9). *P <0.05.

Deposited calcium was assayed by AR staining at days 21 and 28 (fig. 5.10a-c) as a marker of late stage differentiation. Cells cultured in OM on both fibre orientations showed strong staining at both time points, which increased 1.87-fold (random) and 2.44-fold (aligned) from days 21-28. Calcium deposition was significantly higher (p<0.05) on random scaffolds than aligned scaffolds at both time points. Normalising the deposited calcium to total DNA did not change the results

149

significantly. Almost no staining was observed for cells cultured in NM at day 21 but by day 28 there was a noticeable increase in the amount of staining on both fibre orientations (Fig 5.10c).

5.3.2.5 SEM

All cell seeded constructs were well covered with cells and matrix at both time points (Fig. 5.11-12). Cells and matrix on random scaffolds appeared to have no preferential direction of orientation but there was a high degree of alignment observed on aligned scaffolds. At day 21, constructs cultured in NM had a relatively smooth appearance, while constructs cultured in OM had a rougher appearance with some obvious mineral particles on the surface. On random scaffolds in particular, there appeared to be many particulate bumps residing under the top layer of cells and matrix. These particles are most likely bone mineral and support the observed AR staining in OM cultured constructs and not in NM cultured constructs. At day 28, constructs cultured in OM showed an increase in the occurrence and size of the mineral particles. Small mineral particles were also observed to occur in constructs cultured in NM, agreeing with the faint AR staining, indicating that cells were beginning to deposit calcified matrix. At both time points, deposited mineral appeared better organised on aligned scaffolds and in the direction of overall cell/matrix alignment.
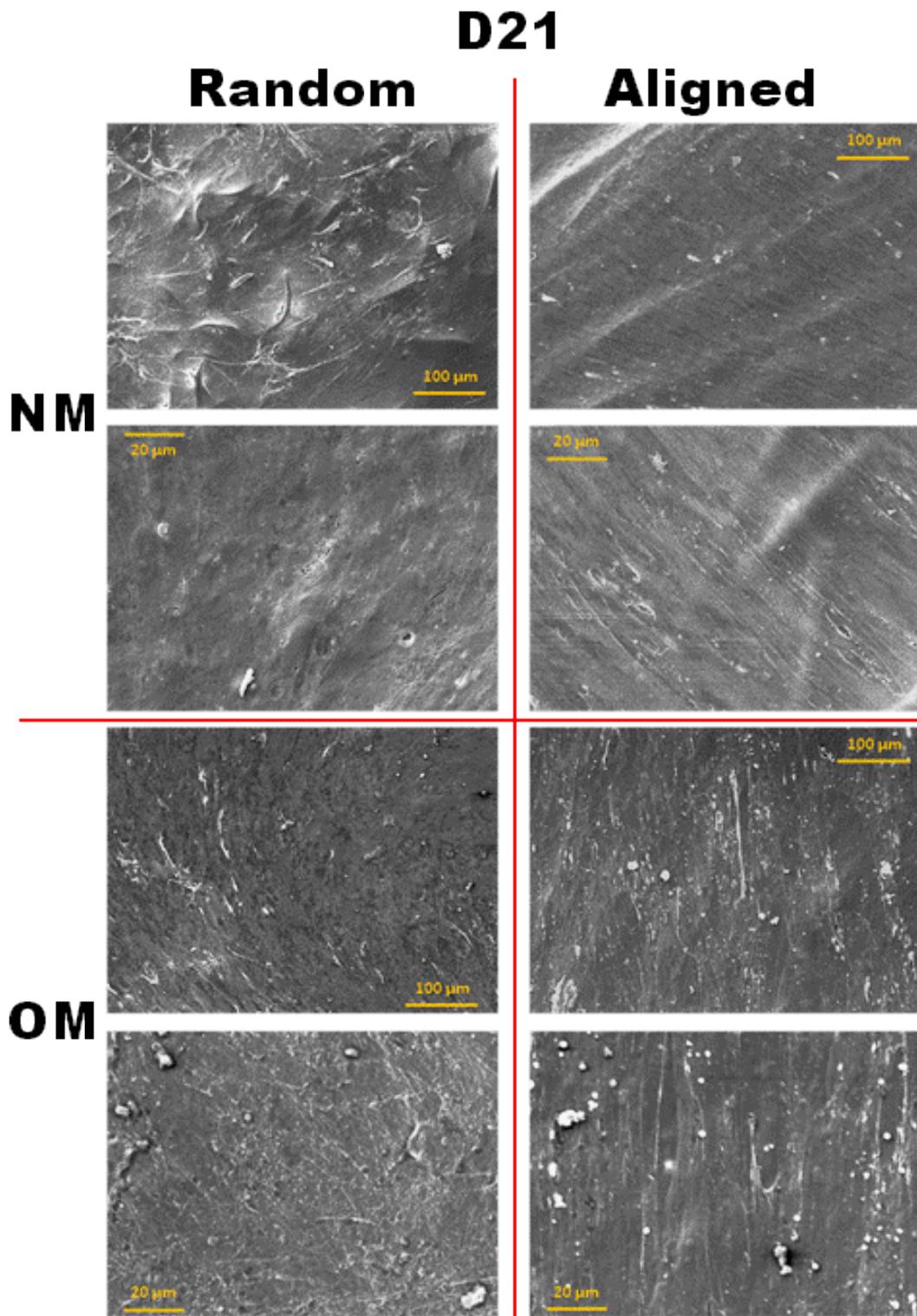
Figure 5.11: SEM micrographs of hESMP-seeded random and aligned PCL fibres cultured in NM or OM was performed at day 21. Constructs cultured in NM do not show any signs of mineral deposition, however constructs cultured with OM appear to show mineral deposits. Each condition shows two images at differing magnifications and images are representative of n = 3.
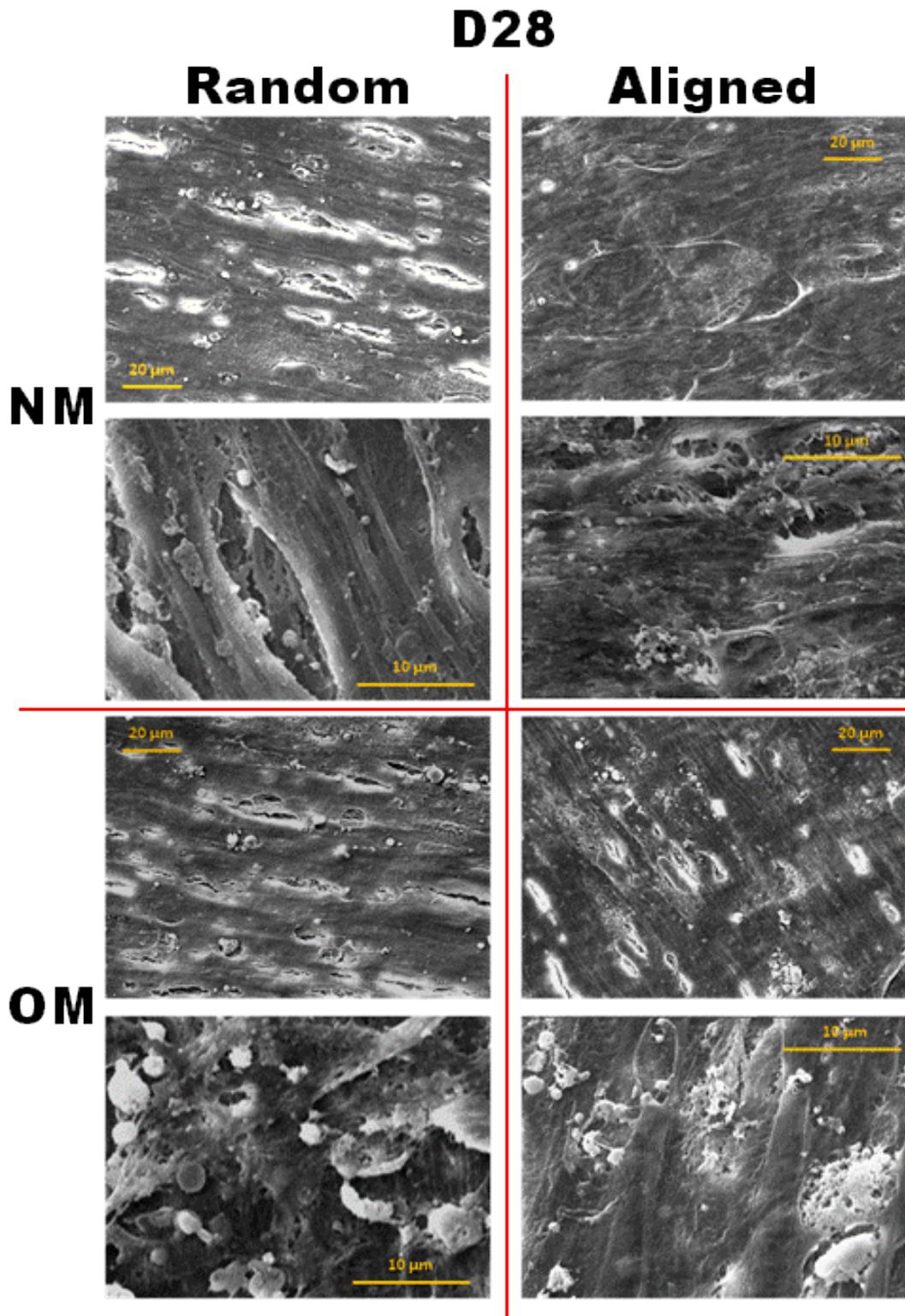
Figure 5.12: SEM micrographs of hESMP-seeded random and aligned PCL fibres cultured in NM or OM was performed at day 21. Notice the accumulation of mineral deposits compared with day 21 SEM micrographs. Each condition shows two images at differing magnifications and images are representative of n = 3.

5.3.2.6 Mechanical properties of constructs

Tensile testing of constructs seeded with hESMPs and cultured in OM was performed at days 2, 7, 14, and 21 (Fig. 5.13a). All constructs had a significantly higher Young's modulus of elasticity (E) at day 2 compared with blank constructs. Constructs of all fibre orientations showed an increasing E at each time point tested over the culture period. For random and parallel fibres this increase was significant at all time points compared with the previous time point ($p<0.05$). Perpendicular fibres showed the biggest increase in E from day 14 to 21. At day 21, the E of each construct compared with non-cell containing constructs was 2.17, 1.88, and 5.26 higher for random, parallel, and perpendicular fibres respectively.
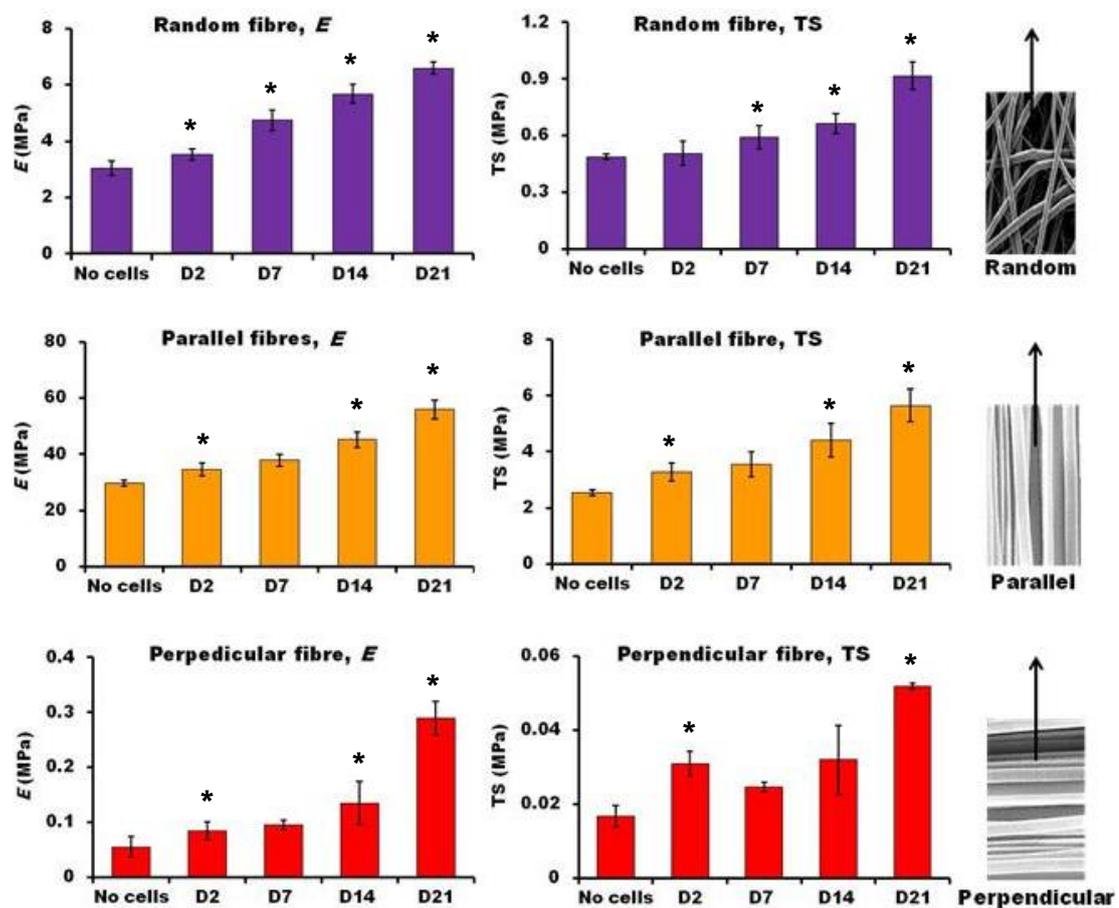
Figure 5.13: Young's modulus of elasticity (E) and tensile strength at 50 % strain (TS) of blank fibrous scaffolds (no cells) and hESMP seeded fibrous constructs cultured in OM (D2, 7, 14 and 21). Notice the difference in the size of the scales for each scaffold orientation (parallel > random > perpendicular). Images on right hand side indicate respective scaffold orientation along with arrow showing direction of tensile force applied. All data is mean ± SD (n = 4 (perpendicular) or n = 6). *P <0.05 verses previous day tested.

A similar trend was observed for the tensile strength at 50 % strain (TS) for all fibre orientations. However, random fibrous constructs did not show a significantly higher TS until day 7 compared with the blank, no-cell scaffolds. The biggest increases in TS were observed from day 14 to 21 for all constructs. Perpendicular fibres actually had a lower TS at day 7 compared with day 2 and day 14 was also similar to day 2. By day 21, the TS of each construct compared with non-cell containing constructs was 1.88, 2.23, and 3.11 higher for random, parallel, and perpendicular fibres respectively.

5.4 Discussion

The main aim of this study was to observe what affect micro-fibre orientation (random or aligned) had on hESMP behaviour, osteogenic differentiation, and matrix production. Controlling each of these aspects is crucial for regenerating new bone from progenitor cells and finding ways to speed up the healing process. The results showed that fibre orientation can influence the differentiation of progenitor cells with a random fibre orientation apparently favouring osteogenesis, while aligned fibres supported better matrix organisation. In contrast to the hESMPs, aligned fibres appeared to support the osteogenesis of MLOA5 mature bone cells more so than random fibres.

The reasoning behind the selection of random and aligned fibres is that MSCs are undifferentiated progenitor cells that will be present in a healing wound representing immature bone that is relatively porous and not yet well organised (represented here by random fibres). They do not reside amongst developed bone, where mature bone cells exist, and this consists of a foundation of highly orientated array of densely packed collagenous fibres (represented here by aligned fibres). It has been shown previously that physical properties can affect cell differentiation and so it was reasonable to assume that there may be some influence on MSC differentiation. Secondly, it was seen in chapter 5 that fibre orientation can also influence matrix organisation and resulting construct mechanical properties. Matrix orientation and structure dictates the mechanical properties of bone which is highly important for bone to function properly in its role of supporting the body. This is the first study I

know of to directly monitor collagen-matrix production of MSCs in fibrous scaffolds of controllable orientation and to subsequently determine what effects its orientation has on construct mechanical properties.

Scaffold fibre orientation influenced cell behaviour and osteogenic differentiation of hESMPs. Aligned fibres caused cells to orientate along the direction of fibre alignment and cell migration was fastest in the direction of fibre orientation, compared with perpendicular to fibre orientation and across randomly orientated fibres. However, cell viability (MTT) at days 5 and 10 was lower most likely due to restricted movement perpendicular to fibre orientation. While both fibre orientations supported osteogenic differentiation and matrix deposition by hESMPs, the random fibrous architecture appeared to favour osteogenesis of hESMPs showing significantly increased ALP activity, collagen and calcium deposition. However, aligned constructs did present a higher degree of mineralised matrix organisation which resulted in a 10-fold increase in mechanical properties compared with random constructs. What was also interesting is that hESMPs cultured on fibres had higher ALP activity in both media conditions compared with cells cultured on TCP and this was most pronounced for cells cultured in NM.

There is a large wealth of evidence indicating that cell behaviour and differentiation is heavily influenced by cell morphology and spreading (Bhadriraju *et al.* 2007; Chen *et al.* 1997). MSCs that spread out over a larger area have been seen to favour osteogenesis compared with those that occupy a small area favouring adipogenesis (McBeath *et al.* 2004b). Cells that spread out over a large area are able to form numerous focal adhesion complexes that geometrically oppose one another and so generating significant cytoskeletal tension. It has been suggested that MSCs must develop cytoskeletal tension above a threshold value in order to undergo osteogenic differentiation (Rowlands *et al.* 2008), and also be bound to an osteogenic ligand. Cells that are not well spread have less permanent, more mobile anchors (Discher *et al.* 2005), whereas cells that are well spread develop permanent anchors through focal adhesions and generate high cytoskeletal tension, which is seen by enhanced actin stress fibres. On both fibre orientations, cells are well spread with well-defined actin stress fibres. When compared with TCP, cells on fibres had a more defined cytoskeletal network in both media types.

Cells are sensitive to matrix elasticity and features and sense them by anchoring via integrin adhesions to ECM molecules and pulling via cytoskeletal contractions. Substrate stiffness also increases cytoskeletal tension even in cells that are restricted in their spreading and it has been shown that stiffer substrates favour osteogenesis over softer substrates (Engler *et al.* 2006; Rowlands *et al.* 2008). TCP is a much stiffer substrate than electrospun PCL and so one would expect TCP to favour osteogenesis. This indicates that the features of the electrospun scaffold enhance osteogenesis in hESMPs compared with planar substrates and this has been seen elsewhere (Watari *et al.* 2012). PCL fibres also contained nano-pores on the fibres (see chapter 4), giving the surface an inherent roughness and this has also shown to be favourable for osteogenesis compared to smooth surfaces (Woo *et al.* 2003; Kumar *et al.* 2011).

In contrast to hESMPs, osteogenic differentiation of MLOA5 cells appeared to be favoured by aligned substrates. Although ALP activity at day 12 was higher on random scaffolds than aligned, there was significantly less deposited mineral. Some authors report ALP activity as a biphasic process, rising to a peak level before gradually decreasing again upon reaching the end of differentiation (Bancroft *et al*. 2002; Datta *et al*. 2006). ALP activity in aligned scaffolds may have peaked before day 12 and earlier on than random scaffolds. The AR staining and the SEM images clearly show that there is more deposited mineral on the aligned scaffolds compared with the random ones implicating that aligned fibres enhance osteogenesis over random ones. Aligned fibres also caused cells to orientate in the fibre direction, whereas cells on random fibres were more star-like and attached to multiple fibres. The SEM images also show the mineralised matrix orientated in the direction of the fibres on aligned scaffolds producing a more organised construct than random fibres. This organisation is much more representative of mature bone and suggests that mature bone cells prefer substrates that mimic their natural environment in the body.

As mature bone consists of alternating layers of parallel-aligned collagen fibres it would be reasonable to speculate that the use of aligned fibrous scaffolds mimicking the native tissue would better enhance osteogenesis. But the work in this chapter indicates that random fibres better supported the osteogenic differentiation of hESMP cells compared with aligned fibres. There are a number of previous studies

that have studied the effect of fibre properties on MSC differentiation but results have been conflicting.

Lu *et al.* (2012) seeded mouse bMSCs on random macro- and random and aligned nano-fibres. The random-orientated nanofibrous scaffolds showed the best cellular compatability in terms of initial attachment and subsequent proliferation. In another study, rat BMSCs were seeded on random and aligned nano-fibres of PLA and while both had similar ALP activity and osteogenic gene expression (OP and OC), calcium content was significantly higher on aligned substrates at day 21 (Ma *et al.* 2011). Wang *et al.* (Wang *et al.* 2012) cultured rat MSCs on random and aligned PHBHHx fibres and noticed differences in cell morphology, and actin and vinculin staining. Markers of osteogenesis (osteocalcin and RUNX2) were higher on aligned fibres than on random in both normal and adipogenic media. However, in osteogenic media, osteogenic markers were expressed similarly. Interestingly, PPARgamma levels were lower on aligned scaffolds than random suggesting that aligned fibre orientation inhibited PPARgamma signalling. The ratio of the phosphorylated form of ERK 1/2 increased when MSCs underwent osteogenesis and this was higher for MSCs on aligned by 3 times than MSCS on random fibres in normal medium. Martins *et al.* (Martins *et al.* 2011) seeded hBMSCs on random and aligned electrospun PCL nanofibrous meshes and did not observe any differences in the expression of osteogenic genes but mineralised ECM was deposited along the fibre direction. Kishore *et al.* (2012) cultured hMSCs on aligned and randomly orientated collagen fibres and noticed suppression of osteocalcin on aligned collagen but increased expression of tendon specific markers scleraxis and tenomodulin. Rat MSCs were seeded on non-woven fibres with different diameters (2-42 µm) (Takahashi and Tabata 2004) and showed the poorest cell attachment and migration on the smallest fibres, most likely due to the cells being greater than the fibre diameter. ALP activity and osteocalcin expression was greatest on fibres with diameters of 9-12 µm. Wang *et al.* (Wang *et al.* 2012) showed that osteogenesis of MSCs was promoted on poly(3-hydroxybutyrate-co-3-hydroxyhexanoate) PHBHHx surfaces with 10um grooves.

A small number of similar studies have been performed on progenitor cells sourced from tissue types other than bone marrow. Yin et al., (Yin *et al.* 2010) seeded human tendon stem /progenitor cells (hTSPCs) on random and aligned PLA nano-fibrous

scaffolds. They observed that tenogenesis (scleraxis and eya2) was favoured by aligned fibres while OCN expression and ALP activity was significantly higher on random fibres. hTSPCs reside within a niche in the tendon composed of highly aligned collagen fibres, with this niche playing an important role in regulating their function and differentiation (Hoffmann and Gross 2007). Both fibre orientations showed similar levels of collagen types I and III however in the presence of osteogenic media, there was a large amount of deposited calcium on random fibres compared with very little on aligned (Yin *et al.* 2010). Foldberg *et al.* (Foldberg *et al.* 2012) cultured adipose derived stem cells (ADSCs) on flat and patterned PLA substrates and saw higher mRNA expression for genes associated with bone, adipose, cartilage, and skeletal/cardiac muscle, than cells cultured on TCP. However, there were no significant differences between flat and patterned PLA surfaces in osteogenic gene expression.

Other physical properties of scaffolds have been examined for their influence on MSC behaviour. Kumar *et al.* (2011) compared the effect of different scaffold types on their ability to promote hBMSC proliferation and differentiation. They found that smooth freeform fabricated (FFF) scaffolds with an open pore structure supported the fastest cell proliferation but did not induce osteogenic differentiation. Whereas nanofibrous scaffolds did (Kumar *et al.* 2011). The authors concluded that the morphology adopted by the hBMSCs as a direct result of the nanofibrous scaffold, induced them towards osteogenesis. In another study by Kumar *et al.* (Kumar *et al.* 2012), hBMSCs were cultured on etched and un-etched porous scaffolds with and without osteogenic media. In the absence of OM, there was no mineral formation at day 21 but by day 62, alizarin stain was present on etched scaffolds but not un-etched. In the presence of OM, deposited calcium was present on both etched and un-etched but more staining was present on etched surfaces. This suggests that in the absence of OM, osteogenic differentiation can still occur, although it takes much longer. It is possible that a similar situation occurred on the PCL scaffolds cultured in NM as a small amount of calcium was deposited at day 28.

While evidence suggests that cell morphology can dictate cell lineage commitment, many of the studies involved with controlling MSC morphology through substrate topography or stiffness tend to focus on individual cells that are not in contact with other cells in a 2D environment. When cells become confluent, as would be the case

in order to develop sufficient matrix, cells will most likely change in their morphology as space is limited and cell-contacts will come into play. When these environments are translated into a 3D environment it will also become more complex and it is unknown whether this will affect the cell phenotype.

With regards to mature bone cells, mouse osteocarcoma cells were seeded on random and aligned PLLA with nano- or micro- hydroxyapatite (HA) particles incorporated (Peng *et al.* 2011). Improved cell viability and superior ALP activity was observed on fibres with micro-HA over no-HA or nano-HA however, aligned fibres with nano-HA had higher ALP than random fibres with nano-HA but not with micro-HA. These results could be due to a combination of surface roughness influence as well as biomimetic effect. In another study, Wang *et al.* (Wang *et al.* 2011)saw decreased ALP activity and production of collagen type I and osteocalcin with increasing alignment of PLLA nanofibres when seeded with MG63 cells. Sisson *et al.* (Sisson *et al.* 2010) seeded osteoblastic MG63 cells on electospun gelatine nano-fibres and initially observed higher ALP activity on the smallest fibres (100nm) but by day 14 ALP levels were the same for both scaffolds. Woo *et al.* (Woo *et al.* 2003) observed enhanced differentiation of ostelblastic cells when seeded on scaffolds with rough struts compared with smooth struts and suggested this was due to the increase they saw in cell adhesive protein (fibronectin and vitronectin) adsorption on scaffolds with rough surfaces.

There are a number of reasons that could explain these differences between studies including the species of origin and the stage of maturity of the progenitor cell. Other scaffold properties may affect the outcome including pore size and fibre diameter, as well as substrate compliance, the material used and the surface properties (chemistry and roughness).

While most studies measure earlier markers of osteogenic differentiation, the presence of a lineage-specific transcription factor within the cell nucleus does not necessarily mean that the cell is committed to that phenotype. It is also not known at what level gene transcription factors need to be at in order to initiate full differentiation and translate the cell into a matrix-secreting specialised cell. Therefore, it is important to observe matrix production and how it is organised. Collagen production was higher on random fibres of both media types compared

with aligned fibres. SHG images of collagen also revealed a more intense signal from random fibrous constructs compared with aligned fibrous constructs for both media conditions. While it was clearly seen that collagen on aligned fibres was more organised and orientated, which would enhance SHG, the fact the signal was weaker indicates reduced collagen formation. However, both collagen and calcium appeared well organised and orientated in the same direction on aligned scaffolds compared with random scaffolds. Interestingly there was an observable deviation of the matrix away from the direction of scaffold fibre orientation on aligned scaffolds from day 14 but the tensile modulus of the cell-seeded scaffolds continued to increase up to day 21. It has been shown previously that when the fibre deviation is $<30^{o}$ from the direction of externally applied tensile strain, this will not significantly affect the tensile modulus compared with no deviation (Nerurkar et $al.$ 2007). Nerurkar et $al.$ (Nerurkar et $al.$ 2009) subjected cell-seeded aligned nanofibrous constructs to tensile testing and observed a large reduction in the tensile modulus when the direction of the fibre and cell alignment deviated more than 30° from the principle direction of strain. The tensile data is largely in agreement with that of the HDF-seeded constructs from chapter 5 and this is also due to matrix orientation. Aligned scaffolds strained parallel to fibre orientation had a near 10-fold increase in mechanical properties compared with randomly orientated scaffolds. Scaffolds strained perpendicular to the fibre direction became much stiffer at day 21 compared with day 14 and this may indicate that the cells are beginning to lose their unidirectional orientation.

5.5 Conclusions and future work

This study has shown that scaffold fibre orientation can influence osteogenesis of progenitor cells and the organisation of deposited matrix. Random scaffolds favoured osteogenesis of hESMPs while aligned scaffolds supported greater matrix organisation and enhanced mechanical properties. Fibrous scaffolds also supported greater ALP activity than conventional TCP suggesting that surface features or substrate composition also greatly affects differentiation. For mature bone cells, aligned fibres supported greater matrix production, suggesting that cell maturity could influence response to substrate. There exists a wide variety of signals that affect MSC differentiation, including, chemical stimulus, substrate topography and

stiffness, and mechanical forces, and it is very likely that a network of signalling pathways are responsible for regulating the differentiation step. Future work will need to try to decipher the specific effects of each of these under well controlled conditions. Most of the previous work has also been performed on 2D substrates but a successful tissue engineered construct will be 3D in nature and differences may be observed between 2D and 3D. It may be that the most suitable scaffold for osteogenesis of MSCs is a scaffold combining both random and orientated elements to enhance differentiation and control matrix organisation. This could involve a scaffold multilayer approach, whereby aligned fibrous mats are stacked on top of each other with differing orientations to mimic the concentric layers of bone. Cylindrical tubes of orientated fibres could also be formed by wrapping sheets of fibres around each other to mimic the Haversian system found in the osteons of bone. Mechanical forces to help guide matrix deposition may also be important as well as the use of bioreactors to improve nutrient flow/waste removal.

5.6 Summary

- Micro-PCL random fibres seeded with hESMPs had increased ALP activity, collagen, and calcium production compared with aligned fibres.
- Aligned fibres supported a greater degree of cell and matrix orientation.
- Aligned constructs had superior mechanical properties compared with random constructs, when strained parallel to fibre orientation.
- Both fibrous constructs had greater ALP activity than TCP for both media formulations.
- MLOA5 cells showed enhanced mineral deposition on aligned constructs along with greater matrix organisation.
- Future work should study combined random/aligned scaffold layers, fibres of varying substrate stiffness, and the incorporation of mechanical forces.

CHAPTER SIX: Dynamic tensile conditioning of collagen producing cells

6.1 Introduction

Many types of cells exist in an environment subjected to daily mechanical loading including fibroblastic cells, osteoblasts, chondrocytes, smooth muscle cells, and endothelial cells, all of which are load-sensitive. Cells of the fibroblast family are the dominant cell type in dense connective tissue like skin, tendon and ligaments and are vital for development and maintenance of connective tissues. They are also responsible for secreting and organizing the ECM during growth and wound repair (Eckes *et al.* 2010). Tendons and ligaments are stretched when muscle contraction causes movement and skin is stretched during growth and when we bend our joints. Structural support tissues like bone require constant loading in order to maintain tissue homeostasis and they are remodelled to resist the forces they experience. A number of studies have shown that when fibroblasts are subjected to cyclic strain, they upregulate collagen expression and synthesis (Breen 2000; Carver *et al.* 1991). However, there are multiple loading parameters and variables available when subjecting cells to a cyclic loading regime and diverse outcomes have been recorded amongst different cell types and experimental setups.

Most of the forces experienced *in vivo* are dynamic, that is they are not constant and often the tissue is loaded then rested in cycles. For example, when a human walks, bones in the leg undergo cycles of compression and tension as the foot impacts on the ground and then lifts off again. Another example is when a muscle contracts to allow movement, which in turn causes tendons and ligaments to stretch, before returning to the start position as the muscle relaxes. Therefore, it seems important that cells be subjected to cyclic loading as opposed to continuous loading, which could cause cells to lose their responsiveness to the loading.

A key area of research in TE is concerned with finding ways of enhancing matrix production to allow the creation of suitable constructs fit for implantation that will assist with wound repair and also speed up the healing time. The construct must also be strong enough to withstand the forces that are experienced *in vivo* and so it would ideally be conditioned pre-implantation. Studies have shown that when cells are

cultured under dynamic conditions in a bioreactor, the result is improvements in matrix production (Cartmell *et al.* 2003). In 3D constructs, this also tends to result in a more evenly spread matrix and better infiltration into the scaffold (Nerurkar *et al.* 2011; Sikavitsas *et al.* 2005). Cell responses to dynamic stimulation in 2D occur mainly as a response to the primary mechanical stimulus, although there may be some small additional fluid flow affects (Donahue *et al.* 2003). For cell stimulation in 3D constructs, responses are related to both the mechanical forces generated within the system, either tension or FSS for example, and a more efficient nutrient transport mechanism caused by fluid movement through the scaffold.

As mentioned in Chapter 1, various techniques have been used *in vitro* to explore the response of cells to mechanical forces. However, many of these stimulation techniques have involved cells adhered to simple 2D surfaces, such as plastics or glasses. While we can learn important information from 2D testing, it does not reflect the true nature of the *in vivo* 3D environment and so it does not fulfil the requirement for the regeneration of functional organs. Culture of cells on 3D scaffolds will provide a more suitable physiological model for studying loading-induced biological responses in cells.

Tensile forces seem to favour a more fibrous matrix compared with compression forces that seem to favour a more GAG-rich matrix (Delaine-Smith and Reilly 2011). The main function of collagen is to resist tensile forces and in tissues where it is found in abundance, it is always organized in a way so as to resist the tensile forces that the tissue receives (Reilly *et al.* 1997). Therefore, *in vitro* tensile conditioning is physiologically relevant for collagen-producing cells and it seems likely that if collagen producing cells were repeatedly stretched then they would respond by synthesizing more collagen.

Previous work has been carried out in our group using a 3D model for bone tissue engineering that included use of a cell-seeded open porous PU foam loaded into a biodynamic chamber for stimulation by dynamic compression forces (Sittichockechaiwut *et al.* 2009). The chamber allows the sample to be maintained in a fluid-filled environment and so the effect of strain induced fluid flow is not ignored. Dynamic compression was applied for 2 hours at three time points over a period of 20 days and it was found that loaded samples had an increase in deposited

collagen and calcium compared with static controls (Sittichockechaiwut *et al.* 2009). This system has shown potential as a way of investigating the effects of mechanotransduction but so far it has only been used with compression as the mechanical stimulus. This model is also capable of producing tensile forces and so cell-seeded scaffolds can be subjected to dynamic tensile conditioning.

The aim of the work in this chapter was to use two types of scaffold material as a support substrate for collagen producing cells (MC3T3-E1 and MG63 bone cells, and HDFs) to simulate a 3D environment and to subject the cells to dynamic tensile conditioning. The main purpose was to monitor if short bouts of dynamic tensile loading had an effect on collagen production. The previous loading regime established by Sittichockechaiwut *et al.* (2009) was used as a starting point for tensile stimulation of all cells. The effect of strain level on collagen production in HDFs was also studied with the hypothesis that higher strains would induce more collagen production. HDFs were also cultured on electrospun tecoflex, which has a more physiologically relevant architecture than the PU foam.

6.2 Methods

6.2.1 Cell culture

Two different bone cells types were used in these experiments; the murine MC3T3 pre-osteoblast cell line and; the human osteocarcoma cell line MG63, both cultured on the PU foams. HDFs from one patient were also used and seeded on PU foams and electrospun tecoflex. All cells were allowed to adhere for 90 min before being submerged in fresh media and then adding AA after 24 h.

6.2.2 Dynamic tensile conditioning

PU foam scaffolds were cut into dog bone shaped scaffolds with the central portion measuring 5x5x25 mm (width/thickness/length) and scaffolds were mounted in groups of 2-3 onto brackets made from dental wire. All cells were seeded at a density of 250, 000 cells per scaffold in a volume of 60 μl on the central portion of the dog bone shaped PU foam substrate. The cycle time (1Hz) and the number of cycles (7200) were kept constant for all experiments. The loading days were also constant for each individual experiment but were altered depending on the cell type. The main

variable in these series of experiments was the magnitude of strain. All conditions for each cell type can be seen in table 6.1.

Regime	Cell Type	Scaffold	Strain %	Load days	Assay Day
1	MC3T3	PU foam	5	5, 10, 15	20
2	MG63	PU foam	5	5, 10, 15	20
3	HDF	PU foam	5	5, 15, 15	20
4	HDF	PU Foam	5, 10, 15	6, 9, 12, 15, 18	21
5	HDF	PU Foam	10	6, 9	12
6	HDF	Electrospun Tecoflex	5, 10, 20	6, 9, 12, 15, 18	21

Table 6.1: A list of the different tensile loading regimes that were carried out including cell type, scaffold type, amount of global tensile strain (%), days the cells were loaded, and the assay day. All cells had a cycle time of 1Hz and experienced 7200 cycles per loading day.

6.3 Results

6.3.1 MC3T3 seeded PU foam

MC3T3 cells were assayed at day 20 for cell viability and collagen deposition after 3 bouts of loading. Both MTS activity and collagen deposition increased almost two-fold with loading and this was statistically significant ($p < 0.05$) when compared with static controls (Fig. 6.1). Collagen deposition normalised to MTS did not show any differences between culture conditions. Scaffolds were cut in half to view the Sirius red staining on the top and middle portion of the scaffolds. Loaded samples showed darker collagen staining than static controls, especially on the surface of the PU foam scaffolds. Loaded samples also showed darker staining towards the middle and bottom of the scaffold. Magnified phase contrast images of the scaffolds showed that Sirius red staining was patchy in static samples, whereas loaded samples showed dense staining located around the struts of the PU foam, while the large pores remained collagen-free.
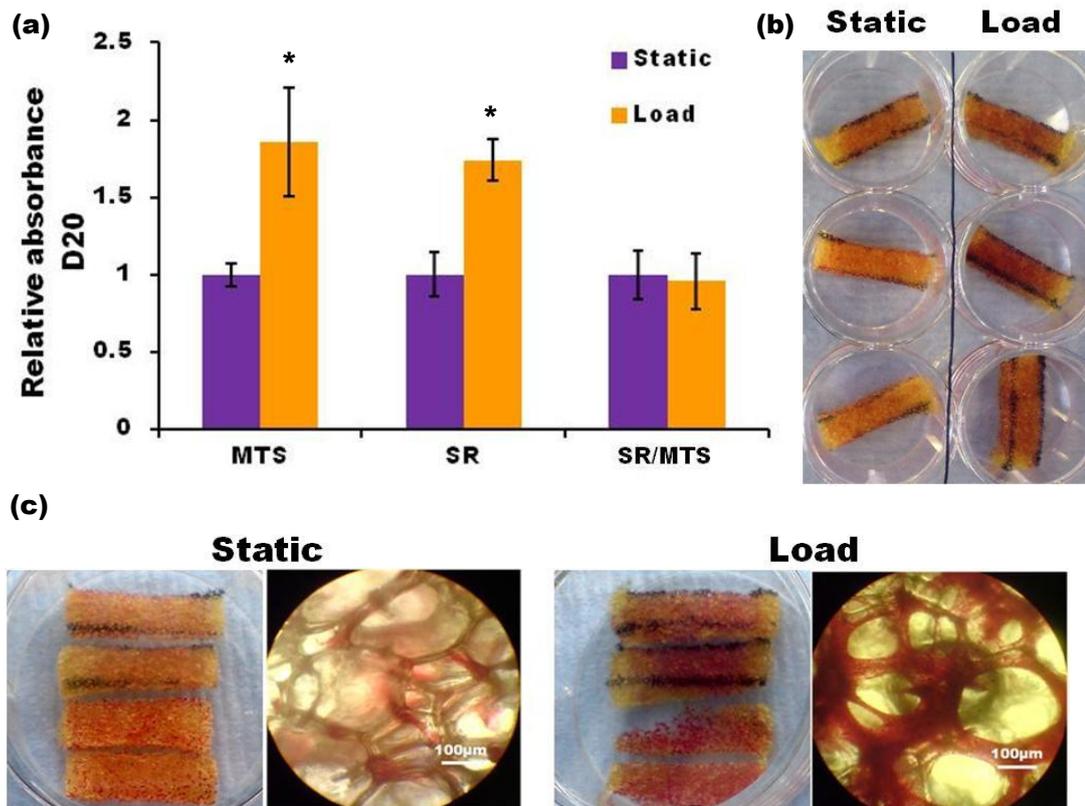
Figure 6.1: MC3T3 cells were subjected to 5 % global cyclic tension at days 5, 10 and 15 or cultured statically, and assayed for cell viability (MTS) and collagen deposition (SR) at day 20. Two scaffolds (c) of both conditions were cut in half to show collagen deposition throughout the scaffold (top half at top and bottom half at bottom). Black lines show pen markings. Phase contrast images of collagen deposition around the scaffold struts can are also shown. Data is mean ± SD (n = 6). *P < 0.05.*

6.3.2 MG63 seeded PU foam

MG63 cells seeded on PU foam were subjected to the same 3 day loading regime as MC3T3 cells and assayed at day 20 for cell viability and collagen deposition. MTS activity and collagen production was slightly higher in loaded samples compared with static controls but this was not statistically significant (Fig. 6.2a). This was a result of the large SD associated with the statically cultured samples. During each experimental run, there were two static samples that had relatively low MTS and collagen but also one that had a higher MTS and collagen similar to the loaded samples. The results were plotted again after removal of static outliers showing loaded samples had significantly more collagen deposition than static samples (Fig. 6.2b). Loaded samples showed dense collagen staining across the whole surface of the scaffold while static controls generally showed patchy staining across the surface (Fig. 6.2c) (with exception of the outlier).
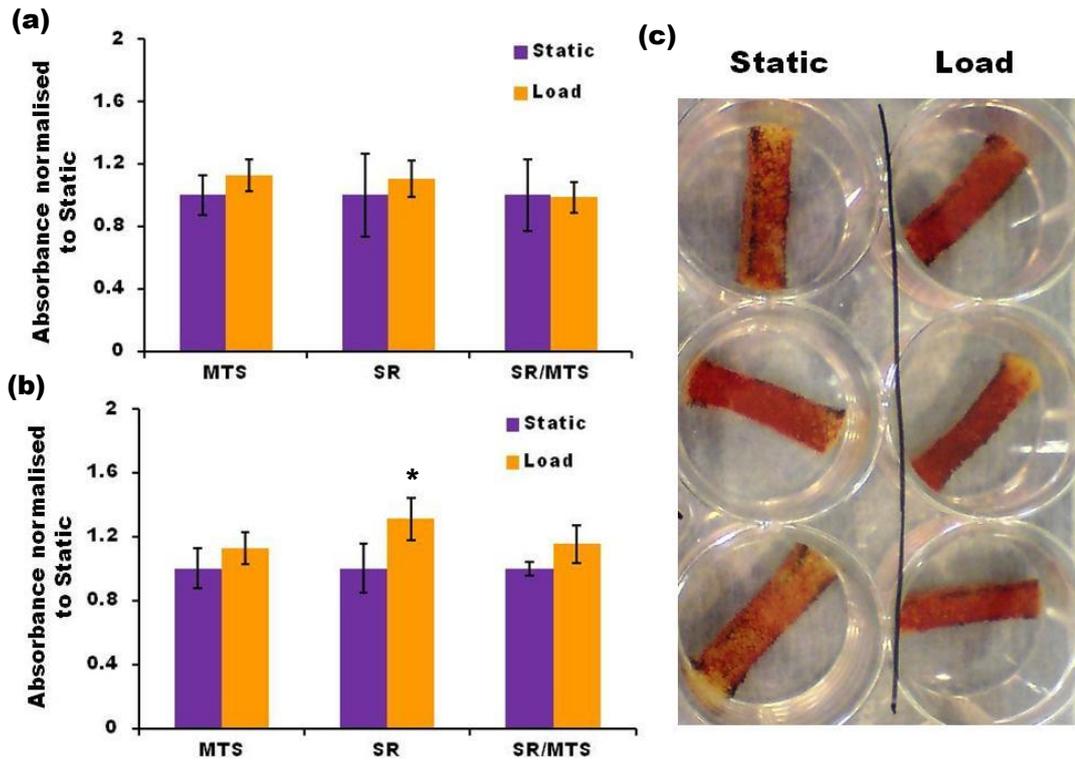
Figure 6.2: MG63 seeded PU foam scaffolds were subjected to 5 % global cyclic tension at days 5, 10 and 15 or cultured statically, and assayed for cell viability (MTS) and collagen deposition (SR) at day 20. Graph (a) shows results that include the static outliers, while graph (b) shows results with the removal of static outliers. Sirius red staining of scaffolds can be seen in (c) including a static outlier (middle static sample). Data is mean ± SD (n = 6 (a) or n = 4 (b)). *P < 0.05.

6.3.3 HDF seeded PU foam
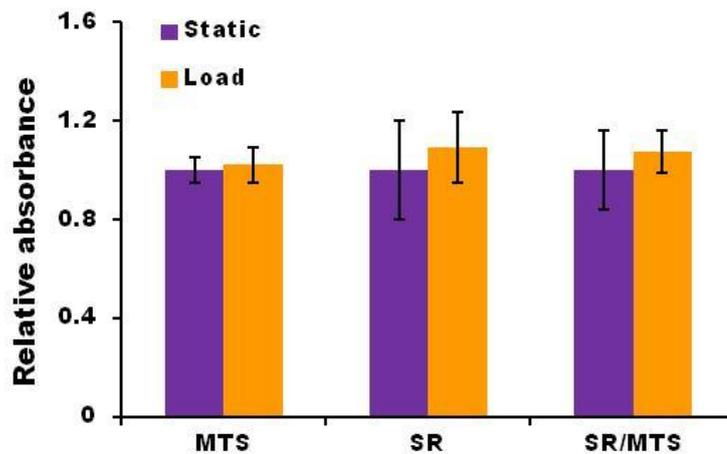
Figure 6.3: HDF seeded PU foams were subjected to 5 % global cyclic tension at days 5, 10 and 15 or cultured statically, and assayed for cell viability (MTS) and collagen deposition (SR) at day 20. Data is mean ± SD (n = 6).

HDF cells seeded on PU foam scaffolds were first subjected to 5 % strain at days 5, 10 and 15 and assayed at day 20 for MTS and collagen. Loading did not cause any significant increases in cell viability or collagen deposition (Fig. 6.3). The number of loading days was increased from 3 (5 days apart) to 5 (3 days apart) with the assay time point at day 21 and 5, 10 and 15 % strain was performed (Fig. 6.4). This regime resulted in a significant increase in MTS activity for samples stretched at 5 and 10 % strain and only slightly increased in samples stretched at 15 % strain.
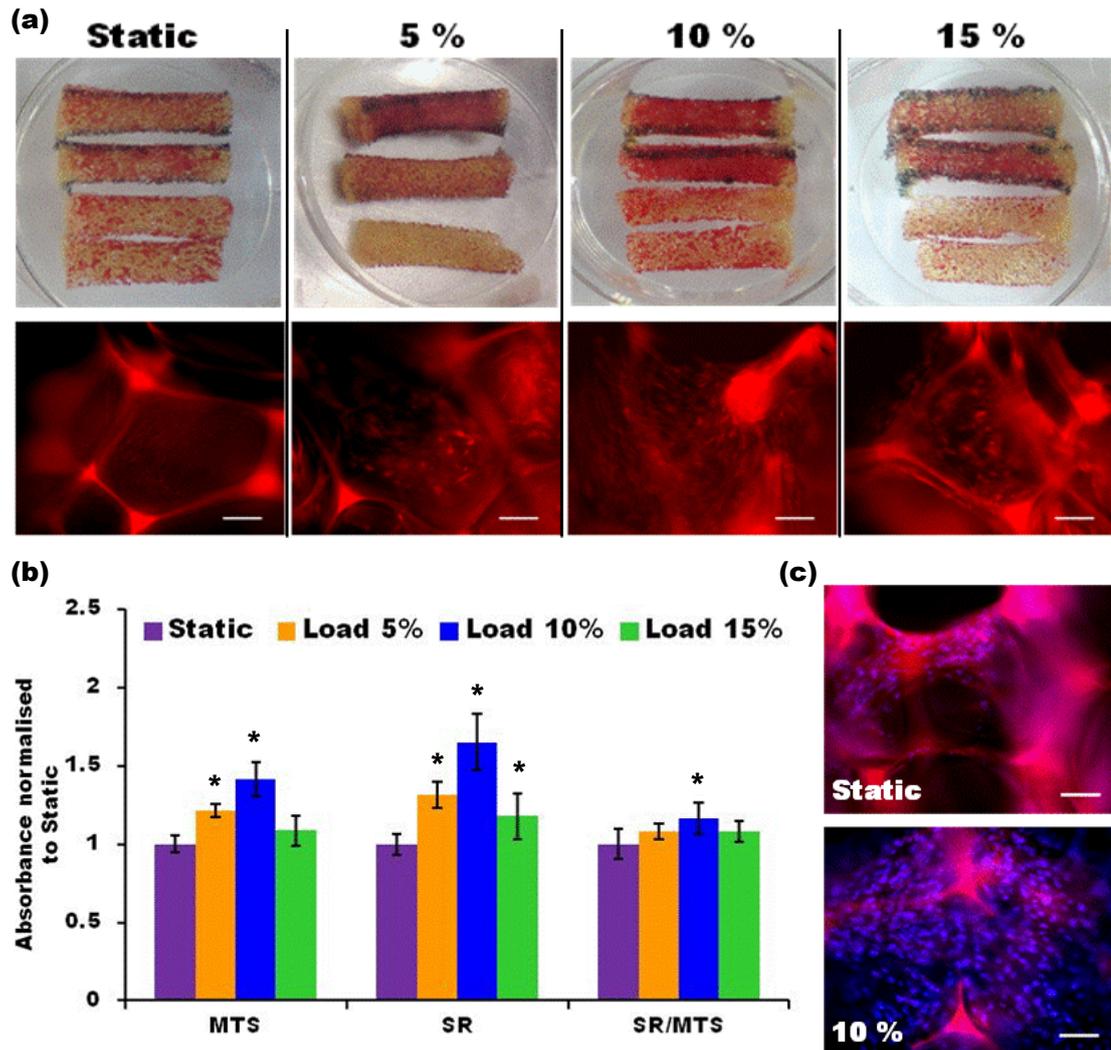
Figure 6.4: HDF seeded PU foam cultured statically or subjected to dynamic load with 5, 10 or 15 % strain at days 6, 9, 12, 15 and 18, and assayed at day 21. SR staining of scaffolds cut in half (a) shows that cells under load had denser staining on the top side (top two scaffolds) and closer inspection using fluorescent microscopy shows distribution of collagen within the pores. DAPI staining (c) (in blue) shows that cells in 10 % strain group had a denser cell coverage that statically cultured cells. Autofluorescence of scaffold struts can be seen in bright red (a) and in pink (c). Data is mean $\pm$ SD (n = 6). Scale bar is 100 μm. *P <0.05* verses static sample.

Collagen production in loaded samples was significantly higher in all groups compared with static controls. The 10 % strain group had higher cell viability and collagen deposition than all other conditions. When collagen was normalised to MTS, 5 % and 15 % strain groups had slightly higher collagen per cell compared with static controls but this was not significant. However, the 10 % strain group had significantly higher collagen per cell compared with static controls ($p < 0.05$). When scaffolds were cut in half, it was seen that SR staining on loaded groups was denser on the surface than static controls and the staining was more evenly spread in the scaffold centre in 5 % and 10 % strain groups than the other conditions (Fig. 6.4a). Interestingly, the 15 % strain group had less visible SR staining in the scaffold centre than the static group. Closer inspection of SR staining using fluorescent microscopy on the surface showed that static samples only deposited collagen around the pore wall whereas loaded samples produced collagen that spread across the pores.

Samples were also subjected to 10 % strain at days 6 and 9 and assayed at day 12 for any short-term effects on cell viability and collagen production. However, two days of loading did not appear to affect cell viability or collagen production (Fig. 6.5).
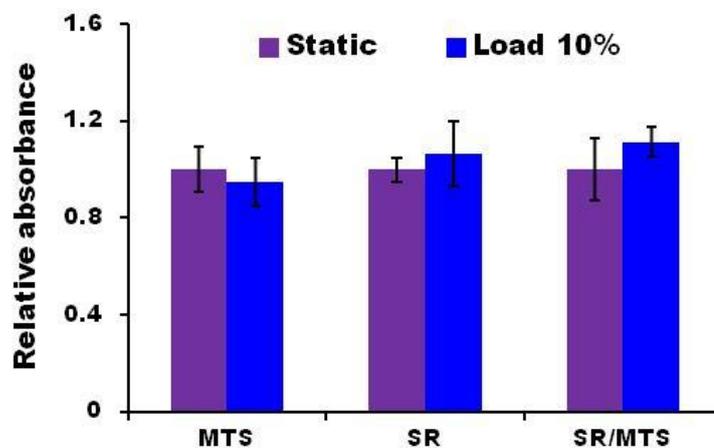
Figure 6.5: HDF seeded PU foam cultured statically or subjected to 5 % dynamic strain at days 6 and 9 and assayed at day 12 for cell viability (MTS) and collagen deposition (SR). No significant differences were observed between conditions. Data is mean ± SD (n = 4).

6.3.4 HDF seeded electrospun tecoflex

HDFs seeded on electrospun tecoflex were subjected to 5 bouts of dynamic tensile loading at 5, 10 and 20 % strain and assayed at day 21 (Fig. 6.6). A global strain of 5 % did not have any effect on cell viability or collagen deposition compared with

static controls. At 10 % and 20 % strain, cell viability was reduced, and this was statistically significant at 20 % compared with static controls. Collagen deposition was higher in samples subjected to 10 % and 20 % strain compared with static controls and this was statistically significant for 20 % strain. When collagen deposition was normalised to MTS, samples subjected to 10 % and 20 % strain had statistically higher values than static controls.
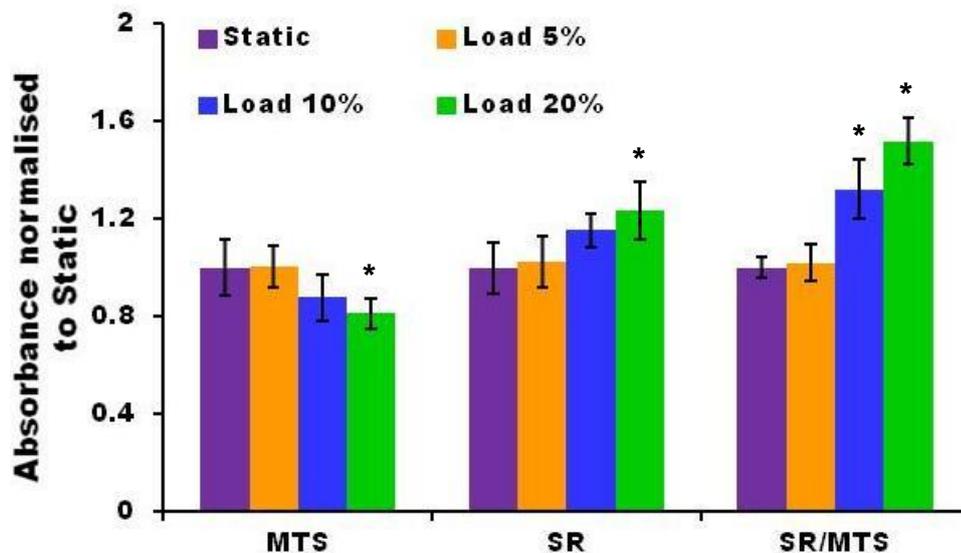
Figure 6.6: HDFs were seeded on random fibres of electrospun Tecoflex and cultured statically or subjected to 5 % dynamic strain at days 6, 9, 12, 15 and 18, and assayed at day 21 for cell viability (MTS) and collagen deposition (SR). Cell viability was assayed by MTS activity and collagen deposition by Sirius red staining at day 21. Values were normalised to static controls. Data is mean ± SD (n = 6). *P <0.05 verses static.

Cell-seeded tecoflex was held statically at each strain level (0, 5, 10, and 20 %) and then immediately fixed and fluorescently labelled to observe cell morphology (Fig. 6.7). Under 0% strain, cells appeared densely packed and well spread with no preferential orientation. As the strain level increased, gaps between the cells began to open up and the scaffold fibres increasingly unravelled, becoming straighter and more aligned parallel to the direction of load. This in turn caused more cells to appear elongated in the direction of the load, especially at 20 % strain.
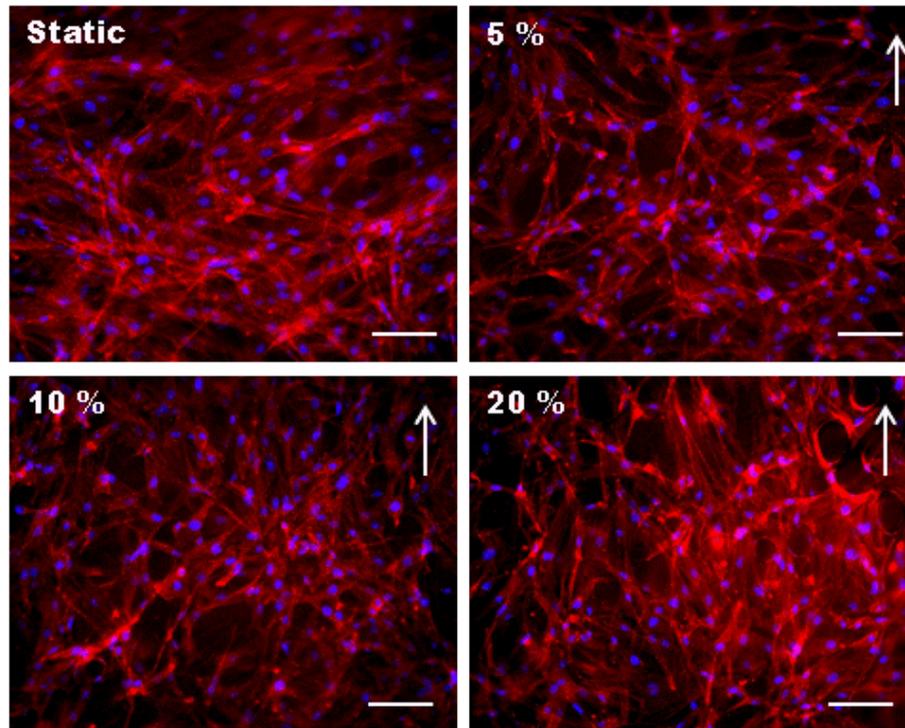
Figure 6.7: Fluorescent labelling of HDFs for nuclei (DAPI in blue) and actin cytoskeleton (phalloidin TRITC in red) cultured on random fibres of electrospun tecoflex and held statically at 0, 5, 10, or 20 % strain followed by immediate fixation. A greater number of cells are seen to orientate in the direction of strain with increasing strain magnitude. Arrows show direction of statically held strain. Scale bar is 100 μm.

6.4 Discussion

Mechanical forces play a key role in tissue homeostasis and are essential for tissue growth, remodelling and maintenance as well as normal function. Static culture does not mimic the dynamic conditions that occur in connective tissue *in vivo* including mechanical forces, nutrient delivery and waste removal. In this chapter, bone cells and HDFs were seeded onto 3D matrices and subjected to intermittent, dynamic tensile conditioning to assess what affect this form of loading had on collagen deposition. The effect of global strain magnitude was also studied on HDFs. For all cell types, loading increased collagen deposition to a certain extent, which was dependent on the number of loading sessions, the global strain, and the scaffold material. These results suggest that the cells were responding to the dynamic loading imposed on them through one of three possible mechanisms; direct sensing of

substrate strain; stress from fluid shearing caused by media movement in and out of the scaffolds; or improved nutrient transfer and waste removal.

There is still little consensus on the optimal regimes of mechanical stimulation due to the wide variety of parameters and possible interactions between chemical supplements. However, ascorbic acid (AA) is well known to play an essential role in the synthesis of stable collagen by mediating the hydroxylation of proline to enable the formation of the collagen triple helix. AA has been seen to support collagen synthesis in fibroblasts and bone cells, and also appears to be necessary for strain-induced increases of the mechanical properties of fibroblast-seeded scaffolds (Garvin *et al.* 2003). So it would seem that AA may be an essential requirement for loading-induced responses of mature fibroblastic cells which is why it was included in this study.

Dynamic loading was performed intermittently for short periods of time (2hrs) and yet cells responded under most conditions with an increase in total collagen. A previous *in vivo* study demonstrated that primary cells seeded in a porous scaffold and subjected to short bouts of loading (30 min, 3 times per week for 2 weeks) had a higher mineral content than non-loaded samples (Duty *et al.* 2007). It has been shown that prolonged mechanical stretching of tendon fibroblasts (TF) can have an inhibitory effect on cell proliferation. For example, hTF were stretched repetitively at 5 % strain for one day and proliferation increased, but when this stretching regime was applied for two days it was inhibited (Barkhausen *et al.* 2003). In another study, tendon fibroblasts were seeded on porous PU substrates and subjected to a wide range of dynamic strain conditions to study the effect this had on the resulting construct elastic modulus (Joshi and Webb 2008). It was observed that the stiffest constructs were those that were subjected to low-subphysiological strains (2.5 %), strain rates and loading frequencies (0.1-0.5 Hz), although both 5 and 10 % strain increased EM. A cycle number of 7200 (considered intermediate loading) increased EM compared with static controls, 1800 (low) and 43200 (high) cycle numbers. This suggests that cells do not need long bouts of dynamic culture in order for a response to occur. On the PU foam scaffold, MC3T3 bone cells responded to 3 days of loading (day 5, 10 and 15) at 5 % strain with an almost 2-fold increase in cell viability and collagen deposition at day 20. HDFs did not show any significant increases in collagen deposition with the same 3 days of loading but the addition of two extra

days of loading resulted in an increase in cell viability and total collagen deposition at all strains. This suggests that HDFs require more loading sessions in order to induce a behavioural response compared to the MC3T3s. MG63 cells seemed to respond to the same 3 day loading regime, however on each experimental run there was one statically cultured sample that also showed a high collagen deposition. This may be due to the heterogeneous nature of the PU foam and the ability of MG63 cells to form colonies enabling them to bridge the large pores.

Studies performed with pedometers have stated that humans walk between 6,700 and 11,900 cycles/day (Sequeira *et al.* 1995) with a frequency in the range of 1Hz. It has also been shown that delaying loading beyond the first few days of culture after seeding supports greater increases in collagen matrix production (Chen *et al.* 2006). In adult bone tissue, Duncan et al. (1995) showed that mechanical loading applied at a frequency of less than 0.5 Hz results in no mechanically-induced bone formation, but increases four-fold when the loading frequency is around 2 Hz (Duncan and Turner 1995). The loading cycle time of 1 Hz with a sinusoidal wave form was selected to simulate walking, and the number of cycles was kept constant throughout all experiments at 7200. This 1 Hz cycle time is commonly used for bone cell mechontransduction studies, however it has also been seen that high frequency and low magnitude loading can induce bone formation *in vitro* (Cowie *et al.* 2006) and *in vivo* (Judex *et al.* 2007).

Maximum strains experienced in bone during exercise have been estimated at around 0.005-0.2 % strain (50-2000 µstrain), which is dependent on the bone type and position as well as area in the bone (Burr *et al.* 1996). However, the local strain that each individual cell feels is under question (Bonivtch *et al.* 2007) and these physiological strains often fail to upregulate relevant bone markers. Often, mechanical strains at 'supraphysiological' levels of more than 0.2 % are used to stimulate cells *in vitro* and have been shown to be capable of upregulating relevant signalling factors (Owan *et al.* 1997). Many loading studies carried out *in vitro* are based on estimations of the forces experienced in the body and most studies also try to replicate those forces experienced in a mature tissue. However, with a tissue-engineered construct we are dealing with an immature and developing tissue and so it is likely that the physiological conditions found in a mature tissue are not optimal at this early stage. Although mature bone cells experience micro-strain levels, the

experimental model used here resembles that of a healing wound and it has been previously estimated that a healing bone wound can experience strains of up to 5 % (Claes and Heigele 1999). Also, the use of strain levels in the supra-physiological region is desirable if they are able to speed up the process of healing and increase matrix production as seen here.

Powell et al., (2010) showed that dermal fibroblast seeded fibrous collagen scaffolds held under 10 and 20 % static strain had greater strength than those cultured at 0 % strain. In addition, 10, 20 and 40 % strain showed greater stiffness but there were no differences amongst these loaded groups (Powell *et al.* 2010). In this study, HDFs showed the greatest level of cell viability and collagen deposition at 10 % strain on the PU foam scaffolds. Unexpectedly, on the PU foam scaffolds at 15 % strain, HDFs produced less collagen than at 10 % strain and similar levels to 5 % strain. This may be due to the fact that the scaffold appeared to undergo plastic deformation during the tensile conditioning regime. This loss of scaffold elasticity would mean that the scaffold no longer returns to its original position upon relaxation and so the cells would no longer feel any strain. This deformed scaffold may also interfere with the media flowing in and out of the scaffold and so it may alter the effects of FSS or nutrient transfer. On electrospun Tecoflex, cell viability of HDFs was lowest for samples subjected to the highest strain levels of 10 % and 20 % compared with 5 % and 0 % strain. This reduced viability may be due to slower cell proliferation or that the higher levels of stretching caused some cells to detach from the scaffold, especially if they were weakly adhered in the first place. However, collagen deposition was greatest with increasing strain and other studies have shown that collagen production increases in a strain magnitude-dependent manner (Yang *et al.* 2004b)

An important point to consider is that the strain level applied here is not reflective of what each individual cell experiences within the scaffolds. The PU foam is composed of many different sized struts and the cells are attached all around these and therefore those cells that are attached to the struts facing perpendicular to the load will experience very low strains compared with those that are attached parallel to the load, which will experience high strains. In an attempt to understand cell behaviour relative to the strain profile an individual cell receives, Woods *et al.* (2008) designed a model to provide insight to the strain distributions experienced across a single pore of a 3D

porous scaffold subjected to perfusion-compression conditioning (Wood *et al.* 2008). Through modelling of strain-induced flow patterns and their application to static constructs, it may be possible to elucidate the independent contributions of each mechanism. The strain profile was vastly different around a single pore including tensile and compression forces. Cells subjected to 0.61 % compression were seen to be rounded while those subjected to tensile force were flat and well-spread. Only cells that experienced intermediate levels of strain (relative to the maximum levels) produced mineralized osteoid and formed multicellular aggregates with their neighbours. This last point suggests that not all cells need to directly feel the optimal strain to undergo differentiation (Woods *et al.* 2009).

A similar situation occurs in the electrospun tecoflex where cells are attached in all directions and so those on fibres facing perpendicular to the load direction will initially only experience strain once the scaffold is stretched so much that the fibre orientates in the load direction. By holding the cells in static strain it was seen that HDFs on Tecoflex became more elongated in the direction of the strain as the strain level became higher. This is due to the fibres beginning to unravel and orientate in the strain direction and any cells attached to these straightened fibres will begin to stretch as the fibre stretches. Upon relaxation the fibres and cells then return back to their normal starting position. It has also been shown that in systems where one end of the substrate is fixed in position while the other end moves to produce substrate strain results in variability in actual substrate strain as a function of position (Joshi and Webb 2008). It would therefore be advisable for future bioreactor designs to simultaneously strain both ends of the substrate in order to produce and even strain distribution. There will also be local variations in the fluid flow-induced shear stress that the cells feel for similar reasons.

How the cell 'feels' the forces it is being subjected to will depend strongly on the substrate it is attached to. For example, a microporous foam scaffold, where the pore size greatly exceeds the cell size, effectively presents a flat or slightly curved substrate to the cell as it adheres to the wall of a strut (Reilly and Engler, 2010). By only attaching its basal surface to the material, mechanotransduction mechanisms of the cell may be similar to those already elucidated on planar substrates where large forces are observed on stiff strut materials (Stevens and George 2005). Interestingly, micropatterns that induce cell curvature on surfaces (McBeath *et al.* 2004b; Ruiz and

Chen 2008) as well as micropores of varying size within a scaffold (O'Brien *et al.* 2005) appear to directly regulate force production in stem cells, indicating that there may exist a gradual transition from a highly tensed, spread cell to a low tension, more rounded cell that contacts the material in all dimensions. However, there are a number of critical points to note. Cells deposit their own matrix with time and in response to the load and thus interactions between the cell, its self-synthesized ECM, and neighbouring cells may rapidly change. With time the self-synthesised matrix may become a more critical guidance variable and cellular interactions with the original scaffold matrix may decrease, especially if it degrades. Such thinking is the reason why degradable scaffolds composed of materials like PLA and PCL are often employed for tissue engineering, as they are replaced by self-synthesized ECM. That said, fate decisions may be made within the first days of seeding cells, i.e. cell plasticity may be limited (Engler *et al.* 2006) and cell fate could be programmed in the first few days of interaction with a material.

On scaffolds with relatively small pores, such as those of the electrospun tecoflex, cells form a confluent layer and pack in very densely, which may also alter the way in which they respond to applied force. In contrast, on the open porous PU foam scaffolds, MC3T3 cells were unable to traverse the larger pore sizes by day 20 regardless of whether they received static or dynamic culture. HDFs cultured on PU foam and subjected to loading were able to bridge the large pores. Loading in these cells may have caused increases in collagen production to allow the cells to use it as a bridge and also it may have encouraged proliferation. MC3T3 cells are much smaller than HDFs and subsequently their size is probably limiting them from bridging the gaps.

It is important to note that in a three-dimensional cyclic strain culture system, mechanical stimulation may result from direct substrate strain, increased nutrient transfer, as well as fluid shear resulting from strain-induced fluid flow around and within the porous substrate. Loading-induced fluid flow will also enhance chemotransport due to convection or mass transport, which will affect the biochemical environment around the cells and within the constructs (Allen *et al.* 2000; Donahue *et al.* 2003). Allen *et al.* (2000) showed that bone cell response to fluid flow is modulated by the cells surroundings. Serum-supplemented medium enhanced the intracellular calcium response of bone cells to fluid flow compared with

serum-free fluid flow (Allen *et al.* 2000). Donahue et al. (2003) used oscillatory FSS to stimulate MC3T3 cells to varying shear stresses and flow rates and found that this type of stimulation can enhance chemotransport in the presence of calf serum with increasing flow at constant shear stress (Donahue *et al.* 2003). However, a study by Bakker et al. (Bakker *et al.* 2001) using steady flow did not see these enhancements, which suggests that the type of stimulation may be important. The FSS experienced in this model system are likely to be oscillatory as they are drawn in and out of the scaffold.

The distribution of nutrients and oxygen levels are highly important factors in the development of many tissues *in vivo* (Zahm *et al.* 2008). Tissues in the body are provided with nutrients and oxygen by networks of blood vessels, which either penetrate directly into well-vascularised tissues like skin and bone, or are passed diffusion into poorly-vascularised tissues such as cartilage. There are also many systems in place that control waste removal and waste gas exchange enabling the tissues access to a constant supply of oxygen and fresh nutrients. For cell-seeded scaffolds *in vitro*, nutrients are provided by the surrounding culture medium and waste removal occurs by removing the media manually. In 3D static cultures, media cannot easily reach the centre of the scaffold and so less nutrients and oxygen are delivered to cells in the middle. The use of dynamic culture, whereby fluid is drawn in and out of the entirety of the scaffold allows for more nutrients and oxygen to reach the scaffold centre and allows for more viable cells and even distribution of matrix (El Haj and Cartmell 2010). This study showed that PU foam scaffolds subjected to loading had a more even distribution of collagen matrix across the scaffold and matrix was present in greater amounts towards the scaffold centre. The loading period was relatively short compared to the static culture time and so any effect from improved nutrient and oxygen transport would be small.

Previous studies have highlighted the importance of rest periods. For long term culture, it seems likely that the optimum loading regimes may involve a combination of dynamic culture along with static rest periods. The dynamic portion will subject cells to mechanical stimulus for increased production of ECM while also providing sufficient nutrients and waste product exchanges. The static portion will allow recovery time for the cells to produce matrix in response to load and to migrate into the construct.

6.5 Conclusions and future work

Dynamic tensile conditioning of cell-seeded constructs caused an increase in deposited collagen either as a consequence of increased cell viability or due to individual cells producing more collagen than their static counterparts. The electrospun tecoflex scaffold mimics the fibrous ECM networks found in connective tissue better than the PU foam, while the PU foam may be a mimic for cancellous bone. However both scaffolds are non-biodegradable and so would not be suitable for implantation and therefore future studies would ideally use biodegradable polyurethanes (Guelcher *et al.* 2007) for example, in order to study the effects of scaffold degradation. Cell-seeded aligned tecoflex was not used in this study due to the scaffold being very elastic and contracting when not restrained, causing the fibres to buckle and lose alignment. Even when the scaffold was held taut to preserve fibre alignment, it was almost impossible to mount it in the loading system without disrupting fibre alignment and so no experiments could be performed using these scaffolds. In order to study the effects of cells on aligned substrates that mimic anisotropic tissues (tendon or ligament), durable aligned substrates that can be easily handled need to be utilised.

The loading system employed here is capable of testing a wide variety of parameters, however, it is limited to the number of samples it can stimulate simultaneously, it requires large volumes of media, and it cannot fit inside an incubator so there are likely to be some effects of loading at room temperature. Therefore, the ideal bioreactor would be easy to use, and able to accommodate multiple samples that can be held in the system throughout the culture period. As well as looking at matrix production and distribution, it would be ideal to monitor matrix orientation and so future studies should incorporate SHG imaging to look at collagen organisation in response to strain.

6.6 Summary

- MC3T3s and HDFs cells seeded in 3D porous foams respond to short periods of intermittent dynamic tensile loading with increased cell viability and collagen matrix deposition.

- The response of HDFs to tensile loading was strain dependent with a strain of 10 % being optimal on the PU foam and 20 % on electrospun Tecoflex.

- HDFs required more days of loading throughout the culture period than MC3T3 cells for a response to occur.

- Loaded constructs had improved matrix deposition in the scaffold centre.

- Dynamic loading of this nature in a fluid-filled environment is likely to elicit additional effects from FSS and improved nutrient delivery.

- A combination of dynamic culture and static conditions may be optimal for developing a suitable tissue engineered construct for clinical use.

CHAPTER SEVEN: The effect of a simple fluid shear stress stimulus on osteoprogenitor matrix production

7.1 Introduction

Our understanding of the behaviour and capabilities of stem cells have come a long way in recent years but we are still unable to precisely control their differentiation, which is a major factor limiting the development of successful tissue engineering strategies. My previous chapters have shown, amongst other researchers, that MSC behaviour and function can be controlled by biochemical stimuli (see chapter 3) as well as physical and environmental cues (see chapter 5). More recently, researchers have become aware that mechanical forces can also have an influence on MSC behaviour and may be important in directing their differentiation and maturation to obtain a fully-developed tissue engineered construct.

One of the major forces that contribute to the mechanical environment of bone cells are oscillatory fluid shear forces caused by fluid movement through interstitial bone space caused by repetitive loading and unloading of the bone. It is also thought that oscillatory fluid shear stresses (FSS) would be experienced by cells in the bone marrow cavity. The magnitudes of the FSSs experienced by cells in mature bone have been predicted to be in the range of 0.8-3 Pa (Weinbaum *et al.* 1994). It is also thought that FSSs occur in the bone marrow cavity itself, and although the magnitude of these stresses are not known, they are predicted to be much less due to the higher porosity and lower stiffness of the marrow (Gurkan and Akkus 2008). It is also expected that progenitor cells residing in other tissues may also be exposed to external mechanical stimuli. Recent *in vitro* stimulation of osteoprogenitors using FSS have shown that osteogenic differentiation can be induced or enhanced on 2D substrates as well as 3D scaffolds, see recent reviews Delaine-Smith and Reilly (2011) and McCoy and O'Brien (2010).

While it is has been established that mechanical forces can influence osteogenic progenitor differentiation, it is not clear what the best conditions are to achieve this. The simple rocking platform system introduced in chapter 3 may be a suitable method for studying the effect of fluid flow-induced shear stress on osteogenic progenitor cell differentiation. The simplicity of the apparatus also allows for fast

and easy monitoring of the production of collagen by the minimally-invasive technique of SHG. The ability to monitor long-term matrix development is important as the successful production of a tissue-engineered construct requires a well-defined body of differentiated cells and ECM. Therefore, this system seems ideal for testing the effect of FSS on osteogenic progenitor cells and how they influence their differentiation and matrix production in a rapid and straightforward manner.

For this study, hESMPs and HDFs were chosen to represent two different osteogenic progenitor cell types. In chapter 3, both cell types were shown to undergo osteogenic differentiation in osteogenic media and had the ability to produce a mineralised matrix. Previous results chapter have also shown that the differentiation of both these cell types are influenced by external physical cues and so they seem ideal for use in this work.

In summary this chapter had four objectives. The first objective was to calculate the magnitude and nature of the shear stresses being experienced in the well at the conditions selected. The second objective was to use the simple platform rocking model to mechanically stimulate osteogenic progenitor cells to see if the oscillatory FSS created could influence their differentiation and matrix production. The third was to examine if FSS were able to enhance the osteogenic differentiation of dermal fibroblasts cultured in osteogenic media. The final objective was to monitor the effect FSS had on the production and organisation of cell secreted tissue engineered collagen using SHG.

7.2 Methods

7.2.1 Cell Culture

Two cell types were used in this study; primary human dermal fibroblasts (HDFs) isolated from dermal tissue taken from one donor and the human embryonic cell-derived mesenchymal progenitor cell line hES-MP 002.5 (hESMP). HDFs were used between passages 2-3 for FSS experiments (HDFs at passage 4 were also used but not included in quantitative data due to minimal calcium staining) and hESMPs were used between passages 3-7. Media groups were either non-dex containing media (NM) or osteogenic media (OM) for hEMSPs, and HDFs were cultured in fibroblastic media (FM) or OM.

7.2.2 Application of fluid shear stress

For experiments, both cells were seeded onto gelatine coated standard 6-well plates at a density of 10,000 cells per well in their respective basal media. Starting from day 4 of culture, cells were exposed to periods of rocking consisting of 45 cycles/min for 1 h/day, 5 days/week. For imaging cell morphology at day 7, cells were also seeded at a lower density of 5, 000 cells/well. The FSS generated were calculated for three separate points in space along the well bottom using a previously described lubrication-based model for a circular well (Zhou *et al.* 2010). Values of FSS were obtained using the equation for calculating the characteristic shear stress, where μ is the fluid viscosity (10^{-3} Pa s), θ_{max} is the maximal tilt angle, δ is the ratio of the fluid depth to the well length, and T is the time for one cycle. Briefly, the model assumes that fluid movement is mainly driven by gravity, and that the fluid free surface remains horizontal. Secondly, the centrifugal forces acting on the fluid are neglected due to the low angular acceleration and velocity.

$$\left|\tilde{\tau}_w\right| = \frac{\pi\mu\theta_{max}}{2\delta^2 T}$$

7.2.3 Cellular assays

- Cell morphology: DAPI and phalloidin TRITC at day 7 visualised by Image Express™ fluorescent microscope.
- Total DNA measurement for cell number at days 7, 14, and 21.
- ALP activity at days 7, 14 and 21.
- Quantitative collagen staining using 0.1 % Picrosirius red solution at days 7, 14, and 21.
- Qualitative and quantitative deposited calcium staining using 1 % Alizarin red S at day 21.
- Qualitative collagen production and organisation visualised using SHG at days 7, 14 and 21. Images were obtained from the centre region of the sample at a depth of approximately 10 µm.

7.2.4 Statistics

FSS experiments were performed three times in triplicate (n = 9) (for HDFs at P4 n = 3). For collagen visualisation using SHG, one sample of each condition was imaged at each time point (n = 2-3). Cells of the same type and cultured using the same media conditions were compared for significant differences between statically cultured and rocked groups.

7.3 Results

7.3.1 Fluid shear stress profiles
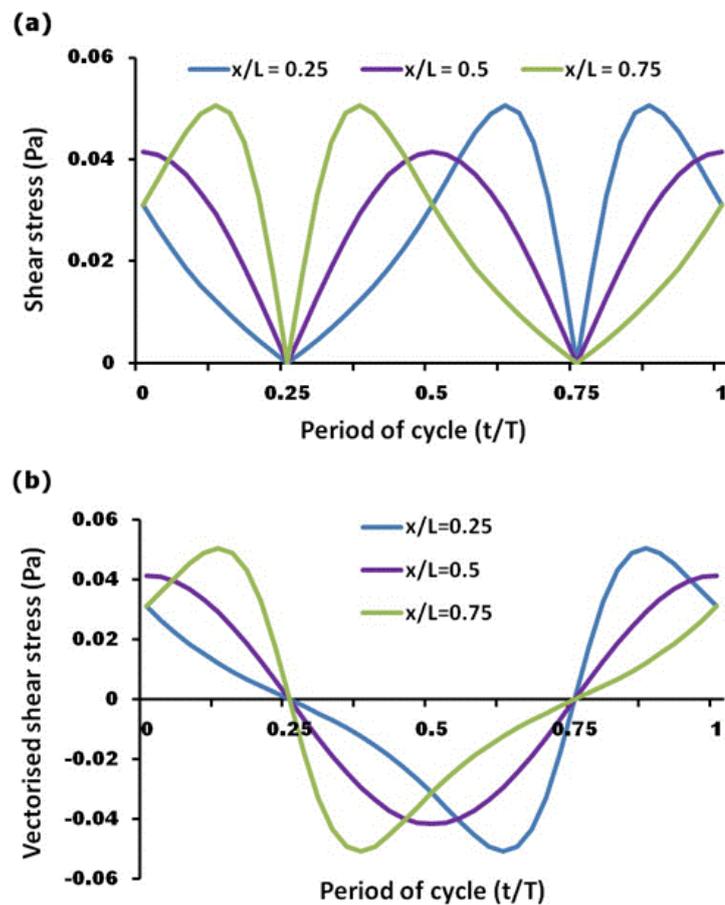
Figure 7.1: FSS profiles for one cycle experienced at the base of a 6-well plate for three different locations, x/L = 0.25, 0.5, or 0.75, where x is the distance from the edge of the well and L is the diameter of the well. (b) The oscillatory nature of the fluid flow induced shear stresses indicated by positive and negative stress.

The FSSs at the base of the culture wells were calculated at 3 separate points in space (x/L = 0.25, 0.5, 0.75, where x is the distance from the edge of the well and L

is the diameter of the well) along the middle of the well parallel to the fluid movement during one rocking cycle. The FSS varied in a spatiotemporal fashion and was oscillatory in nature (Fig. 7.1a-b). Under the conditions used, the shear stress at the centre of the well ($x/L = 0.5$) was found to vary in a sinusoidal manner peaking at 0.041 Pa, while at the other two locations ($x/L = 0.25$ or 0.75) the stress peaked at 0.051 Pa and deviated from a typical sinusoidal wave. The stress profiles at locations $x/L = 0.25$ and 0.75 were identical except for a phase difference of 180 degrees.

7.3.2 The effect of FSS on the morphology of progenitor cells
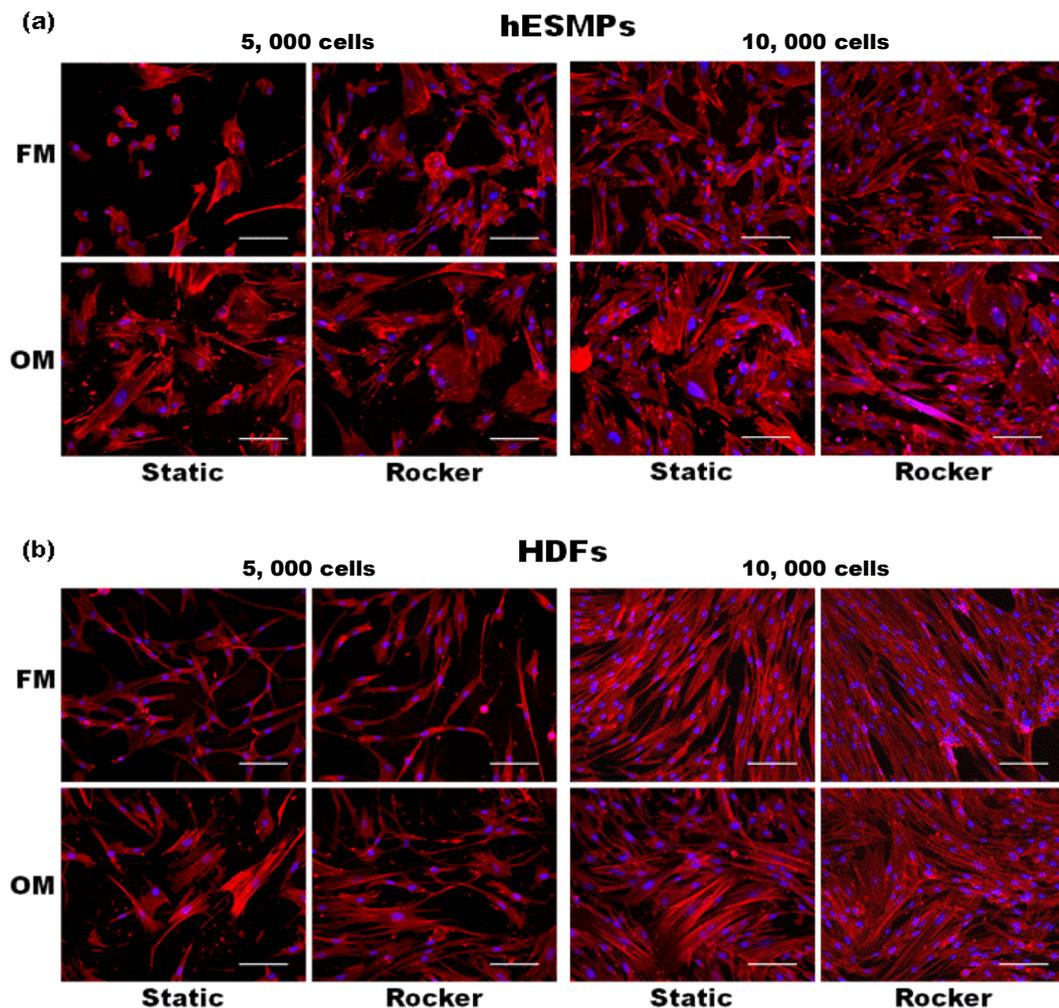
Figure 7.2: Fluorescent staining of cell nucleus (DAPI-blue) and actin cytoskeleton (phalloidin TRITC-red) at day 7 of (a) hESMPs cultured in either NM or OM and (b) HDFs cultured in either FM or OM under static or rocked conditions. Cells cultured in FM and NM show a more fibroblastic morphology whereas cells cultured in OM show a more osteoblastic morphology. (Scale bars are 100 μm).

hESMP cells cultured under static conditions in NM had a fibroblastic, spindle-shaped morphology, whereas hESMPs cultured in osteogenic media (OM) were larger and more cuboidal in shape, indicative of an osteoblastic cell (Figure 7.2a). Application of FSS appeared to cause hESMPs to become more elongated under both media conditions. HDFs cultured in fibroblastic media (FM) showed a typical fibroblastic morphology, however when cultured in OM they showed a more cuboidal morphology (Fig. 7.2b) similar to the hESMP cells and generally appeared larger than those cultured in FM. When HDFs were rocked they also tended to become more elongated than cells cultured under static conditions especially when cultured in fibroblastic media. Cellular alignment did not appear to be influenced by fluid flow induced by rocking in any areas of the culture well for either cell type.

7.3.3 The effect of FSS on total DNA and ALP activity of HDFs and hESMPs

Total DNA content, an indicator of total cell number, increased for both cell types in all cell groups between days 7 and 14 and then remained constant up to day 21 (Fig. 7.3 a-b). There were no significant statistical differences in total DNA between cells that were rocked or cultured under static conditions but it was noticed that hES-MP cells cultured in OM did have 20% less DNA at days 14 and 21 compared with cells cultured in NM. Normalised ALP activity increased in both cell types for all cell groups up to day 21 (Fig. 7.3 c-d), however no ALP activity was detectable in any HDF culture groups at day 7. When OM was combined with FSS, normalised ALP activity in hESMPs was 2-fold higher at day 14 compared with their static counterparts. It appears that the rocking accelerated the upregulation of ALP activity as by day 21 the static controls were as high as the rocked samples. However, there was no effect seen when NM was combined with rocking. HDFs cultured in FM only produced ALP just detectable above baseline values at days 14 and 21, however when cultured in OM they began producing sufficiently detectable levels of ALP at day 14. By 21 ALP activity had increased 4 times compared to day 14. When OM cultured HDFs were subjected to FSS, ALP activity increased by 20% over static counterparts at day 21, which was statistically significant.
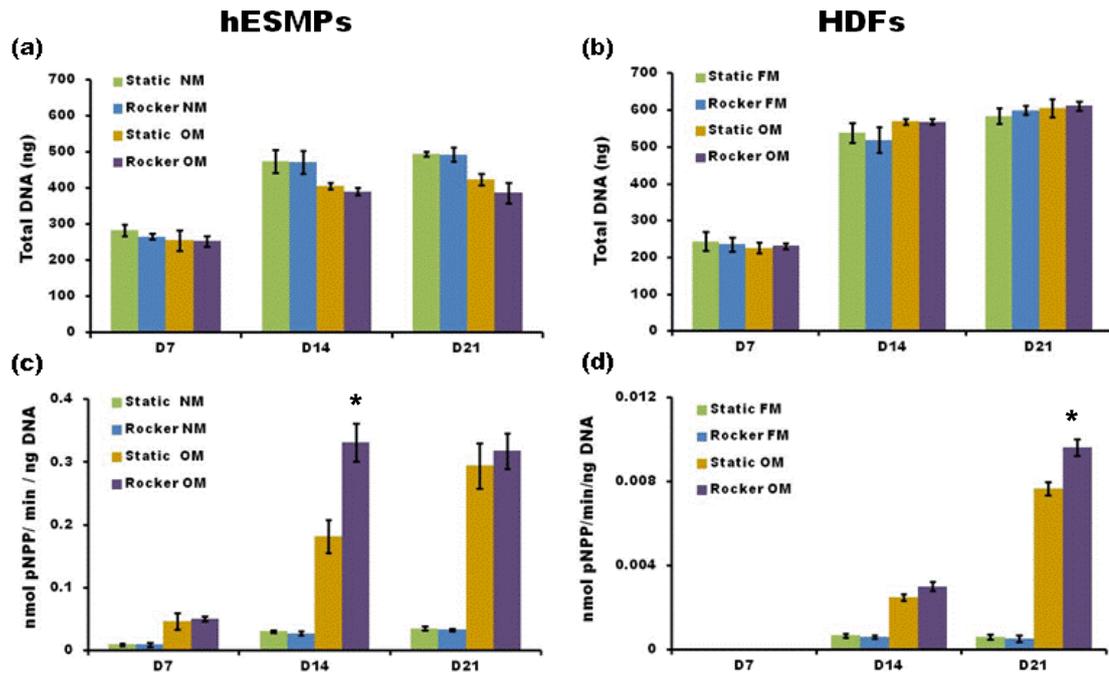
Figure 7.3: Affect of FSS on DNA content of hESMPs (a) and HDFs (b) and ALP activity (normalised to DNA) for hESMPs (c) and HDFs (d) measured at days 7, 14 and 21. Note the y axis range for HDFs is smaller than that of the hESMPs due to a lower ALP activity. All data is mean ± SD ($n = 9$). *$P < 0.05$.

7.3.4 The effect of FSS on total collagen and calcium production

Total collagen production quantified by Picrosirius red staining showed that cells cultured with Dex had produced less collagen at all time points compared to those cultured without Dex (Fig. 7.4-7.5). For hESMPs cultured in either media group, the application of rocking caused the total amount of collagen deposited by day 21 to be 20% higher ($p < 0.05$) (Fig. 7.4 a). For HDFs subjected to rocking, significantly more total collagen ($p < 0.05$) was seen at days 14 and 21 for both media groups (Fig. 7.5 a). Calcium deposition assayed at day 21 was 3-fold higher in OM treated hESMPs subjected to rocking compared to static counterparts and this staining was more uniform across the culture dish while static cells showed patchy staining (Figure 7.4 b). In comparison, HDFs cultured in OM showed a relatively small amount of calcium staining at day 21 but rocking significantly increased the amount deposited by 50% (Fig. 7.5 b). The alizarin stain was seen to concentrate more around the centre of the wells and became fainter towards the outside of the well.

186
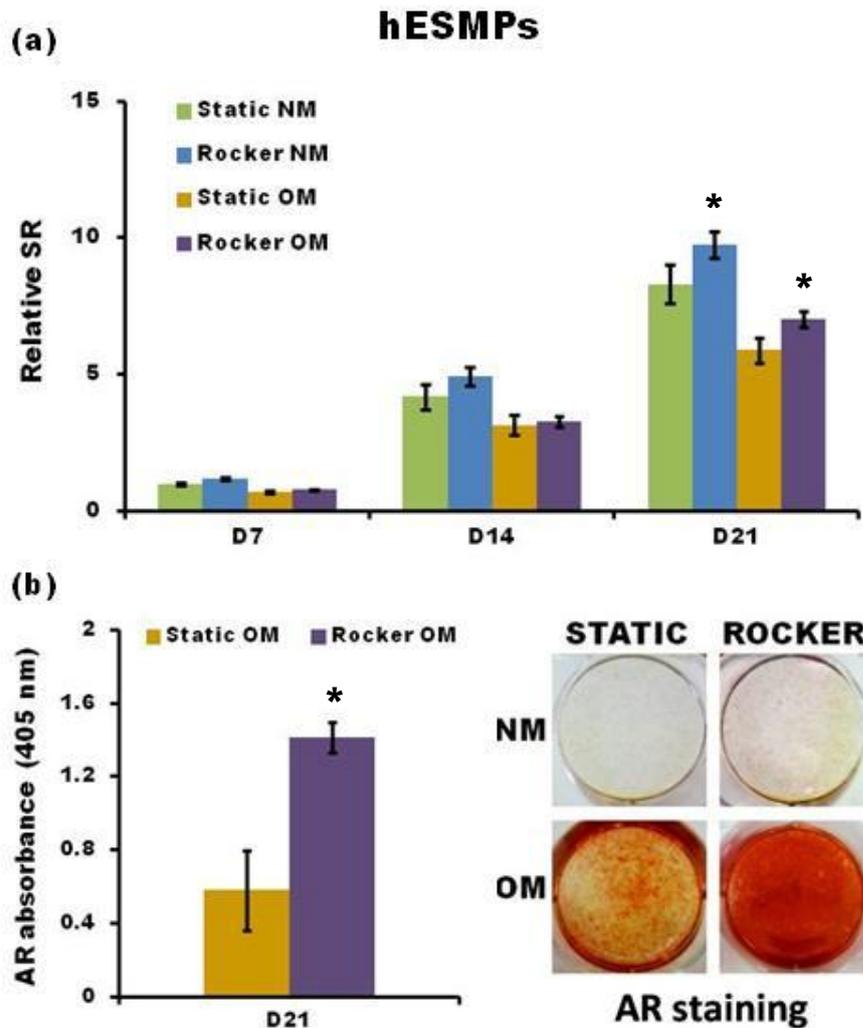
Figure 7.4: Total collagen production (a) and calcium deposition (b) at days 7, 14 and 21 as quantified by SR and AR staining respectively for hESMPs subjected to rocking or cultured statically. Calcium deposition was visualised at day 21 by AR staining (b). Non-Dex containing media (NM) or FSSs alone did not induce calcium deposition. Data is mean ± SD (n = 6 for collagen; n = 9 for calcium) *P <0.05.

HDFs cultured in OM at P4 appeared to also produce more calcium in response to FSS as visualised by Alizarin staining (Fig. 7.6) but the level was too small to quantify. Both hESMP cells and HDFs cultured without Dex did not produce any calcium as visualised by the absence of alizarin red stain.
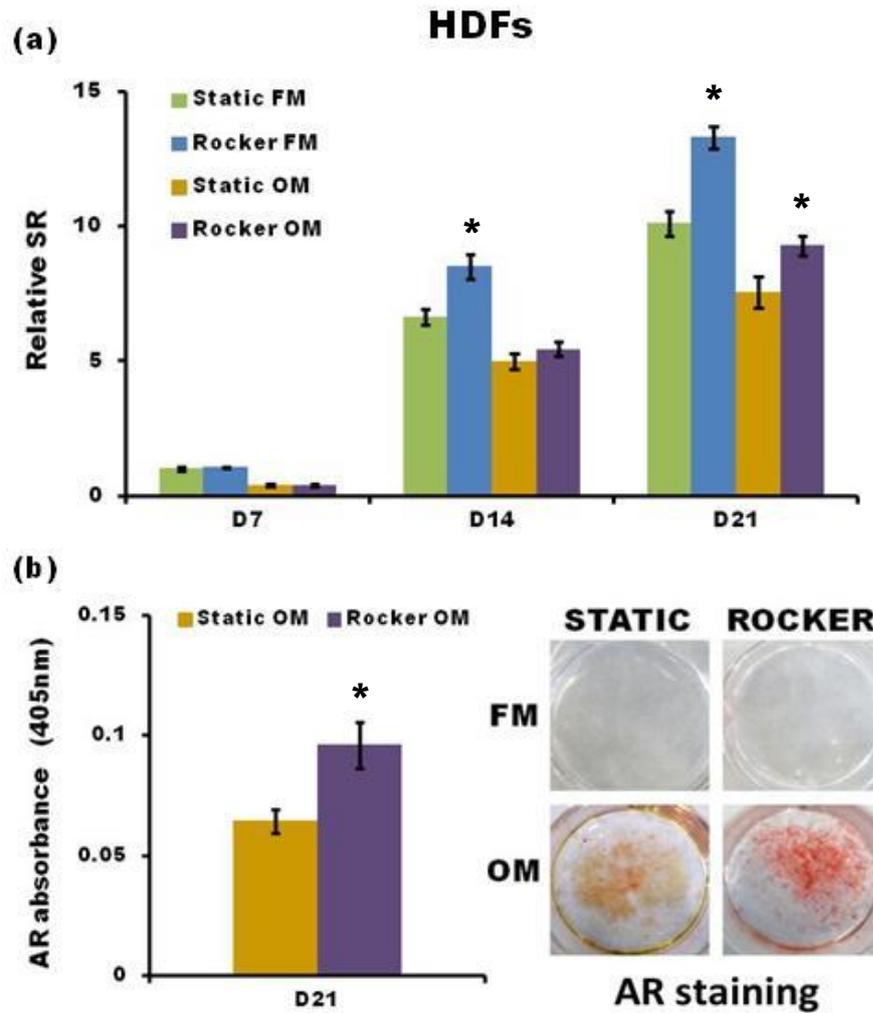
Figure 7.5: Total collagen production (a) and calcium deposition (b) at days 7, 14 and 21 as quantified by SR and AR staining respectively for HDFs subjected to rocking or cultured statically. Calcium deposition was visualised at day 21 by AR staining (b). Fibroblastic media or FSSs alone did not induce calcium deposition. Data is mean $\pm$ SD (n = 6 for collagen; n = 9 for calcium) *P <0.05*.
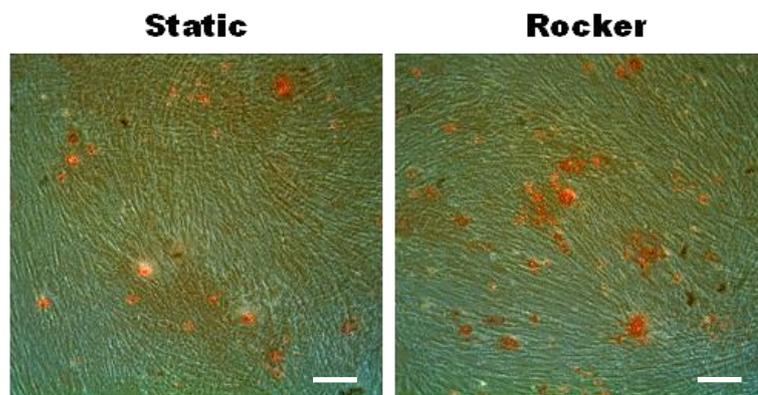
Figure 7.6: HDFs cultured in OM at the fourth passage (P4) appeared to have greater Alizarin staining (D21) when subjected to FSS compared with static culture. Scale bar is 100 μm.

7.3.5 Assessment of collagen production by second harmonic generation

The effect of FSS on collagen deposition and maturation was monitored in both HDFs and hESMP cells using SHG at days 7, 14 and 21 (Figure 7.7 a-b). Signal intensity increased for all samples from day 7 to 21 indicating an accumulation of collagen over the culture period. When both cell types were cultured in the presence of Dex, the signal intensity was lower at all time points compared to those cultured without Dex. At day 7, SHG signal from both cell types cultured in OM was barely visible and therefore no noticeable differences between static and rocking groups were evident. However, when both cell types were cultured without Dex and subjected to rocking, an increase in SHG signal was seen at all time points compared with static counterparts. It was not until day 21 that a noticeable difference in SHG intensity was seen for both cell types when cultured in OM with those subjected to rocking giving a stronger signal compared with statically cultured counterparts. Rocking appeared to have a smaller effect on SHG intensity in hESMPs (Fig. 7.7 a) than in HDFs (Fig. 7.7 b) when compared with static counterparts. While rocking did not appear to induce a preferred direction of collagen orientation with either cell types in any media groups, rocking did appear to improve collagen organisation at day 14 and even more clearly at day 21. Statically cultured groups were seen to contain short and disorganised collagen fibres, whereas FSS groups had thicker and longer bundles of fibres and this effect was more evident in groups cultured without Dex.
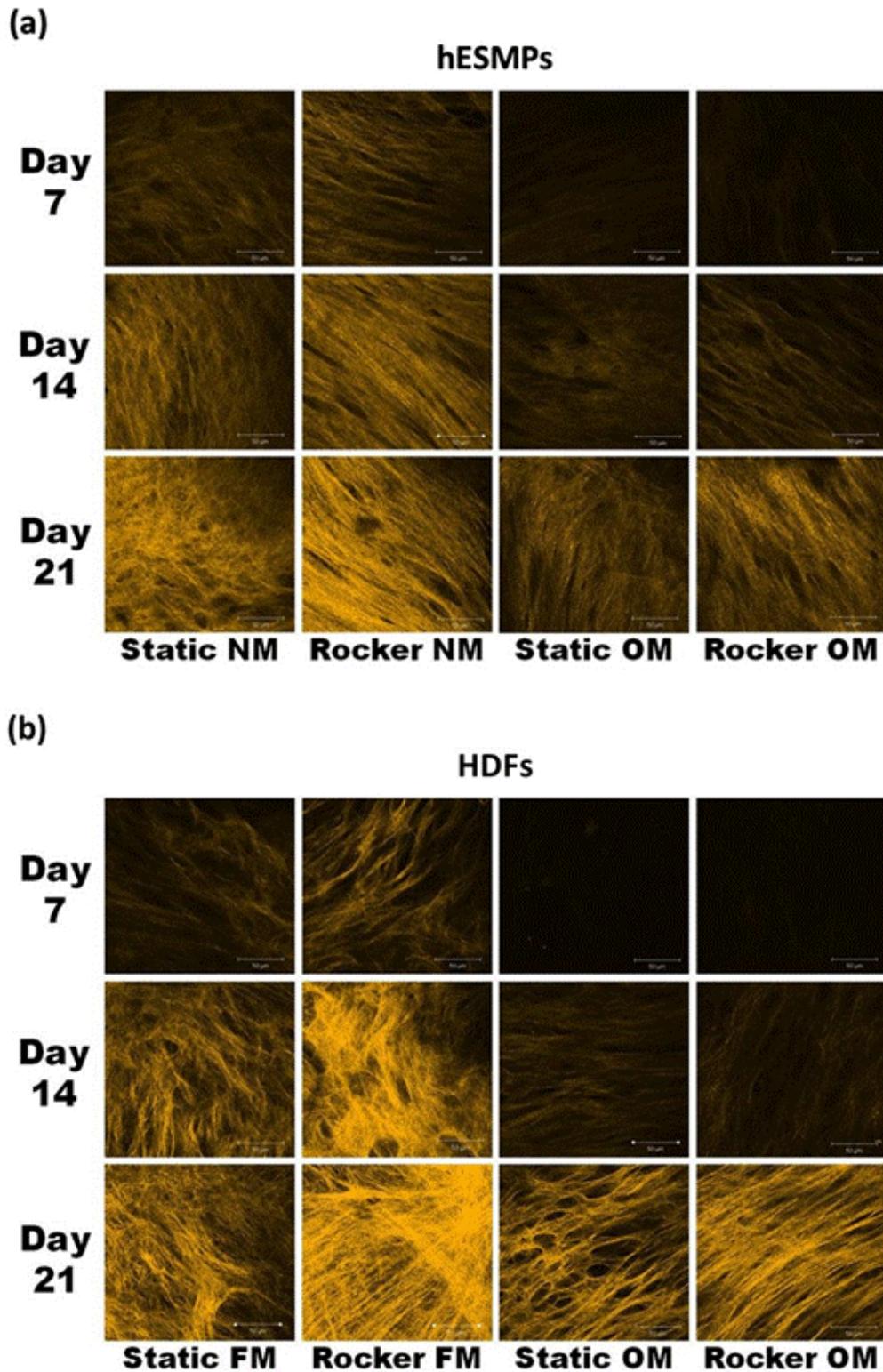
Figure 7.7: Second harmonic generation (SHG) images of deposited collagen fibres produced by hESMPs (a) and HDFs (b) at days 7, 14 and 21. Increases in collagen deposition and organisation are indicated by an increase in SHG intensity and area coverage. A more organised collagen matrix can be observed in cells subjected to FSSs indicated by the appearance of thicker collagen bundles and more defined fibres. Images with a dark appearance did not produce enough detectable SHG signal at the set conditions. Images are typical of 3 images for n = 2. Scale bars are 50 μm.

7.4 Discussion

The main aim of the work in this chapter was to assess the effectiveness of a simple methodology (a rocking platform) to apply oscillatory FSS to osteoprogenitor cells for enhancing differentiation and production of a mineralised collagenous matrix. This study was the first, to our knowledge, to use this simple methodology on progenitor cells. As a potential convenient source of cells for bone tissue engineering, we also wanted to see if the osteogenesis of HDFs could be enhanced using this stimulus. This is also the first study we know of to subject dermal fibroblasts and the hESMP cell line, both cultured in osteogenic media, to oscillatory FSS. I have also demonstrated the potential of the novel and minimally-invasive technique of SHG to monitor the effect of oscillatory FSSs on collagen production by cells, and the ease at which it could be performed with this system.

It has been demonstrated that osteoprogenitor MSCs respond to a variety of mechanical stimuli in a range of 2D and 3D bioreactor conditions (Delaine-Smith and Reilly 2011). However, here I present the interesting result that dermal fibroblasts cultured in osteogenic media produce a mineralised collagenous matrix that is further enhanced by oscillatory FSS. The reasons for selecting HDFs for use in this study is that isolating progenitor cells from the dermis would have many advantages over other osteoprogenitor sources in that any donor will have large quantities of easily accessible skin and operations to remove it are simple and less painful than procedures to remove bone marrow. HDFs also have a high proliferative potential and can be expanded into large numbers *in vitro.*

The FSSs calculated in this study were much lower than those estimated to occur within mature bone (0.8-3 Pa) (Weinbaum *et al.* 1994), peaking at 0.041 Pa in the well centre and are also much lower than the FSSs generally used by others for mechanically stimulating osteoblastic cells, particularly in 2D (McCoy and O'Brien, 2010). However, in chapter 3 it was seen that the mature osteoblast MLO-A5 cell line responded to this FSS with a noticeable increase calcium production at day 21. Collagen production and organisation was improved in both the hESMP cells and the HDFs after they were subjected to these FSS. When cultured in combination with osteogenic media and FSS, both cells upregulated ALP activity and calcium production. Previous studies have also shown that hMSCs cultured in osteogenic

supplements are mechanosensitive to relatively small shear forces (0.036 Pa) applied for only short periods of time (Kreke *et al.* 2005). In a recent study, a T-75 flask rocking system was used to enhance osteogensis in osteoblasts and osteocytes to condition media for MSCs (Hoey *et al.* 2011), and although they did not calculate the FSSs present, it is likely they would have also been relatively low. Recently, computational fluidics has been used to more accurately model the fluid-flow induced shear stresses occurring at the base standard 6-well on a rocking platform, yielding similar values to the lubrication-based model (Tucker *et al.* 2011).

It has been noted by our group and numerous other researchers that higher magnitudes of shear stress and longer periods of exposure to FSS can result in detachment of both progenitor cells and mature bone cells (McCoy and O'Brien 2010). Mature bone cells *in vivo* are encased in a mineralised collagen matrix and so are likely to better resist the shear stresses they are exposed to compared with cells *in vitro*, which are not encased in the same dense matrix. High shear stresses such as those experienced *in vivo* may not be suitable or even required for *in* vitro development of tissue engineered constructs. While the magnitude of fluid shear forces in bone marrow are not know, it is highly likely that they will be lower than those found in mature bone due to higher porosity and lower stiffness of the marrow (Gurkan and Akkus 2008). Additionally, it is unclear whether tissue engineers should be attempting to replicate the mature bone environment or rather a developmental or facture healing environment where bone cells differentiate *in vivo*. Immature, developing bone tissue resembles a healing wound and not a mature tissue and so the forces experienced are likely to be different from those of a fully developed tissue, although little is known about what these forces are (Willie *et al.* 2010).

The shear stress profiles and the peak shear force varied for different locations within the well plate, but the resulting calcium staining for hESMPs showed a rather uniform pattern across the well. This indicates that either the range of forces being experienced by the cells have a similar effect on their differentiation or that the cells are communicating with each other, such as via gap junctions (Donahue 2000; Taylor *et al.* 2007). Another contributing factor could be that the fluid flow is inducing chemotransport (Donahue *et al.* 2003) and so biochemical factors regulating bone cell metabolism, such as prostaglandin E_2 (Genetos *et al.* 2005), are

released into the media by the cells and moved around due to mass transport. While we did not test the mechanisms by which fluid flow enhances osteogenic differentiation, the data presented combined with other studies suggests that osteoblastic differentiation may be guided by soluble factors that accumulate in the media from a combination of externally applied chemical stimulants and direct mechanical stress on the cells (Hoey *et al.* 2011).

This study showed that hESMPs and HDFs cultured in osteogenic media had significantly higher ALP activity than those cultured in non-Dex containing media and this level continued to rise up to day 21. While some authors report ALP activity as a biphasic process (Bancroft *et al*., 2002; Datta *et al*., 2006), this was not seen to occur here and so both cell types may have not reached their peak levels yet. FSS increased ALP activity in both sets of progenitor cells when cultured in osteogenic media and both cells subsequently increased their calcium deposition. ALP activity in the hESMPs was at least ten-fold higher than that in HDFs. A possible reason for this is that the hESMPs are a relatively homogeneous population of cells derived from a single source of embryonic stem cells already characterised as mesenchymal lineage specific and able to undergo osteogenesis in induction media (Karlsson *et al.* 2009). However, HDFs are a much more variable cell population from a mature adult donor and it is likely that only a sub-population of the cells can undergo osteogenic differentiation, or that the cells have varying levels of differentiation potential (Chen *et al.* 2007).

Cells derived from dermal tissue have previously been reported to show osteogenic differentiation potential (Bartsch *et al.* 2005; Chen *et al.* 2007). This study showed that HDFs produced ALP and deposited calcium when cultured in osteogenic supplements. Previous studies have tended to culture HDFs under static conditions but this study showed that the application of oscillatory FSS could further enhance this osteogenic differentiation. In a previous study by Sommar *et al.,* (2009), HDFs were cultured in a macroporous gelatine construct in the presence of osteogenic media and subjected to FSS in a rotating spinner flask. They noticed the formation of bone-like tissue, with further enhancements in the amount of deposited mineral in constructs cultured in spinner flasks (Sommar *et al.* 2009). This observation, along with the work in this chapter, suggests that FSS can enhance mineralized matrix in HDFs cultured in osteogenic media. This revelation that HDFs can be induced

towards an osteogenic lineage using osteogenic supplements and FSS highlights their potential use in the repair of bone.

In this study, quantitative data for HDFs were only obtained using cells at passages 2-3 because after this they did not consistently make calcium at day 21 although they did continue to upregulate ALP activity to similar levels (See Chapter 3). However, an experiment was carried out using HDFs at P4 and Alizarin staining showed a visual increase in the amount of deposited calcium when subjected to rocking. The majority of studies have used dermal fibroblast populations taken from fetal or juvenile skin (Lavoie *et al.* 2009; Xue and Li 2011) with the authors reporting loss of osteogenic potential or decreased potential at higher passage numbers. Some have reported that dermal progenitor populations display a delayed differentiation potential, often taking longer to mineralize than other MSC populations, anywhere between 4-8 weeks (Buranasinsup *et al.* 2006; Jaager and Neuman 2011; Lorenz *et al.* 2008). However, there are a number of studies that have shown osteogenic differentiation to occur in cells from mature and aged dermis (Xue and Li 2011; Young *et al.* 2001). This loss of differentiation potential, and donor variation could be a potential limitation with the future use of these cells for autologous bone repair, and so it is clear that more studies from a larger number of donors are required to assess their bone forming potential. On the other hand, this study combined with that of Sommar *et al.* (2009) indicates the potential of FSS to enhance osteogenic differentiation in HDFs and this should be further exploited.

While some studies have shown that mechanical forces alone can induce osteogenic differentiation in MSCs (Chen *et al.* 2008; Sumanasinghe *et al.* 2006; Yourek *et al.* 2010), in this study FSS alone did not enhance ALP activity or calcium deposition. Supplementation with Dex was required to induce osteogenesis and the addition of FSS enhanced this response. However, FSS alone did increase collagen production, in all cells under all conditions and this has been seen in other studies using fluid flow as a stimulatory source (Augst *et al.* 2008; Morris *et al.* 2010; Sharp *et al.* 2009). As well as being the major extracellular matrix (ECM) protein of bone, collagen is of course the main component of all mesenchymal tissues and of dermis. The Picrosirius red assay cannot distinguish between the different types of collagen, which may indicate that ECM in general is upregulated by matrix synthesising cells under this low FSS stimulus.

Monitoring matrix development by progenitor cells is very important for a successful tissue construct to be developed. SHG has been used successfully in this present work to monitor the effect of different media formulations and fluid shear stress on the tissue engineered collagen produced from cells. When hESMP cells and HDFs were treated with Dex, they produced less collagen at all time points, compared with those cultured without Dex. This is visualised very clearly from the SHG images and this is the first study to show the true extent of this effect of Dex on collagen production using SHG. It has been reported that MSCs treated with Dex *in vitro* show a reduction in collagen production (Leboy *et al.* 1991; Ogston *et al.* 2002) and large concentrations of Dex used to treat patients for various conditions can cause bone loss or impairment of bone formation leading to osteoporosis (Scutt *et al.* 1996). Cells subjected to FSSs, also appeared to be more organised into thicker and longer bundles of fibres when imaged using SHG; information that could not be obtained from Picrosirus red staining. This enhanced collagen organisation suggests that cells subjected to these FSSs would produce tissues with stronger tensile properties.

The process of converting mechanical stimulation into a biochemical response, is thought to occur through a number of mechanically-sensitive mechanisms including the cytoskeleton and integrins, ion channels, the glycocalyx and the primary cilia (Jacobs *et al.* 2010; Morris *et al.* 2010; Reilly *et al.* 2003; Weinbaum *et al.* 2007). Through these mechanisms, the application of FSS initiates a number of signalling events, including the synthesis and release of nitric oxide and prostaglandins (Klein-Nulend *et al.* 2005), a calcium signalling response and phosphorylation of mitogen-activated protein (MAP) kinases ERK (You *et al.* 2001).

During osteogenic differentiation, the actin cytoskeleton in hMSCs remodels resulting in a morphological switch from a fibroblastic fusiform shape to a square shape which is more osteoblast-like. This was observed to happen with the hESMP cells cultured in osteogenic media and a very similar morphological switch was observed when HDFs were cultured in osteogenic media. When subjected to flow, both cells appeared to be more elongated in either media condition. This is thought to be due to a stiffening of the cell cytoskeleton and it has been seen that stiffer cells tend to become more mechano-responsive perhaps due to the forces being transmitted more efficiently (Yourek *et al.* 2010). Previous studies have shown that

actin cytoskeletal tension is required for the activation of mechanosensors or signalling mechanisms involved in the regulation of intracellular processes and protein expression resulting from fluid shearing (Arnsdorf *et al.* 2009). Also a number of studies have shown that remodelling of the cell cytoskeleton can induce changes in the organisation and distribution of deposited collagen (Brammer *et al.* 2009; Koepsell *et al.* 2011). It was also observed in chapter 4 that HDFs elongated in the direction of scaffold fibre alignment and then deposited collagen fibres organised in the same direction as cell elongation. HDFs that were spread across fibres with no favoured orientation also showed a collagen fibre network spread in all directions.

7.5 Conclusions and future work

Isolating progenitor cells from the dermis for use as an autologous source of bone cells would have many advantages in that any donor will have large quantities of easily accessible skin and biopsies undertaken under local anaesthetic to remove it are straightforward. However, more work is needed to fully characterise this apparently diverse pool of multipotent cells in order to realise their full capabilities, including determining the effect that patient age and *in vitro* passaging conditions may have on their bone forming potential. The effect that mechanical forces have on progenitor cells is now one of the major focal points for musculoskeletal tissue engineers and their potential to aid healing and direct differentiation are being realised. It is also likely that the formation of a suitable tissue-engineered construct requires mechanical forces to condition it so that it is ready for the forces it will experience in the body. The simple system employed here created FSSs that enhanced osteogenic differentiation and matrix production in bone progenitor cells in the presence of osteogenic supplements.

This system has many advantages in that it is simple to use, it can accommodate many experimental samples and could be easily scaled up for large defects. This system could be used for a number of tissue engineering strategies as well as mechanistic studies;

- Pre-treating cells before injection into a scaffold or directly into a tissue defect.

- Stimulating cells cultured on thin scaffold sheets to be layered to form a 3D implantable tissue.

- Studying a wide range of loading parameters e.g. load frequency, load days, load period, and in combination with various supplements.

- Mechanotransduction studies.

- Conditioning media for cells for cell communication studies.

For other future work relating to HDFs, it would be ideal to study the effects of osteogenic media in combination with FSS for multiple donors to see how responsive different populations are. It is also necessary to analyse what effect this combined stimulus has on the regulation of genes with regards to osteogenesis to see if the HDFs in particular are truly being enhanced towards osteogenesis.

7.6 Summary

- A simple rocking platform is able to produced oscillatory FSSs that can enhance osteogenesis in progenitor cells.

- The hESMP cell line is responsive to FSSs and may therefore be a suitable model MSC line for fluid flow studies.

- ALP activity and deposited calcium are enhanced by FSSs for HDFs cultured in osteogenic media.

- FSSs enhanced collagen deposition and apparent organisation in both progenitor cells and this was easily monitored using SHG.

CHAPTER EIGHT: Primary cilia response to fluid flow in bone cells

8.1 Introduction

Bone cells are mechanically sensitive and are exposed to oscillatory fluid shear stress (FSS) *in vivo* and as shown previously in chapters 3 and 7, bone cell behaviour is also influenced by oscillatory fluid flow *in vitro* resulting in a significant increase in calcium deposition. Applying dynamic oscillatory fluid flow to osteoblasts has been show to upregulate a number of bone-related markers including the enzyme cyclooxygenase-2 (COX-2) and release of PGE_2 (You *et al.* 2001; Donahue *et al.* 2003).

Until recently, it was largely unknown how bone cells were able to convert an external mechanical stimulus into a biochemical signal. A number of possible mechanisms have been identified including mechanosensitive calcium channels (Jacobs *et al.* 1998), integrins (Iqbal and Zaidi 2005), G-coupled protein receptors (Liedert *et al.* 2008), and the cell glycocalyx (Weinbaum *et al.* 1994; Morris *et al.* 2010). However, recent work by Jacobs and his colleagues has identified the primary cilium as a promising candidate as a mechanotransducer in bone cells (Malone *et al.* 2007; Hoey *et al.* 2011). Application of a continuous 0.036 Pa flow caused the primary cilia to deflect in MC3T3-E1 osteoblasts (Malone *et al.* 2007). Malone *et al.* (2007) then subjected MC3T3-E1 (osteoblasts) and MLO-Y4 (osteocytes) cells to oscillatory fluid flow (OFF) and saw increases in OPN and COX2 mRNA compared with no flow. However, when primary cilia were removed or its formation was inhibited, the fluid flow-induced response was no longer observed. In another study, OFF stimulated osteocyte conditioned media was applied to MSCs causing a significant upregulation in OPN and COX-2 mRNA compared to statically conditioned media. When primary cilia formation was inhibited in the osteocytes prior to OFF stimulation, the upregulation of osteogenic genes in the MSCs did not occur (Hoey *et al.* 2011). These findings implicate the primary cilia as a sensory mechanism for fluid flow in bone cells.

While previous studies have shown that the primary cilia are responsible for the upregulation of specific osteogenic genes in response to OFF, so far there have been

no *in vitro* studies concerning the role of the primary cilia and load-induced mineral matrix deposition, which is ultimately the end stage of bone differentiation. The deflection of the primary cilia under low shear stress (0.036 Pa) (Malone *et al.* 2007) means that the platform rocker used in the previous chapter could be a suitable method for investigating the role of the primary cilia as a mechanical sensor.

The cilium's mechanosensory ability relies on its mechanical properties and it has been seen that the primary cilium is able to regulate its length in response to the extracellular environment in an apparent attempt to adjust its sensitivity. Overloading of chondrocytes resulted in a decrease in cilia length (McGlashan *et al.* 2010) and strain deprivation in tendon cells resulted in a significant cilia length increase, which was reduced upon application of load in a strain-dependent manner (Gardner *et al.* 2011). As of yet, there is no evidence that bone cell primary cilia also adjust their length in response to load.

There are two commonly used methods for primary cilia removal *in vitro*; application of the drug chloral hydrate (CH), which breaks down microtubules (Praetorius and Spring 2003); or siRNA-mediated depletion of the intraflagellar transport (IFT) component polaris (Malone *et al.* 2007), which is required for primary cilium biogenesis and function (Yoder *et al.* 2002). Polaris knockout prevents the primary cilia from forming while CH removes existing primary cilia and stops the formation of new primary cilia while the drug is still present. CH treatment has been shown to be very effective for primary cilia removal in a number of different cell types (Preatorius and Spring 2002; Malone *et al.* 2007), but can take between 24 and 96 h to completely remove all the primary cilia. However, between the beginning of the application of CH and the moment with which the primary cilia is removed, damaged is caused to the primary cilia, which results in it shrinking and bending. This allows for the modelling of a damaged primary cilia or one that is not fully healthy, and so one can study how this affects its function.

MLOA5 bone cells are an ideal candidate with which to study the role of the primary cilia as a mechanotransducer in the modulation of mineralised matrix deposition in response to load. Studies performed in chapter 4 showed that these cells produce dense calcium staining after 12 days and are very responsive to different loading conditions. The mineral deposited by MLOA5 cells has been well characterised

using energy dispersive spectrometry and a variety of high resolution microscopy techniques and has been shown to be more like the mineral found in bone than other osteoblast cells such as MC3T3-E1 cells (Kato *et al.* 2001).

The main aim of this chapter was to further investigate the role of the primary cilia as a mechanotransducer in bone cells using MLO-A5s and the previously established rocking platform system. The two main objectives were to 1. Observe if oscillatory fluid flow affected primary cilia appearance 2. Elucidate whether primary cilia inhibition affects oscillatory FSS-induced calcium deposition.

8.2 Materials and Methods

8.2.1 Cell Culture

MLO-A5 cells between passages 25-28 were seeded at a density of 10, 000 cells/well on 0.1 % gelatin coated six-well plates containing 2 ml of complete α-MEM and supplemented with AA and βGP at day 1 of culture for all experiments. Media was changed every 2-3 days.

8.2.2 Primary cilia visualisation and CH treatment

Primary cilia were visualised using anti-acetylated α-tubulin (see Chapter 2: Materials and Methods). Primary cilia damage/removal was carried out by exposing MLO-A5 cells to 4 mM chloral hydrate (CH) for 0, 24, 48 or 72 h followed by a recovery period whereby cells were washed once with PBS and cultured in fresh media for 0, 24, 48 or 72 h after which cells were fixed and stained for imaging.

8.2.3 FSS experiments

In order to study the response of primary cilia to FSS, cells were subjected to rocking on days 3-7 at 45 cycles/min for 2 h/day, or cultured under static conditions. After rocking on day 7, cells were immediately fixed and labelled with anti-acetylated α-tubulin and visualised using fluorescent microscopy. Total DNA was also quantified at day 7 to monitor any differences in cell number.

In order to observe the effect of primary cilia damage/removal on the FSS-induced responses of MLO-A5s, cells were exposed to CH (4 mM) for either 0 (positive control), 24, 48 or 72 h. Upon removal, cells were washed once with PBS and 2 ml

of fresh media was added for 24 h before subjecting cells to two periods of FSS (Fig. 8.1) at 45 cycles/min for 2 h. Media samples were collected two hours after FSS-1 on day 7 for PGE_2 analysis and then cells were assayed at day 12 for calcium deposition.
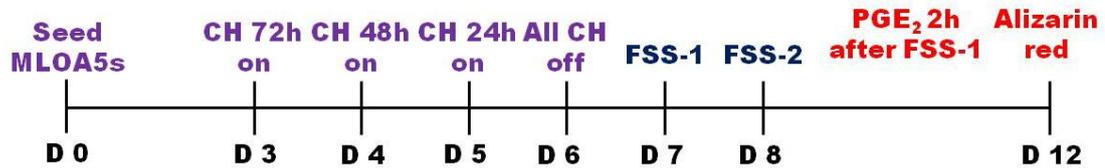
Figure 8.1: Culture regime used to observe the effect of primary cilia damage/removal on the load-induced responses of MLO-A5 cells. MLO-A5 cells were exposed to CH for either 72, 48, or 24 h at days 3, 4 and 5 respectively before removal of all CH at day 6 followed by culture in fresh media for 24 h. Control cells were not exposed to CH. Cells were then subjected to FSS (FSS-1 and FSS-2 at 45 cycles/min for 2 h at days 7 and 8) or cultured statically. Cell culture media was assayed for PGE_2 release 2 h after rocking on day 7 and calcium deposition was analysed at day 12.

8.2.4 Cellular assays

- Cell morphology: DAPI and phalloidin TRITC at day 7 after FSS.
- Anti-acetylated α tubulin antibody staining for primary cilia visualisation with or without after CH treatment, and for FSS experiments.
- Primary cilia counts were conducted on > 600 cells (n = 3-4).
- PicoGreen assay for total DNA at day 7.
- Extracellular PGE_2 collected on day 7, 2 hours after loading.
- Qualitative and quantitative deposited calcium staining using 1 % Alizarin red S at day 12 after FSS.

8.3 Results

8.3.1 Affect of Oscillatory FSS on cell morphology

MLO-A5 cells were visualised after periods of rocking and appeared to be more spread out across the culture well compared with cells cultured statically (Fig. 8.2). Cells subjected to FSS also appeared to have longer dendritic extensions than static counterparts and in areas of the well-plate were cells were overly confluent, the dendrites appeared to extend across many of the neighbouring cells. Rocking the cells did not induce and preferential direction of cellular alignment.
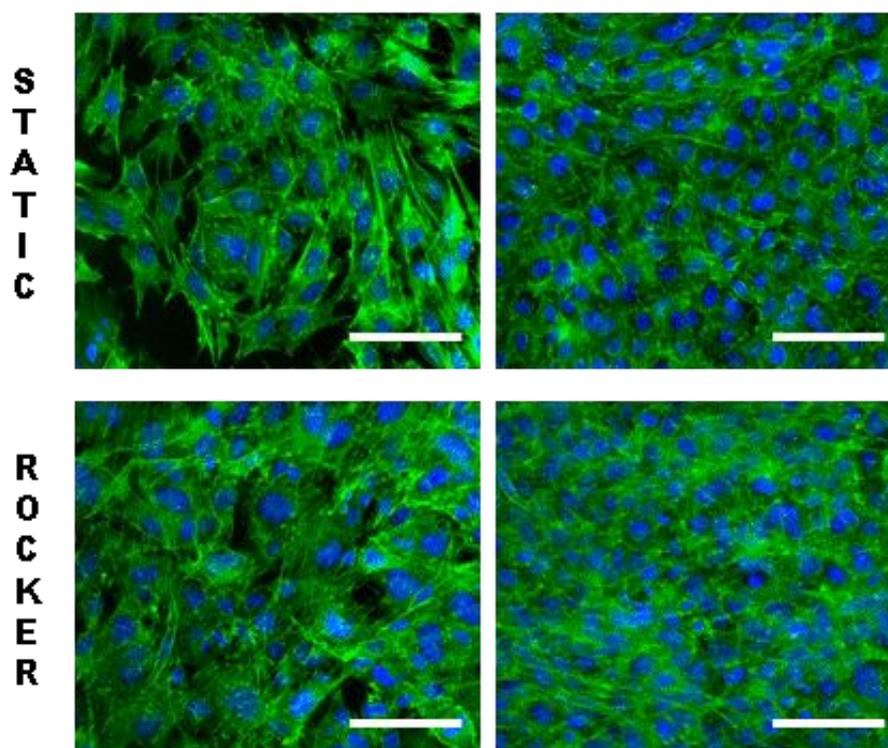
Figure 8.2: Cell nucleus (DAPI-blue) and actin cytoskeleton (phalloidin TRITC-green) of MLO-A5 cells after 7 days of static culture or five consecutive days of rocking (D3-7, 1h, 45 cycles/min). Cells at the edges of the culture well were less-confluent (left hand images) compared with overly confluent cells in the well centre (right hand images). Images are representative of samples from two experimental runs. Scale bars are 100 μm.

8.3.2 Primary cilia identification in MLO-A5 cells and CH treatment

MLOA5 cells labelled with anti-acetylated α tubulin can be seen in figure 8.3a. The microtubule network (in green) was visualised within the cell cytoplasm and was well organised and surrounding the cell nucleus (in blue). A small, bright protrusion was also seen emanating from most cells (67.2 ± 4 %), which is the primary cilium. In figure 8.3b, the plane of focus was adjusted towards the top of the cells and here most of the primary cilium can still be visualised. This indicates that the primary cilium protrudes from the apical surface of the cell and is generally located just to the side of the nucleus.

When MLO-A5 cells were treated with CH for 24 h, the cell microtubule network became disrupted and disorganised (Fig. 8.4a) and primary cilia either reduced in length or disappeared. When the cells were allowed to recover for 24 h in fresh media absent of CH, the microtubule network reorganized and appeared to return back to its normal state (Fig. 8.4b). By this point, primary cilia had returned to their

normal state on only a small number of cells, whereas in other cells, primary cilia were either absent or had a structural impairment i.e. curved (Fig. 8.4b).
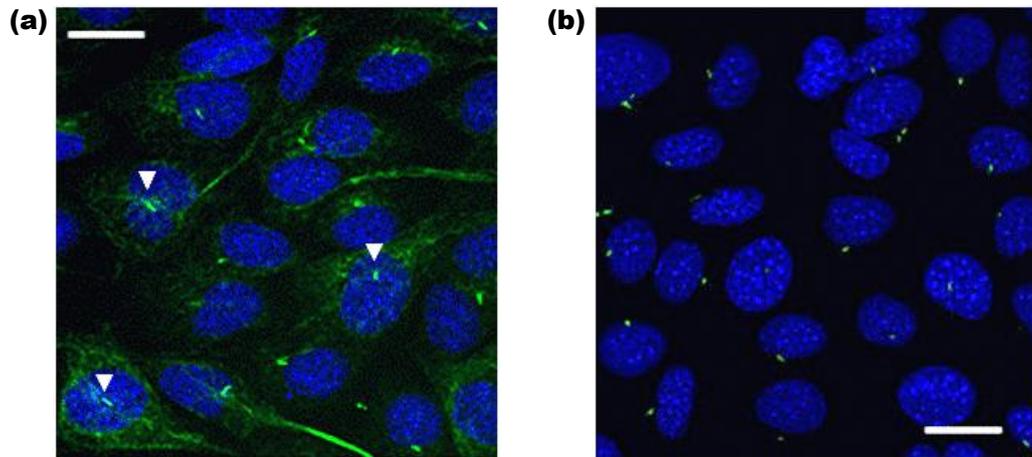
Figure 8.3: Cell nuclei (DAPI-blue) and anti-acetylated α tubulin (green) staining of MLO-A5s. The microtubule network within the cell can be seen surrounding the nucleus and primary cilia can be seen protruding out of most cells and are indicated by the arrows (a). Primary cilia are located away from the cell nucleus (b) and stands out of the apical surface of the cell. Scale bars are 25 μm.

CH 24 h   CH 24 h + 24 h recovery
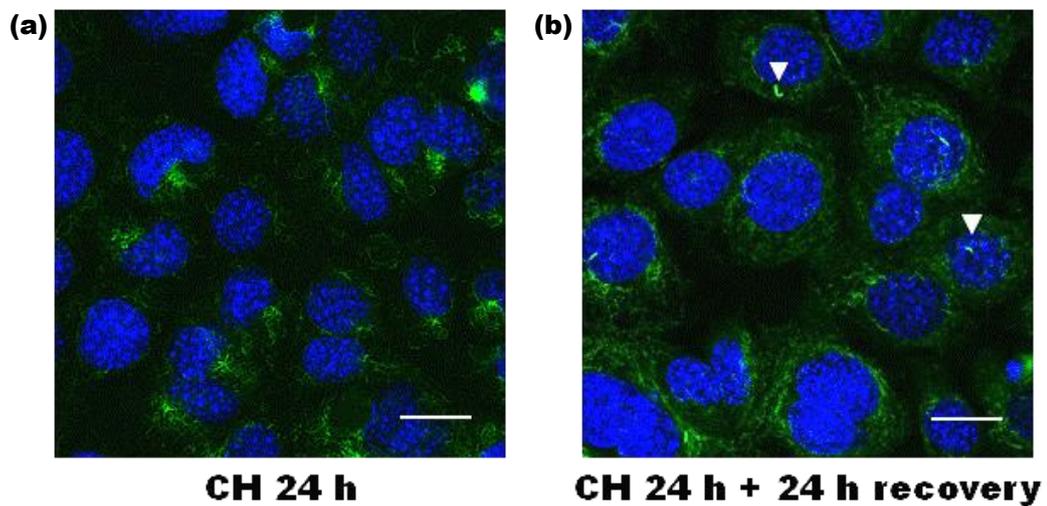
Figure 8.4: Nuclei (DAPI in blue) and anti-acetylated α tubulin (green) staining of MLO-A5 cells after CH treatment for 24 h (a) and CH treatment for 24 h followed by recovery for 24 h (b). CH treatment damages the microtubule network, which appears disorganised, and removes most primary cilia. After 24 h recovery, the microtubule network has recovered and some of the primary cilia have grown back, while others appear shortened or curved (indicated by arrows). Scale bars are 20 μm.

More primary cilia were removed with increasing exposure time to CH and after CH treatment for 72 h all primary cilia were removed (Fig. 8.5). Although the

microtubule network within the cells appeared to be increasingly disrupted with increasing CH exposure time, the microtubules returned to their normal after 24 h in fresh media regardless of exposure time. However, primary cilia took longer to grow back or return to their normal state with increasing treatment time. After 72 h recovery in fresh media, the number of cells with primary cilia was almost back to normal for all exposure times.
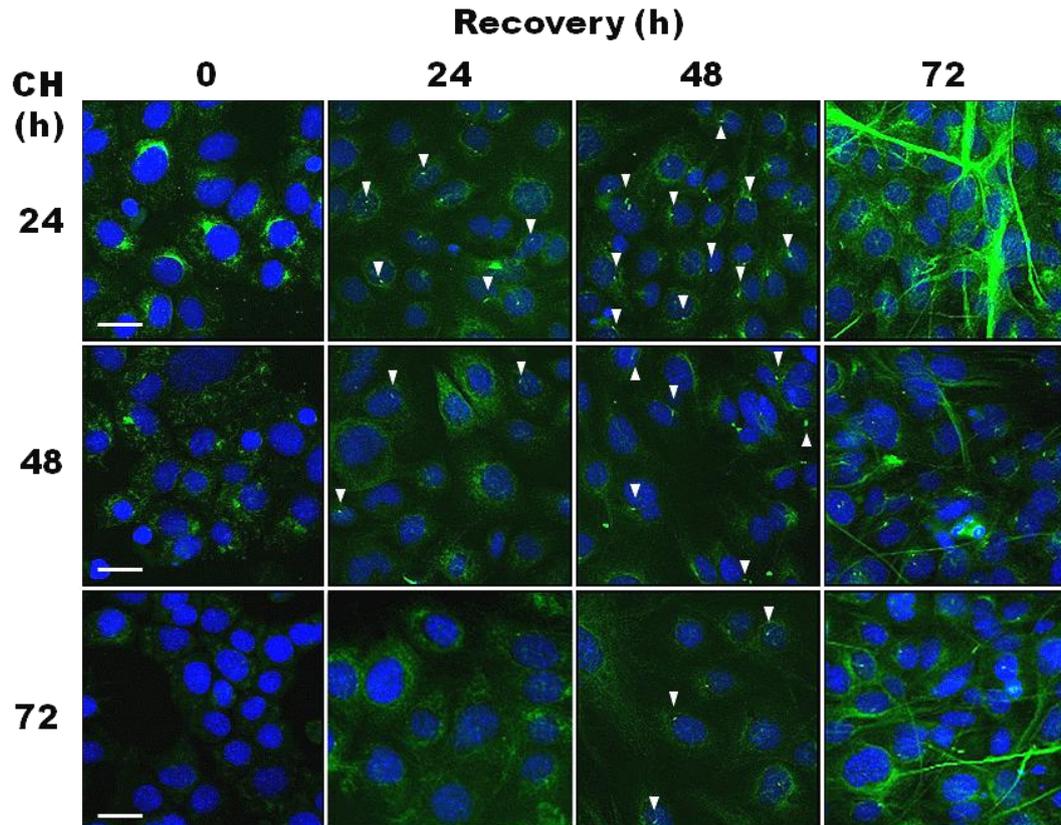
Figure 8.5: Cell nuclei (DAPI-blue) and anti-acetylated α tubulin (green) staining of MLO-A5 cells after CH treatment (24-72 h) and recovery in fresh media (0-72 h). Primary cilia were removed entirely after 72 h CH exposure. The microtubule network appeared normal after 24 h regardless of CH exposure time. Increased exposure time to CH resulted in a greater primary cilia recovery times. Primary cilia presence and frequency is represented by white arrows. Scale bars are 25 μm.

8.3.3 Oscillatory FSS regulation of primary cilia

The application of oscillatory fluid flow using the rocker for 2 h on 5 consecutive days had an effect on the number of primary cilia present as well as the primary cilia appearance. At day 7, cells cultured in static conditions appeared to have longer, more defined primary cilia than those subjected to rocking (Fig. 8.6a), which appeared less well-defined, and more stub-like. Rocking also significantly ($p < 0.05$)

reduced the number of cells with primary cilia from 73.47 ± 12.76 (Static) to 52.47 ± 10.85 (Rocker) (Fig. 8.6b). There was no difference in total DNA between statically cultured cells and cells subjected to rocking at day 7 (Fig. 8.6c) and so the observed responses is not due to increased cell number in the rocking group. This suggests that primary cilia are responsive to oscillatory FSS.
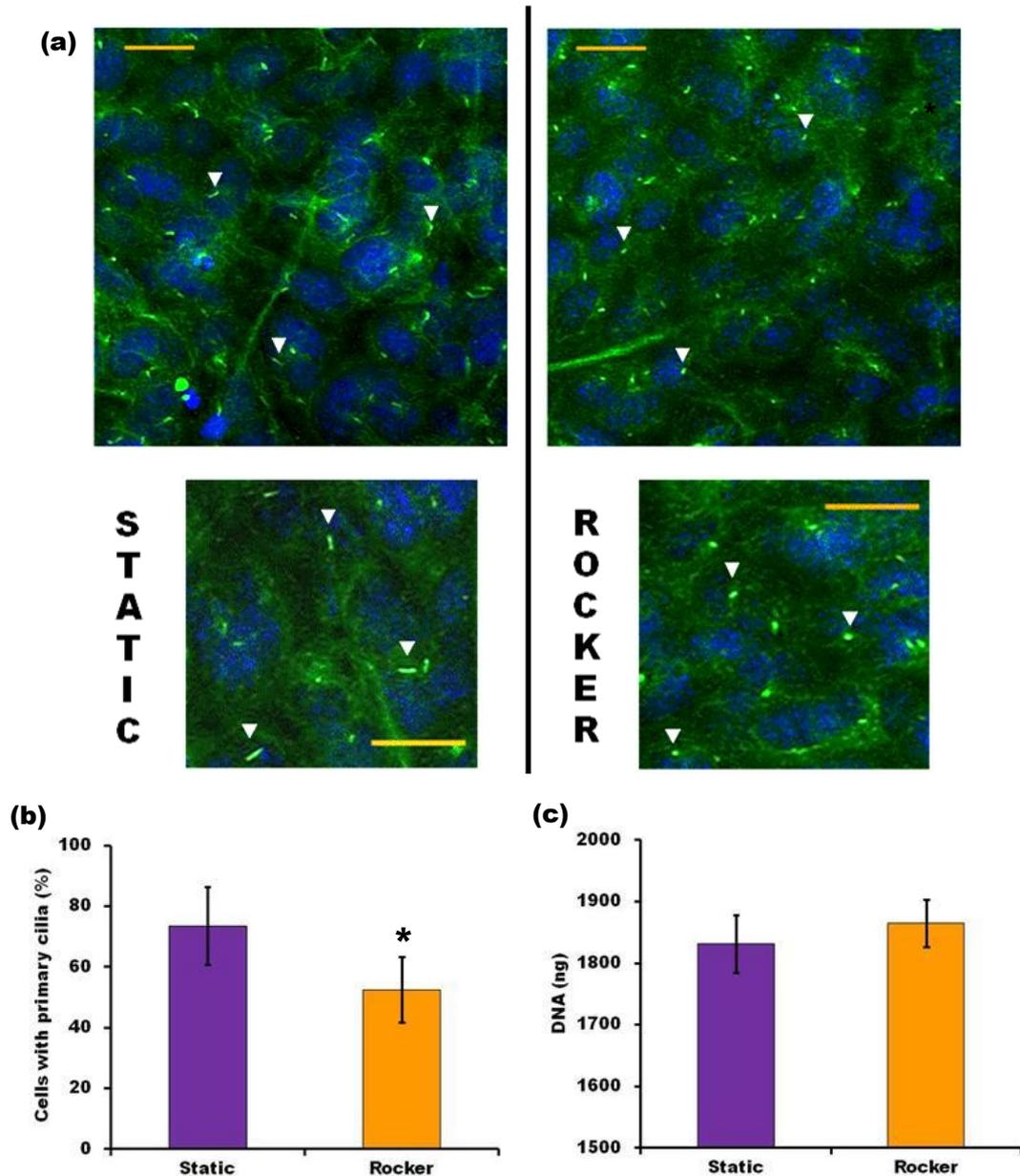
Figure 8.6: MLO-A5 cells labelled with DAPI (nuclei-blue) and anti-acetylated α tubulin (green) after 7 days of culture under static conditions or rocked for 2 h on 5 consecutive days. Arrows indicate primary cilia; cells subjected to rocking have shorter primary cilia compared with statically cultured cells (a). Total DNA was measured at day 7 (b) and the percentage of cells with primary cilia were counted for static and rocked samples (c). Data is mean ± SD (n = 6 for DNA and n > 600 cells from n = 4 for (c)). Scale bars are 50 μm. *$P < 0.05$.

8.3.4 CH treatment and MLO-A5 response to FSS

MLO-A5 cells were treated with CH for 0, 24, 48 or 72 h and then cultured in fresh media for 24 h before being subjected to two bouts of rocking at days 7 and 8. At day 7 after cells (CH 0) were subjected to one period of FSS, a 3-fold increase in the level of extracellular PGE_2 was detected compared with statically cultured cells (Fig. 8.7). Following the application of CH, no statistically significant differences were found in the level of extracellular PGE_2 between cells subjected to FSS or cultured under static conditions. The application of FSS combined with CH for 24 h resulted in a 1.6-fold increase in PGE_2 levels, while CH treatment for 48-72 h showed no observed increase, all of which were significantly different from the normalised response of CH 0 cells to rocking.
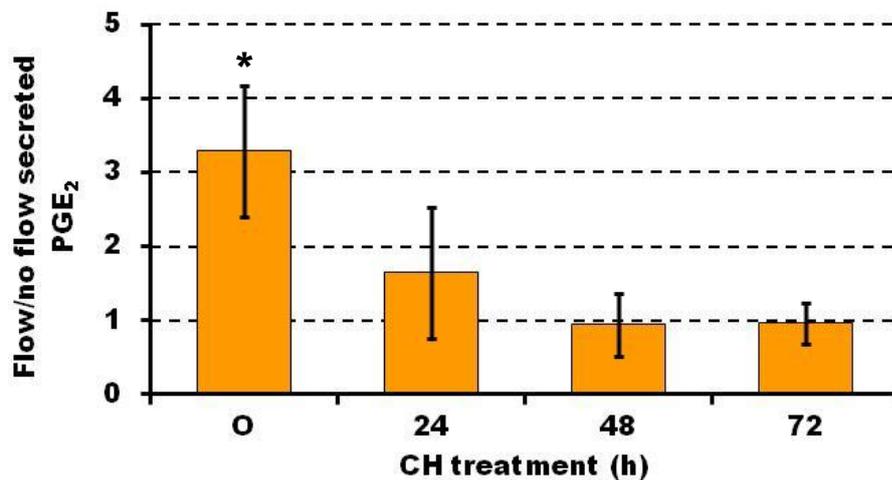
Figure 8.7: Extracellular PGE_2 produced by MLO-A5 cells subjected to CH treatment (0-72 h) was quantified at day 7 after static culture or 2 h of FSS, followed by 2 hours of culture in fresh medium. Data is mean $\pm$ SD (n = 4-5). *P <0.05* verses respective static sample.

Deposited calcium, visualised by AR staining, can be seen in figure 8.8a for rocked cells and static controls. With no CH treatment (0 h), cells subjected to FSS showed darker and more uniform staining compared with the patchy staining of the static controls indicating a load-induced matrix forming response. When cells were cultured in CH for 24 h, cells subjected to rocking showed a more uniform stain across the well compared with its static control, but this was less dense than CH 0 h rocked cells. Cells cultured in CH for 48 h and subjected to rocking also showed a more uniform stain than its static control, however, this was less dense and more speckled than rocked cells with CH 0 and 24 h. With 72 h of CH treatment, there did

not appear to be any difference between the staining of cells exposed to FSS or cultured under static conditions, both of which appeared patchy.
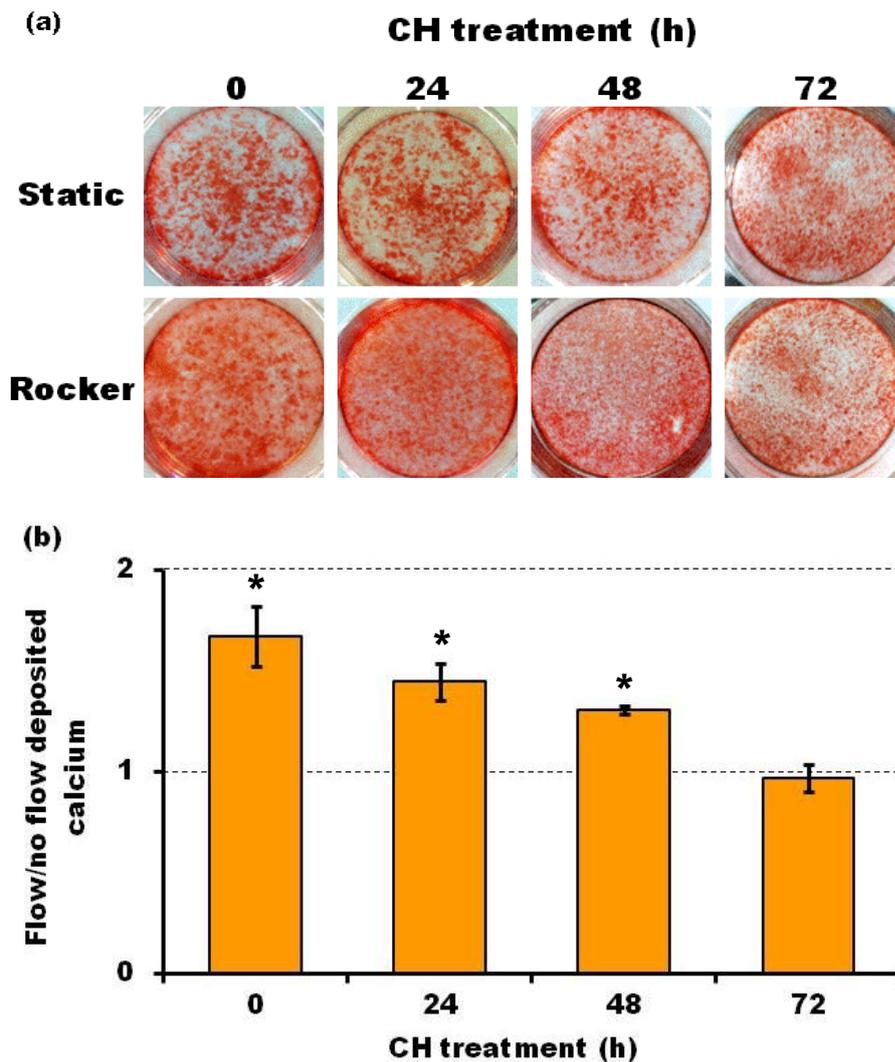
Figure 8.8: Calcium deposited by MLO-A5 cells at day 12 visualised by AR staining (a) after CH treatment (0-72 h), followed by 24 h recovery and then exposure to FSS on a rocking platform for 2 days (2 h, 45 cycles) or static culture. FSS caused cells to deposit more calcium (CH 0), but after treatment with CH cells deposited less calcium in response to FSS with increasing treatment time (b). CH treatment for 72 h completely removed the load-induced response. Data is mean ± SD (n = 9). *P <0.05* verses respective static samples.

Quantifying the AR stain (Fig. 8.8b) showed a decrease in the amount of deposited calcium in response to load, normalised to static controls, with increasing exposure to CH. Deposited calcium in rocked samples treated with CH for 0, 24, 48, and 72 h was 1.66, 1.44, 1.31, and 0.97 (respectively) times the level of their respective static

controls. The amount of calcium produced in response to rocking was reduced by 33 % with CH 24 h, 50 % with CH 48 h, and was completely removed with CH 72 h.

8.4 Discussion

Mechanical sensitivity is essential for maintaining homeostasis and correct physiological function in many tissues. For bone TE purposes, conditioning cells with mechanical forces is most likely required in order to produce a more suitable construct and reduce healing time. However, little is known about the exact mechanisms by which mechanical forces regulate ECM production in bone cells and how this translates into mechanically induced bone formation *in vivo*.

The ultimate aim of bone tissue engineering is to control osteogenic cell differentiation and to produce sufficient amounts of mineralised collagenous matrix in a short amount of time. Early signalling-responses to mechanical load are important in order to monitor cellular responses and initiation of the correct differentiation pathway. Understanding which signals correspond to downstream matrix formation is a key step for controlling the production of a suitable bone construct for transplantation. However, the relationships between early and late responses to mechanical load still remain unclear. While it has been seen that the primary cilia play a role in load-induced gene expression in bone cells (Malone *et al.* 2007; Hoey *et al.* 2011), the present work shows that it also plays a role in the load-induced deposition of calcium matrix.

Prostaglandin E_2 (PGE_2) is released by osteoblasts and osteocytes after mechanical stimulation *in vivo* and *in vitro* with the primary role of regulating bone metabolism (You *et al.* 2001). Malone *et al.* (2007) observed that the load-induced increase in extracellular PGE_2 was abolished when primary cilia formation was inhibited in both immature osteoblasts (MC3T3-E1) and osteocytes (MLO-Y4). In this study, PGE_2 levels in the medium increased when MLOA5 cells were subjected to rocking and this response was removed with the application of CH. We also showed that mineral deposition in response to load is primary cilia-dependent. After two bouts of loading, calcium deposition was increased compared with static controls, and this flow-induced response was reduced with increasing CH treatment time until it was abolished with CH 72 h. However, it was seen that CH treatment at 48-72 h induced

higher levels of PGE_2 in static samples compared with CH 0-24 h and so loading responses in the 48-72 h groups may have been masked. On the other hand the 24 h group did show a reduction in the loading response of PGE_2 suggesting that this is still primary cilia dependent. This suggests that the primary cilium plays a vital role in the formation of calcium matrix deposits in response to loading.

It is thought that the primary cilia can adjust its sensitivity to the load it receives either to avoid overloading or in order to detect minor forces, indicating that it plays a role in mechanotransduction. Chondrocytes seeded in a 3D agarose culture model were subjected to cyclic compressive strain and chondrocyte primary cilia were found to reduce in incidence and length compared with free-swelling culture (McGlashan *et al.* 2010). In another study, freshly harvested rat tail tendons were stress-deprived and after 24 h demonstrated an increase in cilia length compared with fresh controls (Gardner *et al.* 2011). Stress deprived tendons were then subjected to 24 h of cyclic loading and cilia length returned to normal levels. In my study, the application of 5 days of oscillatory FSS appeared to cause a reduction in the length of primary cilia in MLOA5 cells compared with statically cultured primary cilia which appeared more defined. Liu *et al.* (2003) developed a model for fluid flow around an array of primary cilia and calculated that the drag force and torque experienced was significantly greater in a cilium of 8 µm length compared with one of 2.5 µm (Liu *et al.* 2003). This supports the hypothesis that cilia adjust their length in order to regulate their mechanosensitivity (Besschetnova *et al.* 2010).

One of the major differences between microtubules within the cytoplasm and the primary cilium is that ciliary microtubules undergo reversible post-translational modifications including acetylation and phosphorylation (Westermann and Weber 2003). Microtubule associated protein 1(MAP1) has been shown to localize to the axoneme of the cilium. The occurrence of MAPs is known to coincide with acetylation and the binding of MAPs has been shown to increase flexural rigidity of microtubules as much as 8-fold (Felgner *et al.* 1996). Recently, Geiger et al. (2009) demonstrated that physiological levels of cyclic stretch *in vivo* and *in vitro* result in a significant increase in acetylation of microtubules in a magnitude and duration dependent manner, due to a decrease in deacetylation enzyme HDAC6 activity (Geiger *et al.* 2009). The microtubules in the primary cilium are known to be heavily acetylated, and so this suggests another possible mechanism by which it is able to

tune its sensitivity to the extracellular environment by altering its flexural rigidity in response to load.

Correct function of the primary cilia relies on its structural integrity as defects in this sensory mechanism have shown to be responsible for numerous diseases such as arthritis, osteoporosis, and cancer (Badano *et al.* 2006). The mechanical properties of the cilium dictate how it will be deformed by external stimuli such as FSS and how much this translates into a cellular response. By increasing the CH treatment time, more primary cilia were damaged and removed and load-induced calcium deposition decreased. This indicates that structural integrity of the primary cilia is essential for proper function. It is often hypothesized that bending of the cilium contributes to the opening of ion channels such as polycystin 2 (PC2). Upon applying a set bending force, a stiffer cilium will experience lower membrane strain compared with a more flexible one. Therefore, it would be expected that the stiffer cilium was less mechanoresponsive.

There may well be several other pathways by which fluid-flow induced shear stress is transduced and modulated. When a cell is mechanically stimulated, pronounced cytoskeletal alterations can occur, including actin reorientation, microtubule polymerization/depolymerisation and reorganization of focal adhesion sites. It is thought that cytoskeletal reorganization is partly due to minimize cell internal stresses caused by external stress (Geiger *et al.* 2009) and this reorganization has been shown to be dependent on the type, magnitude, and duration of the external stress. It has been shown that steady flow applied to osteoblasts for a sufficient amount of time results in reorganisation of the actin fibre network into distinct stress fibers (Pavalko *et al.* 1998) and an apparent increase in actin fibre density (Malone *et al.* 2007b). However, this did not appear to occur with the application of oscillatory fluid flow (Malone *et al.* 2007b). It was proposed that adaptations in the actin cytoskeleton occur over a time period that is relatively longer (a few seconds) than the time it takes for oscillatory flow to switch direction, whereas unidirectional steady flow is continuous (Malone *et al.* 2007b). Therefore, it seems likely that the cell needs to experience this stress level in one direction for a certain period of time in order for stress fibre formation to occur. In my study, the actin cytoskseleton appeared different between statically cultured osteocytes and those subjected to oscillatory FSS. Cells subjected to oscillatory flow appeared to be more spread with

a greater number of dendritic extensions. In areas of over confluence, cells subjected to flow had a denser network of actin than static counterparts. It has been shown that osteocytes are more sensitive to mechanical forces than osteoblasts and progenitor cells (Ponik *et al.* 2007) and so this may explain the reason for seeing this apparent actin reorganisation, which was not observed in immature osteoblasts (Malone *et al.* 2007b). Norvell *et al.* (2004) subjected osteoblasts to steady fluid flow (1 Pa) and individually disrupted actin microfilaments, micro-tubules, and intermediate filaments. They showed that none of these three major cytoskeletal networks were required for FSS-induced prostaglandin release (Norvell *et al.* 2004).

Another proposed mechanotransducer, the cell glycocalyx (a pericellular glycosaminoglycan (GAG)-proteoglycan (PG) layer), has been shown to play a sensory role in bone cells (Reilly *et al.* 2003; Morris *et al.* 2010). Using laminar flow, Morris et al. (2010) induced FSSs on mature bone cells causing an increase in collagen production, a response that was absent upon removal of hyaluronan (HA), a key glycocalyx component. In an earlier study, Reilly et al. (2003) inhibited the ability of osteocyte-like cells to upregulate PGE_2 release in response to flow by removal of HA. However, this did not affect intracellular calcium signalling which is produced by OFF suggesting that different mechanisms play different roles in moderating mechanotransduction. This is consistent with the possibility that oscillatory fluid shear stress may stimulate different mechanotransduction pathways from steady/dynamic fluid shear stress. It is likely that multiple mechanosensitive mechanisms are present in bone cells and that these mechanisms are activated at different levels of stimulus. A previous PhD student in our group showed that the cell glycocalyx was also found covering the primary cilia suggesting that they possibly work together. Multiple response mechanisms would be advantageous in terms of biologic redundancy or may be associated with distinct mechanically regulated functions such as turnover or repair.

Mechanotransduction in bone in vivo may or may not be comparable given the differences in cell orientation, morphology, and cell–matrix interactions. Studies such as this provide potential targets for in-vivo investigation of mechanically induced bone formation. The relationship between cells and their matrix differs in a 2D environment compared with that of the 3D *in-vivo* environment and so cellular responses in 2D may not necessarily be the same as in 3D. In cartilage, it has been

shown that primary cilia interact with the ECM proteins (Jensen *et al.* 2004), and it is possible that this may occur in bone cells also. In this case, integrins on the primary cilia may sense deformations of the ECM and convert these into biological signals, causing an increased load-induced response. However, in a scaffold with relatively large pores, cells attach to the strut walls in a similar way that cells attach to a 2D surface (Reilly and Engler 2010). These similarities mean that the regions of the cell shielded and exposed to flow will also be similar and therefore responses to flow within this rocking well environment could provide information on the optimization of flow conditions for 3D porous scaffold bioreactors. Primary cilia may also be responsible for cellular responses to other types of mechanical stimulation other than oscillatory fluid flow. Chondrocyte primary cilia have been shown to be essential for cartilage matrix synthesis (sulphated glycsoaminosglycan) in response to compressive strain (Wann *et al.* 2012).

Studies like this also as provide potential targets for *in vivo* investigation of mechanically induced bone formation. An *in vivo* study by Temiyasathit *et al.* (2012), observed that the response of bone formation to load was reduced in Kif3a knockout mice. Deletion of Kif3a (an essential subunit of the kinesin II IFT motor protein) has been linked to cell signalling dysfunction through disruption of IFT. Intraflagellar transport (IFT) along the microtubule core of the primary cilium is required for its formation, maintenance, and function (Yoder *et al.* 2002). Although the bone forming response of Kif3a knockout mice to load was reduced, it was not completely abolished (Temiyasathit *et al.* 2012). This response may be due to the type of loading stimulus, cyclic axial ulna loading, which induces strain as well as fluid movement through bone and so other mechanotransduction mechanisms may have been activated. It is also possible that primary cilia are involved in a strain response.

CH treatment to disrupt the primary cilia has limitations and could have non-specific effects on cell physiology. CH removes the primary cilia by disrupting the microtubules and the junction of the cilium and the basal body (Chakrabarti *et al.* 1998). It also disrupts the microtubules within the cell cytoplasm and is known to interfere with mitosis (Lee *et al.* 1987). However, it is currently one of the only pharmaceutical ways of removing the primary cilia and is highly efficient. CH treatment disrupted the microtubules within the cell but this was seen to recover after

24 h in fresh media regardless of the length of treatment time. It was also seen that CH treatment induced PGE_2 release which may have masked any response to load in the 48 and 72 h treatment groups. Other methods for abrogation of primary cilia include polaris siRNA treatment, but in a previous study this only caused the number of cells with primary cilia to decrease by 50 % (Malone *et al.* 2007).

Understanding which signals correspond to downstream matrix formation is a key step for controlling the production of a suitable construct for transplantation. Cultured kidney cells exposed to fluid flow showed a primary cilium dependent extracellular Ca^{2+}-dependent intracellular Ca^{2+} release (Praetorious and Spring 2003). This cilium-mediated Ca^{2+} entry also required the stretch-activated ion channel polycystin 2 (Nauli *et al.* 2003). In bone cells, flow-induced Ca^{2+} flux was shown to be independent of primary cilia (Malone *et al.* 2007) and inhibition of polcystin 2 also did not remove the flow-induced flux of Ca^{2+}. In chondrocytes, the primary cilium is required for compression-induced Ca^{2+} signalling mediated by ATP release but this was only for downstream ATP reception and not in response to exogenous ATP (Wann *et al.* 2012). These findings suggest that different cell types contain distinctly different mechanisms that are responsible for cilium-mediated mechanosensation.

8.5 Conclusions and future work

Understanding the mechanisms behind how a cell senses a mechanical force and converts this into a biological response is important for tissue engineering strategies involving the use of mechanical stimulation. Assessing the pathways involved in mechanotransduction responses will also aid research into fracture healing and osseointegration, which would greatly benefit from knowing the exact mechanical stimuli that will produce more rapid bone growth. The present study showed that bone cell primary cilia adjust their structure in response to oscillatory fluid flow in an apparent attempt to alter sensitivity to loading. Mineralised matrix deposition is the end stage of bone cell differentiation and the primary cilium seems to play an essential role in load-induced bone formation, which did not occur when it was completely removed. The evidence presented here for primary cilia as a mechanosensor in bone cells highlights that these could be targeted for optimising loading regimes and controlling the subsequent production of a suitable construct.

Future work needs to address the role that the primary cilia plays at the different stages of cell differentiation, including undifferentiated progenitor cells, immature osteoblastic cells, and fully differentiated osteocytes. Most of the work up until now concerning the primary cilia and mechanotransduction has focused on mature cells. However, a recent study by Hoey *et al.* (2012) suggests that increases in osteogenic responses of MSCs to oscillatory fluid flow are also dependent on a fully functioning primary cilium. The progenitor cell line hESMPs contain primary cilia as do the HDFs and this can be visualised in figure 8.9 and their role in fluid-flow mediated responses should be explored.
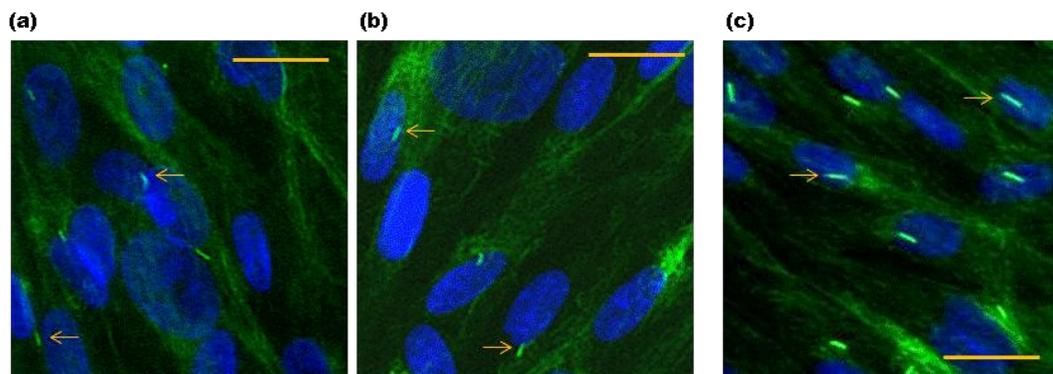
Figure 8.9: Primary cilia was visualised in osteoprogenitor cells. hESMPs were cultured in expansion media (a) or osteogenic media containing Dex (b), and HDFs were cultured in fibroblastic media (c) for 10 days. Fluorescent staining of cell nucleus (DAPI-blue) and microtubules and primary cilia (anti-acetylated α-tubulin in green) are shown. Arrows indicate primary cilia. Scale bars are 25 μm.

The effect that different types of mechanical stimuli have on primary cilia-dependent load-induced cellular responses should be elucidated. As one of the main aims in TE is to use mechanical forces to produce a more suitable construct and reduce healing time, it would be essential to understand fully the adaptive role that the primary cilia has to loading and how it responds to different conditions and loading parameters. It may be that matrix deposition is limited to a maximum rate without manipulation of the primary cilia. Simple models like the plate rocker platform used here can be used for high-through put screening to address these issues, however, CH treatment is not suitable for long term culture and so other methods for primary cilia inhibition such as knock out components of the IFT are required.

8.6 Summary

- Primary cilia are present in MLO-A5 mature bone cells.

- CH treatment was effective at damaging/removing primary cilia.

- Oscillatory fluid flow caused primary cilia to shorten in length and reduce in incidence compared with unloaded primary cilia.

- Primary cilia removal inhibited the load-induced mineral deposition response of MLO-A5 cells to oscillatory fluid flow.

- Primary cilia are present in hESMP and HDF osteoprogenitor cells.

CHAPTER NINE: Conclusions and future directions

The main aim of this research project was to study the effect that mechanical force and physical cues have on cell differentiation (more specifically osteogenesis) and matrix production. The overall goal was to see if cell differentiation and matrix production could be guided in order to produce a more developed and structured ECM and speed up development time. The hypothesis was that both physical and mechanical cues were able to influence matrix production and organisation. My results showed that physical cues (electrospun fibre architecture) and external mechanical forces (dynamic tension and oscillatory FSS) both influenced cell behaviour and matrix production, and more interestingly collagen organisation.

9.1 Scaffold guidance

Physical cues from the scaffold architecture influenced matrix organisation resulting in a collagenous fibre network that mimicked the scaffold fibre orientation. Aligned scaffolds supported the formation of a highly organised collagen network orientated in the scaffold fibre direction. This occurred as a result of cell alignment, which yielded anisotropic mechanical properties that were strongest in the direction parallel to fibre alignment. Meanwhile, cell-seeded randomly orientated fibrous mats showed isotropic properties that were 10-fold lower than parallel fibrous scaffolds.

Scaffold architecture also influenced the osteogenic differentiation of MLO-A5 and hESMP cells but not in the same way. MLO-A5 cells deposited more mineralised matrix on aligned fibres whereas hESMP cells had the highest ALP activity, collagen deposition, and calcium deposition on randomly orientated substrates. This suggests that cell maturity and the stage of cell differentiation may affect how the cell responds to physical cues. Interestingly, hESMP cells cultured without the osteogenic inducer Dex showed a significant increase in ALP activity on both fibre orientations at day 21 compared with TCP and by day 28 there were signs of some mineral formation. This indicates that surface features of electropsun fibres may promote the osteogenesis of progenitor cells.

Stem cell differentiation *in vitro* is most commonly directed using chemical stimulation with well defined growth factors. Controlling cell function with scaffold structure would be beneficial over strategies involving the use of growth factors or

biomolecules, including reduced cost, increased shelf-life, avoiding associated side effects, and it would also significantly reduce regulatory procedures. Reapplication of chemical stimulants could also prove challenging once a construct is implanted into the patient. Scaffolds with topographic cues are advantageous over traditional osteoinductive agents in that they can influence the cell for longer than the residence time of the supplements (Watari *et al.* 2012). At present, routine cell expansion and tissue culture is carried out using 2D stiff plastic or glass substrates. These environments are not found *in vivo* and so it is likely that cell behaviour is being compromised and it is also unknown whether later down the line this will affect the cell's ability to perform the desired function. Producing substrates that mimic the native tissue environment for routine *in vitro* cell culture will most likely provide more insights into the behaviour of cells and provide important insights into processes such as cell differentiation, wound healing and disease modelling.

Future work

- Alternating scaffold orientations; random with aligned or alternating aligned.
- Longer term studies to further study how cell behaviour and matrix organisation changes with time.
- Use of fast degrading scaffolds to see how this affects cells and their matrix once the scaffold degrades.
- Bioreactors for nutrient diffusion in layered scaffolds and combination of external mechanical forces.
- Substrate stiffness affect with fibre arrangement.

9.2 External mechanical forces

Mechanical stimulation in the form of dynamic tensile loading and oscillatory fluid flow was shown to influence matrix production in a number of different cells. Short bouts of tensile loading caused an increase in collagen production by cells cultured in a 3D environment. Oscillatory FSS promoted mineral deposition, collagen production and organisation in two types of osteoprogenitor cell.

Future work will need to decipher which type of load is the most appropriate along with the magnitude of this load, the frequency at which it is applied, and at what time point it should be applied in order to design culture systems that are capable of being scaled-up to commercially viable processing techniques. The simple rocking platform used here has the potential to test a wide variety of conditions as demonstrated in Chapter 3 and is suitable for stimulating osteogenic progenitors (Chapter 7). This could help translate optimal loading strategies to larger, more complex loading systems without the need for trying numerous loading parameters. However, it is not a straight forward process to convert these directly into 3D human models for clinical applications. Bioreactors will need to be designed on a much larger scale using well-defined parameters and characteristics with precisely predictable outcomes. What also must not be forgotten is that a cell-seeded construct in vitro initially resembles a healing wound and not a fully differentiated tissue, and so the dynamics of the construct will be very different to that of a fully developed in vivo tissue (Willie *et al.* 2010).

There also needs to be a better characterization of the forces cells experience from these loading systems. While most loading systems employ a common force type (e.g., tension or compression), there may also be other forces at work causing significant side effects (e.g., shear forces from fluid flow in compression systems). These other forces along with loading effects on mass transport and biochemical availability may have more of an effect on the cell differentiation process than the specific regimen the investigator intended to apply, causing a misinterpretation in the reason for the obtained results. Although a tissue engineer may only be concerned with the overall response and not the specific mechanism behind the response, it is important to know what forces are actually inducing the improved tissue formation to help simplify the design of future systems. Mathematical and computer modelling of loading systems can help better characterize the stresses and strains that are being experienced throughout the construct and subsequently provide a better understanding of what the cell is sensing and responding to (Thompson *et al.* 2010).

Future work

- Test a variety of loading parameters and culture conditions using simple platform rocker.

- See how optimal conditions translate into 3D fluid flow systems.

- Combine the use of a suitable orientated substrate with mechanical forces.

- Observe the effect of tensile loading on matrix production using SHG.

- Use fast degrading scaffolds to study the effect loading has on cells and their matrix production as the scaffold degrades.

9.3 Mesenchymal progenitor/stem cells

Our understanding of the capabilities of MSCs and the cues affecting their differentiation and development has advanced greatly over the past few decades. Numerous factors have been identified that are able to induce or enhance MSC differentiation into a wide variety of tissue-specific cells including chemical reagents, scaffold composition and topography, surface chemistry, and internal and external physical or mechanical forces. This makes MSCs a very promising cell source for future regenerative medicine and TE strategies. However, precisely controlling the timing and outcome of this differentiation process is still a challenge facing tissue engineers. Therefore, there are a number of issues that need to be addressed in order to successfully use MSCs in a clinical context.

While many relevant markers (gene expression and matrix synthesis) for tissue-specific differentiation and their temporal expression have been identified, complete profiling of each tissue-specific differentiation process is required in order to better understand how to fully induce the desired phenotype in MSC. While most studies measure earlier markers of osteogenic differentiation, the presence of a lineage-specific transcription factor within the cell nucleus does not necessarily mean that the cell is committed to that phenotype. It is also not known at what level gene transcription factors need to be at in order to initiate full differentiation and translate the cell into a matrix-secreting specialised cell.

Many studies have demonstrated that dermal tissue harbours different populations of multi-potent cells, but considering the abundance of this tissue, interest in its use as a source of progenitor cells has not been prolific. In order to determine the potential of this tissue as a suitable source of cells for bone tissue engineering, much further work is required.

- Analysis of osteogenic transcription factors and genes

- Analysis of deposited mineral by FT-IR

- Analysis of multiple donors, from different anatomical sights

- Further investigation of mechanical forces for enhancing osteogenesis

- Promotion of osteogenesis on electrospun fibres

The main limitation to creation of large scale implantable constructs from MSCs is the lack of a vascular network, at present, cell survival rate toward the center of tissue engineered constructs are low, even in the smallest cell-seeded scaffolds due to poor nutrient diffusion and gas exchange into the center of the scaffold. It has been suggested that TE constructs should have the rudiments of a vascular system incorporated within them by seeding with endothelial progenitor cells possessing angiogenic differentiation capabilities and using appropriate growth factors to direct these cells toward the center of the scaffold and induce them to form a vascular network (McCoy and O'Brien, 2010). The constructs would then be seeded with MSCs and directed toward the required tissue type using the appropriate cues. Since MSCs also produce angiogenic growth factors themselves they should aid the formation of the vascular network and here mechanical loading may form a dual role since it has also been shown to be a modulator of angiogenic growth factor release by MSCs (Kasper *et al.* 2007; Kasten *et al.* 2010).

9.4 Mechanotransduction

Understanding the process of converting a mechanical signal into a biological response is highly important for tissue engineering and regenerative medicine strategies. Unravelling these mechanisms will not only allow us to understand and treat diseases in a therapeutic setting, but also perform targeted loading regimes to produce a more clinically relevant construct in a more rapid fashion.

In this work I demonstrated that the primary cilium in MLO-A5 cells is responsible for the increase in calcium deposited in response to oscillatory fluid shear stress. I also showed that the primary cilium is able to adjust its length in response to this fluid stimulus, perhaps in an attempt to adjust its sensitivity. It is not entirely clear how the primary cilia in osteogenic cells and progenitors transfer an external

mechanical stimulus into a biological function inside the cell and how they interact with the ECM. Although oscillatory FSS is thought to be the primary stimulus in mature bone, the space around bone cells is very small (less than the typical length of the primary cilia seen *in vitro*) and it is likely that the primary cilia tethers to the ECM and may sense matrix deformation (Jensen, *et al.* 2004). Therefore, more 3D bone models are needed in order to study these interactions.

Other suspected mechanosensors have been identified, and it is highly possible that there is interaction between numerous mechanosenors which until now has had little investigation. Previously, it has been shown that the glycocalyx is responsible for uni-directional fluid flow responses (Reilly *et al.* 2003; Morris *et al.* 2010) and a previous student in our lab has shown that the glycocalyx appears to be present around the outside of the primary cilium. Both of my fluid flow studies (Chapters 7 and 8) also appeared to show cells spreading in response to the applied stimulus and it was seen that collagen matrix was well organized in the loaded groups. Chapter 4 showed that cell morphology dictates the organisation of deposited collagen and so cytoskeletal changes and integrin pulling are suspected mechanisms for the controlling of matrix organisation. The orientation of the primary cilia is also of interest with regards to matrix organisation and in confluent HDFs, I observed the primary cilium on most HDFs pointing in the direction of cell elongation.

While I showed that primary cilia are present in osteogenic progenitor cells (hESMPs and HDFs), a recent study by Hoey *et al.* (2012) has shown that primary cilia are required for loading-induced responses in MSCs. As it is likely that MSCs will be the cell of choice used instead of mature bone cells for clinical applications, mechanotransduction studies need to be performed on osteoprogenitors.

Future work

- Primary cilia interaction with ECM using SHG.
- Orientation of primary cilia on random and aligned scaffolds.
- Response of primary cilia to loading in 3D fluid flow systems.
- Localization of integrins on primary cilia.

9.5 Final conclusions

In conclusion, physical cues and mechanical loading are potent modulators of mature- and progenitor-cell differentiation, and can be used to guide matrix production. Harnessing their effects may allow for improved pre-culture methods of MSCs in implantable constructs or the design of exercise/tissue stimulation regimens that a patient can undergo after construct implantation. They will also allow for the production of a more organised and suitable construct which up to now has been a major reason for construct failure. Methods to monitor matrix production in a non-invasive fashion will be important to this extent and SHG has been demonstrated to useful tool for monitoring collagen organisation. A better understanding of the mechanical environment of MSCs niche could also lead to non-invasive methods of amplifying the MSC pool, stimulating their migration, or directing their differentiation toward a target tissue. Multiple laboratories have designed a wide range of scaffolds and cell loading devices however comparison of results between laboratories is very difficult due to the high variety of scaffold materials, loading devices and loading regimens, as well as cell sources available to the investigator. Contrasting results may be explained by the exquisite sensitivity of MSCs to very a specific combination of biochemical factors and physical stimuli at a specific time-point within their life, proliferative and differentiation cycles. Optimal pre-culture conditions for MSCs will vary without a doubt dependant on the clinical procedures they are aimed to treat so it is likely that a range of application dependant culture conditions will need to be developed over the coming years. Identifying the mechanisms by which a cell converts external stimuli into a biological response will aid with the production of targeted regimes.

APPENDIX 1

Oral presentations

1. UK BOSE Users Meeting: 'Simulating Physiological Environment using Electrospun Scaffolds and Tensile Loading', June 2010, Kings Collage, London.

2. EXPERTISSUES 8th International Symposium: 'Simulating Physiological Tissue Function through the Fabrication of Electrospun Scaffolds', May 2010, Portugal.

3. UK Bioengineering 11: 'A Simple Fluid Shear Force Method for Enhancing Osteogenesis in Progenitor Cells', September 2011, Queen Mary University, London.

4. 18th Congress of the European Society of Biomechanics (ESB2012): 'A Simple Shear Stress Stimulus for Enhancing Mineralised Matrix', July 2012, Lisbon, Portugal.

Poster presentations

1. Tissue and Cell Engineering Society: 'Response of Collagen Forming Cells to Dynamic Tensile Loading', July 2010, University of Manchester, UK.

2. UK Society of Biomaterials: 'Simulating Physiological Tissue Environment Through the Fabrication of Electrospun Scaffolds', July 2010, University of Glasgow, UK.

3. Orthopedic Research Society Annual Meeting: 'Osteogenic Media and Fluid Shear Forces can Induce Osteogenic Differentiation in Dermal Fibroblasts', Jan 2011, Long Beach, CA, USA.

4. 3rd Tissue Engineering and Regenerative Medicine World Congress 2012: 'Primary Cilia Removal Inhibits Osteoblastic Matrix-forming Response to Fluid-Induced Shear Stress', September 2012, Vienna, Austria.

Awards

1. Travel grant from Expert Tissues (2009), £350.
2. Four travel grants awarded from Sheffield University Learned Society (2011-2012), £350 and £300.
3. Travel grant awarded from the Royal Academy of Engineering, UK (2011), £600
4. Travel grant from Tissue and Cell Engineering Society UK (2011), £100.
5. **1st place prize** for 2nd year PhD departmental poster presentation (University of Sheffield 2010).

Publications

1. Delaine-Smith R.M. and Reilly G.C. (2011). The effect of mechanical loading on mesenchymal stem cell differentiation and matrix production. *Vitam Horm*, **87**: 417-80.
2. Delaine-Smith R.M., MacNeil S., Reilly G.C. (2012). Matrix production and collagen structure are enhanced in two types of osteogenic progenitor cells by a simple fluid shear stress stimulus. *Eur Cells Mater,* **24**: 162-174.
3. Delaine-Smith R.M. and Reilly G.C. (2012). Mesenchymal stem cell responses to mechanical stimuli. *Muscles, Ligaments, and Tendons J.* **2** (3): 169-180.

APPENDIX 2

Appendix 3

MATRIX PRODUCTION AND COLLAGEN STRUCTURE ARE ENHANCED IN TWO TYPES OF OSTEOGENIC PROGENITOR CELLS BY A SIMPLE FLUID SHEAR STRESS STIMULUS

R. M. Delaine-Smith[1], S. MacNeil[1] and G. C. Reilly[1*]

[1]Kroto Research Institute, Department of Materials Science and Engineering, University of Sheffield, Sheffield, UK.

Abstract

Mesenchymal progenitor cells play a vital role in bone regenerative medicine and tissue engineering strategies. To be clinically useful osteoprogenitors should be readily available with the potential to form bone matrix. While mesenchymal stromal cells from bone marrow have shown promise for tissue engineering, they are obtained in small numbers and there is risk of donor site morbidity. Osteogenic progenitor cells derived from dermal tissue may provide a more abundant and easily expandable source of cells. Bone turnover *in vivo* is regulated by mechanical forces, particularly oscillatory fluid shear stresses (FSS), and *in vitro* osteogenic progenitors have been shown to be regulated by mechanical stimuli. The aim of this study was to assess what effect osteogenic media and FSS, generated by a simple rocking platform, had on cell behaviour and matrix production in human progenitor dermal fibroblasts (HDFs) and the embryonic stem cell-derived mesenchymal progenitor cell line (hES-MP).

Osteogenic media stimulated alkaline phosphatase activity (ALP) and calcium deposition in HDFs. The addition of FSS further enhanced ALP activity and mineralised matrix deposition in both progenitor cells cultured in osteogenic media. Both types of progenitor cell subjected to FSS showed increases in collagen secretion and apparent collagen organisation as imaged by second harmonic generation.

Keywords: Mesenchymal stem cells; dermal fibroblasts; fluid shear stress; second harmonic generation; osteogenesis; matrix production; collagen.

*Address for correspondence:
Gwendolen Reilly
Department Materials Science and Engineering
Kroto Research Institute
University of Sheffield
Broad Lane
Sheffield , S3 7HQ, UK.
　　　　Telephone Number: +44 (0)114 222 5986
　　　　FAX Number: +44 (0) 114 222 5945
　　　　E-mail: g.reilly@shef.ac.uk

Introduction

Mesenchymal progenitor cells play a vital role in bone regenerative medicine and tissue engineering strategies, and to be clinically useful they should be readily available with the potential to undergo osteogenesis. Mesenchymal stem or stromal cells (MSCs) harvested from bone marrow have shown great potential as an autologous bone cell source with self-renewing and multipotent properties capable of *in vitro* differentiation along the osteogenic lineage (Jaiswal *et al.*, 1997; Mauney *et al.*, 2004; Pittenger *et al.*, 1999). However, bone marrow extraction carries the risk of donor site morbidity and only a small number of MSCs are obtained from bone marrow, which are difficult to expand to sufficient numbers *in vitro*. This has led researchers to search for alternative multipotent cell reservoirs. Progenitor cells with similar phenotypic characteristics and differentiation capabilities have been obtained from a variety of other adult tissues including adipose (De Ugarte *et al.*, 2003; Zuk *et al.*, 2001), tendon (Rui *et al.*, 2011), and skeletal muscle (Asakura *et al.*, 2001; Bosch *et al.*, 2000), as well as foetal tissues such as umbilical cord blood (Erices *et al.*, 2000; Goodwin *et al.*, 2001) and amniotic fluid (Soncini *et al.*, 2007). Another recently identified tissue that might harbour a suitable cell source for bone repair is the dermis of skin. Dermal fibroblasts were initially thought to be terminally differentiated, but it has been reported that dermal fibroblasts may be more plastic than first thought and are able to switch their lineage preference (Rutherford *et al.*, 2002; Sommar *et al.*, 2009) while numerous studies report that multipotent progenitor cells reside in the dermal tissue of rodents and humans (Bartsch *et al.*, 2005; Chen *et al.*, 2007; Toma *et al.*, 2001; Xue and Li, 2011; Young *et al.*, 2001). Chen *et al.* (2007) established single cell clones from dermal foreskin fibroblasts and found that around 30 % upregulated alkaline phosphatase (ALP) and osteocalcin (OCN) mRNA along with strong staining of deposited calcium when cultured in osteogenic media. Others have observed osteogenic differentiation from a population of skin cells (Buranasinsup *et al.*, 2006; Lorenz *et al.*, 2008). Lorenz *et al.* (2008) observed an upregulation in OCN and osteonectin (ON) mRNA in cells derived from human juvenile foreskin when cultured in osteogenic media, while Buranasinsup *et al.* (2006) observed positive ALP and mineral staining in cells derived from middle-age human skin biopsies. This suggests that dermal tissue has the potential to be an easily accessible source of cells suitable for use in bone tissue engineering.

MSC behaviour and function can be controlled by biochemical stimuli such as growth factors, cytokines and signalling events (Augello and De Bari, 2010) as well as

References

Agata, H.*, et al.* 2010. "Characteristic Change and Loss of In Vivo Osteogenic Abilities of Human Bone Marrow Stromal Cells During Passage." Tissue Eng. Part A **16**(2):663-673.

Allen, F. D.*, et al.* 2000. "Serum modulates the intracellular calcium response of primary cultured bone cells to shear flow." J. Biomech. **33**(12):1585-1591.

Anderson, E. J. and M. L. K. Tate. 2007. "Open access to novel dual flow chamber technology for in vitro cell mechanotransduction, toxicity and pharamacokinetic studies." Biomedical Engineering Online **6**.

Angle, S. R.*, et al.* 2011. "Osteogenic differentiation of rat bone marrow stromal cells by various intensities of low-intensity pulsed ultrasound." Ultrasonics **51**(3):281-288.

Archer, R. and D. J. Williams. 2005. "Why tissue engineering needs process engineering." Nat. Biotechnol. **23**:1353-1355.

Arnsdorf, E. J.*, et al.* 2009. "Mechanically induced osteogenic differentiation - the role of RhoA, ROCKII and cytoskeletal dynamics." Journal of Cell Science **122**(4):546-553.

Asakura, A., M. Komaki and M. A. Rudnicki. 2001. "Muscle satellite cells are multipotential stem cells that exhibit myogenic, osteogenic, and adipogenic differentiation." Differentiation **68**(4-5):245-253.

Aubin, J.E. and E. Bonnelye. 2000. "Osteoprotegerin and its ligand: a new paradigm for regulation of osteoclastogenesis and bone resorption." Osteoporos. Int. **11**(11):905-913.

Augello, A. and C. De Bari. 2010. "The Regulation of Differentiation in Mesenchymal Stem Cells." Hum. Gene Ther. **21**(10):1226-1238.

Augst, A.*, et al.* 2008. "Effects of chondrogenic and osteogenic regulatory factors on composite constructs grown using human mesenchymal stem cells, silk scaffolds and bioreactors." J Roy Soc Interface **5**(25):929-939.

Badami, A. S.*, et al.* 2006. "Effect of fiber diameter on spreading, proliferation, and differentiation of osteoblastic cells on electrospun poly(lactic acid) substrates." Biomaterials **27**(4):596-606.

Badano, J. L.*, et al.* 2006. "The ciliopathies: an emerging class of human genetic disorders." Annu. Rev. Genom. Hum. Genet. **7**:125-148.

Bakker, A. D.*, et al.* 2001. "The production of nitric oxide and prostaglandin E-2 by primary bone cells is shear stress dependent." J. Biomech. **34**(5):671-677.

Balu, M.*, et al.* 2009. "Effect of excitation wavelength on penetration depth in nonlinear optical microscopy of turbid media." J Biomed Opt **14**:010508.

Barkhausen, T.*, et al.* 2003. "Modulation of cell functions of human tendon fibroblasts by different repetitive cyclic mechanical stress patterns." Exp. Toxicol. Pathol. **55**(2-3):153-158.

Barocas, V. H. and R. T. Tranquillo. 1997. "An anisotropic biphasic theory of tissue-equivalent mechanics: the interplay among cell traction, fibrillar network deformation, fibril alignment, and cell contact guidance." J. Biomech. Eng. **119**(2):137-145.

Bartsch, G.*, et al.* 2005. "Propagation, expansion, and multilineage differentiation of human somatic stem cells from dermal progenitors." Stem Cells Dev **14**(3):337-348.

Bashur, C. A., L. A. Dahlgren and A. S. Goldstein. 2006. "Effect of fiber diameter and orientation on fibroblast morphology and proliferation on electrospun poly(D,L-lactic-co-glycolic acid) meshes." Biomaterials **27**(33):5681-5688.

Bassey, E. J. and S. J. Ramsdale. 1994. "Increase in femoral bone-density in young-women following high-impact exercise." Osteoporos. Int. **4**(2):72-75.

Bayan, C.*, et al.* 2009. "Fully automated, quantitative, noninvasive assessment of collagen fiber content and organization in thick collagen gels." J Appl Phys **105**:102042.

Baylink, D. J. and J. E. Wergedal. 1971. "Bone formation by osteocytes." Am. J. Physiol. **221**(3):669-678.

Ben-David, U. and N. Benvensity. 2011. "The tumorigenicity of human embryonic and induced pluripotent stem cells." Nat Rev Cancer **11**:268-277.

Berbari, N. F.*, et al.* 2009. "The primary cilium as a complex signaling center." Curr. Biol. **19**:R526-535.

Beresford, J. N.*, et al.* 1992. "Evidence for an inverse relationship between the differentiation of adipocytic and osteogenic cells in rat marrow stromal cell-cultures." J. Cell Sci. **102**:341-351.

Besschetnova, T. Y.*, et al.* 2010. "Identification of Signaling Pathways Regulating Primary Cilium Length and Flow-Mediated Adaptation." Curr. Biol. **20**(2):182-187.

Bhadriraju, K.*, et al.* 2007. "Activation of ROCK by RhoA is regulated by cell adhesion, shape, and cytoskeletal tension." Exp. Cell Res. **313**(16):3616-3623.

Bissell, M. J. and M. H. Barcellos-Hoff. 1987. "The influence of extracellular matrix on gene expression: is structure the message?" J. Cell Sci. **8**:327343.

Blackwood, K. A.*, et al.* 2008. "Development of biodegradable electrospun scaffolds for dermal replacement." Biomaterials **29**(21):3091-3104.

Blasi, Antonella*, et al.* 2011. "Dermal fibroblasts display similar phenotypic and differentiation capacity to fat-derived mesenchymal stem cells, but differ in anti-inflammatory and angiogenic potential." Vascular cell **3**(1):5-5.

Boland, E. D.*, et al.* 2006. "Electrospinning of bioresorbable polymers for tissue engineering scaffolds." In Polymeric Nanofibres: American Chemical Society.

Bonivtch, A. R., L. F. Bonewald and D. P. Nicolella. 2007. "Tissue strain amplification at the osteocyte lacuna: A microstructural finite element analysis." J. Biomech. **40**(10):2199-2206.

Bosch, P.*, et al.* 2000. "Osteoprogenitor cells within skeletal muscle." J. Orthop. Res. **18**(6):933-944.

Brammer, K. S.*, et al.* 2009. "Improved bone-forming functionality on diameter-controlled TiO2 nanotube surface." Acta Biomater. **5**(8):3215-3223.

Breen, E. C. 2000. "Mechanical strain increases type I collagen expression in pulmonary fibroblasts in vitro." J. Appl. Physiol. **88**(1):203-209.

Brown, T. D. 2000. "Techniques for mechanical stimulation of cells in vitro: a review." J. Biomech. **33**(1):3-14.

Buranasinsup, S.*, et al.* 2006. "In vitro osteogenesis from human skin-derived precursor cells." Dev. Growth Differ. **48**(4):263-269.

Burger, C., B. S. Hsiao and B. Chu. 2006. "Nanometre diameter fibres of polymer, produced by electrospinning." Ann Rev Mater Res **36**:216-223.

Burr, D. B.*, et al.* 1996. "In vivo measurement of human tibial strains during vigorous activity." Bone **18**(5):405-410.

Campagnola, P. J. and L. M. Loew. 2003. "Second-harmonic imaging microscopy for visualizing biomolecular arrays in cells, tissues and organisms." Nat Biotechnol **21**:1356-1360.

Campagnola, P. J.*, et al.* 2002. "Three-dimensional high-resolution secondharmonic generation imaging of endogenous structural proteins in biological tissues." Biophysics **81**:493-508.

Canton, I.*, et al.* 2010. "Development of an ibuprofen-releasing biodegradable PLA/PGA electrospun scaffold for tissue regeneration." Biotechnol Bioeng **105**(2):396-408.

Caplan, A. I. 2007. "Adult mesenchymal stem cells for tissue engineering versus regenerative medicine." J Cell Physl **213**(2):341-347.

Cartmell, S. H.*, et al.* 2003. "Effects of medium perfusion rate on cell-seeded three-dimensional bone constructs in vitro." Tissue Eng. Part A **9**(6):1197-1203.

Carver, W.*, et al.* 1991. "COLLAGEN EXPRESSION IN MECHANICALLY STIMULATED CARDIAC FIBROBLASTS." Circ. Res. **69**(1):116-122.

Chakrabarti, A.*, et al.* 1998. "Chloral hydrate alters the organization of the ciliary basal apparatus and cell organelles in sea urchin embryos." Cell Tissue Res. **293**(3):453-462.

Chanda, D., S. Kumar and S. Ponnazhagan. 2010. "Therapeutic potential of adult bone marrow derived mesenchymal stem cells in diseases of the skeleton." Journal of Cellular Biochemistry **111**:249-257.

Chang, H. Y., *et al.* 2002. "Diversity, topographic differentiation, and positional memory in human fibroblasts." Proc. Natl. Acad. Sci. U. S. A. **99**(20):12877-12882.

Chang, Y. L., C. M. Stanford and J. C. Keller. 2000. "Calcium and phosphate supplementation promotes bone cell mineralization: Implications for hydroxyapatite (HA)-enhanced bone formation." J. Biomed. Mater. Res. **52**(2):270-278.

Chen, C. S., *et al.* 1997. "Geometric Control of Cell Life and Death." Science **276**(5317):1425-1428.

Chen, F. G., *et al.* 2007. "Clonal analysis of nestin(-) vimentin(+) multipotent fibroblasts isolated from human dermis." J. Cell Sci. **120**(16):2875-2883.

Chen, Y. J., *et al.* 2008. "Effects of cyclic mechanical stretching on the mRNA expression of tendon/ligament-related and osteoblast-specific genes in human mesenchymal stem cells." Connective Tissue Research **49**(1):7-14.

Claes, L. E. and C. A. Heigele. 1999. "Magnitudes of local stress and strain along bony surfaces predict the course and type of fracture healing." J. Biomech. **32**(3):255-266.

Cowie, R., R. D. Walker and A. Scutt. 2006. "The use of high-frequency, low-intensity vibration to stimulate the proliferation and differentiation of primary rat bone marrow cells." Cytotherapy **8**:63-63.

Cukierman, E., *et al.* 2001. "Taking Cell-Matrix Adhesions to the Third Dimension." Science **294**(5547):1708-1712.

Dalby, M. J., *et al.* 2007a. "Nanomechanotransduction and interphase nuclear organization influence on genomic control." J. Cell. Biochem. **102**(5):1234-1244.

Dalby, M. J., *et al.* 2007b. "The control of human mesenchymal cell differentiation using nanoscale symmetry and disorder." Nature Materials **6**(12):997-1003.

Daud, M. F. B., *et al.* 2012. "An aligned 3D neuronal-glial co-culture model for peripheral nerve studies." Biomaterials **33**(25):5901-5913.

De Ugarte, D. A., *et al.* 2003. "Comparison of multi-lineage cells from human adipose tissue and bone marrow." Cells Tissues Organs **174**(3):101-109.

Delaine-Smith, R. M., S. Macneil and G. C. Reilly. 2012. "Matrix production and collagen structure are enhanced in two types of osteogenic progenitor cells by a simple fluid shear stress stimulus." Eur cells mater **24**:162-174.

Delaine-Smith, R. M. and G. C. Reilly. 2011. "The effects of mechanical loading on mesenchymal stem cell differentiation and matrix production." Vitam Horm. **87**:417-480.

Deligianni, D. D., *et al.* 2001. "Effect of surface roughness of hydroxyapatite on human bone marrow cell adhesion, proliferation, differentiation and detachment strength." Biomaterials **22**:87-96.

den Braber, E. T., *et al.* 1998. "Orientation of ECM protein deposition, fibroblast cytoskeleton, and attachment complex components on silicone microgrooved surfaces." J. Biomed. Mater. Res. **40**(2):291-300.

Deng, D., *et al.* 2009. "Engineering human neo-tendon tissue in vitro with human dermal fibroblasts under static mechanical strain." Biomaterials **30**(35):6724-6730.

Deshpande, P., *et al.* 2010. "Using poly(lactide-co-glycolide) electrospun scaffolds to deliver cultured epithelial cells to the cornea." Regen Med **5**(3):395-401.

Detta, N., *et al.* 2010. "Novel electrospun polyurethane/gelatin composite meshes for vascular grafts." J Mater Sci Mater Med **21**(5):1761-1769.

Diefenderfer, D. L., *et al.* 2003. "BMP responsiveness in human mesenchymal stem cells." Connect Tissue Res **44**:305-311.

Discher, D. E., P. Janmey and Y. L. Wang. 2005. "Tissue cells feel and respond to the stiffness of their substrate." Science **310**(5751):1139-1143.

Dominici, M., *et al.* 2006. "Minimal criteria for defining multipotent mesenchymal stromal cells. The International Society for Cellular Therapy position statement." Cytotherapy **8**(4):315-317.

Donahue, H. J. 2000. "Gap junctions and biophysical regulation of bone cell differentiation." Bone **26**(5):417-422.

Donahue, T. L. H., *et al.* 2003. "Mechanosensitivity of bone cells to oscillating fluid flow induced shear stress may be modulated by chemotransport." J Biomech **36**(9):1363-1371.

Doshi, J. and D. H. Reneker. 1995. "Electrospinning Process and Applications of Electrospun Fibers." J. Electrostatics **35**(2-3):151-160.

Duncan, R. L. and C. H. Turner. 1995. "Mechanotransduction and the functional-response of bone to mechanical strain." Calcif. Tissue Int. **57**(5):344-358.

Duty, A. O., M. E. Oest and R. E. Guldberg. 2007. "Cyclic mechanical compression increases mineralization of cell-seeded polymer scaffolds in vivo." J Biomech Engineering-Transactions of the Asme **129**(4):531-539.

Eckes, B., R. Nischt and T. Krieg. 2010. "Cell-matrix interactions in dermal repair and scarring." Fibrogenesis Tissue Repair **3**(4):1-12.

Edwards, J. H. and G. C. Reilly. 2011. "Low magnitude, high frequency vibration modulates mesenchymal progenitor differentiation." Trans Annu Mee Orthop Res Soc **57**.

El Haj, A. J. and S. H. Cartmell. 2010. "Bioreactors for bone tissue engineering." P I Mech Eng H **224**(H12):1523-1532.

Engler, A. J.*, et al.* 2008. "Embryonic cardiomyocytes beat best on a matrix with heart-like elasticity: scar-like rigidity inhibits beating." J Cell Science **121**:3794-3802.

Engler, A. J.*, et al.* 2006. "Matrix elasticity directs stem cell lineage specification." Cell **126**(4):677-689.

Erices, A., P. Conget and J. J. Minguell. 2000. "Mesenchymal progenitor cells in human umbilical cord blood." Brit J Haematol **109**(1):235-242.

Felgner, H., R. Frank and M. Schliwa. 1996. "Flexural rigidity of microtubules measured with the use of optical tweezers." J. Cell Sci. **109**:509-516.

Fenn, J. B.*, et al.* 1989. "Electrospray ionization for mass spectrometry of large biomolecules." Science **246**(4926):64-71.

Foldberg, S.*, et al.* 2012. "Patterned poly(lactic acid) films support growth and spontaneous multilineage gene expression of adipose-derived stem cells." Colloid Surface B **93**:92-99.

Frangos, J. A., L. V. McIntire and S. G. Eskin. 1988. "Shear-stress induced stimulation of mammalian-cell metabolism." Biotechnol Bioeng **32**(8):1053-1060.

Freund, I., M. Deutsch and A. Sprecher. 1986. "Connective tissue polarity, Optical second-harmonic microscopy, crossed-beam summation, and small-angle scattering in rat-tail tendon." Biophys J **50**:693-712.

Friedenstein, A. J., I. I. Piatetzk-Shapiro and K. V. Petrakov. 1966. "Osteogenesis in transplants of bone marrow cells." J Embryol Exp Morph **16**:381-90.

Fu, X. L. and H. J. Wang. 2012. "Spatial Arrangement of Polycaprolactone/Collagen Nanofiber Scaffolds Regulates the Wound Healing Related Behaviors of Human Adipose Stromal Cells." Tissue Eng Part A **18**(5-6):631-642.

Gabbiani, G. 2003. "The myofibroblast in wound healing and fibrocontractive diseases." J Pathol **200**:500-503.

Gardner, K., S. P. Arnoczky and M. Lavagnino. 2011. "Effect of In vitro Stress-Deprevation and Cyclic Loading on the Length of Tendon Cell Cilia in situ." J Orthop Res **29**(4):582-587.

Garvin, J.*, et al.* 2003. "Novel system for engineering bioartificial tendons and application of mechanical load." Tissue Eng **9**(5):967-979.

Geiger, R. Christopher*, et al.* 2009. "Tubulin Acetylation and Histone Deacetylase 6 Activity in the Lung under Cyclic Load." Am J Respir Cell Mol Biol **40**(1):76-82.

Genetos, D. C.*, et al.* 2005. "Fluid shear-induced ATP secretion mediates prostaglandin release in MC3T3-E1 osteoblasts." J Bone Miner Res **20**(1):41-49.

Glossop, J. R. and S. H. Cartmell. 2009. "Effect of fluid flow-induced shear stress on human mesenchymal stem cells: Differential gene expression of IL1B and MAP3K8 in MAPK signaling." Gene Expr Pattern **9**(5):381-388.

Glossop, J. R. and S. H. Cartmell. 2010. "Tensile strain and magnetic particle force application do not induce MAP3K8 and IL-1B differential gene expression in a similar manner to fluid shear stress in human mesenchymal stem cells." J Tissue Eng Regen Med **4**(7):577-579.

Goodwin, H. S.*, et al.* 2001. "Multilineage differentiation activity by cells isolated from umbilical cord blood: Expression of bone, fat, and neural markers." Biol Blood Marrow Tr **7**(11):581-588.

Guan, J.*, et al.* 2005. "Preparation and characterization of highly porous, biodegradable polyurethane scaffolds for soft tissue applications." Biomaterials **26**(18):3961-3971.

Guelcher, S. A. 2008. "Biodegradable polyurethanes: synthesis and applications in regenerative medicine." Tissue Eng Part B Rev **14**(1):3-17.

Guelcher, S.*, et al.* 2007. "Synthesis, in vitro degradation, and mechanical properties of two-component poly(ester urethane)urea scaffolds: effects of water and polyol composition." Tissue Eng Part A **13**(9):2321-2333.

Guilak, F.*, et al.* 2009. "Control of Stem Cell Fate by Physical Interactions with the Extracellular Matrix." Cell Stem Cell **5**(1):17-26.

Gurkan, U. A. and O. Akkus. 2008. "The Mechanical Environment of Bone Marrow: A Review." Ann Biomed Eng **36**(12):1978-1991.

Hasirci, V. and H. Kenar. 2006. "Novel surface patterning approaches for tissue engineering and their effect on cell behavior." Nanomedicine **1**(1):73-89.

Hay, E. D. 1991. Cell biology and extracellular matrix. 2nd edn. Edition. New York: Plenum Press.

He, J.*, et al.* 2011. "Bone morphogenetic protein receptor IB as a marker for enrichment of osteogenic precursor-like cells in human dermis." Arch. Dermatol. Res. **303**(8):581-590.

Heino, J. 2007. "The collagen family members as cell adhesion proteins." Bioessays **29**:1001-1010.

Henderson, J. H.*, et al.* 2007. "Rapid growth of cartilage rudiments may generate perichondrial structures by mechanical induction." Biomech Model Mechanobiol **6**(1-2):127-137.

Hoey, D. A., M. E. Downs and C. R. Jacobs. 2012a. "The mechanics of the primary cilium: An intricate structure with complex function." J Biomech **45**:17-26.

Hoey, D. A., D. J. Kelly and C. R. Jacobs. 2011. "A role for the primary cilium in paracrine signaling between mechanically stimulated osteocytes and mesenchymal stem cells." Biochem Biophys Res Commun **412**(1):182-187.

Hoey, D. A.*, et al.* 2012b. "Primary Cilia Mediated Mechanotransduction in Human Mesenchymal Stem Cells." Stem Cells **30**:Epub Ahead of print.

Hoffmann, A., and G. Gross. 2007. "Tendon and ligament engineering in the adult organism: mesenchymal stem cells and gene-therapeutic approaches." Int. Orthop. **31**(6):791-797.

Hollinger, J. O.*, et al.* 2005. Bone Tissue Engineering: CRC Press.

Hong, J. K., and S. V. Madihally. 2010. "Three-dimensional scaffold of electrosprayed fibers with large pore size for tissue regeneration." Acta Biomater **6**(12):4734-4742.

Huang, C. H.*, et al.* 2009. "Interactive Effects of Mechanical Stretching and Extracellular Matrix Proteins on Initiating Osteogenic Differentiation of Human Mesenchymal Stem Cells." J Cell Biochem **108**(6):1263-1273.

Huang, Z. M.*, et al.* 2004. "Electrospinning and mechanical characterization of gelatin nanofibers." Polymer **45**(15):5361-5368.

Hubbe, M. A. 1981. "Adhesion and detachment of biological cells-invitro." Prog Surf Sci **11**(2):65-138.

Ignatius, A.*, et al.* 2005. "Tissue engineering of bone: effects of mechanical strain on osteoblastic cells in type I collagen matrices." Biomaterials **26**(3):311-318.

Inai, R., M. Kotaki and S. Ramakrishna. 2005. "Structure and properties of electrospun PLLA single nanofibres." Nanotechnology **16**(2):208-213.

Iqbal, J. and M. Zaidi. 2005. "Molecular regulation of mechanotransduction." Biochem Biophys Res Com **328**:751-755.

Jaager, K. and T. Neuman. 2011. "Human Dermal Fibroblasts Exhibit Delayed Adipogenic Differentiation Compared with Mesenchymal Stem Cells." Stem Cells Dev **20**(8):1327-1336.

Jaasma, M. J. and F. J. O'Brien. 2008. "Mechanical stimulation of osteoblasts using steady and dynamic fluid flow." Tissue Eng Part A **14**(7):1213-1223.

Jacobs, C. R., S. Temiyasathit and A. B. Castillo. 2010. "Osteocyte Mechanobiology and Pericellular Mechanics." Ann RevBiomed Eng **12**:369-400

Jacobs, C. R.*, et al.* 1998. "Differential effect of steady versus oscillating flow on bone cells." J. Biomech. **31**(11):969-976.

Jaiswal, N.*, et al.* 1997. "Osteogenic differentiation of purified, culture-expanded human mesenchymal stem cells in vitro." J Cell Biol **64**(2):295-312.

Janmey, P. A. and C. A. McCulloch. 2007. "Cell mechanics: Integrating cell responses to mechanical stimuli." Ann Rev Biomed Eng **9**:1-34.

Jensen, C. G.*, et al.* 2004. "Ultrastructural, tomographic and confocal imaging of the chondrocyte primary cilium in situ." Cell Biol Int **28**(2):101-110.

Johnson, D. L., T. N. McAllister and J. A. Frangos. 1996. "Fluid flow stimulates rapid and continuous release of nitric oxide in osteoblasts." Am. J. Physiol. **271**(1 Pt 1):E205-208.

Joshi, S. D., and K. Webb. 2008. "Variation of cyclic strain parameters regulates development of elastic modulus in fibroblast/substrate constructs." J Orthop Res **26**(8):1105-1113.

Judex, S.*, et al.* 2007. "Low-magnitude mechanical signals that stimulate bone formation in the ovariectomized rat are dependent on the applied frequency but not on the strain magnitude." J Biomech **40**(6):1333-1339.

Kaewkhaw, R., A. M. Scutt and J. W. Haycock. 2011. "Anatomical site influences the differentiation of adipose-derived stem cells for Schwann cell phenotype and function." Glia **59**(5):734-749.

Karageorgiou, V. and D. Kaplan. 2005. "Porosity of 3D biornaterial scaffolds and osteogenesis." Biomaterials **26**(27):5474-5491.

Karlsson, C.*, et al.* 2009. "Human embryonic stem cell-derived mesenchymal progenitors-Potential in regenerative medicine." Stem Cell Res **3**(1):39-50.

Kasper, J. M.*, et al.* 2007. "Mesenchymal stem cells regulate angiogenesis according to their mechanical environment." Stem Cells **25**:903-910.

Kasten, A.*, et al.* 2010. "Mechanical Integrin Stress and Magnetic Forces Induce Biological Responses in Mesenchymal Stem Cells Which Depend on Environmental Factors." J Cellular Biochem **111**(6):1586-1597.

Kato, Y.*, et al.* 2001. "Establishment of an osteoid preosteocyte-like cell MLO-A5 that spontaneously mineralizes in culture." J Bone Miner Res **16**(9):1622-1633.

Khademhosseini, A.*, et al.* 2006. "Microscale technologies for tissue engineering and biology." Proc Natl Acad Sci U. S. A. **103**(8):2480-2487.

Khademhosseini, A., J. P. Vacanti and R. Langer. 2009. "Progress in tissue engineering." Sci Am **300**(5):64-+.

Khan, A. S.*, et al.* 2008. "Preparation and characterization of a novel bioactive restorative composite based on covalently coupled polyurethane-nanohydroxyapatite fibres." Acta Biomater **4**(5):1275-1287.

Kielty, C. M., I. Hopkinson and M. E. Grant. 1993. "Collagen: The collagen family: Structure, assembly, and organization in the extracellular matrix." In Connective tissue and its heritable disorders: Molecular, genetic, and medical aspects.

Kim, S. H.*, et al.* 2007. "Erk 1/2 activation in enchanced osteogenesis of human mesenchymal stem cells in poly(lactic-glycolic acid) by cyclic hydrostatic pressure." J Biomed Mater Res A **80A**:826-836.

Kishore, V.*, et al.* 2012. "Tenogenic differentiation of human MSCs induced by the topography of electrochemically aligned collagen threads." Biomaterials **33**(7):2137-2144.

Kjaer, M. 2004. "Role of extracellular matrix in adaptation of tendon and skeletal muscle to mechanical loading." Physiol Rev **84**:649-698.

Klein-Nulend, J., R. G. Bacabac and M. G. Mullender. 2005. "Mechanobiology of bone tissue." Pathol Biol (Paris). **53**(10):576-580.

Koc, O. N.*, et al.* 2002. "Allogeneic mesenchymal stem cell infusion for treatment of metachromatic leukodystrophy (MLD) and Hurler syndrome (MPS-IH)." Bone Marrow Transplantation **30**(4):215-222.

Koepsell, L., *et al.* 2011. "Tissue engineering of annulus fibrosus using electrospun fibrous scaffolds with aligned polycaprolactone fibers." J Biomed Mater Res Part A **99A**(4):564-575.

Koroleva, A., *et al.* 2012. "Two-photon polymerization-generated and micromolding-replicated 3D scaffolds for peripheral neural tissue engineering applications." Biofabrication **4**:025005.

Krajewska, E., *et al.* 2011. "New insights into induction of early-stage neovascularization in an improved tissue-engineered model of psoriasis." J Tissue Eng Regen Med **5**(5):363-374.

Kreke, M. R., W. R. Huckle and A. S. Goldstein. 2005. "Fluid flow stimulates expression of osteopontin and bone sialoprotein by bone marrow stromal cells in a temporally dependent manner." Bone **36**(6):1047-1055.

Krieg, M., *et al.* 2008. "Tensile forces govern germ-layer organization in zebrafish." Nat Cell Biol **10**:429-436.

Kumar, G., *et al.* 2011. "The determination of stem cell fate by 3D scaffold structures through the control of cell shape." Biomaterials **32**(35):9188-9196.

Kumar, G., *et al.* 2012. "Freeform fabricated scaffolds with roughened struts that enhance both stem cell proliferation and differentiation by controlling cell shape." Biomaterials **33**(16):4022-4030.

Kumbar, S. G., *et al.* 2008. "Electrospun poly(lactic acid-co-glycolic acid) scaffolds for skin tissue engineering." Biomaterials **29**(30):4100-4107.

Kwon, I. K., S. Kidoaki and T. Matsuda. 2005. "Electrospun nano- to microfiber fabrics made of biodegradable copolyesters: structural characteristics, mechanical properties and cell adhesion potential." Biomaterials **26**(18):3929-3939.

Lacroix, D., *et al.* 2002. "Biomechanical model to simulate tissue differentiation and bone regeneration: application to fracture healing." Med Biol Eng Comp **40**(1):14-21.

Laurencin, C. T., J. W. Freeman and M. D. Woods. 2006. "A novel tissue engineered scaffold for anterior Cruciate ligament repair: Relation of functional properties to scaffold structure." In Proceedings of the 5th World Congress of Biomechanics.

Lavoie, J. F., *et al.* 2009. "Skin-Derived Precursors Differentiate Into Skeletogenic Cell Types and Contribute to Bone Repair." Stem Cells Dev **18**(6):893-905.

Leboy, P. S., *et al.* 1991. "Dexamethansone induction of osteoblast messenger-RNAs in rat marrow stromal cell-cultures." J Cell Physiol **146**(3):370-378.

Lee, C. H., *et al.* 2005a. "Nanofiber alignment and direction of mechanical strain affect the ECM production of human ACL fibroblast." Biomaterials **26**(11):1261-1270.

Lee, G. M., *et al.* 1987. "Chloral hydrate disrupts mitosis by increasing intracellular free calcium." J Cell Sci **88**:603-612.

Lee, J. B., *et al.* 2011. "Highly Porous Electrospun Nanofibers Enhanced by Ultrasonication for Improved Cellular Infiltration." Tissue Eng Part A **17**(21-22):2695-2702.

Lee, S. B., *et al.* 2005b. "Study of gelatin-containing artificial skin V: fabrication of gelatin scaffolds using a salt-leaching method." Biomaterials **26**(14):1961-1968.

Li, W. J., *et al.* 2007. "Engineering controllable anisotropy in electrospun biodegradable nanofibrous scaffolds for musculoskeletal tissue engineering." J Biomech **40**(8):1686-1693.

Liedert, A., L. Claes and A. Ignatius. 2008. "Signal transduction pathways involved in mechanotransduction in osteoblastic and mesenchymal stem cells." Mechanosensitivity in Cells and Tissues **1**:253-265

Liu, W., *et al.* 2003. "Effect of flow and stretch on the [Ca(2+)](i) response of principal and intercalated cells in cortical collecting duct." Am J Physiol-Renal **285**(5):F998-F1012.

Liu, Ying, *et al.* 2009. "Effects of fiber orientation and diameter on the behavior of human dermal fibroblasts on electrospun PMMA scaffolds." J Biomed Mater Res Part A **90A**(4):1092-1106.

Lorenz, K., *et al.* 2008. "Multilineage differentiation potential of human dermal skin-derived fibroblasts." Exp Dermatol **17**(11):925-932.

Lowery, J. L., N. Datta and G. C. Rutledge. 2010. "Effect of fiber diameter, pore size and seeding method on growth of human dermal fibroblasts in electrospun poly(epsilon-caprolactone) fibrous mats." Biomaterials **31**(3):491-504.

Lu, Lan-Xin*, et al.* 2012. "The effects of PHBV electrospun fibers with different diameters and orientations on growth behavior of bone-marrow-derived mesenchymal stem cells." Biomed Mater **7**(1):015002.

Luo, Z. J. and B. B. Seedhom. 2007. "Light and low-frequency pulsatile hydrostatic pressure enhances extracellular matrix formation by bone marrow mesenchymal cells: an in-vitro study with special reference to cartilage repair." P I Mech Eng H **221**(H5):499-507.

Lynch, H. A. *, et al.* 2003. "Effect of fiber orientation and strain rate on the nonlinear uniaxial tensile material properties of tendon." J Biomech Eng **125**(5):726-731.

Lysy, P. A., *et al.* 2007. "Human skin fibroblasts: From mesodermal to hepatocyte-like differentiation." Hepatology **46**(5):1574-1585.

Ma, J., X. He and E. Jabbari. 2011. "Osteogenic Differentiation of Marrow Stromal Cells on Random and Aligned Electrospun Poly(L-lactide) Nanofibers." Ann Biomed Eng **39**(1):14-25.

Ma, Z.*, et al.* 2005. "Grafting of gelatin on electrospun poly(caprolactone) nanofibers to improve endothelial cell spreading and proliferation and to control cell Orientation." Tissue Eng Part A **11**(7-8):1149-1158.

Maehata, Y.*, et al.* 2007. "Type III collagen is essential for growth acceleration of human osteoblastic cells by ascorbic acid 2-phosphate, a long-acting vitamin C derivative." Matrix Biol **26**(5):371-381.

Malone, A. M. D.*, et al.* 2007a. "Primary cilia mediate mechanosensing in bone cells by a calcium-independent mechanism." Proc Natl Acad Sci U. S. A. **104**(33):13325-13330.

Malone, A. M. D.*, et al.* 2007b. "The role of actin cytoskeleton in oscillatory fluid flow-induced signaling in MC3T3-E1 osteoblasts." Am J Physiol-Cell Physiol **292**:C1830-C1836.

Mao, Y. and J. E. Schwarzbauer. 2005. "Fibronectin fibrillogenesis, a cell-mediated matrix assembly process." Matrix Biol **24**:389-399.

Martin, R. B., D. B. Burr and N. A. Sharkey. 1998. Skeletal Tissue Mechanics: Springer.

Martins, Albino*, et al.* 2011. "The Influence of Patterned Nanofiber Meshes on Human Mesenchymal Stem Cell Osteogenesis." Macromol Biosci **11**(7):978-987.

Matcher, S. J. 2009. "A review of some recent developments in polarization-sensitive optical imaging techniques for the study of articular cartilage." J App Phys **105**:102041.

McBeath, R.*, et al.* 2004a. "Cell Shape, Cytoskeletal Tension, and RhoA Regulate Stem Cell Lineage Commitment." Dev Cell **6**:483-495.

McBeath, R.*, et al.* 2004b. "Cell shape, cytoskeletal tension, and RhoA regulate stem cell lineage commitment." Dev Cell **6**(4):483-495.

McCoy, R. J. and F. J. O'Brien. 2010. "Influence of Shear Stress in Perfusion Bioreactor Cultures for the Development of Three-Dimensional Bone Tissue Constructs: A Review." Tissue Eng Part B-Rev **16**(6):587-601.

McGlashan, S. R.*, et al.* 2010. "Mechanical loading modulates chondrocyte primary cilia incidence and length." Cell Biol Int **34**:441-446.

Meirelles, L. D., *et al.* 2009. "Mechanisms involved in the therapeutic properties of mesenchymal stem cells." Cytokine Growth F Rev **20**(5-6):419-427.

Menard, C., S. Mitchell and M. Spector. 2000. "Contractile behavior of smooth muscle actin-containing osteoblasts in collagen-GAG matrices in vitro: implant-related cell contractions." Biomaterials **21**(18):1867-1877.

Milleret, Vincent*, et al.* 2011. "Tuning electrospinning parameters for production of 3D-fiber-fleeces with increased porosity for soft tissue engineering applications." Euro cells mater **21**:286-303.

Min, B. M.*, et al.* 2004. "Chitin and chitosan nanofibers: electrospinning of chitin and deacetylation of chitin nanofibers." Polymer **45**(21):7137-7142.

Mizuno, M. and Y. Kuboki. 2001. "Osteoblast-related gene expression of bone marrow cells during the osteoblastic differentiation induced by type I collagen." J Biochem (Tokyo). **129**(1):133-138.

Mo, X., *et al.* 2000. "Soft tissue adhesive composed of modified gelatin and polysaccharides." J Biomater Sci Polym Ed **11**(4):341-351.

Morgan, E. F., *et al.* 2008. "Mechanotransduction and fracture repair." J Bone Joint Surg Am **90A**:25-30.

Morris, H. L., *et al.* 2010. "Mechanisms of fluid-flow-induced matrix production in bone tissue engineering." P I Mech Eng H **224**(H12):1509-1521.

Murray-Dunning, C., *et al.* 2011. "Three-dimensional alignment of Schwann cells using hydrolysable microfiber scaffolds: strategies for peripheral nerve repair." Methods Mol Biol **695**:155-166.

Murugan, R. and S. Ramakrishna. 2004. "Bioresorbable composite bone paste using polysaccharide based nano hydroxyapatite." Biomaterials **25**(17):3829-3835.

Murugan, R. and S. Ramakrishna. 2007. "Design strategies of tissue engineering scaffolds with controlled fiber orientation." Tissue Eng **13**(8):1845-1866.

Nauli, S. M., *et al.* 2003. "Polycystins 1 and 2 mediate mechanosensation in the primary cilium of kidney cells." Nat Genet **33**:129-137.

Nerurkar, N. L., *et al.* 2011. "Dynamic culture enhances stem cell infiltration and modulates extracellular matrix production on aligned electrospun nanofibrous scaffolds." Acta Biomater **7**(2):485-491.

Nerurkar, N. L., *et al.* 2009. "Nanofibrous biologic laminates replicate the form and function of the annulus fibrosus." Nat Mater **8**(12):986-992.

Nerurkar, N. L., D. M. Elliott and R. L. Mauck. 2007. "Mechanics of oriented electrospun nanofibrous scaffolds for annulus fibrosus tissue engineering." J Orthop Res **25**(8):1018-1028.

Ngiam, M., *et al.* 2011. "Effects of mechanical stimulation in osteogenic differentiation of bone marrow-derived mesenchymal stem cells on aligned nanofibrous scaffolds." J Bioact Compatible Polym **26**(1):56-70.

Nombela-Arrieta, C., J. Ritz and L.E. Silberstein. 2011. "The elusive nature and function of mesenchymal stem cells." Nat Rev Mol Cell Biol **12**:126-131.

Nomura, S. and T. Takano-Yamamoto. 2000. "Molecular events caused by mechanical stress in bone." Matrix Biol **19**(2):91-96.

Norvell, S. M., *et al.* 2004. "Fluid shear stress induction of COX-2 protein and prostaglandin release in cultured MC3T3-E1 osteoblasts does not require intact microfilaments or microtubules." J Appl Physiol **96**(3):957-966.

O'Brien, F. J., *et al.* 2005. "The effect of pore size on cell adhesion in collagen-GAG scaffolds." Biomaterials **26**(4):433-441.

Ogston, N., *et al.* 2002. "Dexamethasone and retinoic acid differentially regulate growth and differentiation in an immortalised human clonal bone marrow stromal cell line with osteoblastic characteristics." Steroids **67**(11):895-906.

Oh, S., *et al.* 2009. "Stem cell fate dictated solely by altered nanotube dimension." P Natl Acad Sci USA **106**(7):2130-2135.

Oheim, M., *et al.* 2006. "Principles of two-photon excitation fluorescence microscopy and other nonlinear imaging approaches." Adv Drug Del Rev **58**:788-808.

Ondarcuhu, T. and C. Joachim. 1998. "Drawing a single nanofibre over hundreds of microns." Europhys Lett **42**(2):215-220.

Orr, A. W., *et al.* 2006. "Mechanisms of mechanotransduction." Dev Cell **10**(1):11-20.

Osyczka, A. M. and P. S. Leboy. 2005. "Bone morphogenetic protein regulation of early osteoblast genes in human marrow stromal cells is mediated by extracellular signal-regulated kinase and phosphatidylinositol 3-kinase signaling." Endocrinology **146**(8):3428-3437.

Owan, I., *et al.* 1997. "Mechanotransduction in bone: osteoblasts are more responsive to fluid forces than mechanical strain." Am J Physiol **273**(3 Pt 1):C810-815.

Pavalko, F. M.*, et al.* 1998. "Fluid shear-induced mechanical signaling in MC3T3-E1 osteoblasts requires cytoskeleton-integrin interactions." Am J Physiol-Cell Physiol **275**(6):C1591-C1601.

Pedersen, J. A. and M. A. Swartz. 2005. "Mechanobiology in the third dimension." Ann Biomed Eng **33**(11):1469-1490.

Pedicini, A. and R. J. Farris. 2003. "Mechanical behavior of electrospun polyurethane." Polymer **44**(22):6857-6862.

Peng, F., X. Yu and M. Wei. 2011. "In vitro cell performance on hydroxyapatite particles/poly(L-lactic acid) nanofibrous scaffolds with an excellent particle along nanofiber orientation." Acta Biomater **7**(6):2585-2592.

Peterlin, A. 1983. "The strength and stiffness of polymers." eds. A. E. Zachariades and R. S. Porter. New York: Dekker.

Phillips, C. L., S. B. Combs and S. R. Pinnell. 1994. "Effects of ascorbic acid on pro-liferation and collagen synthesis in relation to the donor age of human dermal fibroblasts." J Invest Dermatol **103**:228-232.

Phipps, M. C., Y. Xu and S. L. Bellis. 2012. "Delivery of Platelet-Derived Growth Factor as a Chemotactic Factor for Mesenchymal Stem Cells by Bone-Mimetic Electrospun Scaffolds." PloS one **7**(7):e40831.

Pitaval, A.*, et al.* 2010. "Cell shape and contractility regulate ciliogenesis in cellcycle-arrested cells." J Cell Biol **191**(2):303-312.

Pittenger, M. F.*, et al.* 1999. "Multilineage potential of adult human mesenchymal stem cells." Science **284**(5411):143-147.

Ponik, S. M., J. W. Triplett and F. M. Pavalko. 2007. "Osteoblasts and osteocytes respond differently to oscillatory and unidirectional fluid flow profiles." J Cell Biochem **100**(3):794-807.

Porter, R. M., W. R. Huckle and A. S. Goldstein. 2003. "Effect of dexamethasone withdrawal on osteoblastic differentiation of bone marrow stromal cells." J Cell Biochem **90**(1):13-22.

Powell, H. M.*, et al.* 2010. "Uniaxial Strain Regulates Morphogenesis, Gene Expression, and Tissue Strength in Engineered Skin." Tissue Eng Part A **16**(3):1083-1092.

Praetorius, H. A. and K. R. Spring. 2003. "Removal of MDCK cell primary cilium abolishes flow sensing." J Membr Biol **191**(1):69-76.

Praetorius, H. A. and K. R. Spring. 2005. "A physiological view of the primary cilia." Ann Rev Physiol **67**:515-529.

Prasad, P. N. 2003. "Introduction to Biophotonics." Nwe Jersey: John Wiley and Sons, Inc.

Rehman, J.*, et al.* 2004. "Secretion of angiogenic and antiapoptotic factors by human adipose stromal cells." Circulation **109**(10):1292-1298.

Reilly, G. C., J. D. Currey and A. E. Goodship. 1997. "Excercise of young thorougbred horses increases impact strength and the third metacarpal bone." J Orthop Res **15**(6):862-868.

Reilly, G. C. and A. J. Engler. 2010. "Intrinsic extracellular matrix properties regulate stem cell differentiation." J Biomech **43**(1):55-62.

Reilly, G. C.*, et al.* 2003. "Fluid flow induced PGE(2) release by bone cells is reduced by glycocalyx degradation whereas calcium signals are not." Biorheology **40**(6):591-603.

Reneker, D. H. and I. Chun. 1996. "Nanometre diameter fibres of polymer, produced by electrospinning." Nanotechnology **7**(3):216-223.

Reneker, D. H.*, et al.* 2000. "Bending instability of electrically charged liquid jets of polymer solutions in electrospinning." J App Phys **87**:4531.

Rho, J. Y., L. Kuhn-Spearing, P. Zioupos. 1998. "Mechanical properties and the hierarchical structure of bone." Med Eng Phy **20**(2):92-102.

Riggs, C .M.*, et al.* 1993. "Mechanical implications of collagen fibre orientation incortical bone of the equine radius." Anat Embryol (Berl) **187**(3):239-248.

Rowlands, A. S., P. A. G. and J. J. Cooper-White. 2008. "Directing osteogenic and myogenic differentiation of MSCs: interplay of stiffness and adhesive ligand presentation." Am J Physiol-Cell Physiol **295**(4):C1037-C1044.

Rui, Y. F., *et al.* 2011. "Mechanical Loading Increased BMP-2 Expression which Promoted Osteogenic Differentiation of Tendon-Derived Stem Cells." J Orthop Res **29**(3):390-396.

Ruiz, S. A., and C. S. Chen. 2008. "Emergence of Patterned Stem Cell Differentiation Within Multicellular Structures." Stem Cells **26**(11):2921-2927.

Rutherford, R. B., *et al.* 2002. "Bone morphogenetic protein-transduced human fibroblasts convert to osteoblasts and form bone in vivo." Tissue Eng **8**(3):441-452.

Rutledge, G. C. and S. V. Fridrikh. 2007. "Formation of fibers by electrospinning." Adv Drug Del Rev **59**(14):1384-1391.

Salasznyk, R. M., *et al.* 2004. "Adhesion to vitronectin and collagen I promotes osteogenic differentiation of human mesenchymal stem cells." J Biomed Biotechnol (1):24-34.

Salgado, A. J., O. P. Coutinho and R. L. Reis. 2004. "Bone tissue engineering: state of the art and future trends." Macromol Biosci **4**(8):743-765.

Schenke-Layland, K. , *et al.* 2006. "Two-photon microscopes and in vivo multiphoton tomographs - Powerful diagnostic tools for tissue engineering and drug delivery." Drug Deliv Rev **58**:878-896.

Schoof, H. , *et al.* 2001. "Control of pore structure and size in freeze-dried collagen sponges." J Biomed Mater Res **58**(4):352-357.

Screen, H. R. C. , *et al.* 2004. "Local strain measurement with tendon." Strain **40**(4):157-163.

Scutt, A., P. Bertram and M. Brautigam. 1996. "The role of glucocorticoids and prostaglandin E(2) in the recruitment of bone marrow mesenchymal cells to the osteoblastic lineage: Positive and negative effects." Calcified Tissue Int **59**(3):154-162.

Selim, M., *et al.* 2011. "Developing biodegradable scaffolds for tissue engineering of the urethra." Brit J Urol Int **107**(2):296-302.

Sen, B., *et al.* 2008. "Mechanical Strain Inhibits Adipogenesis in Mesenchymal Stem Cells by Stimulating a Durable beta-Catenin Signal." Endocrinology **149**(12):6065-6075.

Seong, J. M., *et al.* 2010. "Stem cells in bone tissue engineering." Biomed Mater **5**:062001.

Sequeira, M. M., *et al.* 1995. "Physical-activity assessment using pedometer and its comparison with a questionnaire in a large population survey." Am J Epidemiol **142**(9):989-999.

Sharp, L. A., Y. W. Lee and A. S. Goldstein. 2009. "Effect of Low-Frequency Pulsatile Flow on Expression of Osteoblastic Genes by Bone Marrow Stromal Cells." Ann Biomed Eng **37**(3):445-453.

Siddappa, R., *et al.* 2007. "Donor variation and loss of multipotency during in vitro expansion of human mesenchymal stem cells for bone tissue engineering." J Orthop Res **25**(8):1029-1041.

Sikavitsas, V. I., *et al.* 2005. "Flow perfusion enhances the calcified matrix deposition of marrow stromal cells in biodegradable nonwoven fiber mesh scaffolds." Ann Biomed Eng **33**(1):63-70.

Simmons, C. A., *et al.* 2003. "Cyclic strain enhances matrix mineralization by adult human mesenchymal stem cells via the extracellular signal-regulated kinase (ERK1/2) signaling pathway." J Biomech **36**(8):1087-1096.

Sioud, M., *et al.* 2011. "Mesenchymal stem cell-mediated T cell suppression occurs through secreted galectins." Int J Oncol **38**(2):385-390.

Sisson, K., *et al.* 2010. "Fiber diameters control osteoblastic cell migration and differentiation in electrospun gelatin." J Biomed Mater Res Part A **94A**(4):1312-1320.

Sittichockechaiwut, A., *et al.* 2009. "Use of rapidly mineralising osteoblasts and short periods of mechanical loading to accelerate matrix maturation in 3D scaffolds." Bone **44**(5):822-829.

Sittichokechaiwut, A., *et al.* 2010. "Short bouts of mechanical loading are as effective as dexamethasone at inducing matrix production by human bone marrow mesenchymal stem cells " Eur Cells Mater **20**:45-57.

Skedros, J. G. and K. J. Hunt. 2004. "Does the degree of laminarity correlate with site-specific differences in collagen fibre orientation in primary bone?" J Anat **205**(2):121-134.

Sodek, J. and M. D. McKee. 2000. "Molecular and cellular biology of alveolar bone." Periodontol 2000 **24**:99-126.

Sommar, P*., et al.* 2009. "Engineering three-dimensional cartilage- and bone-like tissues using human dermal fibroblasts and macroporous gelatine microcarriers." J Plast Reconstr Aesthet Surg **63**(6):1036-1046.

Sommerfeldt, D.W. and C. T. Rubin. 2001. "Biology of bone and how it orchestrates the form and function of the skeleton." Eur Spine J **10**:S86-S95.

Soncini, M*., et al.* 2007. "Isolation and characterization of mesenchymal cells from human fetal membranes." J Tissue Eng Regen Med **1**(4):296-305.

Stevens, M. M. 2005. "Exploring and Engineering the Cell Surface Interface." Science **310**:1135-1138.

Stevens, M. M. and J. H. George. 2005. "Exploring and engineering the cell surface interface." Science **310**(5751):1135-1138.

Stock, U. A. and J. P. Vacanti. 2001. "Tissue engineering: Current state and prospects." Ann Rev Med **52**:443-451.

Sumanasinghe, R. D., S. H. Bernacki and E. G. Loboa. 2006. "Osteogenic differentiation of human mesenchymal stem cells in collagen matrices: Effect of uniaxial cyclic tensile strain on bone morphogenetic protein (BMP-2) mRNA expression." Tissue Eng **12**(12):3459-3465.

Summitt, M. C. and K. D. Reisinger. 2003. "Characterization of the mechanical properties of demineralized bone." J Biomed Mater Res Part A **67A**(3):742-750.

Sun, J*., et al.* 2004. "In vivo multimodal nonlinear optical imaging of mucosal tissue." Optics Express **12**:2478-2486.

Takahashi, Y. and Y. Tabata. 2004. "Effect of the fiber diameter and porosity of non-woven PET fabrics on the osteogenic differentiation of mesenchymal stem cells." J Biomater Sci-Polym Ed **15**(1):41-57.

Tan, E. P. S. and C. T. Lim. 2006. "Effects of annealing on the structural and mechanical properties of electrospun polymeric nanofibres." Nanotechnology **17**:2649-2654.

Taskiran, D*., et al.* 1999. "Quantification of Total Collagen in Rabbit Tendon by the Sirius Red Method." J Med Sci **29**:7-9.

Tatsumi, S. *, et al.* 2007. "Targeted ablation of osteocytes induces osteoporosis with defective mechanotransduction." Cell Metabolism **5**(6):464-475.

Taylor, A. F*., et al.* 2007. "Mechanically stimulated osteocytes regulate osteoblastic activity via gap junctions." Am J Physiol-Cell Physiol **292**(1):C545-C552.

Taylor, G. I. 1964. "Disintegration of water drops in an electric field." Proc R Soc Lon A Mat **A280**:383-397.

Temiyasathit, S*., et al.* 2012. "Mechanosensing by the Primary Cilium: Deletion of Kif3A Reduces Bone Formation Due to Loading." PloS one **7**(3).

Theodossiou, T. A*., et al.* 2006. "Second Harmonic Generation Confocal Microscopy of Collagen Type I from Rat Tendon Cryosections." Biophys J **91**:4665-4677.

Thompson, M. S*., et al.* 2010. "In vitro models for bone mechanobiology: applications in bone regeneration and tissue engineering." P I Mech Eng H **224**(H12):1533-1541.

Toma, J. G*., et al.* 2001. "Isolation of multipotent adult stem cells from the dermis of mammalian skin." Nat Cell Biol **3**(9):778-784.

Tuan, R. S., G. Boland and R. Tuli. 2003. "Adult mesenchymal stem cells and cell-based tissue engineering." Arthrit Res Ther **5**(1):32-45.

Tucker, R. P*., et al.* 2011. "Validated in vitro cyclic shear stress alters human tenocyte ECM synthesis." Histol Histopathol **26**(S1):27.P26.

Tummala, P., E. J. Arnsdorf and C. R. Jacobs. 2010. "The role of the primary cilia in mesenchymal stem cell differentiation: A pivotal switch in guiding lineage commitment." Cell Mol Bioeng **3**:207-212.

Ugryumova, N*., et al.* 2005. "The collagen structure of equine articular cartilage, characterized using polarization-sensitive optical coherence tomography." J Phys D **38**:2612-2619.

Ugryumova, N., S. V. Gangus and S. J. Matcher. 2006. "Three-dimensional optic axis determination using variable-incidence-angle polarozation-optical coherence tomography." Optics Letters **31**:2305-2307.

Vater, C., P. Kasten and M. Stiehler. 2011. "Culture media for the differentiation of mesenchymal stromal cells." Acta Biomater **7**(2):463-477.

Vogel, V. 2006. "Mechanotransduction involving multimodular proteins: Converting force into biochemical signals." Annu Rev Biophys Biomol Struct **35**:459-488.

Wagner, W.*, et al.* 2005. "Comparative characteristics of mesenchymal stem cells from human bone marrow, adipose tissue, and umbilical cord blood." Exp Hematol **33**(11):1402-1416.

Walker, N. G.*, et al.* 2012. "A Chemically Defined Carrier for the Delivery of Human Mesenchymal Stem/Stromal Cells to Skin Wounds." Tissue Eng Part C-Meth **18**(2):143-155.

Walsh, B. J.*, et al.* 1992. "Micorplate reader-based quantitation of collagens." Anal Biochem **203**(2):187-190.

Wang, Bo*, et al.* 2011. "The effect of poly (L-lactic acid) nanofiber orientation on osteogenic responses of human osteoblast-like MG63 cells." J Mech Behav Biomed **4**(4):600-609.

Wang, J. H. C.*, et al.* 2003. "Cell orientation determines the alignment of cell-produced collagenous matrix." J Biomech **36**(1):97-102.

Wang, Yang*, et al.* 2012. "The differential effects of aligned electrospun PHBHHx fibers on adipogenic and osteogenic potential of MSCs through the regulation of PPAR gamma signaling." Biomaterials **33**(2):485-493.

Wann, A. K. T.*, et al.* 2012. "Primary cilia mediate mechanotransduction through control of ATP-induced Ca2+ signaling in compressed chondrocytes." FASEB J. **26**(4):1663-1671.

Watari, S.*, et al.* 2012. "Modulation of osteogenic differentiation in hMSCs cells by submicron topographically-patterned ridges and grooves." Biomaterials **33**(1):128-136.

Weinbaum, S., S. C. Cowin and Y. Zeng. 1994. "A model for the excitation of osteocytes by mechanical loading-induced bone fluid shear stresses." J. Biomech. **27**(3):339-360.

Weinbaum, S., J. M. Tarbell and E. R. Damiano. 2007. "The structure and function of the endothelial glycocalyx layer." Ann Rev Biomed Eng **9**:121-167.

Weiner, S. and H. D. Wagner. 1998. "The materials bone: Structure-Mechanical Function Relations." Ann Rev Mater Sci **28**:271-298.

Westermann, S. and K. Weber. 2003. "Post-translational modifications regulate microtubule function." Nat Rev Mol Cell Biol **4**(12):938-947.

Wheatley, D. N., A. M. Wang and G. E. Strugnell. 1996. "Expression of primary cilia in mammalian cells." Cell Biol Int Rep **20**(1):73-81.

Whitesides, G. M. and M. Boncheva. 2002. "Beyond molecules: Self-assembly of mesoscopic and macroscopic components." Proc Natl Acad Sci USA **99**(8):4769-4774.

Whitfield, J. F. 2003. "Primary cilium - is it an osteocyte's strain-sensing flowmeter?" J Cell Biochem **89**(2):233-237.

Whitfield, J. F. 2007. "The solitary (primary) cilium-A mechanosensory toggle switch in bone and cartilage cells." Cell Signal **20**(6):1019-1024.

Williams, R. M., W. R. Zipfel and W. W. Webb. 2005. "Interpreting second-harmonic generation images of collagen I fibrils." Biophys J **88**(2):1377-1386.

Willie, B. M.*, et al.* 2010. "Designing biomimetic scaffolds for bone regeneration: why aim for a copy of mature tissue properties if nature uses a different approach?" Soft Matter **6**(20):4976-4987.

Wong, J. Y., J. B. Leach and X. Q. Brown. 2004. "Balance of chemistry, topography, and mechanics at the cell-biomaterial interface: Issues and challenges for assessing the role of substrate mechanics on cell response." Surf Sci **570**(1-2):119-133.

Woo, K. M., V. J. Chen and P. X. Ma. 2003. "Nano-fibrous scaffolding architecture selectively enhances protein adsorption contributing to cell attachment." J Biomed Mater Res Part A **67A**(2):531-537.

Wood, M. A., *et al.* 2008. "Correlating cell morphology and osteoid mineralization relative to strain profile for bone tissue engineering applications." J Roy Soc Interface **5**(25):899-907.

Xie, J. W., X. R. Li and Y. N. Xia. 2008. "Putting Electrospun Nanofibers to Work for Biomedical Research." Macromol Rapid Comm **29**(22):1775-1792.

Xue, S. and L. Li. 2011. "Upregulation of collagen type 1 in aged murine dermis after transplantation of dermal multipotent cells." Clin Exp Dermatol **36**(7):775-781.

Yang, F., *et al.* 2004a. "Fabrication of nano-structured porous PLLA scaffold intended for nerve tissue engineering." Biomaterials **25**(10):1891-1900.

Yang, G. G., R. C. Crawford and J. H. C. Wang. 2004b. "Proliferation and collagen production of human patellar tendon fibroblasts in response to cyclic uniaxial stretching in serum-free conditions." J Biomech **37**(10):1543-1550.

Yin, Zi, *et al.* 2010. "The regulation of tendon stem cell differentiation by the alignment of nanofibers." Biomaterials **31**(8):2163-2175.

Yoder, B. K., X. Y. Hou and L. M. Guay-Woodford. 2002. "The polycystic kidney disease proteins, polycystin-1, polycystin-2, polaris, and cystin, are co-localized in renal cilia." J Am Soc Nephrol **13**(10):2508-2516.

Yoshimoto, H., *et al.* 2003. "A biodegradable nanofiber scaffold by electrospinning and its potential for bone tissue engineering." Biomaterials **24**(12):2077-2082.

You, J., *et al.* 2001. "Osteopontin gene regulation by oscillatory fluid flow via intracellular calcium mobilization and activation of mitogen-activated protein kinase in MC3T3-E1 osteoblasts." J Biol Chem **276**(16):13365-13371.

You, Y., *et al.* 2006. "Effect of solution properties on nanofibrous structure of electrospun poly(lactic-co-glycolic acid)." J Appl Polym Sci **99**(3):1214-1221.

Young, H. E., *et al.* 2001. "Human reserve pluripotent mesenchymal stem cells are present in the connective tissues of skeletal muscle and dermis derived from fetal, adult, and geriatric donors." Anat Rec **264**(1):51-62.

Yourek, G., *et al.* 2010. "Shear stress induces osteogenic differentiation of human mesenchymal stem cells." Regen Med **5**(5):713-724.

Zahm, Adam M., *et al.* 2008. "Oxygen tension regulates preosteocyte maturation and mineralization." Bone **43**(1):25-31.

Zamir, E. A., *et al.* 2003. "Mechanical asymmetry in the embryonic chick heart during looping." Ann Biomed Eng **31**:1327-1336.

Zamir, E. and B. Geiger. 2001. "Molecular complexity and dynamics of cell-matrix adhesions." J Cell Sci **114**(20):3583-3590.

Zeugolis, D. I., *et al.* 2008. "Electro-spinning of pure collagen nano-fibres - just an expensive way to make gelatin?" Biomaterials **29**(15):2293-2305.

Zhong, S., *et al.* 2006. "An aligned nanofibrous collagen scaffold by electrospinning and its effects on in vitro fibroblast culture." J Biomed Mater Res **79**(3):456-463.

Zhou, X. Z., *et al.* 2010. "Quantifying fluid shear stress in a rocking culture dish." J Biomech **43**(8):1598-1602.

Zimmerman, H. D. 1971. "Cilia in the fetal kidney of man." Beitraege zur Pathologie **143**(3):227-240.

Zipfel, W. R. , *et al.* 2003. "Live tissue intrinsic emission microscopy using multiphoton-excited native fluorescence and second harmonic generation." Proc Natl Acad Sci USA **100**:7075-7080.

Zoumi, A. , A. Yeh and Tromberg B. J. 2002. "Imaging cells and extracel-lular matrix in vivo by using second-harmonic generation and two-photon excited fluorescence." Proc Natl Acad Sci USA **99**:11014-11019.

Zuk, P. A., *et al.* 2001. "Multilineage cells from human adipose tissue: Implications for cell-based therapies." Tissue Eng **7**(2):211-228.